UNIVERSITÀ
DEGLI STUDI
DI MILANO

DEPARTMENT OF PHARMACEUTICAL SCIENCES

DOCTORAL SCHOOL IN PHARMACEUTICAL SCIENCES

XXXII Ph.D. Cycle

Lipid and protein oxidation in human heart failure: in search of potential biomarkers and insights into their biological function

Scientific Supervisor: Dr. Cristina Banfi

Academic Supervisor: Prof. Giancarlo Aldini

Ph.D Coordinator: Prof. Giancarlo Aldini

Alma E. Martínez Fernández
Ph.D. Candidate
R11562

Academic year 2019/2020

MasstrplAn
Grant Agreement 675132

Centro Cardiologico
Monzino

FUNDING

This work has been funded by the European Union's Horizon 2020 research and innovation programme under the Marie Sklowdowska- Curie grant agreement number 675132 (http://cordis.europa.eu/ project/rcn/198275_en.html).

TABLE OF CONTENTS

ABBREVIATIONS

•OH,	Hydroxyl radical
4-HNE,	4-hydroxy-2-nonenal
8-OHdG,	8-hydroxydeoxyguanosine
ACN,	Acetonitrile
ACR,	Acrolein
AGE-HSA,	Advanced glycation products of HSA
AGEs,	Advanced glycation end-products
ALEs,	Advanced lipoxidation end-products
BMI,	Body mass index
BNP,	Brain natriuretic peptide
CAM,	Carbamidomethylation
ChE,	Cholesteryl ester
CML,	Carboxymethyl lysine
CVD,	Cardiovascular disease
cys-HSA,	Cysteinylated human serum albumin
DCF,	2',7' dichlorofluorescein
DCF-DA,	2',7' –dichlorofluorescein diacetate
DDA,	Data dependent acquisition mode
DF,	Deoxy-fructosyl
DFK,	Deoxy-fructosyl lysine
DFR,	Deoxy-fructosyl arginine
DLCO,	Carbon monoxide lung diffusion
DNPH,	2,4-Dinitrophenylhydrazine
DTT,	Dithiothreitol
ECM,	Extracellular matrix
EF,	Ejection fraction
ELISA,	Enzyme-linked immunosorbent assay
ESI,	Electrospray ionization
FA,	Formic acid
FDR,	False discovery rate
GA,	Glycated human serum albumin
GAPDH,	Glyceraldehyde-3-phosphate dehydrogenase
GO,	Glyoxal
H_2O_2,	Hydrogen peroxide
HF,	Heart failure

HILIC, Hydrophilic interaction chromatography
HPLC, High-performance liquid chromatography
HSA, Human serum albumin
IL-6, Interleukin-6
L•, Lipid radicals
LC, Liquid chromatography
LDLs, Low density lipoproteins
LOO•, Peroxyl radical
LOOH, Lipid hydroperoxides
LPC, Lysophosphatidylcholine
LPPs, Lipid peroxidation products
LVEF, Left ventricular ejection fraction
MDA, Malondialdehyde
MGO, Methylglyoxal
MRM, Multiple reaction monitoring
MS, Mass spectrometry
MTT, 3-(4,5-dimethylthiazol-2-yl)-2,5-diphenyltetrazolium bromide tetrazolium
NADPH, Nicotinamide adenine dinucleotide phosphate
NO, Nitric oxide
NOS, Nitric oxide synthase
Nrf2, Nuclear factor erythroid 2-related factor 2
NYHA, New York Heart Association
$O_2^{\bullet-}$, Superoxide anion
oxPLs, Oxidized phospholipids
oxPTMs, Oxidative post-translational modifications
PC, Phosphatidylcholine
PE, Phosphatidylethanolamine
PGC-1α, Transcriptional coactivator peroxisome proliferator-activated receptor γ coactivator-1 α
PGC-1β, Transcriptional coactivator peroxisome proliferator-activated receptor γ coactivator-1 β
PI, Phosphatidylinositol
PLs, Phospholipids
PLS-DA, Projection to latent structures discriminant analysis
PRM, Parallel reaction monitoring
PTMs, Post-translational modifications

PUFAs,	Polyunsaturated fatty acids
RAGE,	Receptor for advanced glycation end products
RCS,	Reactive carbonyl species
RNS,	Reactive nitrogen species
ROS,	Reactive oxygen species
rt,	Retention time
SDS-PAGE,	Sodium dodecyl sulfate–polyacrylamide gel electrophoresis
SEM,	Standard error of the mean
SM,	Sphingomyelin
TFA,	Trifluoroacetic acid
TNF-α,	Tumor necrosis factor α
UPLC,	Ultra Performance Liquid Chromatography
VIP,	Variable importance in projection
VO_2,	Oxygen consumption

General introduction

GENERAL INTRODUCTION

1. THE PATHOLOGY OF HEART FAILURE

Heart failure (HF) is a condition characterized by the inability of the heart to supply enough blood to the peripheral tissues. Consequently, body organs and tissues are not well perfused and cannot meet their metabolic demands giving rise to cell death and multiple organ dysfunction that may eventually result in a fatal outcome. HF is one of the leading causes of death worldwide and is rapidly becoming a major public health problem, constituting an enormous economic burden for the healthcare systems in industrialized countries [1]. Moreover, HF is an age-related syndrome and its prevalence is increasing in accordance with the longer life expectancy.

HF is considered a progressive disorder triggered from a previous cardiac injury. Coronary artery disease, mainly originated from atherosclerotic coronary arteries, represents the predominant cardiac injury in industrialized western countries that can lead to HF. Other main risk factors are hypertension, diabetes, cardiomyopathies, valvular diseases, congenital defects or hypercholesterolemia [2].

In the first place, upon cardiac damage, the harmed heart undergoes cardiac remodeling as compensatory effect in order to maintaining or restore the normal cardiac function. Cardiac remodeling is strictly associated with the progression of HF, is a determinant of its clinical course after a cardiac insult, and might be associated with changes at genome expression, molecular, cellular and interstitial levels, which are clinically manifested as changes in size, shape, and function of the heart [3].

Hence, several compensatory mechanisms may take place at first, such as the activation of the renin-angiotensin-aldosterone system and the sympathetic adrenergic nervous system, as well as the increase of cytokine production, which in turn trigger the release of neurohormonal factors and stimulation of stretch receptors in the circulatory system [4]. These changes trigger a structural adaptation of the heart pursuing to enhance the impaired pumping function. For example, cardiomyocytes become hypertrophic, with the result of a heightened wall mass, aiming to pump the blood stronger within each beat, while ventricles enlarge holding larger volumes of blood inside the chamber [3]. However, after sustained stress, those changes cause in turn more stress to the heart leading to uncontrolled cardiac hypertrophy, myocyte loss, alteration of extracellular matrix homeostasis, fibroblast proliferation or metalloproteinases activation [5,6], which lead to decompensation and failure. Indeed, the damaged heart muscle declines in the number of functional cardiomyocytes, therefore reducing the myocardium's ability to fill with or eject blood; thus, the systolic and/or diastolic function is weakened (i.e., reduced contractility and/or relaxation finally precluding the heart from contracting normally [7]), contributing to a progressive and irreversible dysfunction that ultimately leads to heart failure progression.

Indeed, therapies targeting pathological cardiac remodeling have demonstrated significant effectiveness in reducing morbidity and mortality in HF patients [8]. Although cardiac remodeling is multifactorial, in the last decades, considerable experimental evidence has demonstrated the involvement of oxidative stress as a key player in the pathophysiology of HF (**Figure 1**) [9–11]. This relationship will be explained hereinafter.

HF is often characterized either by non-specific clinical symptoms (breathlessness, fluid retention in ankles, legs or lungs, nocturnal dyspnea, tiredness or fatigue even at rest) or by signs (elevated jugular venous pressure, pulmonary crackles, kidney dysfunction and peripheral edema). Owing to pulmonary congestion, gas exchange in the alveoli is hampered and the maximum amount of oxygen used during intense exercise is reduced, meaning that HF patients usually show a reduced value of peak of oxygen uptake (VO_2 peak/Kg).

HF diagnosis relies mainly on history and clinical examination, and therefore, it is detected once severe damage has already occurred in the heart. (**Figure 1**) [12]. Furthermore, the non-specificity of symptoms and signs might not help to discriminate between HF and other pathologies.

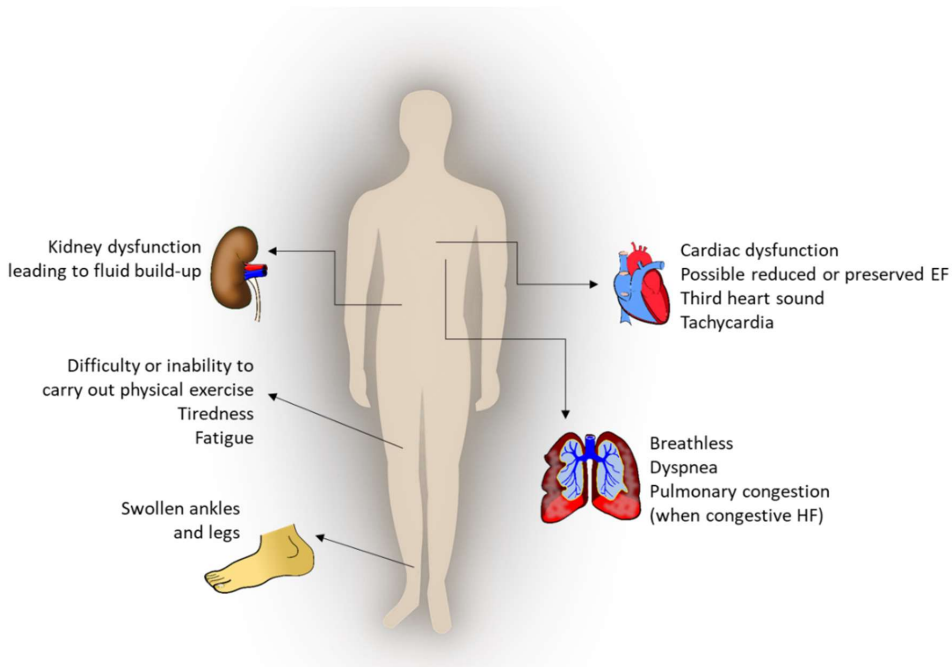

Figure 1. Most common symptoms and signs of heart failure [13].

Many imaging modalities, such as echocardiography, give assistance in the evaluation of myocardial performance at rest and allow the measurement of the left ventricular ejection fraction (LVEF), which is the central measure of left ventricular systolic function [14]. LVEF represents the ratio of blood volume ejected in systole (stroke volume) in relation to the blood volume in the ventricle at the end of diastole, expressed in percentage units [15]. HF patients are typically

classified in 3 groups according to the LVEF value: patients with normal (≥50%) LVEF; patients with mid-range ejection fraction or preserved EF (HFpEF) that present a LVEF in the range of 40-49%; and those with reduced EF (HFrEF), typically considered as <40%. Differentiation of patients with HF based on LVEF is important due to different underlying etiologies, demographics, co-morbidities, and response to therapies [12].

Likewise, HF patients can also be classified according to the severity of the symptoms and impairment of physical activity. Thus, the New York Heart Association (NYHA) has clinically graded HF severity into four classes (**Table 1**).

NYHA Class	Symptoms description
I.	No limitation of physical activity. Ordinary physical activity does not cause undue fatigue, palpitation, dyspnea (shortness of breath).
II.	Slight limitation of physical activity. Comfortable at rest. Ordinary physical activity results in fatigue, palpitation, and dyspnea.
III.	Marked limitation of physical activity. Comfortable at rest. Less than ordinary activity causes fatigue, palpitation, or dyspnea.
IV.	Unable to carry on any physical activity without discomfort. Symptoms of heart failure at rest. If any physical activity is undertaken, discomfort increases.

Table 1. New York Heart Association (NYHA) functional classification

2. INVOLVEMENT OF OXIDATIVE STRESS IN HEART FAILURE

2.1. Oxidative stress, ROS and ROS sources

Oxidative stress is defined as an imbalance between the production of reactive oxygen and nitrogen species (ROS and RNS respectively) and the antioxidant capacity levels in favor of the former, disrupting the redox equilibrium [16]. When low and balanced, reactive species participate in a great number of physiological processes (proliferation, host defense, signal transduction, gene expression, etc.). However, when ROS levels increase uncontrolled, either due to its excessive production or due to a decrease in the antioxidant capacity, they are prone to react with all biomolecules, altering their properties and resulting in cell damage and, ultimately, cell death.

ROS are chemical species containing oxygen characterized by a high reactivity and capable of initiating deleterious reactions. The variety of ROS-dependent effects relies on their distinct properties and their different sites of distribution.

For the majority of cardiovascular diseases (CVDs) some of the most important sources of ROS are the mitochondrial respiratory chain, the nicotinamide adenine dinucleotide phosphate (NADPH) oxidases, xanthine oxidase (XO), uncoupled nitric oxide synthase (NOS), and myeloperoxidase (MPO) [17].

Mitochondria are the primary source of ROS in the cardiovascular system and, simultaneously, the major target of ROS-induced cellular damage [18]. Since the heart meets high energy requirements to maintain sustained contraction and relaxation activities, mitochondria are especially abundant in the heart owing to its important role as ATP generators [19]. However, during the aerobic synthesis of ATP carried out by the electron transport chain (ETC), an amount of molecular oxygen is converted into superoxide anion ($O_2^{\bullet-}$) by the NADH-ubiquinone oxidoreductase or complex I and the ubiquinone-cytochrome c oxidoreductase or complex III. Thus, a small amount of $O_2^{\bullet-}$ escapes as byproduct, becoming into the primary radical [20]. $O_2^{\bullet-}$ can bring eventually on the formation of more reactive secondary species.

Xanthine oxidase represents another source of ROS and catalyses the oxidation of hypoxanthine and xanthine at the expense of molecular oxygen reduction to form $O_2^{\bullet-}$ and hydrogen peroxide (H_2O_2), the latter being able to penetrate biological membranes [21].

In the cardiac context, the multi-subunit cytoplasmic NADPH oxidase enzymes is a ROS source of particular interest, specifically those containing a Nox2 or Nox4 catalytic subunits, the most abundant in the heart. NADPH oxidases catalyze $O_2^{\bullet-}$ production by transferring electrons from NADPH to molecular oxygen [22]. Moreover, myeloperoxidase, a member of the heme peroxidase family of enzymes, consumes H_2O_2 to produce hypochlorous acid, among other oxidizing products [23] (**Figure 2**).

Together with the endogenous mechanisms for ROS generation, exogenous sources such as UV radiation, pollution, or cigarette smoking amid others may contribute to the overproduction of ROS.

In biological systems, $O_2^{\bullet-}$ is rapidly dismutated by superoxide dismutase (SOD) enzymes into H_2O_2 which, in turn, in the presence of iron or other transition metals, is reduced leading to the formation of the highly reactive hydroxyl radical (•OH) via the Fenton reaction (**Figure 2**) [24]. Likewise, the interaction between superoxide ($O_2^{\bullet-}$) and hydrogen peroxide (H_2O_2) can trigger the formation of •OH through the iron-catalyzed Harber-Weiss reaction, which easily oxidizes the surrounding biomolecules [25].

On the other hand, reactive nitrogen species are also secondary products of superoxide anion. When $O_2^{\bullet-}$ and NO (nitric oxide) -the latter synthesized by nitric oxide synthase enzymes- are spatially close enough, both molecules may interact with each other yielding peroxynitrite ($ONOO^-$) that has the capacity to oxidize lipids and proteins (**Figure 2**) [26].

To certain extent, both the intracellular non-enzymatic (β -carotene, ascorbic acid, and tocopherols) and the enzymatic antioxidant defense systems neutralize ROS to maintain the redox

balance. Some antioxidant enzymes are superoxide dismutase (SOD) that catalyzes the reduction of superoxide anion into hydrogen peroxide [9,11]; glutathione peroxidase (GSHPx) and catalases, involved in the neutralization of hydrogen peroxide with the production of water [11,27]; or thioredoxin, which reduces oxidized thiol groups by cysteine thiol-disulfide exchange [28].

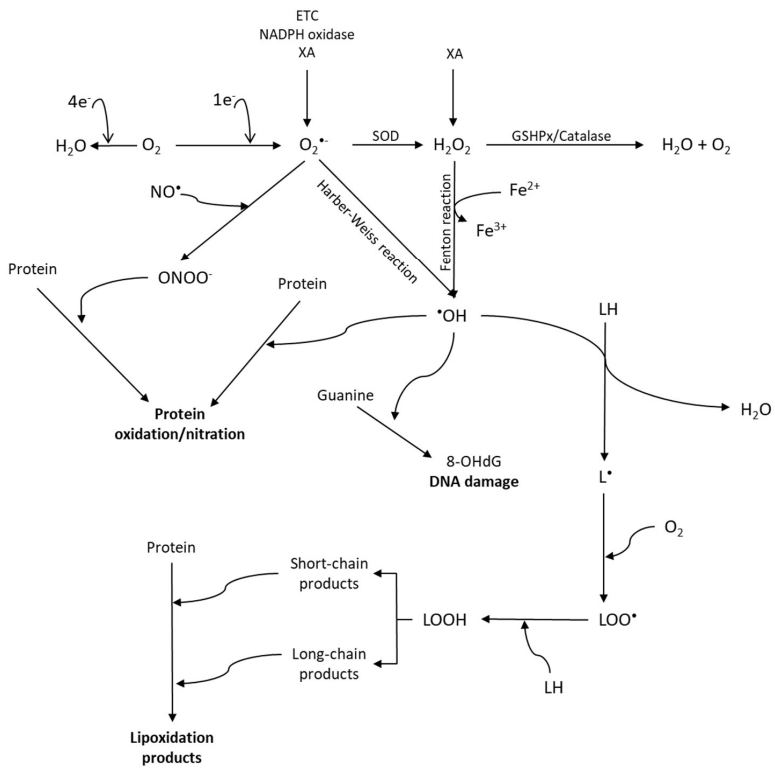

Figure 2. Schematic representation of reactive oxygen and nitrogen free radical-mediated oxidation of proteins, lipids and DNA with the subsequent formation of protein nitration/oxidation, DNA damage, lipid peroxidation and lipoxidation products.

However, when ROS production is uninterrupted, and the antioxidant defense capacity reaches its maximum, the balance is disrupted and oxidative stress becomes harmful to the organism significantly contributing to the onset and worsening of a wide set of diseases.

2.2. Oxidative damage to biomolecules

All the above-mentioned reactive oxygen species can mediate to some extent reversible or irreversible oxidative modifications on the neighboring macromolecules (lipids, proteins or nucleic acids), thus regulating their redox status and triggering the formation of protein oxidation,

lipid peroxidation and lipoxidation products, as well as DNA damage [29]. Oxidative modification of these biomolecules may impair their physiological role giving rise to the development of diseases such as cardiovascular diseases, including HF.

2.2.1. Protein oxidation

Proteins are the major target of ROS due to their abundance and ubiquity in the organism. Among all amino acid, the majority of reversible and irreversible oxidative modifications take place mainly in cysteine, methionine, histidine, lysine, arginine, tyrosine, and threonine residues, owing to their chemical characteristics [30]. Proteins might undergo various forms of oxidation. For example, ROS radicals, mainly •OH, can abstract a hydrogen from target residues (**Figure 2**) giving rise to carbon-centered radicals (or protein thiyl radicals if cysteine is the target residue) that react rapidly with molecular oxygen to form hydroxyl protein derivatives [31]. On the other side, carbon-containing radical proteins may also react with another protein carbon radical to form protein-protein cross-linked derivatives. Additionally, oxidized proteins may undergo fragmentation, unfolding or altered conformation [32]. All forms of protein oxidation may eventually participate in human diseases.

Direct oxidation of the amino acid side chains or peptide bond cleavage ROS-mediated might lead to carbonylated proteins. Protein carbonylation is known to be a significant hallmark of oxidative stress. In addition, protein carbonyl derivatives may be formed when reactive carbonyl groups derived from reducing sugar or their oxidation products interact with the amino group of lysine or arginine residues, eventually triggering the formation of advanced glycation end-products (AGEs), or by the adduction of lipid peroxidation products to proteins, giving rise to advanced lipoxidation end-products (ALEs) [33,34]. Carbonylated proteins tend to lose their function forming degradation-resistant aggregates, owing to the augmented hydrophobicity of side-chain residues [34].

2.2.2. Lipid oxidation

Lipids are well known structural elements of biological membranes and mediate key signaling pathways in several biological mechanisms. Modifications that hamper these roles, such as lipid peroxidation, can result into cell death.

Unsaturated and, specially, polyunsaturated fatty acids (PUFAs) are susceptible targets of lipid peroxidation due to the presence of reactive double bonds in their structure that facilitate the abstraction of an allylic hydrogen atom by oxidants such as ROS, which leads to the formation of lipid radicals (L•) [35]. This is known to be the initiation step of the lipid peroxidation process. Further, within the propagation step, molecular oxygen is added to the radical L•, which generates the formation of peroxyl radicals (LOO•), the main primary unstable oxidation product. Lipid peroxyl radicals may successively be transformed into lipid hydroperoxides (LOOH) after

abstracting a hydrogen from another unsaturated lipid (LH), in a vicious propagation circle [36] (**Figure 2**).

This chain reaction mechanism stops when two radicals react and produce non-radical derivative. Because of the instability of LOOH, a wide range of secondary reactive products are generated, from full-chain length to chain-shortened oxidized lipids as well as small fragmentation products. As well-reviewed by Domingues et al., lipid peroxidation breakdown products can be classified into 5 reactive groups: alkanals, 2-alkenals, 4-hydroxy-2-alkenals, keto-alkenals, and dialdehydes [37]. The identification of lipid peroxidation products has largely relied on the assessment of small lipid oxidation breakdown products. Indeed, two of the major and most studied aldehyde-derivative secondary products in HF are 4-hydroxy-2-nonenal (4-HNE) and malondialdehyde (MDA), 4-hydroxyalkenal and dialdehyde products, respectively. Those, in turn, may react with proteins that results in the formation of lipoxidation adducts (**Figure 2**) [38].

2.2.3. DNA damage

Hydrogen peroxide can interact with DNA by its addition to double bonds of DNA bases and by abstraction of a hydrogen atom from the methyl group of thymine. Indeed, hydrogen peroxide easily modifies guanine bases, which are particularly sensitive to oxidation, giving rise to 8-hydroxydeoxyguanosine (8-OHdG) formation, a reliable biomarker for DNA oxidative injury (**Figure 2**). Additionally, hydroxyl radical may abstract a hydrogen from the sugar moiety of DNA leading to sugar modification and strand breaks [32].

2.3. Evidence of oxidative stress and oxidative damage in the clinical course of heart failure

Increasing body of evidence supports that oxidative stress is involved systolic and diastolic myocardial dysfunction in HF. Indeed, it has been well established an association between cardiac remodeling (hypertrophy, apoptosis or contractile dysfunction) and oxidative stress [40,41], as summarized in **Figure 3**.

The development of chemical, chemiluminescent or fluorogenic assays has greatly contributed to demonstrate a relation between HF and oxidative stress. For example, raised levels of ROS have been detected in rat hearts suffering from HF [42], while enhanced superoxide production was pointed out in left and right ventricles from failing human hearts [43]. Additionally, the measurement of the expression level and/or the activity of ROS sources, as indirect markers of oxidative stress, have also confirmed the redox imbalance statement in the pathology of HF. For example, elevated plasma levels of myeloperoxidase were detected in HF patients compared to control subjects, and this increase was more marked when raising the severity degree of HF, a

fact that may provide prognostic value in predicting long-term clinical outcome [44]. Moreover, activity of NADPH oxidase and xanthine oxidase were significantly higher in end-stage hearts and in plasma samples from HF patients, respectively, when compared to the control subjects [45,46].

In turn, ROS can modulate downstream hypertrophy and inflammatory signaling pathways, such as the activation of the nuclear factor kappa-light-chain-enhancer of activated B cells (NF-κB) [47] or the p38MAP kinase [48] that enhance cardiac hypertrophy finally driving to maladaptive hypertrophy and cardiac remodeling. Oxidative stress also induces the dysregulation of cardiac excitation-contraction coupling processes, for instance cysteine residues in the cardiac ryanodine receptor (RyR2) become oxidized leading to an activated form that enlarges Ca^{2+} leakage into the cytosol affecting the cardiac contraction, while elevated ROS levels irreversibly oxidize the cardiac Sarco-/endoplasmic reticulum Ca^{2+}-ATPase (SERCA2a) inhibiting its function and, hence, impairing the systolic and/or diastolic cardiac function [49]. In addition, Canton et al. detected raised levels of S-nitrosylated tropomyosin in human failing hearts and demonstrated that S-nitrosylated tropomyosin contributed to contractile function impairment [50].

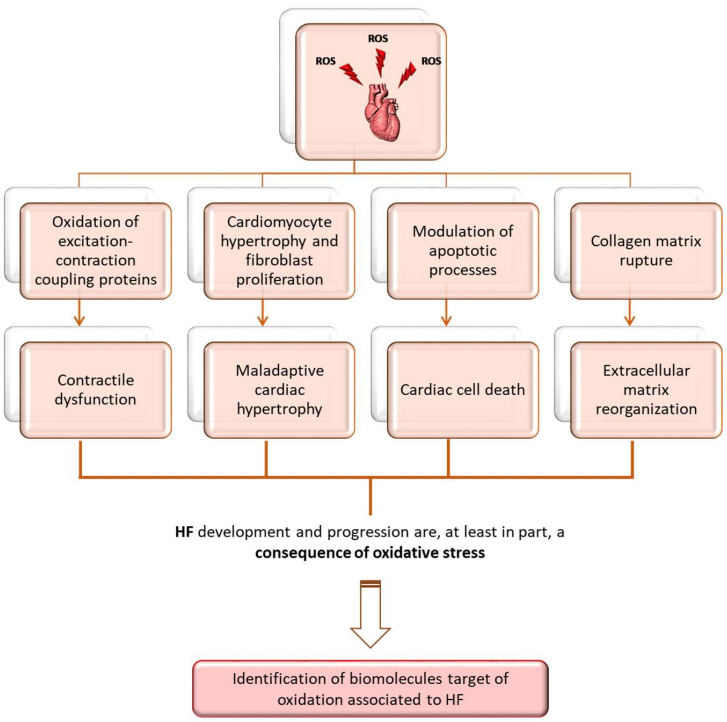

Figure 3. Consequences of oxidative stress in the development of heart failure. Increased reactive oxygen species in the heart lead to the activation of hypertrophic and apoptotic signaling pathways together with a contractile dysfunction and reorganization of the extracellular matrix (ECM). All these changes in turn induce the development and progression of heart failure.

The contribution of ROS to cardiac death processes has been also well documented. For example, ROS activate the c-Jun N-terminal kinase protein (JNK) that successively phosphorylates p53 which in turn stimulates cardiomyocyte apoptosis [51]. In addition, cardiolipin peroxidation-ROS dependent could lead to the release of cytochrome C into the cytoplasm and, ultimately, in the onset of apoptosis through caspase activation [52].

Finally, oxidation of matrix metalloproteinase-1 thiol group ROS-mediated boost the enzymatic activity whereby collagen, the major component of the extracellular matrix (ECM), is degraded, which results in ECM remodeling [53]. Interestingly, the expression of matrix metalloproteinases is up-regulated in the end-stage failing human myocardium [54].

Despite the myriad of evidence relating oxidative stress with HF, specific biomarkers of oxidative stress in plasma of HF are still needed. Only conventional biomarkers have been validated and daily used in clinical practice.

3. PLASMA BIOMARKERS IN HEART FAILURE ASSOCIATED TO OXIDATIVE STRESS: ADVANTAGES AND LIMITATIONS

Since oxidative stress is involved in the pathology of HF, the identification of reactive species and oxidized biomolecules present in HF patients can contribute not only to understand the mechanisms responsible for disease development but also as biological markers, where plasma stands out as the most advantageous biological sample to look for biomarkers since it is abundant, easy to be collected, and its composition reflects the physiological or pathological state of the body. Because ROS are highly reactive and have a short lifetime, the majority of research performed so far has been focused both in the assessment of the general plasma redox status and in the detection and quantification of the classical and more stable derivatives of oxidative stress and oxidative damage (**Table 2**). To summarize, levels of 4-HNE, MDA, carboxymethyl lysine (CML) derivatives, carbonyl adducts, isoprostanes, and other oxidative stress biomarkers have been found significantly increased in the plasma of patients belonging to the four NYHA classes (from NHYA I to IV), being most prominent in the most severe HF group. Conversely, lower plasma levels of free sulfhydryl groups within proteins are present in HF patients with respect to the healthy group [55–60]. Interestingly, the higher the amount of oxidized proteins or lipids, the worse the severity of HF and the cardiac outcome. However, an important limitation of the mentioned biomarkers is that they are not cardiac- or HF-specific but rather inform about a general oxidative status common to other diseases. Hence, to understand the role of the oxidized biomolecules in HF development and progression and to translate this information into biomedical and biotechnological applications, it is required to apply comprehensive methods in order to provide precise and quantitative information on the specific modified protein and type of

Biomarker		Utility as oxidative stress biomarker of heart failure	Ref.
Free thiol group (-SH)		- positive correlation between plasma free thiols and left ventricular ejection fraction	[58]
		- positive correlation with severity degree of HF	[57]
		- negative correlation between free thiols and disease outcome	[61]
Nitrotyrosine protein derivative		- positive correlation between nitrotyrosine levels and the severity degree of HF	[56]
Carbonyl groups		- carbonylated proteins lose their function	[34,62,63]
		- increased carbonyl levels are most prominent in severe CHF - association between reactive carbonyl plasma levels and the degree of left ventricular remodeling	[57]
AGEs	CML	- CML levels at baseline were associated with a higher mortality rate - predicted hospitalization events	[64]
		- increased levels are associated with severity and prognosis of patients with HF	[65]
	Pentosidine	- contribution to risk stratification of patients (increased levels in patients with cardiac events than in those without cardiac events)	[66]
		- increased pentosidine levels are associated with worse prognosis	[64]
Lipid hydroperoxides		- significantly positive relation between NYHA class and LPO levels	[67]
Aldehyde derivatives		- significantly inverse relationship between total aldehyde concentration and cardiac output	[60]
MDA		- MDA levels negatively correlate with the LVEF - MDA contributes as predictor of death	[57,68]
		- MDA levels are strongly associated with the chronicity of heart failure	[59]
		- significantly positive relation between MDA levels and the severity degree of HF	[59,67]
4-HNE		- increased 4-HNE levels correlate with higher heart rate and impaired left ventricular contractility	[60]
		- decreased levels after therapy with beta-blockers along with amelioration of cardiac function	[69]
Isoprostanes		- association between increased levels and clinical severity of HF - raised levels are positively correlated with the progression of the disease, ventricular remodeling and deterioration of functional cardiac capacity	[55,70]
Oxidized LDL		- levels inversely correlates with survival rate and positively correlates with cardiac event. Prognostic value - contribution in predicting hospitalization events	[71,72]
8-OHdG		- increased levels in HF patients. Therapy with beta-blockers along with amelioration of cardiac function	[73]

Table 2: Summary table of products of oxidative stress and oxidative damage found in plasma or serum samples from heart failure patients, and their utility as potential oxidative biomarkers.

modification. While well validated methods have been implemented for detecting the general status of oxidative stress in clinical samples, the development of protocols aiming to detect and characterize either particular proteins target of oxidation or specific target residues undergoing redox reactions in HF patients is still one step behind. Indeed, the analysis of heterogeneous oxidative post-translational modifications (oxPTMs) is not standard and continues to be very challenging, where further multidisciplinary research is required.

A similar situation occurs with the identification of long-chain lipid peroxidation products. Although several groups have determined that plasma of patients with HF presented significantly higher levels of lipid hydroperoxides with respect to the healthy subjects, which correlated with NYHA class severity [67], their specific characterization is still lacking.

Fully characterization of oxidized biomolecules requires the development of sample handling methods that avoid adventitious atmospheric oxidations, and specially tailored instrument routines, often combined with chemical labelling and enrichment strategies and advanced chromatographic separations, supported by extensive and complex manual data analysis. A powerful method for detecting not only oxPTMs of proteins but also lipid peroxidation and lipoxidation products at molecular level is mass spectrometry (MS) that allows distinguishing between modified and native biomolecules owing to the shifted m/z value [74], though the lack of databases hinder the process.

A reduced number of works have resolved which are the specific proteins and residues undergoing the oxPTMs in HF plasma samples. For instance, Brioschi et al. identified two proteins, alpha-1-antitrypsin and fibrinogen, which underwent carbonylation in a higher extent in the plasma of HF patients than in the plasma of healthy subjects [62]. Also, ATP synthase alpha-subunit Cys294 has been identified as a sensitive target for S-glutathionylation and S-nitrosylation in the left ventricle myocardium of a HF dog model, which trigger a profound conformational change in the protein leading to its inactivation, hence diminishing the essential ATP cardiac supplies [75]; however, heart tissue is not the prototype biological sample for biomarker detection due to tissue collection complexity. Nevertheless, much remains to be done.

On the other hand, plasma is a rich source of biomarkers with clinical relevance since it contains traces of all activities in the body. As such, it is a valuable biological sample. However, the overall protein dynamic range in human plasma is greater than ten orders of magnitude. While the levels of high abundance proteins, such as human serum albumin (HSA) or immunoglobulin G (IgG), range from mg/L to g/L, those of low abundance proteins, such as oxidized or tissue leakage proteins, are usually less than one µg/L [76], meaning that their straightforward identification is not possible. Additionally, levels of oxPMTs may fluctuate according to disease state. Because of these issues, plasma immunodepletion, affinity enrichment or fractionation methods arise as key tools to reduce plasma complexity [76]. Immunodepletion of the high abundance proteins is the most applied strategy to increase the proportion of potential low abundance proteins of clinical

interest. However, depletion of non-specific bound proteins with resin and antibodies, or even of proteins that specifically interact with the removed abundant proteins may also happen. Moreover, the most abundant proteins are more prone to undergo oxidative modifications due, indeed, to the higher concentration in circulation, as in the case of HSA. By contrast, affinity enrichment methods, such as the enrichment strategy based on the affinity of RAGE (receptor for advanced glycation end products) [77], have been generally designed in order to trap the low abundance proteins. Unfortunately, these methods present elevated costs and limited sample capacity [76]. Finally plasma fractionating is another method used to simplify plasma complexity but, in this case, plasma components are separated according to their biophysical properties, such as molecular weight or solubility. However, fractionation has showed a limitation in the standardization of methods and reproducibility of the results.

Hence, for the detection of oxPTMs and lipid peroxidation products in HF plasma samples it is urgently needed the development and evolution of efficient protocols for reducing plasma complexity, aiming to raise the presence of the low abundant oxidized species, together with improved untargeted and semi-targeted bottom-up mass spectrometry-based methods [78].

Considering that the current guidelines for the diagnosis of HF are based mainly on clinical examination, its diagnosis is often confirmed once severe damage to the heart has already happened. Thus, the identification of specific oxidized proteins, lipids, and lipoxidation products in easy-to-collect human samples, such as plasma, may be used as potential biomarkers of HF. Therefore, they could assist the clinicians in the early diagnosis, prognosis, stratification or treatment effectiveness to achieve the best possible outcomes. Moreover, understanding the residues target of oxidative damage within proteins might be of relevance as therapeutic targets for drug candidates.

4. REFERENCES

[1] G. Savarese, L.H. Lund, Global Public Health Burden of Heart Failure, Card. Fail. Rev. (2017). doi:10.15420/cfr.2016:25:2.

[2] G.Y.H. Lip, C.R. Gibbs, D.G. Beevers, ABC of heart failure: Aetiology, BMJ. (2000). doi:10.1136/sbmj.000219.

[3] J.N. Cohn, R. Ferrari, N. Sharpe, Cardiac remodeling—concepts and clinical implications: a consensus paper from an international forum on cardiac remodeling, J. Am. Coll. Cardiol. 35 (2000) 569 LP – 582. doi:10.1016/S0735-1097(99)00630-0.

[4] M.A. Konstam, D.G. Kramer, A.R. Patel, M.S. Maron, J.E. Udelson, Left ventricular remodeling in heart failure: Current concepts in clinical significance and assessment, JACC Cardiovasc. Imaging. (2011). doi:10.1016/j.jcmg.2010.10.008.

[5] L. Schirone, M. Forte, S. Palmerio, D. Yee, C. Nocella, F. Angelini, F. Pagano, S. Schiavon, A. Bordin, A. Carrizzo, C. Vecchione, V. Valenti, I. Chimenti, E. De Falco, S. Sciarretta, G. Frati, A Review of the Molecular Mechanisms Underlying the Development and Progression of Cardiac Remodeling, Oxid. Med. Cell. Longev. (2017). doi:10.1155/2017/3920195.

[6] D. Fan, A. Takawale, J. Lee, Z. Kassiri, Cardiac fibroblasts, fibrosis and extracellular matrix remodeling in heart disease, Fibrogenes. Tissue Repair. (2012). doi:10.1186/1755-1536-5-15.

[7] M. Lainscak, I. Spoletini, A. Coats, Definition and Classification of Heart Failure, Int. Cardiovasc. Forum J. (2017). doi:10.17987/icfj.v10i0.419.

[8] M. Xie, J.S. Burchfield, J.A. Hill, Pathological ventricular remodeling: Therapies: Part 2 of 2, Circulation. (2013). doi:10.1161/CIRCULATIONAHA.113.001879.

[9] M. Seddon, Y.H. Looi, A.M. Shah, Oxidative stress and redox signalling in cardiac hypertrophy and heart failure, Heart. (2007). doi:10.1136/hrt.2005.068270.

[10] T. Münzel, T. Gori, J.F. Keaney, C. Maack, A. Daiber, Pathophysiological role of oxidative stress in systolic and diastolic heart failure and its therapeutic implications, Eur. Heart J. (2015). doi:10.1093/eurheartj/ehv305.

[11] H. Tsutsui, S. Kinugawa, S. Matsushima, Oxidative stress and heart failure, Am. J. Physiol. Circ. Physiol. 301 (2011) H2181-90. doi:10.1152/ajpheart.00554.2011.

[12] P. Ponikowski, A. Voors, 2016 Esc guidelines for the diagnosis and treatment of acute and chronic heart failure: The Task Force for the diagnosis and treatment of acute and chronic heart failure of the European society of cardiology (ESC): Developed with the special contribution , Russ. J. Cardiol. (2017). doi:10.15829/1560-4071-2017-1-7-81.

[13] R.N. Fogoros, Symptoms and Complications of Heart Failure, (2019). https://www.verywellhealth.com/symptoms-and-complications-of-heart-failure-4161320.

[14] P. Pazos-López, J. Peteiro-Vázquez, A. Carcía-Campos, L. García-Bueno, J.P.A. de Torres, A. Castro-Beiras, The causes, consequences, and treatment of left or right heart failure, Vasc. Health Risk Manag. (2011). doi:10.2147/VHRM.S10669.

[15] T.A. Foley, S. V. Mankad, N.S. Anavekar, C.R. Bonnichsen, M.F. Morris, T.D. Miller, P.A. Araoz, Measuring left ventricular ejection fraction-techniques and potential pitfalls, Eur. Cardiol. (2012). doi:10.15420/ecr.2012.8.2.108.

[16] H. Sies, C. Berndt, D. Jones, Oxidative stress, Annu. Rev. Biochem. 86 (2017) 715–748. doi:10.1146/annurev-biochem-061516-045037.

[17] N. Panth, K.R. Paudel, K. Parajuli, Reactive Oxygen Species: A Key Hallmark of Cardiovascular Disease, Adv. Med. (2016). doi:10.1155/2016/9152732.

[18] Y.R. Chen, J.L. Zweier, Cardiac mitochondria and reactive oxygen species generation, Circ. Res. (2014). doi:10.1161/CIRCRESAHA.114.300559.

[19] Å.B. Gustafsson, R.A. Gottlieb, Heart mitochondria: Gates of life and death, Cardiovasc. Res. (2008). doi:10.1093/cvr/cvm005.

[20] J.F. Turrens, Mitochondrial formation of reactive oxygen species, J. Physiol. (2003). doi:10.1113/jphysiol.2003.049478.

[21] E.E. Kelley, N.K.H. Khoo, N.J. Hundley, U.Z. Malik, B.A. Freeman, M.M. Tarpey, Hydrogen

peroxide is the major oxidant product of xanthine oxidase, Free Radic. Biol. Med. (2010). doi:10.1016/j.freeradbiomed.2009.11.012.

[22] T.M. Paravicini, R.M. Touyz, NADPH oxidases, reactive oxygen species, and hypertension: clinical implications and therapeutic possibilities., Diabetes Care. (2008).

[23] K. Sugamura, J.F. Keaney, Reactive oxygen species in cardiovascular disease, Free Radic. Biol. Med. (2011). doi:10.1016/j.freeradbiomed.2011.05.004.

[24] T. Fukai, M. Ushio-Fukai, Superoxide dismutases: Role in redox signaling, vascular function, and diseases, Antioxidants Redox Signal. (2011). doi:10.1089/ars.2011.3999.

[25] J.P. Kehrer, The Haber-Weiss reaction and mechanisms of toxicity, Toxicology. (2000). doi:10.1016/S0300-483X(00)00231-6.

[26] D. Salvemini, T.M. Doyle, S. Cuzzocrea, Superoxide, peroxynitrite and oxidative/nitrative stress in inflammation, Biochem. Soc. Trans. (2006). doi:10.1042/BST0340965.

[27] E. Birben, U.M. Sahiner, C. Sackesen, S. Erzurum, O. Kalayci, Oxidative stress and antioxidant defense, World Allergy Organ. J. (2012). doi:10.1097/WOX.0b013e3182439613.

[28] Y. Hoshino, K. Shioji, H. Nakamura, H. Masutani, J. Yodoi, From oxygen sensing to heart failure: Role of thioredoxin, in: Antioxidants Redox Signal., 2007. doi:10.1089/ars.2007.1575.

[29] B.C. Dickinson, C.J. Chang, Chemistry and biology of reactive oxygen species in signaling or stress responses, Nat. Chem. Biol. (2011). doi:10.1038/nchembio.607.

[30] Z. Cai, L.-J. Yan, Protein Oxidative Modifications: Beneficial Roles in Disease and Health., J. Biochem. Pharmacol. Res. (2013).

[31] B.S. Berlett, E.R. Stadtman, Protein oxidation in aging, disease, and oxidative stress, J. Biol. Chem. (1997). doi:10.1074/jbc.272.33.20313.

[32] M.J. Davies, Protein oxidation and peroxidation, Biochem. J. (2016). doi:10.1042/BJ20151227.

[33] J.P. Silva, O.P. Coutinho, Free radicals in the regulation of damage and cell death - basic mechanisms and prevention, Drug Discov. Ther. (2010).

[34] I. Dalle-Donne, G. Aldini, M. Carini, R. Colombo, R. Rossi, A. Milzani, Protein carbonylation, cellular dysfunction, and disease progression, J. Cell. Mol. Med. (2006). doi:10.1111/j.1582-4934.2006.tb00407.x.

[35] A. Ayala, M.F. Muñoz, S. Argüelles, Lipid peroxidation: Production, metabolism, and signaling mechanisms of malondialdehyde and 4-hydroxy-2-nonenal, Oxid. Med. Cell. Longev. (2014). doi:10.1155/2014/360438.

[36] H. Yin, L. Xu, N.A. Porter, Free radical lipid peroxidation: Mechanisms and analysis, Chem. Rev. (2011). doi:10.1021/cr200084z.

[37] R.M. Domingues, P. Domingues, T. Melo, D. Pérez-Sala, A. Reis, C.M. Spickett, Lipoxidation adducts with peptides and proteins: Deleterious modifications or signaling mechanisms?, J. Proteomics. (2013). doi:10.1016/j.jprot.2013.06.004.

[38] G. Aldini, M.R. Domingues, C.M. Spickett, P. Domingues, A. Altomare, F.J. Sánchez-Gómez, C.L. Oeste, D. Pérez-Sala, Protein lipoxidation: Detection strategies and challenges, Redox Biol. (2015). doi:10.1016/j.redox.2015.05.003.

[39] M.S. Cooke, M.D. Evans, M. Dizdaroglu, J. Lunec, Oxidative DNA damage: Mechanisms,

mutation, and disease, FASEB J. (2003). doi:10.1096/fj.02-0752rev.

[40] C.M. Sag, C.X.C. Santos, A.M. Shah, Redox regulation of cardiac hypertrophy, J. Mol. Cell. Cardiol. (2014). doi:10.1016/j.yjmcc.2014.02.002.

[41] A.C. Köhler, C.M. Sag, L.S. Maier, Reactive oxygen species and excitation-contraction coupling in the context of cardiac pathology, J. Mol. Cell. Cardiol. (2014). doi:10.1016/j.yjmcc.2014.03.001.

[42] A. Guggilam, M. Haque, E.K. Kerut, E. McIlwain, P. Lucchesi, I. Seghal, J. Francis, TNF-α blockade decreases oxidative stress in the paraventricular nucleus and attenuates sympathoexcitation in heart failure rats, Am. J. Physiol. - Hear. Circ. Physiol. (2007). doi:10.1152/ajpheart.00286.2007.

[43] E. Borchi, V. Bargelli, F. Stillitano, C. Giordano, M. Sebastiani, P.A. Nassi, G. d'Amati, E. Cerbai, C. Nediani, Enhanced ROS production by NADPH oxidase is correlated to changes in antioxidant enzyme activity in human heart failure, Biochim. Biophys. Acta - Mol. Basis Dis. (2010). doi:10.1016/j.bbadis.2009.10.014.

[44] W.H.W. Tang, W. Tong, R.W. Troughton, M.G. Martin, K. Shrestha, A. Borowski, S. Jasper, S.L. Hazen, A.L. Klein, Prognostic Value and Echocardiographic Determinants of Plasma Myeloperoxidase Levels in Chronic Heart Failure, J. Am. Coll. Cardiol. (2007). doi:10.1016/j.jacc.2007.02.053.

[45] C. Heymes, J.K. Bendall, P. Ratajczak, A.C. Cave, J.L. Samuel, G. Hasenfuss, A.M. Shah, Increased myocardial NADPH oxidase activity in human heart failure, J. Am. Coll. Cardiol. (2003). doi:10.1016/S0735-1097(03)00471-6.

[46] U. Landmesser, S. Spiekermann, S. Dikalov, H. Tatge, R. Wilke, C. Kohler, D.G. Harrison, B. Hornig, H. Drexler, Vascular oxidative stress and endothelial dysfunction in patients with chronic heart failure: Role of xanthine-oxidase and extracellular superoxide dismutase, Circulation. (2002). doi:10.1161/01.CIR.0000041431.57222.AF.

[47] H. Shinichi, O. Kinya, N. Kazuhiko, H. Yoshiharu, M. Takashi, N. Hiroyuki, Y. Osamu, M. Toshiaki, M. Yasushi, U. Hikaru, T. Michihiko, H. Masatsugu, Involvement of Nuclear Factor-κB and Apoptosis Signal-Regulating Kinase 1 in G-Protein–Coupled Receptor Agonist–Induced Cardiomyocyte Hypertrophy, Circulation. 105 (2002) 509–515. doi:10.1161/hc0402.102863.

[48] D. Moris, M. Spartalis, E. Tzatzaki, E. Spartalis, G.-S. Karachaliou, A.S. Triantafyllis, G.I. Karaolanis, D.I. Tsilimigras, S. Theocharis, The role of reactive oxygen species in myocardial redox signaling and regulation, Ann. Transl. Med. (2017). doi:10.21037/atm.2017.06.17.

[49] J.R. Burgoyne, H. Mongue-Din, P. Eaton, A.M. Shah, Redox signaling in cardiac physiology and pathology, Circ. Res. (2012). doi:10.1161/CIRCRESAHA.111.255216.

[50] M. Canton, S. Menazza, F.L. Sheeran, P. Polverino De Laureto, F. Di Lisa, S. Pepe, Oxidation of myofibrillar proteins in human heart failure, J. Am. Coll. Cardiol. (2011). doi:10.1016/j.jacc.2010.06.058.

[51] M. Kara, E. Özçağlı, A.T. Jannuzzi, B. Alpertunga, Oxidative stress mediated cardiac apoptosis, J. Fac. Pharm. Istanbul. 45 (2015) 217–232.

[52] K. Nomura, H. Imai, T. Koumura, T. Kobayashi, Y. Nakagawa, Mitochondrial phospholipid hydroperoxide glutathione peroxidase inhibits the release of cytochrome c from mitochondria by

suppressing the peroxidation of cardiolipin in hypoglycaemia-induced apoptosis, Biochem. J. (2000). doi:10.1042/0264-6021:3510183.

[53] S. Koch, C.M. Volkmar, V. Kolb-Bachofen, H.G. Korth, M. Kirsch, A.H.C. Horn, H. Sticht, N. Pallua, C. V. Suschek, A new redox-dependent mechanism of MMP-1 activity control comprising reduced low-molecular-weight thiols and oxidizing radicals, J. Mol. Med. (2009). doi:10.1007/s00109-008-0420-5.

[54] D. Reinhardt, H.H. Sigusch, J. Henße, S.C. Tyagi, R. Körfer, H.R. Figulla, Cardiac remodelling in end stage heart failure: Upregulation of matrix metalloproteinase (MMP) irrespective of the underlying disease, and evidence for a direct inhibitory effect of ACE inhibitors on MMP, Heart. (2002).

[55] M. Cristina Polidori, D. Praticó, K. Savino, J. Rokach, W. Stahl, P. Mecocci, Increased F2 isoprostane plasma levels in patients with congestive heart failure are correlated with antioxidant status and disease severity, J. Card. Fail. (2004). doi:10.1016/j.cardfail.2003.11.004.

[56] E. Eleuteri, A. Di Stefano, F.L.M. Ricciardolo, F. Magno, I. Gnemmi, M. Colombo, R. Anzalone, F. Cappello, G. La Rocca, F.T. Genta, G. Zummo, P. Giannuzzi, Increased nitrotyrosine plasma levels in relation to systemic markers of inflammation and myeloperoxidase in chronic heart failure, Int. J. Cardiol. 135 (2009) 386–390. doi:10.1016/j.ijcard.2008.11.013.

[57] S. Radovanovic, A. Savic-Radojevic, M. Pljesa-Ercegovac, T. Djukic, S. Suvakov, M. Krotin, D. V Simic, M. Matic, Z. Radojicic, T. Pekmezovic, T. Simic, Markers of Oxidative Damage and Antioxidant Enzyme Activities as Predictors of Morbidity and Mortality in Patients With Chronic Heart Failure, J. Card. Fail. 18 (2012) 493–501. doi:10.1016/j.cardfail.2012.04.003.

[58] J.J. Belch, A.B. Bridges, N. Scott, M. Chopra, Oxygen free radicals and congestive heart failure, Br. Heart J. 65 (1991) 245–248. doi:10.1136/hrt.65.5.245.

[59] C.R. Díaz-Vélez, S. García-Castiñeiras, E. Mendoza-Ramos, E. Hernández-López, Increased malondialdehyde in peripheral blood of patients with congestive heart failure, Am. Heart J. (1996). doi:10.1016/S0002-8703(96)90063-0.

[60] S. Mak, D.C. Lehotay, M. Yazdanpanah, E.R. Azevedo, P.P. Liu, G.E. Newton, Unsaturated aldehydes including 4-OH-nonenal are elevated in patients with congestive heart failure, J. Card. Fail. (2000). doi:10.1054/jcaf.2000.7272.

[61] A.M. Koning, W.C. Meijers, A. Pasch, H.G.D. Leuvenink, A.R.S. Frenay, M.M. Dekker, M. Feelisch, R.A. de Boer, H. van Goor, Serum free thiols in chronic heart failure, Pharmacol. Res. (2016). doi:10.1016/j.phrs.2016.06.027.

[62] C. Banfi, M. Brioschi, S. Barcella, F. Veglia, P. Biglioli, E. Tremoli, P.G. Agostoni, Oxidized proteins in plasma of patients with heart failure: Role in endothelial damage, Eur. J. Heart Fail. (2008). doi:10.1016/j.ejheart.2008.01.016.

[63] M. Brioschi, G. Polvani, P. Fratto, A. Parolari, P. Agostoni, E. Tremoli, C. Banfi, Redox proteomics identification of oxidatively modified myocardial proteins in human heart failure: Implications for protein function, PLoS One. (2012). doi:10.1371/journal.pone.0035841.

[64] S. Willemsen, J.W.L. Hartog, D.J. Van Veldhuisen, P. Van Der Meer, J.F. Roze, T. Jaarsma, C. Schalkwijk, I.C.C. Van Der Horst, H.L. Hillege, A.A. Voors, The role of advanced glycation end-

products and their receptor on outcome in heart failure patients with preserved and reduced ejection fraction, Am. Heart J. (2012). doi:10.1016/j.ahj.2012.07.027.

[65] J.W.L. Hartog, A.A. Voors, C.G. Schalkwijk, J. Scheijen, T.D.J. Smilde, K. Damman, S.J.L. Bakker, A.J. Smit, D.J. Van Veldhuisen, Clinical and prognostic value of advanced glycation end-products in chronic heart failure, Eur. Heart J. (2007). doi:10.1093/eurheartj/ehm486.

[66] Y. Koyama, Y. Takeishi, T. Arimoto, T. Niizeki, T. Shishido, H. Takahashi, N. Nozaki, O. Hirono, Y. Tsunoda, J. Nitobe, T. Watanabe, I. Kubota, High Serum Level of Pentosidine, an Advanced Glycation End Product (AGE), is a Risk Factor of Patients with Heart Failure, J. Card. Fail. (2007). doi:10.1016/j.cardfail.2006.11.009.

[67] M. Keith, A. Geranmayegan, M.J. Sole, R. Kurian, A. Robinson, A.S. Omran, K.N. Jeejeebhoy, Increased oxidative stress in patients with congestive heart failure, J. Am. Coll. Cardiol. (1998). doi:10.1016/S0735-1097(98)00101-6.

[68] S. Suzuki, Y. Kodera, T. Saito, K. Fujimoto, A. Momozono, A. Hayashi, Y. Kamata, M. Shichiri, Methionine sulfoxides in serum proteins as potential clinical biomarkers of oxidative stress, Sci. Rep. (2016). doi:10.1038/srep38299.

[69] K. Nakamura, K. Kusano, Y. Nakamura, M. Kakishita, K. Ohta, S. Nagase, M. Yamamoto, K. Miyaji, H. Saito, H. Morita, T. Emori, H. Matsubara, S. Toyokuni, T. Ohe, Carvedilol decreases elevated oxidative stress in human failing myocardium, Circulation. (2002). doi:10.1161/01.CIR.0000018605.14470.DD.

[70] R. Wolfram, A. Oguogho, B. Palumbo, H. Sinzinger, Enhanced oxidative stress in coronary heart disease and chronic heart failure as indicated by an increased 8-epi-PGF2α, Eur. J. Heart Fail. (2005). doi:10.1016/j.ejheart.2004.05.007.

[71] T. Tsutsui, T. Tsutamoto, A. Wada, K. Maeda, N. Mabuchi, M. Hayashi, M. Ohnishi, M. Kinoshita, Plasma oxidized low-density lipoprotein as a prognostic predictor in patients with chronic congestive heart failure, J. Am. Coll. Cardiol. (2002). doi:10.1016/S0735-1097(02)01721-7.

[72] G. Charach, J. George, A. Afek, D. Wexler, D. Sheps, G. Keren, A. Rubinstein, Antibodies to Oxidized LDL as Predictors of Morbidity and Mortality in Patients With Chronic Heart Failure, J. Card. Fail. (2009). doi:10.1016/j.cardfail.2009.05.009.

[73] Y. Kono, K. Nakamura, H. Kimura, N. Nishii, A. Watanabe, K. Banba, A. Miura, S. Nagase, S. Sakuragi, K.F. Kusano, H. Matsubara, T. Ohe, Elevated levels of oxidative DNA damage in serum and myocardium of patients with heart failure, Circ. J. (2006). doi:10.1253/circj.70.1001.

[74] I. Verrastro, S. Pasha, K.T. Jensen, A.R. Pitt, C.M. Spickett, Mass spectrometry-based methods for identifying oxidized proteins in disease: Advances and challenges, Biomolecules. (2015). doi:10.3390/biom5020378.

[75] S.B. Wang, D.B. Foster, J. Rucker, B. O'Rourke, D.A. Kass, J.E. Van Eyk, Redox regulation of mitochondrial ATP synthase: Implications for cardiac resynchronization therapy, Circ. Res. (2011). doi:10.1161/CIRCRESAHA.111.246124.

[76] S. Chutipongtanate, S. Chatchen, J. Svasti, Plasma prefractionation methods for proteomic analysis and perspectives in clinical applications, Proteomics - Clin. Appl. (2017). doi:10.1002/prca.201600135.

[77] G. Degani, A.A. Altomare, M. Colzani, C. Martino, A. Mazzolari, G. Fritz, G. Vistoli, L. Popolo, G. Aldini, A capture method based on the VC1 domain reveals new binding properties of the human receptor for advanced glycation end products (RAGE), Redox Biol. (2017). doi:10.1016/j.redox.2016.12.017.

[78] R. Baetta, M. Pontremoli, A. Martinez Fernandez, C.M. Spickett, C. Banfi, Proteomics in cardiovascular diseases: Unveiling sex and gender differences in the era of precision medicine, J. Proteomics. 173 (2018). doi:10.1016/j.jprot.2017.11.012.

Aim of the project

AIM OF THE PROJECT

Products of oxidative damage, such as lipoxidation or lipid peroxidation, contribute to the onset of a number of inflammatory diseases, including HF, and may be used as biomarkers providing information of pathophysiological and therapeutic interest in the management, treatment, and risk assessment of the patients. Although classic biomarkers of oxidative stress have been identified in plasma of patients suffering from HF, they are not specific of this pathology but report about a general oxidative stress status common to other cardiovascular diseases. Consequently, it is necessary to unveil a more comprehensive oxidative proteomic and lipidomic plasma profile associated to HF for a better understanding of the pathology, which could in turn be helpful either for the clinicians to detect earlier the disease or for drug therapy design.

Thus, the first objective of this project was to identify oxidative post-translational modifications of a wide range of plasma proteins by means of mass spectrometry analysis. Since human serum albumin is the most abundant protein in blood and therefore highly prone to suffer oxidative damage, we aimed to detect, relatively quantify, and fully characterize the most relevant albumin isoforms, as well as to correlate their plasma levels with the severity of the pathology. Likewise, we pursued to characterize medium and low abundant lipoxidation products in circulation, specifically, AGEs and ALEs. However, their analysis is not standard and continues to be very challenging, being essential to apply prefractionation strategies which enhance their concentration and, ultimately, their detection. To circumvent this problem, we took advantage of the VC1 pull-down technique that has been proven to be a promising technique for the enrichment of AGEs/ALEs *in vitro*.

Owing to the relevance of HSA in the circulatory system and aiming to establish a causal role in the etiopathogenesis of HF, our second goal was to investigate the biological significance, in terms of pro-oxidant and pro-inflammatory effects, of the identified oxidized HSA isoforms on cardiac cells, since both biological effects have been widely related with the onset and development of HF

The third objective of this thesis has been focused on the study of the plasma lipidomic profile as a powerful tool to explore novel biomarkers and mechanisms in heart failure, taking advantage of label-free targeted and un-targeted lipidomic approaches provided by partners of MASSTRPLAN (MASS Spectrometry Training network for Protein Lipid adduct Analysis, proposal number 675132). Since gender is a major and often underestimated factor that should be carefully considered when screening lipidomes of pathological processes, we aimed to study for the first time disparities in circulating plasma phospholipids between healthy subjects and HF patients, and between age- and sex-matched male and female HF patients. On the other hand, we also

sought to provide insights about the structure and abundance of long- and short-chain products of lipid peroxidation in plasma of patients suffering from HF, since the majority of the research performed so far has focused mainly in small fragmentation lipid peroxidation products.

Finally, in order to reach the mentioned objectives and considering the benefits provided by plasma as an important source for disease biomarker study, during this project we pursued to establish a plasma biobank of HF patients recruited at Centro Cardiologico Monzino. These patients have been well characterized in terms of cardiac and lung function and classified according to the NYHA.

CHAPTER I:

Analysis of cysteinylated and glycated albumin in plasma of heart failure patients

ANALYSIS OF CYSTEINYLATED AND GLYCATED ALBUMIN IN PLASMA OF HEART FAILURE PATIENTS

1. INTRODUCTION

Human serum albumin (HSA) is the most abundant protein in the circulatory system, constituting up to 60% of total plasma proteins. It exerts immunomodulatory, anti-oxidant, and anti-inflammatory effects, it is well known for binding a large variety of molecules, including fatty acids, drugs, hormones, and metal ions, and contributes to the maintenance of the normal capillary permeability and endothelial stabilization [1]. Owing to its long half-life and high concentration in the circulatory system compared to other proteins, HSA is highly sensitive to undergo oxidative post-translational modifications (oxPTMs), for example cysteinylation or glycation, that easily occur upon oxidative stress.

HSA contains 35 cysteine (cys) residues, of which 34 are involved in the formation of 17 disulfide bonds, where the cys in position 34 (cys34) stands as the only free cysteine in the protein [2], representing the most common cysteine that undergoes cysteinylation. Cysteinylated human serum albumin (cys-HSA) is a post-translational modification of HSA where the free sulfhydryl group (SH) of cysteine becomes oxidized by a different cysteine, a reaction promoted in oxidizing environments [3]. This cysteine residue is more prone to be oxidized by ROS because of the high nucleophilic moiety conferred by the thiol group which, when deprotonated, known as thiolate anion, presents an enhanced reactivity with respect to other residues [4]. This fact, together with its low redox potential in proteins, makes the thiol side chain particularly sensitive to be easily oxidized [5], playing a significant role in the damage to numerous proteins, such as HSA, hampering their biological and structural function [6,7]. Upon oxidation, the free thiol levels become consequently shrunk turning into a useful tool as biomarkers of oxidative damage.

Conversely, free amino groups of proteins might suffer non-enzymatic glycation, also referred to as the Maillard reaction [8]. The reaction that involves the condensation reaction of the carbonyl group of sugar aldehydes, such as glucose, with the N-terminus or free-amino groups of lysine or arginine residues via a nucleophilic attack of the nitrogen atom at the carbonyl group of a reducing sugar. The first step of the Maillard reaction results in the rapid reversible formation of a hemiaminal which spontaneously dehydrates to give an unstable Schiff base products. Over weeks, these intermediate labile Schiff base adducts then undergo Amadori rearrangement giving rise to the relatively more stable Amadori-products, such as deoxy-fructosyl derivatives (e.g. glycated albumin, (GA)), also called early glycation products [9]. Non-enzymatic glycation of HSA is indeed one of the underlying modifications that can modify its native secondary and tertiary structure [8]. However, the effect of glycation appears to vary between different binding regions on HSA since the properties of nearby amino acids in either the primary or the three

dimensional structure play a role in determining whether a given residue has the propensity to be glycated [10].

Several works aimed to elucidate the most common early glycated residues of HSA not only *in vitro* [11–13] but also *in vivo*. The majority of the *in vivo* studies have been primarily focused on diabetes and diabetes-related complications owing to the typical elevated glucose levels in the blood of patients suffering from these pathologies, although *in vivo* glycation tends to occur to a relatively limited extent. Hence, significant effort has been made in order to identify and relatively quantify the lysine and arginine residues within HSA target of glycation in plasma of patients [10,14,15]. Nevertheless, GA does not exclusively happen in hyperglycemia conditions but even at normal glucose levels some degree of glycation may happen, including in HF.
The location of the specific glycated residues present in HSA will allow to broaden the knowledge of HSA in the pathology of HF and would help to better understand its effects. Additionally, it might be of interest for the development of new drugs designed to reduce the levels of glycated HSA.

In this work, we seek to evaluate the plasma levels of cysteinylated and glycated HSA in HF patients by means of quantitative mass spectrometry analysis. Additionally, we pursue to uncover the specific early glycated pattern within isolated HSA from plasma of HF patients.

2. MATERIAL AND METHODS

2.1. Study population

Plasma samples collected at Centro Cardiologico Monzino were selected from a subset of healthy subjects (controls) and HF patients, according to their age, sex, and clinical characteristics. A detailed summary of the clinical characteristics is reported in **Table 1**. The study was approved by the Ethical Committee European Institute of Oncology and Monzino Cardiologic Center (registration number R205-CCFM S208/412). All patients belong to a cohort of HF patients regularly followed at our HF Unit and underwent our standard HF assessment which included full clinical evaluation, standard laboratory tests, echocardiography, spirometry, and alveolar capillary diffusion, as well as cardiopulmonary exercise test. All patients had severe HF, being in New York Heart Association (NYHA) class III and IV, but were in stable clinical conditions. Patients with an established diagnosis of diabetes mellitus or under diabetes treatment were excluded [1].

	Healthy subjects	HF patients NYHA III	HF patients NYHA IV
n	11	7	7
Age	56.27±4.69	67±12.14	67.43±6.24
Gender (m/f)	7/4	5/2	6/1
Hypertension	0/11	5/7	5/7
Dyslipidemia	0/11	4/7	4/7
Smoke	1/11	1/7	3/7
BMI	25.66±3.24	26.68±3.38	27.11±4.81
Glycemia (mg/dL)	102.4±12.76	105±12.39	120.2±12.01
EF (%)	-	39.9±6.57	26.86±11.31
BNP (pg/mL)	-	265.14±310.15	967.8±668.6
DLCO (%predicted)	94.21±21.06	72.09±17.43	65.87±12.21
VO_2 peak/Kg (mL/min/Kg)	34.58±8.46	15.39±8.95	11.05±2.09

Table 1. Clinical characteristics of subjects categorized in healthy subjects, HF patients (NYHA class III), and HF patients (NYHA class IV). Data are expressed as mean ± SD. BMI, body mass index; EF, ejection fraction; BNP, Brain natriuretic peptide; DLCO, carbon monoxide lung diffusion; VO_2, oxygen consumption; m, male; f, female.

2.2. Quantitation of cysteinylated and glycated HSA by intact protein mass spectrometry

The relative composition of albumin isoforms in human plasma samples was evaluated by intact protein analysis using the Xevo TQS micro triple quadrupole mass spectrometer coupled with the M-Class UPLC system (Waters Corporation, Milford, USA) [1]. Briefly, centrifuged plasma samples at 3000 x g for 10 min at 4°C were diluted 200 folds in 50% ACN containing 0.1% FA. After centrifugation at 14000 x g for 10 min at 4°C, 5 µl were injected at 5 µl/min and the spectra were acquired for 6 minutes with the following parameters: positive ESI mode; mass range 1100-1350 m/z; capillary voltage, 3kV; cone, 90V; desolvation temperature 350°C; source temperature 150°C. Data processing for deconvolution was performed with the MaxEnt1 function on the MassLynx software (Waters Corporation, Milford, USA). Mercaptoalbumin (native HSA), cys-HSA (119 ± 2 Da), GA (+160 ± 2 Da), and an albumin isoform characterized by a mass increase of 44 ± 2 Da were detected. Their intensities were used to calculate the relative abundances as described hereafter:

$$\% \text{ cys-HSA} = (\text{cys-HSA intensity} \div \text{Total HSA intensity}) \times 100$$

$$\% \text{ GA} = (\text{GA intensity} \div \text{Total HSA intensity}) \times 100$$

$$\% \Delta 44 \pm 2 = (\Delta 44 \pm 2 \text{ intensity} \div \text{Total HSA intensity}) \times 100$$

Total HSA intensity = (cys-HSA intensity + GA intensity + Δ44±2 intensity + native HSA intensity)

2.3. In-solution digestion of plasma HSA from HF patients

HSA was removed from pooled plasma from HF patients class IV (Pierce Albumin depletion kit (Thermo Fisher Scientific, Milan, Italy)). HSA concentration was determined by means of Bradford's method. 10 µg of protein were reduced with 10 mmol/L DTT at 56 °C for 30 min, and carbamidomethylated with 55 mmol/L iodoacetamide for 20 min at room temperature in the darkness. In-solution digestion was performed by incubating 0.5 µg trypsin (Roche, Monza, Italy) overnight at 37 °C. 2 µg of tryptic peptides from each sample were purified by use of ZipTip C18 pipette tip (Merck Millipore, Milan, Italy). The purified peptides were eluted with 0.1% formic acid (FA) in water/acetonitrile 2/8 (vol/vol). Afterwards, the eluted tryptic peptides were dried and stored at -20 °C until further analysis.

2.4. Mass spectrometry analysis of digested HSA from HF patients

Tryptic peptides were analyzed at UNITECH OMICs (University of Milano, Italy) using a Dionex Ultimate 3000 nano-LC system (Sunnyvale CA, USA) connected to an Orbitrap Fusion™ Tribrid™ Mass Spectrometer (Thermo Scientific, Bremen, Germany) equipped with a nano-electrospray ion source. Peptide mixtures were pre-concentrated onto an Acclaim PepMap 100 - 100µm x 2cm C18 and separated on EASY-Spray column, 15 cm x 75 µm ID packed with Thermo Scientific Acclaim PepMap RSLC C18, 3 µm, 100 Å. The temperature was set to 35 °C and the flow rate was 300 nL/min. Mobile phases were the following: 0.1% formic acid (FA) in water (solvent A); 0.1% FA in water/acetonitrile (solvent B) with 2/8 ratio. Peptides were eluted from the column with the following gradient: 4% to 28% of B for 90 min and then 28% to 40% of B in 10 min, and to 95% within the following 6 min to rinse the column. Column was re-equilibrated for 20 min. Total run time was 130 min. One blank was run between replicates to prevent sample carryover. MS spectra were collected over an m/z range of 375-1500 Da at 120,000 resolutions, operating in the data dependent acquisition mode (DDA), cycle time 3 sec between master scans. HCD was performed with collision energy set at 35 eV. Each sample was analyzed in two technical replicates.

2.5. Identification and localization of protein adducts

The software Proteome Discoverer (version 1.3.0.339, Thermo Scientific, USA), implemented with the algorithm SEQUEST, was used to compare the experimental full and tandem mass

spectra with the theoretical ones obtained by the *in silico* digestion of the HSA sequence (Uniprot P02768). Trypsin was selected as the cleaving protease, allowing a maximum of 2 missed cleavages. Peptide and fragment ion tolerances were set to 5 ppm and 10 mmu, respectively. Cysteine carbamidomethylation was set as fix modification (+57.02147); methionine oxidation was allowed as a variable modification in addition to the known early glycation-derived modification as listed in Table below.

Glycation-derived PTMs	Δm shift (Da)	Residue
Deoxy-fructosyl-derivative	+162.05282	Lys, Arg

Table 2. Glycation-derived PTMs and their corresponding mass shift.

As a quality filter, only peptides with an Xcore value greater than 2.2 were considered as genuine peptide identifications. To ensure the lowest number of false positives, the mass values experimentally recorded were further processed through a combined search with the Database Decoy, where the protein sequences are inverted and randomized. This operation allows the calculation of the false discovery rate (FDR) for each match, so that all the proteins out of range of FDR between to 0.01 (strict) and 0.05 (relaxed) were rejected.
For the localization of glycation-derived modifications, the MS/MS spectra of modified peptides were manually inspected; for the confident mapping of the modification sites, spectra were requested to match the expected ions (b and/or y) neighboring the modified amino acid residue both at the N- and C-termini.

2.6. Semi-quantitative analysis of PTMs in plasma HSA from HF patients

The relative extent of each protein modification has been calculated by determining the amount of the modified peptide in respect of the native one, by assuming that the ionization efficiency of the native and the modified peptides are equal. In particular, the single ion traces (SIC) of the native and modified peptides were firstly reconstituted by setting as filter ion the m/z values of the corresponding precursor protonated peptides. The peak areas were then automatically calculated by the Qual Browser tool of the Xcalibur data system (version 2.0.7, Thermo Scientific Inc., Milan, Italy) and then the relative abundance calculated by using the following equation:

$$Relative\ Abundance\ \% = \frac{Modified\ Peptide\ Peak\ Area}{(Modified\ Peptide\ Peak\ Area + Nativ\ \ Peptide\ Peak\ Area)} * 100$$

2.7. Statistical analysis

Clinical data from controls and HF patients were analyzed using SAS v9.4 (SAS Institute, Cary, NC, USA) and are expressed as mean ± standard deviation (SD), subdividing HF patients according to NYHA class (III vs. IV). Univariate analysis was performed by ANOVA to identify statistically different variables among groups while Pearson correlation was used to identify a possible correlation between the levels of the different albumin isoforms that significantly increased in HF patients with respect to the healthy subjects and the peak VO_2/Kg values.

3. RESULTS

In this study we examined the extent of cys-HSA and GA in plasma of HF patients subdivided according to disease severity as inferable from the NYHA class (III vs. IV) compared with healthy subjects, by using a direct infusion ESI-MS approach. After the identification of the albumin isoforms by the mass increase of 119 ± 2 Da for cys-HSA and 162 ± 2 Da for GA with respect to the native HSA (**Figure 1A)**, their relative quantification was calculated. Results showed an increase of cys-HSA in the patients versus the age-matched healthy subjects (14.79 ± 5.22% and 17.81 ± 3.17% for class III and IV and 9.87 ± 3.07% for healthy subjects) (**Figure 1B**). This increase was statistically significant for HF class IV. The same behavior was observed when comparing the relative abundance of GA between healthy subjects and HF patients without diabetes (6.53 ± 0.54% for healthy subjects, 7.38 ± 1.47% for HF class III, and 8.13 ± 0.77% for HF class IV), as represented in **Figure 1C**. The statistical analysis demonstrated that the percentage of GA was significantly higher in the group HF class IV [1]. Of note, we detected an inverse correlation between the levels of either cys-HSA or GA and the peak VO_2/Kg value (**Figure 1F and 1G, respectively**), a known index of oxygen uptake previously associated with HF severity [16]. We also observed an unknown albumin isoform characterized by a mass shift of 44 ± 2 Da (**Figure 1A**), however its relative abundance remained unchanged among the three groups of subjects (**Figure 1D**). Interestingly, total levels of HSA tended to decrease while increasing the disease severity, although not statistically significant ((2.37 ± 0.74)x10^{10} and (1.72 ± 1.13)x10^{10} for class III and IV, and (1.44 ± 5.72)x10^{10} for healthy subjects) (**Figure 1E**). Considering this results, a deeper characterization of GA associated to HF was addressed in this work. While S-cysteinylation of HSA tends to happen in cys34, HSA-glycation might happen in a large set of lysine or arginine amino acids within the protein. Thus, our next goal was to identify the early glycation pattern of HSA from pooled HF class IV plasma samples. To this purpose, we firstly isolated HSA from the rest of plasma components, we digested in-solution the protein and then we proceed to characterize the glycation sites within the peptides by means of mass spectrometry.

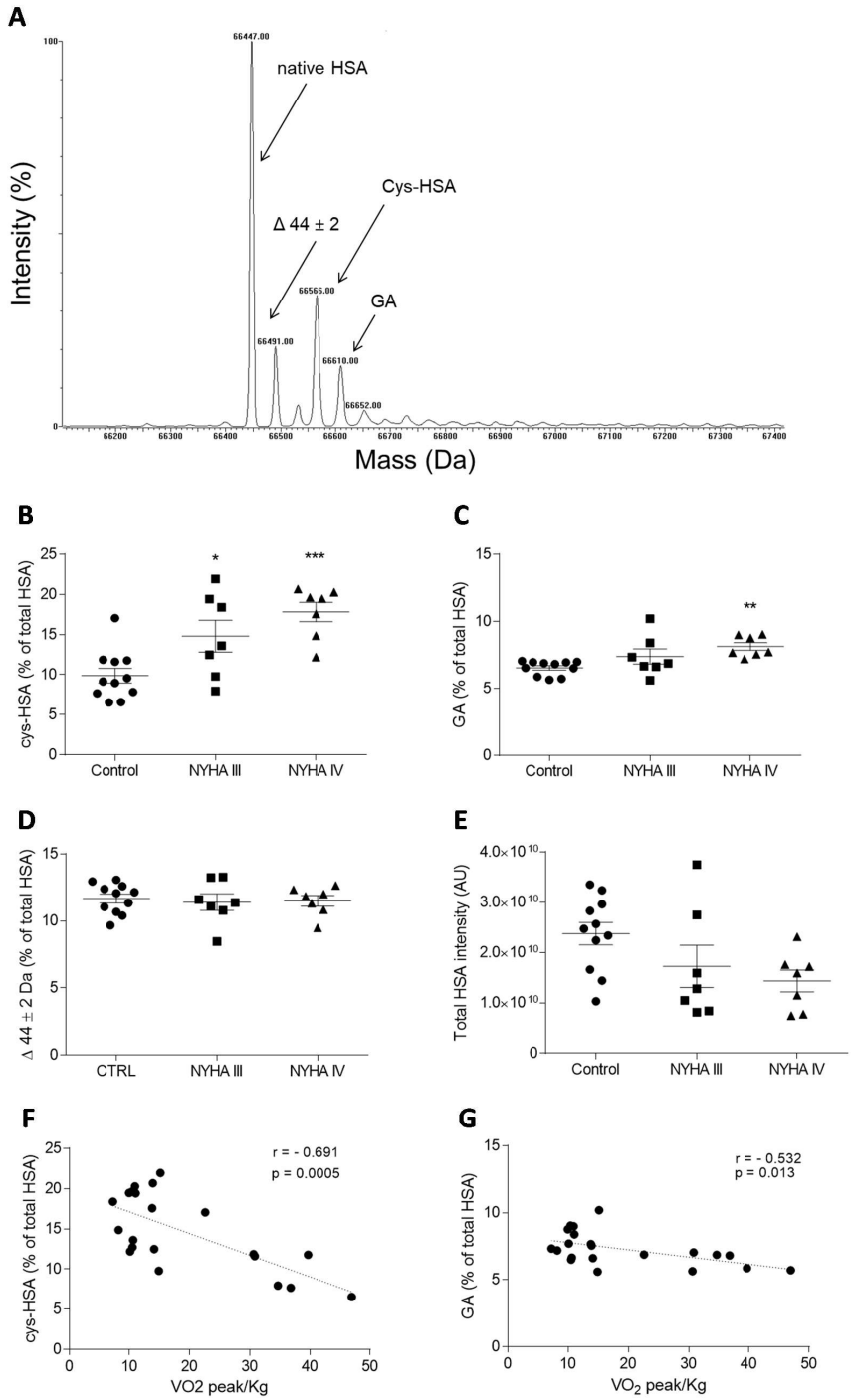

Figure 1. HSA isoforms in plasma of heart failure patients. A) Representative deconvoluted ESI-MS spectrum of albumin from plasma of a HF patient. Arrows indicate the mercaptoalbumin (native HSA),

cys-HSA, GA, and an unknown isoform characterized by a mass shift of 119 ± 2, 162 ± 2, and 44 ± 2 Da with respect to the native HSA, respectively. ESI-MS spectra were acquired in positive ion mode with a scan range of m/z 1100-1350. The relative content (%) of B) cys-HSA, C) GA, and D) the 44 ± 2 isoform with respect to the total amount of albumin has been analyzed by mass spectrometry in healthy subjects (controls) and HF patients divided in NYHA class III and class IV. The intensity of each HSA isoform was used to calculate the relative abundances with respect to the total HSA intensity. E) Total HSA has been calculated by adding the intensities of the native HSA, the GA, the cys-HSA, and the unknown isoform from each group. F) Correlation between the percentage of cys-HSA and peak VO2/Kg. G) Correlation between the percentage of GA and peak VO2/Kg. Values are represented as mean ± SEM and all statistical analyses were performed using GraphPad Prism 6. ***$p < 0.001$ vs. controls, **$p < 0.01$ vs. controls, * $p<0.05$ vs. controls. HSA, human serum albumin; NYHA, New York heart association.

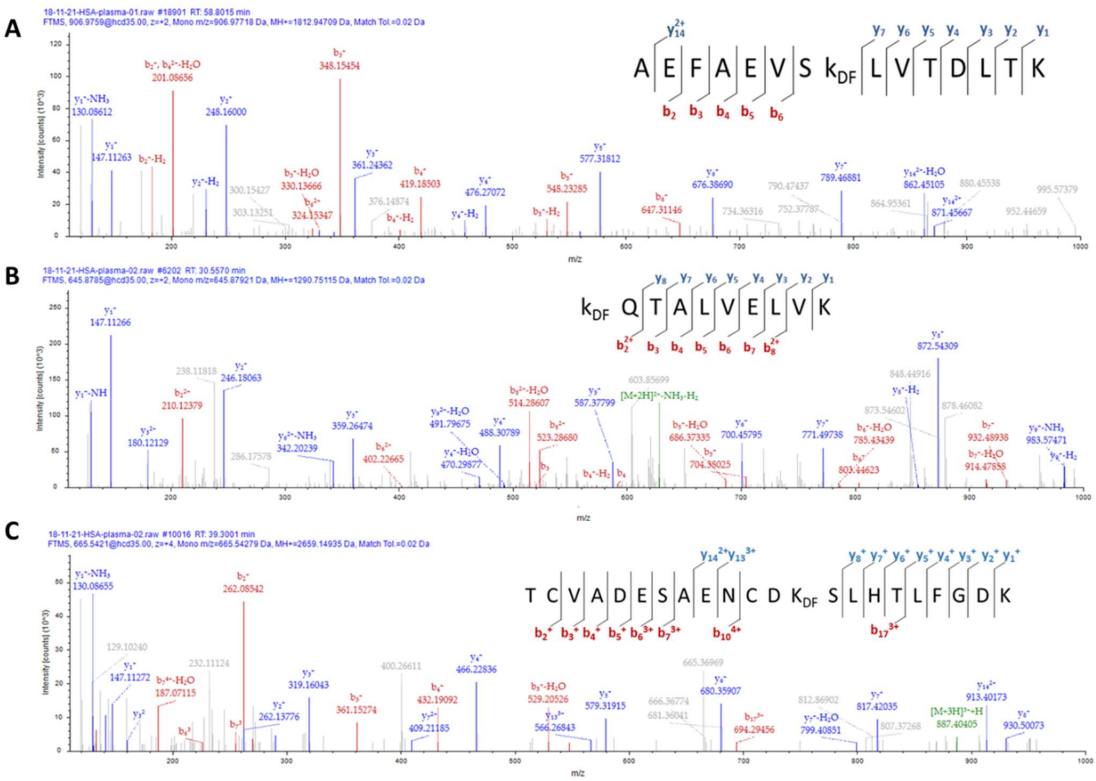

Figure 2. Fragmentation mass spectra (MS/MS) of the three most abundant glycated peptides present in the plasma of HF patients and the relevant fragments for their attribution. A) Spectrum corresponding to the peptide AEFAEVSkLVTDLTK (glycated residue lys233). B) kQTALVELVK (modified residue lys525), and C) TcVADESAENcDkSLHTLFGDK (modified residue lys64). The calculated fragment ions b^+, b^{2+}, b^{3+}, y^+, y^{2+} and y^{3+} of the adducted peptides are highlighted by red (b series) and blue (y series) colors. DF, deoxy-fructosyl.

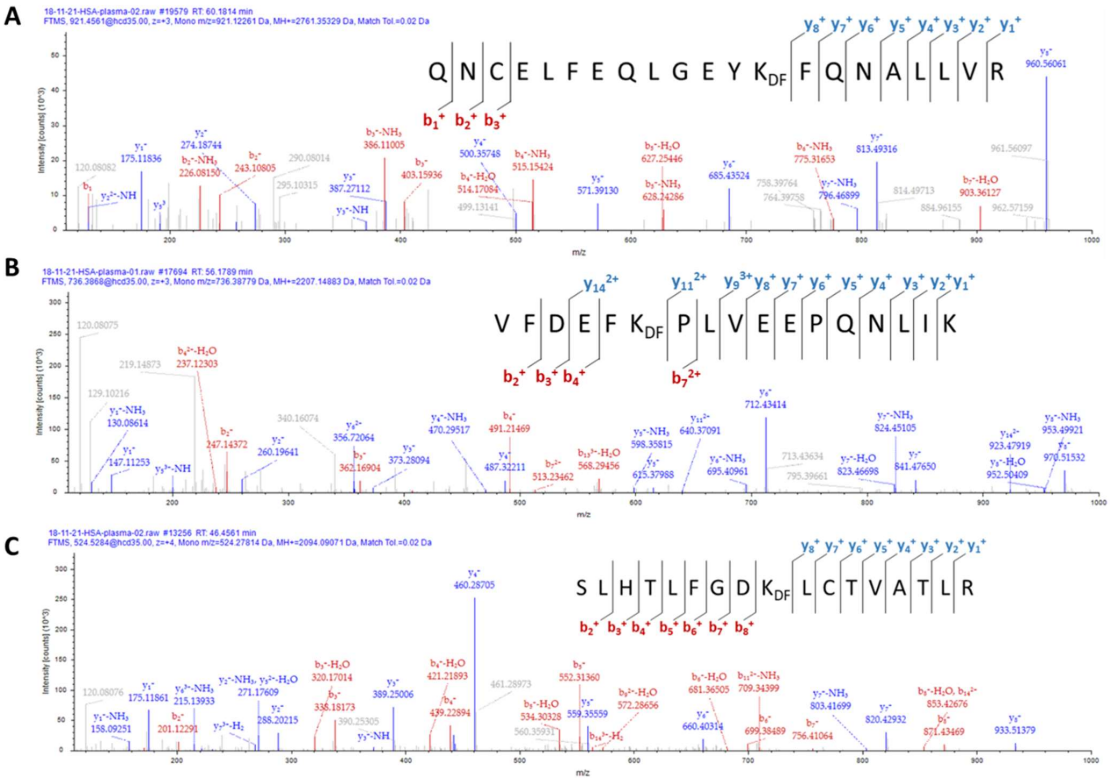

Figure 3. Fragmentation mass spectra (MS/MS) of the three less abundant glycated peptides present in the plasma of HF patients and the relevant fragments for their attribution. A) Spectrum corresponding to the peptide QNcELFEQLGEYkFQNALLVR (glycated residue lys402), B) VFDEFkPLVEEPQNLIK (modified residue lys378), and C) SLHTLFGDkLcTVATLR (modified residue lys73). The calculated fragment ions b^+, b^{2+}, y^+ and y^{2+} of the adducted peptides identified in the MS/MS spectra are highlighted by red (b series) and blue (y series) colors. DF, deoxy-fructosyl.

Proteome Discoverer software was used for the identification of the glycated peptides containing a mass shift of 162 Da, which is characteristic of the known deoxy-fructosyl-lysine or –arginine modifications. After the analysis with Proteome Discoverer we found 9 modified peptides that presented a mass increase that fitted with the addition of deoxy-fructosyl. Fragmentation spectra of some of the found glycated peptides are showed in **Figure 2 and 3**.

Then, the relative extent of each modified residue was calculated by determining the peak area of the modified peptide with respect to the unmodified one, by assuming that the ionization efficiency of the native and the modified peptides are equal (**Table 3**). The adducted residues that presented higher relative abundance were lys233 (79%) followed by lys525 (13%).

We observed that, although the intact protein analysis pointed out the addition of only one molecule of glucose per molecule of HSA, this addition occurred at different lysine or arginine sites.

Annotated Sequence *	Modifications	Residue	Average Peak Area		Relative Abundance [%]
			unmodified peptide	modified peptide	
1	**K8(DFK)**	**Lys233**	8,75E+07	3,37E+08	**79,36**
2	**K1(DFK)**	**Lys525**	3,32E+08	5,25E+07	**13,66**
3	C2(Cam); C11(Cam); **K13(DFK)**	**Lys64**	9,44E+08	2,99E+07	**3,07**
4	**K1(DFK)**	**Lys574**	7,76E+08	1,19E+07	**1,51**
5	C14(Cam); **K21(DFK)**	**Lys41**	1,34E+09	1,37E+07	**1,01**
6	C5(Cam); C6(Cam); C13(Cam); **R17 or K22(DFK or DFR)**	**Arg257 or Lys262**	1,57E+09	1,35E+07	**0,86**
7	C3(Cam); **K13(DFK)**	**Lys402**	4,71E+09	2,34E+07	**0,50**
8	**K6 (DFK);** C20(Cam)	**Lys378**	1,67E+10	4,40E+07	**0,26**
9	**K9(DFK);** C11(Cam)	**Lys73**	6,75E+09	9,25E+06	**0,14**

Table 3. List of deoxy-fructosyl-lysine (DFK) and deoxy-fructosyl-arginine (DFR) residues identified in isolated plasma HSA from HF patients class IV. Lys, lysine; Arg, arginine; Cam, carbamidomethylation.

*1) AEFAEVSkLVTDLTK, 2) kQTALVELVK, 3) TcVADESAENcDkSLHTLFGDK, 4) kLVAASQAALGL, 5) ALVLIAFAQYLQQcPFEDHVkLVNEVTEFAK, 6) VHTEccHGDLLEcADDrADLAk, 7) QNcELFEQLGEYkFQNALLVR, 8) VFDEFkPLVEEPQNLIK, 9) SLHTLFGDkLcTVATLR

4. DISCUSSION

In this study we have evaluated the plasma levels of cysteinylated and glycated HSA in patients with HF class III and IV, according to the NYHA. Using a mass spectrometric approach we have proved that both albumin isoforms in plasma of patients are significantly increased with respect to healthy subjects. Likewise, these increases were more marked when raising the disease severity

and inversely correlated significantly with VO_2 peak/kg, which might assist in stratification and prognosis of HF patients. By means of intact protein MS analysis we observed a 1:1 molecular ratio with respect to the number of glucose added per molecule of HSA. Similarly, results revealed that only one cysteine covalently binds to one molecule of HSA in HF patients.

Cys34 accounted for approximately 40% of the total radical scavenging activity of HSA due to the free thiol group, constituting one of the most powerful antioxidant sources present in circulation [2]. Cysteinylation of this residue can hamper some of the beneficial activities attributed to HSA, in particular a significant loss of the oxidant buffering capacity [17], which could in turn be reflected in the emergence of oxPTM of other proteins, such as low density lipoproteins (LDLs) [18].

The redox status of the free thiol group in HSA can be a very important indicator of oxidative stress and oxidative damage as observed in patients undergoing oxidative stress-related pathologies such as end stage renal disease [18], coronary artery disease [19], chronic liver disease or diabetes mellitus [20], as well as in pregnant women with intrauterine growth restriction [21]. Additionally, it has been demonstrated that HSA goes through conformational changes upon S-cysteinylation making the cleavage sites more accessible to proteases and, hence, more susceptible to proteolytic degradation [22]. Also, structural changes associated to cys34 oxidation impair the binding of HSA ligands.

Likewise, glycation of HSA may reduce its affinity for different ligands (long chain fatty acids, bilirubin, copper) or hamper the antioxidant capacity [2] due mainly to the conformational changes induced upon lysine or arginine modification. In addition, glycation is accompanied by oxidative modifications, which occur during aging of the albumin molecule. Although glycation of HSA shows more than two-folds increase than the glycation of rest of the serum proteins in hyperglycemic conditions [8], in this work we have demonstrated that GA levels also happens in non-diabetic conditions, since diabetic patients were not enrolled in the study.

On the other hand, we also observed an albumin isoform that was not reported previously in other intact protein MS analysis of HSA [3,23,24] characterized by a mass increment of 44 ± 2 Da that could correspond to the addition of ethylene oxide [25]. Ethylene oxide is particularly useful for sterilizing disposable medical equipment in hospitals, such as vacuum blood collection tubes [26]. Nevertheless, no variations in the relative abundance between controls and patients were pointed out, meaning that this is not an interesting HSA isoform as marker of oxidative stress in HF.

Finally, total HSA levels showed a clear tendency to decrease from control subjects to the most severe class of HF, which is in accordance with other studies claiming that hypoalbuminemia is common in HF patients with a prevalence ranging from 18% to 89% [27,28]. Inflammation, liver dysfunction, or malnutrition may reduce serum albumin concentration in HF patients, but the fact that HSA is more prone to be cleaved by proteases upon cysteinylation could also contribute to hypoalbuminemia. The osmotic importance of HSA is related to its abundance, thus reduced

circulating HSA levels contribute to fluid migration towards interstitial space and can eventually result in peripheral edema, such as pulmonary congestion [28].

For a deeper characterization of GA we also identified and relatively quantified for the first time the early glycated residues in plasma samples from HF patients classified in the most severe NYHA group. The employment of ultra-high resolution MS instruments allowed the identification of 9 different glycated positions. Since intact protein MS analysis of HSA revealed a peak shifted 162 Da with respect to the native HSA, while other peaks with a mass shift of 344 Da or any multiple of 162, characteristic of two or more glycated sites, were not present in the spectrum, population of molecules containing at the same time two or more glycation adducts can be ruled out. This indicates that different populations of GA molecules do exist, each one containing only one modification but at different sites. The reactivity of the amino groups and their relative glycation ratios depends on the accessibility of the site [14]. In the case of HF plasma patients, relative quantification results indicated that lys233 and lys525 are the two most abundant populations of GA (79% and 13% respectively).
Lys233 is located in the Sudlow site I acidic drug binding site of HSA, within the subdomain IIA, which is a major drug binding site on HSA, so modifications of this residue may hamper its binding to drugs. On the other hand, lys525 has been depicted in several studies as the predominant site of the non-enzymatic glycation of HSA *in vivo* despite its low surface exposure and accessibility in native conformation [8]. The location of these glycated sites could be explained by the presence in their close vicinity of basic amino acid residues, such as lysine or histidine. However, the glycation pattern of HSA in subjects suffering from pathological conditions, such as diabetes, where lys549 represents the main glycated residue within HSA [14], does not match with the pattern found *in vivo* in HF patients [1], leading to believe in the existence of disease-specific glycation patterns. Therefore, lys233 and lys525 might represent the main potential therapeutic targets to reduce GA levels in HF patients.

In conclusion, this study highlights raised levels of HSA cysteinylation and glycation in patients with HF expanding the current knowledge that different residues on HSA can experience certain post-translational modifications under specific environments in oxidative stress-related diseases. Additionally, we identified and relatively quantified for the first time the HSA glycation pattern associated to the most severe class of HF, which might be useful for drug therapy. Finally, to provide insights about the role of GA, we have assessed the biological effects of GA on *in vitro* cultured cardiomyocytes. Results are reported in the next chapter (Chapter II).

5. REFERENCES

[1] A. Martinez Fernandez, L. Regazzoni, M. Brioschi, E. Gianazza, P. Agostoni, G. Aldini, C. Banfi, Pro-oxidant and pro-inflammatory effects of glycated albumin on cardiomyocytes, Free Radic. Biol. Med. (2019). doi:0.1016/j.freeradbiomed.2019.06.023.

[2] M. Taverna, A.-L. Marie, J.-P. Mira, B. Guidet, Specific antioxidant properties of human serum albumin, Ann. Intensive Care. 3 (2013) 4. doi:10.1186/2110-5820-3-4.

[3] D. Bar-Or, C.G. Curtis, A. Sullivan, L.T. Rael, G.W. Thomas, M. Craun, R. Bar-Or, K.N. MacLean, J.P. Kraus, Plasma albumin cysteinylation is regulated by cystathionine β-synthase, Biochem. Biophys. Res. Commun. (2004). doi:10.1016/j.bbrc.2004.10.191.

[4] K.G. Reddie, K.S. Carroll, Expanding the functional diversity of proteins through cysteine oxidation, Curr. Opin. Chem. Biol. (2008). doi:10.1016/j.cbpa.2008.07.028.

[5] L.B. Poole, The basics of thiols and cysteines in redox biology and chemistry, Free Radic. Biol. Med. (2015). doi:10.1016/j.freeradbiomed.2014.11.013.

[6] D. Pérez-Sala, C.L. Oeste, A.E. Martínez, M.J. Carrasco, B. Garzón, F.J. Cañada, Vimentin filament organization and stress sensing depend on its single cysteine residue and zinc binding, Nat. Commun. 6 (2015). doi:10.1038/ncomms8287.

[7] J.R. Burgoyne, H. Mongue-Din, P. Eaton, A.M. Shah, Redox signaling in cardiac physiology and pathology, Circ. Res. (2012). doi:10.1161/CIRCRESAHA.111.255216.

[8] P. Rondeau, E. Bourdon, The glycation of albumin: Structural and functional impacts, Biochimie. (2011). doi:10.1016/j.biochi.2010.12.003.

[9] J. Anguizola, R. Matsuda, O.S. Barnaby, K.S. Hoy, C. Wa, E. DeBolt, M. Koke, D.S. Hage, Review: Glycation of human serum albumin, Clin. Chim. Acta. (2013). doi:10.1016/j.cca.2013.07.013.

[10] Q. Zhang, M.E. Monroe, A.A. Schepmoes, T.R.W. Clauss, M.A. Gritsenko, D. Meng, V.A. Petyuk, R.D. Smith, T.O. Metz, Comprehensive identification of glycated peptides and their glycation motifs in plasma and erythrocytes of control and diabetic subjects, J. Proteome Res. (2011). doi:10.1021/pr200040j.

[11] C. Wa, R.L. Cerny, W.A. Clarke, D.S. Hage, Characterization of glycation adducts on human serum albumin by matrix-assisted laser desorption/ionization time-of-flight mass spectrometry, Clin. Chim. Acta. (2007). doi:10.1016/j.cca.2007.06.011.

[12] O.S. Barnaby, C. Wa, R.L. Cerny, W. Clarke, D.S. Hage, Quantitative analysis of glycation sites on human serum albumin using 16O/18O-labeling and matrix-assisted laser desorption/ionization time-of-flight mass spectrometry, Clin. Chim. Acta. (2010). doi:10.1016/j.cca.2010.04.007.

[13] A.G. Soudahome, A. Catan, P. Giraud, S.A. Kouao, A. Guerin-Dubourg, X. Debussche, N. Le Moullec, E. Bourdon, S.B. Bravo, B. Paradela-Dobarro, E. Álvarez, O. Meilhac, P. Rondeau, J. Couprie, Glycation of human serum albumin impairs binding to the glucagon-like peptide-1 analogue liraglutide, J. Biol. Chem. (2018). doi:10.1074/jbc.M117.815274.

[14] A. Frolov, R. Hoffmann, Identification and relative quantification of specific glycation sites in human serum albumin, Anal. Bioanal. Chem. (2010). doi:10.1007/s00216-010-3810-9.

[15] A. Soboleva, G. Mavropulo-Stolyarenko, T. Karonova, D. Thieme, W. Hoehenwarter, C. Ihling, V.

Stefanov, T. Grishina, A. Frolov, Multiple glycation sites in blood plasma proteins as an integrated biomarker of type 2 diabetes mellitus, Int. J. Mol. Sci. (2019). doi:10.3390/ijms20092329.

[16] R. Malhotra, K. Bakken, E. D'Elia, G.D. Lewis, Cardiopulmonary Exercise Testing in Heart Failure, JACC Hear. Fail. (2016). doi:10.1016/j.jchf.2016.03.022.

[17] M. Roche, P. Rondeau, N.R. Singh, E. Tarnus, E. Bourdon, The antioxidant properties of serum albumin, FEBS Lett. (2008). doi:10.1016/j.febslet.2008.04.057.

[18] L. Regazzoni, L. Del Vecchio, A. Altomare, K.-J. Yeum, D. Cusi, F. Locatelli, M. Carini, G. Aldini, Human serum albumin cysteinylation is increased in end stage renal disease patients and reduced by hemodialysis: mass spectrometry studies, Free Radic. Res. 47 (2013) 172–180. doi:10.3109/10715762.2012.756139.

[19] K. Kadota, Y. Yui, R. Hattori, Y. Murohara, C. Kawai, Decreased sulfhydryl groups of serum albumin in coronary artery disease, Jpn. Circ. J. (1991). doi:10.1253/jcj.55.937.

[20] K. Nagumo, M. Tanaka, V.T.G. Chuang, H. Setoyama, H. Watanabe, N. Yamada, K. Kubota, M. Tanaka, K. Matsushita, A. Yoshida, H. Jinnouchi, M. Anraku, D. Kadowaki, Y. Ishima, Y. Sasaki, M. Otagiri, T. Maruyama, Cys34-cysteinylated human serum albumin is a sensitive plasma marker in oxidative stress-related chronic diseases, PLoS One. (2014). doi:10.1371/journal.pone.0085216.

[21] D. Bar-Or, K.D. Heyborne, R. Bar-Or, L.T. Rael, J. V. Winkler, D. Navot, Cysteinylation of maternal plasma albumin and its association with intrauterine growth restriction, Prenat. Diagn. (2005). doi:10.1002/pd.1122.

[22] A. Kawakami, K. Kubota, N. Yamada, U. Tagami, K. Takehana, I. Sonaka, E. Suzuki, K. Hirayama, Identification and characterization of oxidized human serum albumin: A slight structural change impairs its ligand-binding and antioxidant functions, FEBS J. (2006). doi:10.1111/j.1742-4658.2006.05341.x.

[23] J.W. Jeffs, S. Ferdosi, H.N. Yassine, C.R. Borges, Ex vivo instability of glycated albumin: A role for autoxidative glycation, Arch. Biochem. Biophys. (2017). doi:10.1016/j.abb.2017.07.004.

[24] K. Kubota, A. Nakayama, K. Takehana, A. Kawakami, N. Yamada, E.I. Suzuki, A simple stabilization method of reduced albumin in blood and plasma for the reduced/oxidized albumin ratio measurement, Int. J. Biomed. Sci. (2009).

[25] H. Grigoryan, W. Edmands, S.S. Lu, Y. Yano, L. Regazzoni, A.T. Iavarone, E.R. Williams, S.M. Rappaport, Adductomics Pipeline for Untargeted Analysis of Modifications to Cys34 of Human Serum Albumin, Anal. Chem. (2016). doi:10.1021/acs.analchem.6b02553.

[26] L. Chen, C. Sloey, Z. Zhang, P. V. Bondarenko, H. Kim, D. Ren, S. Kanapuram, Chemical modifications of therapeutic proteins induced by residual ethylene oxide, J. Pharm. Sci. (2015). doi:10.1002/jps.24257.

[27] J.L. Bonilla-Palomas, A.L. Gámez-López, M. Moreno-Conde, M.C. López-Ibáñez, M. Anguita-Sánchez, Á. Gallego De La Sacristana, F. García-Catalán, A. Villar-Ráez, Hypoalbuminemia in acute heart failure patients: Causes and its impact on hospital and long-term mortality, J. Card. Fail. (2014). doi:10.1016/j.cardfail.2014.01.016.

[28] S. Arques, P. Ambrosi, Human serum albumin in the clinical syndrome of heart failure, J. Card. Fail. (2011). doi:10.1016/j.cardfail.2011.02.010.

CHAPTER II:

Biological effects of glycated albumin on cardiomyocytes

BIOLOGICAL EFFECTS OF GLYCATED ALBUMIN ON CARDIOMYOCYTES

1. PREFACE

PUBLISHED ARTICLE (please see Appendix: Scientific contributions)

Pro-oxidant and pro-inflammatory effects of glycated albumin on cardiomyocytes.
Alma Martinez Fernandez, Luca Regazzoni, Maura Brioschi, Erica Gianazza, Piergiuseppe Agostoni, Giancarlo Aldini, Cristina Banfi. *Free Radical Biology and Medicine*. Jun 2019.
DOI: 10.1016/j.freeradbiomed.2019.06.023

2. INTRODUCTION

Several *in vitro* studies have shown the implication of glycated albumin, mainly advanced stage glycation products of HSA (AGE-HSA), in cardiovascular diseases. For example, platelets activated by both irreversibly and reversibly glycated albumin boost the expression and activation of adhesion molecules, enhance aggregation agonist receptor expression, and raise intracellular calcium concentration and dense body secretion, which promotes endothelial responses promoting CVD development [1]; in endothelial cells, glycated albumin enhanced ROS production by activating multiple signaling pathways that require NF-κB activation, NADPH oxidase, and endothelial nitric oxide synthase (eNOS) uncoupling [2].

Glycated albumin can also trigger damaging effects *in vitro* and *in vivo* on hepatic cells by increasing oxidative stress, attenuating the antioxidant capacity, and by impairment of hepatic proteolytic and respiratory chain enzyme activities [3], all features that contribute to increase the mortality of diabetic patients [4]. Additionally, early glycation of bovine serum albumin (BSA), which has approximately a sequence homology to HSA of 76% [5] stimulates cardiomyocyte ROS production through a protein kinase C-dependent activation of a Nox2-containing NADPH oxidase that results eventually in NF-κB activation and up-regulation of atrial natriuretic factor mRNA suggesting that glycated albumin may play a role in the development of diabetic heart disease [6].

However, the possible implication of early glycation HSA (GA) in cardiovascular diseases has been less studied than the effects of the irreversible AGEs.

Keeping in mind that levels of GA are significantly increased in plasma of non-diabetic HF patients (reported in CHAPTER I: Analysis of cysteinylated and glycated albumin in heart failure patients), in the present chapter we pursued to investigate the effects of GA on cardiomyocytes (HL-1 cells) in order to find a causal role in the etiopathogenesis of HF. Hence, in this study we analyzed the effects of this modified protein on cardiomyocytes *in vitro*.

3. MAIN RESULTS

Considering that raised GA levels in the plasma of HF patients were found in Chapter I, we next investigated the effects of commercial GA on cardiomyocytes (HL-1 cells). To this purpose, the glycation sites present in the purified commercially available GA were firstly characterized by means of mass spectrometry and compared with the ones found in the HSA isolated from plasma of HF patients. Results showed that 8 out of 9 glycated residues found in the human HSA from HF patients were also present in the purified commercially available GA (**Figure 1**).

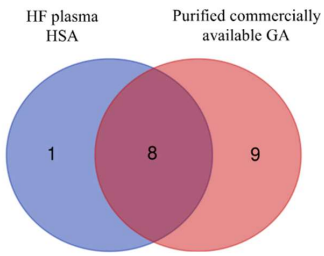

Figure 1. Venn diagram of the glycated residues found in plasma from HF patients and in the purified commercially available GA.

Therefore, HL-1 cells were treated with the commercial GA (100 or 250 µg/mL) for 8 and 16 hours. Cells treated with GA exhibited a very slightly decrease in proliferation (lower than 10%) while apoptotic responses remained unchanged after GA treatment (**Figure 2**).

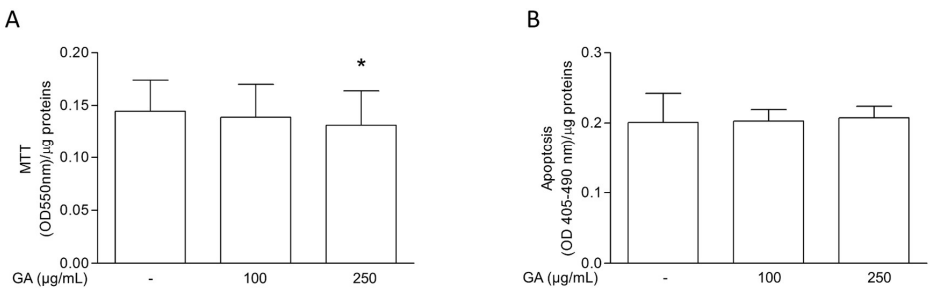

Figure 2. Effects of GA on HL-1 cell proliferation and apoptosis. A) HL-1 cells were stimulated with GA (100 or 250 µg/mL) for 16 h and then cultured in serum-free phenol-free medium for additional 24 h. Cell proliferation assay was performed employing the MTT colorimetric method. Data are expressed as the means ± SEM of absorbance values/µg of proteins from 3 independent experiments. *$p < 0.05$ compared to control cells. B) Analysis of apoptosis. Cells were stimulated with GA for 16 h. Cell lysates were collected to measure apoptosis after 24 h of incubation in serum-free and phenol-free by means of Cell Death Detection ELISA Plus assay. Data are expressed as the means ± SEM of absorbance values/µg of proteins from 3 independent experiments.

Then, we analyzed the secretome from the treated and control cells by LC-MS/MS and several differentially abundant proteins were identified, among them HSP90 beta, Nucleolin and HSP90 alpha. The lists of differentially abundant proteins were analyzed with STRING and gene ontology (GO) analysis. After 16 hours of treatment, some biological processes including response to organic substance and response to stress were significantly enriched (**Figure 3**).

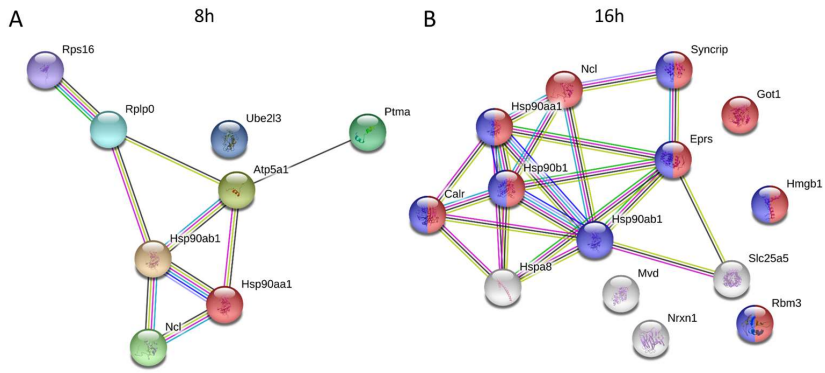

Figure 3. Gene ontology analysis of secreted proteins modulated by GA visualized with STRING. A) Protein network obtained with proteins modulated after 8 h of treatment with GA. B) Protein network obtained with proteins modulated after 16 h of treatment with GA in which enriched biological processes are highlighted. In B, proteins associated with the GO term response to stress are colored in blue ($p = 0.0229$), while proteins associated with the response to organic substances are colored in red ($p = 0.000222$).

In view of the statistically significant enrichment of the GO term related to response to stress, we next assessed the capacity of GA to cause oxidative damage. Exposure of HL-1 cells to GA resulted in the rapid intracellular generation of ROS, assessed by DCF fluorescence (**Figure 4**).

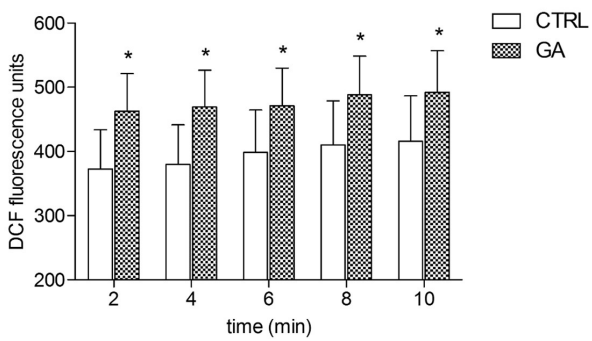

Figure 4. Intracellular generation of reactive oxygen species (ROS) mediated by GA. HL-1 cells were loaded with 10 µmol/L DCF-DA and stimulated with GA (250 µg/mL) for different times. Data shown represent the averages of three independent experiments (mean ± SEM). *$p < 0.05$ vs. untreated cells.

Subsequently, we evaluated, by means of western blot, intracellular 4-hydroxynonenal-protein adducts and carbonylated protein levels, both biomarkers of protein lipoxidation and oxidation. Results unveiled that levels of both biomarkers were enhanced when cells were exposed to GA (**Figure 5**). Specifically, 4-HNE-adducted protein levels increased significantly when cells were treated for 8 h with the highest concentration of GA, while levels of carbonylated proteins increased both after 8 and 16 h, although only after 16 h the increase was statistically significant.

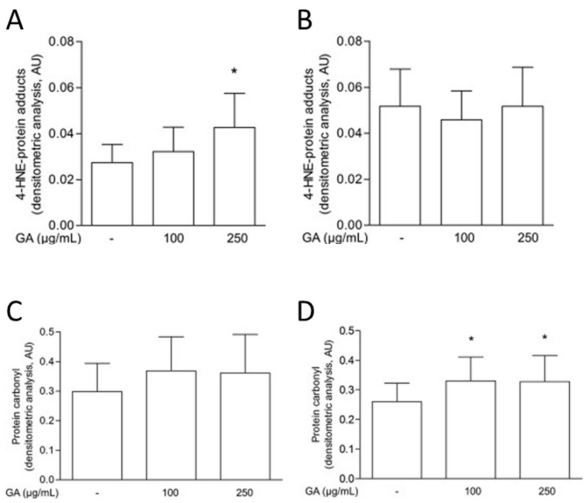

Figure 5. Densitometric analysis of western blots corresponding to 4-HNE immunoreactivity after A) 8 h and B) 16 h of treatment with GA. C) Densitometric analysis relative to carbonylated protein levels after 8 h and D) 16 h of incubation with GA. Values are representative of at least 8 experiments and are expressed as mean ± SEM. *p < 0.05 compared to control cells.

Additionally, we measured mRNA levels of nuclear factor erythroid 2-related factor 2 (Nrf2) and a significant increase of Nrf2 mRNA was detected when cells were treated with GA (**Figure 6**).

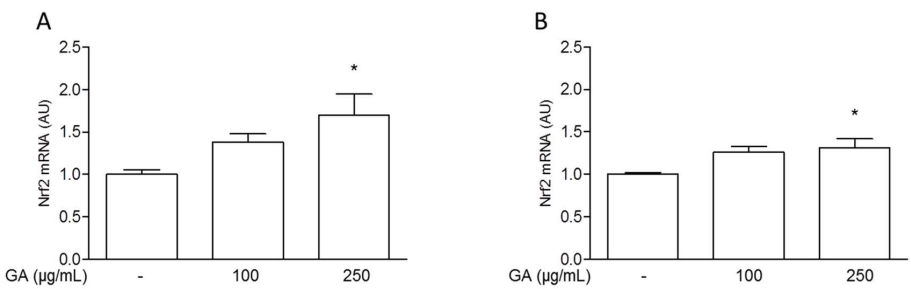

Figure 6. Effect of GA on Nrf2 at mRNA level. Transcript expression levels analyzed by RT-qPCR were measured after A) 8 h and B) 16 h of treatment with 100 or 250 µg/mL GA. Gene expression was normalized relative to the expression of the glyceraldehyde-3-phosphate dehydrogenase (GAPDH). Results are based on 3 independent analysis and data are presented as mean ± SEM. *p < 0.05 vs. control.

We also analyzed the expression levels of the transcriptional coactivator peroxisome proliferator-activated receptor γ coactivator-1 α (PGC-1α) and β (PGC-1 β), that play a role as inducer of many antioxidant-detoxifying enzymes. Results showed an early increase in the expression of PGC-1β but not of PGC-1α (**Figure 7**).

On the other hand, it was also investigated whether GA could induce a pro-inflammatory state on cardiomyocytes. Our results pointed out a significantly enhanced production of IL-6 and TNF-α mRNA levels in the cells treated with GA with respect to the untreated ones (**Figure 7**). Conversely, the anti-inflammatory cytokine interleukin-10 (IL-10) mRNA was not detectable even after stimulation with GA.

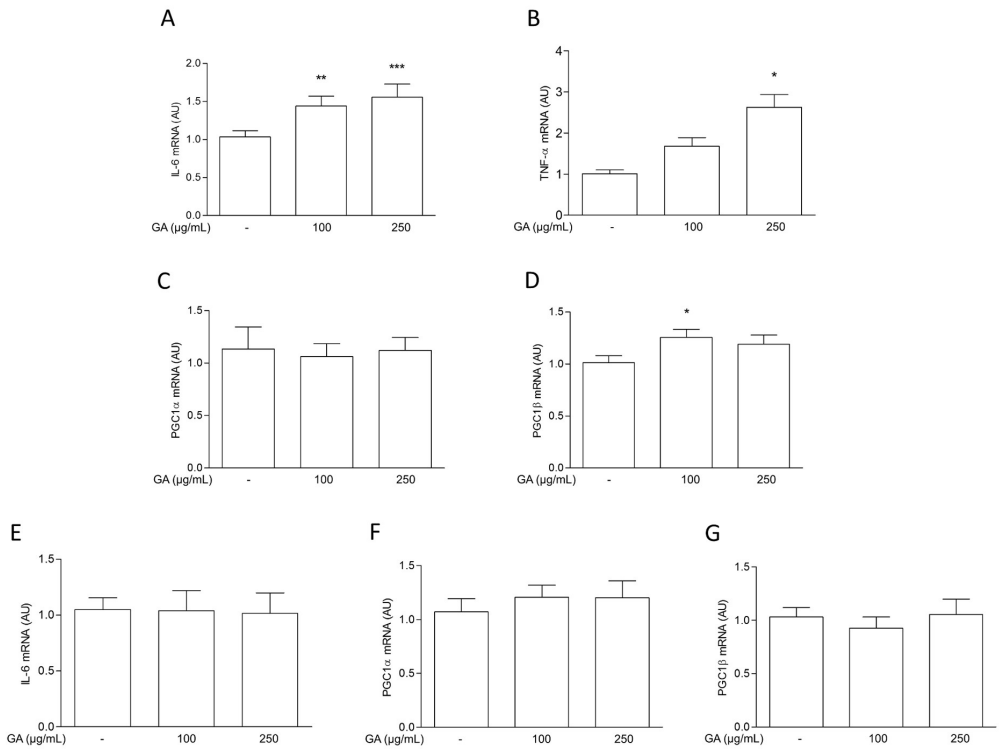

Figure 7. Effect of GA on the mRNA levels of IL-6, TNF-α, PGC1α, and PGC1β. mRNA levels of A) IL-6, B) TNF-α, C) PGC1α, and D) PGC1β after 8 h of treatment with 100 or 250 μg/mL of GA were analyzed by RT-qPCR. mRNA levels of E) IL-6, F) PGC1α, and G) PGC1β were evaluated after 16 h or treatment with 100 or 250 μg/mL GA. Gene expression was normalized relative to the expression of the glyceraldehyde-3-phosphate dehydrogenase (GAPDH). Results are based on 10 independent experiments for IL-6, PGC1α, and PGC1β genes and on 3 independent experiments for TNF-α. Data are presented as mean ± SEM. *P-value < 0.05 vs. control cells, **p-value < 0.01 vs. control cells, ***p-value < 0.001 vs. control cells.

Hence, these findings suggest that GA exerts pro-inflammatory and pro-oxidant effects on murine HL-1 cardiomyocytes. No pro-inflammatory nor pro-oxidant effects were observed when HL-1 cells were exposed to non-glycated HSA.

4. DISCUSSION

Considering the significant increased amount of glycated albumin in the plasma of HF patients pointed out by quantitative mass spectrometry (Chapter I), in this study we pursued to provide insights about the biological effects of GA, in order to understand the potential causal role of GA in the etiopathogenesis of HF. To that purpose, we used HL-1 cardiomyocytes that are currently the only cells available that continuously divide, spontaneously contract, and maintain a differentiated adult cardiac phenotype through indefinite passages in culture. A schematic representation of the most relevant findings is depicted in **Figure 8**.

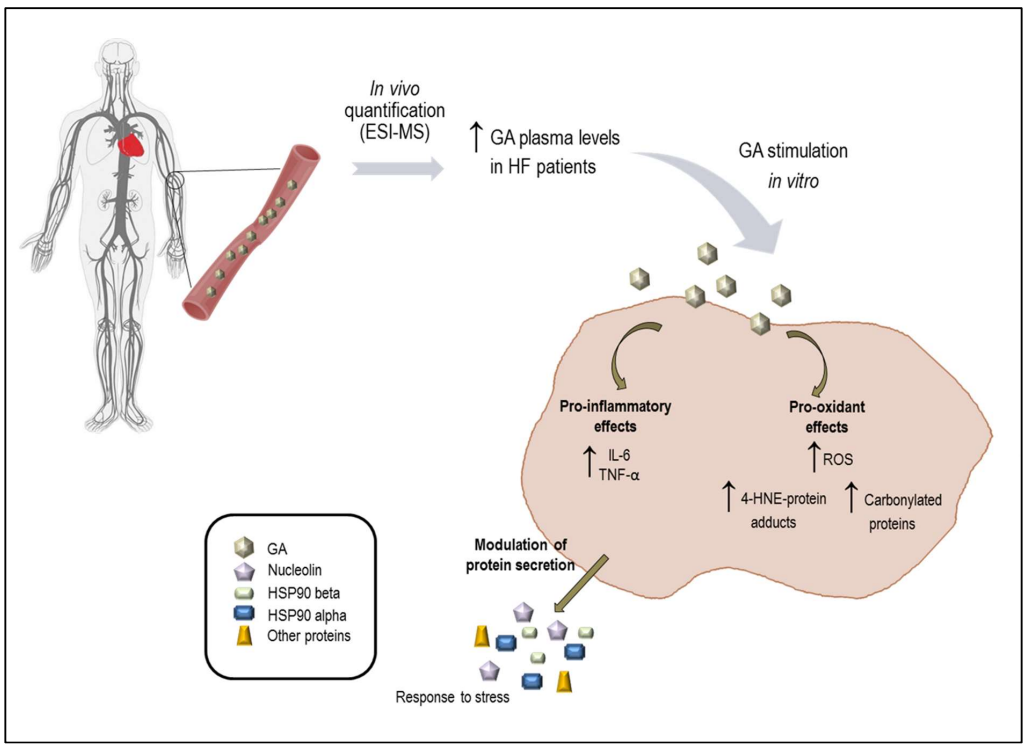

Figure 8. Schematic representation of *in vitro* glycated albumin effects on HL-1 cells. Increased GA plasma levels were found in HF patients. Thus, a similar purified commercially available GA was used to stimulate HL-1 cells. After GA treatment, increased levels of ROS, carbonylated proteins and 4-HNE-adducts were detected, as well a raise at mRNA level of pro-inflammatory cytokines (IL-6, TNF-α). In addition, protein secretion was modulated after GA stimulation, and the differentially abundant proteins take part in response to stress processes.

Upon GA stimulation of cardiomyocytes we took advantage of a proteomics-based approach to assess secretome differences at protein level between treated and untreated cells and, after functional interpretation of the identified proteins, the results revealed that GA is a potential mediator of the response to stress. Hence, we decided to evaluate the effect of GA in the onset of oxidative stress and we detected not only a rapid increased of ROS levels after GA stimulation but also oxidative modifications, specifically carbonylation and HNE-adduction, of a multitude of cellular proteins within cardiac myocytes after GA treatment. Interestingly, previous studies claimed that raised plasma HNE-adduct levels correlate with an elevated heart rate and impaired left ventricular contractility [7], while *ex vivo* experiments highlighted that the higher the levels of carbonylated plasma proteins, the higher the degree of left ventricular remodeling [8], them all characteristics associated to HF. In fact, aggravation of HF positively correlates with higher plasma levels of carbonylated proteins in the patients [8].
Keeping in mind that HF is related with an inflammatory state [9], in this study we also sought to determine whether GA might modulate the expression of pro-inflammatory cytokines. Our *in vitro* results have demonstrated that GA modulates the cardiomyocyte expression of inflammatory cytokines such as IL-6 or TNF-α. Interestingly, up-regulation of IL-6, when remains elevated chronically, induces maladaptive cardiac hypertrophy and decreases the contractile function [10,11]. Moreover, TNF-α was elevated in trials of HF patients with reduced and preserved ejection fraction, which was associated independently with increased mortality [12].
Besides, no pro-oxidant nor pro-inflammatory effects were induced by native HSA, which suggest that a lesser extent of free amino groups along HSA in favor of a higher content of deoxy-fructosyl HSA adducts causes a detrimental effect on cardiomyocytes.

Conversely, it is well known that there exist a relationship between type 2 diabetes and the risk of heart failure. Indeed, the results of the Framingham Heart Study showed that the frequency of HF was twice as high in diabetic men and five times higher in diabetic women compared with control subjects [13]. Raised GA plasma levels are common in diabetic patients [14], being HSA 2–3 times more glycated than the rest of the serum proteins in hyperglycaemic condition, whereas IL-6 and TNF-α might induce the development of insulin resistance and pathogenesis of type 2 diabetes mellitus [15]. Hence, the awareness of the biological effects of GA on cardiomyocytes highlighted in this work might contribute to understand the pathophysiologic mechanisms mediating the association of diabetes and heart failure.

In conclusion, the present work has contributed to expand the current knowledge of GA suggesting a causal role in the etiopathogenesis of HF. Also, our *in vitro* results may contribute to understand the pathophysiological relation between diabetes and HF.

5. REFERENCES

[1] I. Soaita, W. Yin, D.A. Rubenstein, Glycated albumin modifies platelet adhesion and aggregation responses, Platelets. (2017). doi:10.1080/09537104.2016.1260703.

[2] B.K. Rodiño-Janeiro, B. Paradela-Dobarro, S. Raposeiras-Roubín, M. González-Peteiro, J.R. González-Juanatey, E. Álvarez, Glycated human serum albumin induces NF-κB activation and endothelial nitric oxide synthase uncoupling in human umbilical vein endothelial cells, J. Diabetes Complications. (2015). doi:10.1016/j.jdiacomp.2015.07.016.

[3] J. Patche, D. Girard, A. Catan, F. Boyer, A. Dobi, C. Planesse, N. Diotel, A. Guerin-Dubourg, P. Baret, S.B. Bravo, B. Paradela-Dobarro, E. Álvarez, M.F. Essop, O. Meilhac, E. Bourdon, P. Rondeau, Diabetes-induced hepatic oxidative stress: a new pathogenic role for glycated albumin, Free Radic. Biol. Med. (2017). doi:10.1016/j.freeradbiomed.2016.11.026.

[4] K. Nagumo, M. Tanaka, V.T.G. Chuang, H. Setoyama, H. Watanabe, N. Yamada, K. Kubota, M. Tanaka, K. Matsushita, A. Yoshida, H. Jinnouchi, M. Anraku, D. Kadowaki, Y. Ishima, Y. Sasaki, M. Otagiri, T. Maruyama, Cys34-cysteinylated human serum albumin is a sensitive plasma marker in oxidative stress-related chronic diseases, PLoS One. (2014). doi:10.1371/journal.pone.0085216.

[5] A. Arasteh, S. Farahi, M. Habibi-Rezaei, A.A. Moosavi-Movahedi, Glycated albumin: An overview of the In Vitro models of an In Vivo potential disease marker, J. Diabetes Metab. Disord. (2014). doi:10.1186/2251-6581-13-49.

[6] M. Zhang, L.K. Ay, N. Anilkumar, R. Chibber, P.J. Pagano, A.M. Shah, A.C. Cave, Glycated proteins stimulate reactive oxygen species production in cardiac myocytes: Involvement of Nox2 (gp91phox)-containing NADPH oxidase, Circulation. (2006). doi:10.1161/CIRCULATIONAHA.105.581397.

[7] S. Mak, D.C. Lehotay, M. Yazdanpanah, E.R. Azevedo, P.P. Liu, G.E. Newton, Unsaturated aldehydes including 4-OH-nonenal are elevated in patients with congestive heart failure, J. Card. Fail. (2000). doi:10.1054/jcaf.2000.7272.

[8] S. Radovanovic, A. Savic-Radojevic, M. Pljesa-Ercegovac, T. Djukic, S. Suvakov, M. Krotin, D. V. Simic, M. Matic, Z. Radojicic, T. Pekmezovic, T. Simic, Markers of oxidative damage and antioxidant enzyme activities as predictors of morbidity and mortality in patients with chronic heart failure, J. Card. Fail. (2012). doi:10.1016/j.cardfail.2012.04.003.

[9] D.L. Mann, Innate immunity and the failing heart: The cytokine hypothesis revisited, Circ. Res. (2015). doi:10.1161/CIRCRESAHA.116.302317.

[10] L. Tamariz, J.M. Hare, Inflammatory cytokines in heart failure: Roles in aetiology and utility as biomarkers, Eur. Heart J. (2010). doi:10.1093/eurheartj/ehq014.

[11] J.A. Fontes, N.R. Rose, D. Čihák ová, The varying faces of IL-6: From cardiac protection to cardiac failure, Cytokine. (2015). doi:10.1016/j.cyto.2014.12.024.

[12] S.M. Dunlay, S.A. Weston, M.M. Redfield, J.M. Killian, V.L. Roger, Tumor necrosis factor-α and mortality in heart failure: A community study, Circulation. (2008). doi:10.1161/CIRCULATIONAHA.107.759191.

[13] J. Kasznicki, J. Drzewoski, Heart failure in the diabetic population-pathophysiology, diagnosis and management, Arch. Med. Sci. (2014). doi:10.5114/aoms.2014.43748.

[14] N. Furusyo, J. Hayashi, Glycated albumin and diabetes mellitus, Biochim. Biophys. Acta - Gen. Subj. (2013). doi:10.1016/j.bbagen.2013.05.010.

[15] P. Dandona, A. Aljada, A. Bandyopadhyay, Inflammation: The link between insulin resistance, obesity and diabetes, Trends Immunol. (2004). doi:10.1016/j.it.2003.10.013.

CHAPTER III:

Detection of AGEs and ALEs in heart failure plasma samples

DETECTION OF AGEs and ALEs IN HEART FAILURE PLASMA SAMPLES

1. INTRODUCTION

Products of nonenzymatic reactions such as lipid peroxidation and glucose-protein interactions (glycation) are involved in many of the pathophysiologies associated with cardiovascular diseases. Unstable intermediates containing reactive carbonyl moieties arising from these nonenzymatic reactions have the ability to form covalent adducts with proteins leading to the formation of advanced glycation and lipoxidation end products (AGEs and ALEs respectively) [1]. AGEs and ALEs are a very heterogeneous and complex class of damaging molecules that might be capable of binding the transmembrane receptor RAGE (receptor for advanced glycation end products), thereby inducing the inflammatory response and pro-fibrotic response through RAGE activation [2].

On one hand, lipids can go through lipid peroxidation further yielding a wide variety of highly reactive carbonyl species (RCS), such as oxidatively truncated phospholipids and short-chain carbonyl derivatives, including 2-alkenals, 4-hydroxy-2-alkenals and ketoaldehydes or dialdehydes (**Figure 1**). RCS are able to interact and covalently bind to nucleophilic groups of proteins, forming reversible and/or irreversible modifications and generating the so-called advanced lipoxidation end-products (ALEs) [3]. With respect to the 2-alkenals, acrolein (ACR) is by far the strongest electrophile [1]. ACR arises from both peroxidation of polyunsaturated fatty acids and from the metabolism of amino acids, polyamines, and drugs, and has the highest reactivity with protein nucleophiles and selectively reacts with cysteine, histidine, and lysine, being lysine-adducts the most stable products [3]. Prolonged exposure to ACR can cause myocyte dysfunction, myocyte necrosis and apoptosis and ultimately lead to cardiomyopathy and cardiac failure [4]. 4-hydroxy-2-nonenal (4-HNE), the most studied 4-hydroxy-2-alkenal, results from the breakdown of oxidized phospholipids containing omega-6 polyunsaturated fatty acid chains, such as linoleic acid and arachidonic acid [5]. 4-HNE might interact with cysteine and histidine residues triggering Michael addition-type products, while the covalent reaction with lysine residues yields the formation of pyrrole derivatives [6]. 4-HNE is believed to be largely responsible for the cytopathologic effects observed during oxidative stress *in vivo* and directly depresses the contractile function, enhances ROS formation, and can contribute to many cardiovascular diseases, including atherosclerosis, myocardial ischemia-reperfusion injury, HF and cardiomyopathy [7,8]. Ketoaldehydes/dialdehydes is another class of RCS that comprises malondialdehyde and glyoxal. Malondialdehyde (MDA) is the most abundant dialdehyde-derivative small fragmentation product [9] that may result either as side product of enzymatic arachidonic acid oxygenation or as end product of oxidative omega-3 and omega-6 fatty acids

degradation [10,11]. MDA primarily reacts with lysine residues generating enaminal adducts as major reaction product [6]. In the cardiac context, MDA has showed to be directly involved in cardiac dysfunction, a typical feature of HF [12]. Additionally, MDA plasma levels are strongly associated with the chronicity of the HF state [13]. In turn, glyoxal (GO) can be formed during the oxidation of both carbohydrates and lipids and might react with lysine, arginine or histidine residues leading to carboxymethyl derivatives. Glyoxal also reacts with arginine residues to form imidazolone adducts [1].

On the other hand, molecules derived from reducing sugars or their oxidation products may also bind to nucleophilic residues within proteins in a process known as glycation, described by the Maillard reaction [1]. As reported in the Chapter I, the first step of the Maillard reaction explains the formation of Amadori-products (e.g. glycated albumin or glycated hemoglobin), also called early glycation products. After prolonged periods, these products may further undergo multiple dehydration, cyclization, oxidation and rearrangement processes, which might be catalyzed by oxidative stress and ROS, to generate irreversible advanced glycation end-products (AGEs) [14]. Two well characterized reducing sugar metabolites are GO and methyglyoxal (MGO), RCS classified respectively as dialdehyde or ketoaldehydes species (**Figure 1**), that can also undergo the Maillard reaction contributing to carbonyl stress through the formation of AGEs. Importantly, higher plasma levels of MGO have been associated with cardiovascular events in individuals with type 1 diabetes and may explain the increased risk for cardiovascular disease [15]. A well-known product derived from the reaction between GO and lysine residues is carboxymethyl-lysine (CML). CML is the most abundant glycation product and the first discovered, although it can also be formed by the advanced lipoxidation end product pathway. CML is considered a general marker of oxidative stress and protein damage in cardiovascular diseases and aging [16]. For instance, several groups have claimed that circulating CML is significantly raised in HF patients with respect to the control group, and this increase is associated with the severity, mortality rate, and prognosis of HF [17,18].

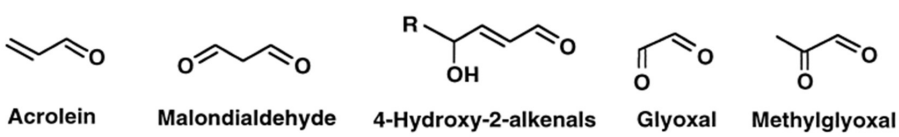

Figure 1. Structure some reactive carbonyl species generated from lipid peroxidation and glycation [1].

Nevertheless, all the above mentioned RCS have the ability to interact with nucleophilic side chains of proteins owing to the strong electrophilic moiety conferred by the carbonyl group. Hence, they act as precursors of AGEs and ALEs. The most relevant and abundant ALEs/AGEs that have been chemically characterized are summarized in **Table 2**.

In this chapter we aimed to detect the presence of either specific AGE-HSA adducts or other low abundant AGEs and ALEs (listed in **Table 2**) in HF plasma samples, together with the identification of target residues within the identified proteins. However, plasma is a complex sample that presents a wide dynamic range. Hence, although challenging, the implementation of enrichment/isolation strategies followed by off target LC-MS approaches is essential for the detection and identification of low abundance AGEs and ALEs. In particular and for this purpose, we pursued to apply a capture method based on the capability of the VC1 domain, a subdomain of RAGE receptor, to bind its natural ligands [19]. Considering that AGEs and ALEs are known to act as binders and activators of the receptor RAGE, this strategy might allow their enrichment. In addition, this system already worked for the enrichment of ALEs generated *in vitro* [20].

2. MATERIAL AND METHODS

2.1. Study population

Plasma samples collected at Centro Cardiologico Monzino were selected from a subset of healthy subjects (controls) and HF patients, according to their age, sex, and clinical characteristics. A detailed summary of the clinical characteristics is reported in **Table 1**.

	Control pool 1	Control pool 2	Control pool 3	HF pool 1	HF pool 2	HF pool 3
n	3	3	3	3	3	3
Age	53 ± 2	53 ± 1	51 ± 3	51 ± 4	66 ± 7	54 ± 5
Gender (m/f)	1/2	½	2/1	1/2	1/2	1/2
Weight (kg)	72.0 ± 3.1	69.0 ± 4.9	63.3 ± 7.7	67.3 ± 8.2	75.7 ± 12.3	77.7 ± 4.5
Height (cm)	170.7 ± 1.3	172.7 ± 2.7	167.7 ± 4.8	168.3 ± 6.7	165.7 ± 2.7	174-3 ± 4.7
BMI	24.7 ± 0.8	23.1 ± 1.0	22.41 ± 1.9	23.6 ± 1.5	27.4 ± 3.6	25.5 ± 0.2
Total cholesterol (mg/dL)	220.7 ± 11.3	190.3 ± 24.1	217.7 ± 3.8	173.3 ± 21.2	184.7 ± 27.4	190.3 ± 19.9
NYHA class III				3	3	3
EF%				31.6 ± 4.9	30.6 ± 3.1	34.1 ± 1.4
VO2 peak/Kg (mL/min/Kg)				22.8 ± 4.8	14.8 ± 1.7	11.2 ± 2.0

Table 1. Clinical characteristics of subjects categorized in healthy subjects, HF patients (NYHA class III), and HF patients (NYHA class IV). Data are expressed as mean ± SEM. BMI, body mass index; EF, ejection fraction; NYHA, New York Heart Association; VO2, oxygen consumption; m, male; f, female.

The study was approved by the Ethical Committee European Institute of Oncology and Monzino Cardiologic Center. All patients belonged to a cohort of HF patients monitored at our HF Unit and underwent a full clinical evaluation, standard laboratory tests, echocardiography, spirometry, and alveolar capillary diffusion, as well as cardiopulmonary exercise test. All patients had severe HF, NYHA class III, but were in stable clinical conditions.

2.2. In-solution digestion of isolated HSA from plasma of HF patients

HSA was removed from pooled plasma from HF patients (Pierce Albumin depletion kit (Thermo Fisher Scientific, Milan, Italy)). HSA concentration was determined by means of Bradford's method. 10 µg of protein were reduced with 10 mmol/L DTT at 56 °C for 30 min, and carbamidomethylated with 55 mmol/L iodoacetamide for 20 min at room temperature in the darkness. In-solution digestion was performed by incubating the samples with 0.5 µg trypsin (Roche, Monza, Italy) overnight at 37 °C. 2 µg of tryptic peptides from each sample were purified by use of ZipTip C18 pipette tip (Merck Millipore, Milan, Italy). The purified peptides were eluted with 0.1% formic acid (FA) in water/acetonitrile 2/8 (vol/vol) respectively, dried and stored at -20 °C.

2.3. *Mass spectrometry analysis of digested HSA from HF patients*

Tryptic peptides were analyzed at UNITECH OMICs (University of Milano, Italy) using a Dionex Ultimate 3000 nano-LC system (Sunnyvale CA, USA) connected to an Orbitrap Fusion™ Tribrid™ Mass Spectrometer (Thermo Scientific, Bremen, Germany) equipped with a nano-electrospray ion source. Peptide mixtures were pre-concentrated onto an Acclaim PepMap 100 - 100µm x 2cm C18 and separated on EASY-Spray column, 15 cm x 75 µm ID packed with Thermo Scientific Acclaim PepMap RSLC C18, 3 µm, 100 Å. The temperature was set to 35 °C and the flow rate was 300 nL/min. Mobile phases were the following: 0.1% formic acid (FA) in water (solvent A); 0.1% FA in water/acetonitrile (solvent B) with 2/8 ratio. Peptides were eluted from the column with the following gradient: 4% to 28% of B for 90 min and then 28% to 40% of B in 10 min, and to 95% within the following 6 min to rinse the column. Column was re-equilibrated for 20 min. Total run time was 130 min. One blank was run between replicates. MS spectra were collected over an m/z range of 375-1500 Da at 120,000 resolutions, operating in the data dependent acquisition mode (DDA), cycle time 3 sec between master scans. HCD was performed with collision energy set at 35 eV. Each sample was analyzed in two technical replicates.

2.4. Identification and localization of AGE-HSA and plasma AGEs and ALEs

The software Proteome Discoverer (version 1.3.0.339, Thermo Scientific, USA), implemented with the algorithm SEQUEST, was used to compare the experimental full and tandem mass spectra with the theoretical ones obtained by the *in silico* digestion of the HSA sequence (Uniprot

P02768) and UniProt human protein database. Trypsin was selected as the cleaving protease, allowing a maximum of 2 missed cleavages. Peptide and fragment ion tolerances were set to 5 ppm and 10 mmu, respectively. Cysteine carbamidomethylation was set as fix modification (+57.02147); methionine oxidation was allowed as a variable modification in addition to the modifications listed in **Table 2**. In the case of HSA, only variable modifications arising from GO and MGO were studied. As a quality filter, only peptide with an Xcore value greater than 2.2 for doubly-charged peptides, 2.5 for triply-charged, 2.75 for quadruply-charged peptide ions, and 3 for charge states quintuple or higher were considered as genuine peptide identifications. To ensure the lowest number of false positives, the mass values experimentally recorded were further processed through a combined search with the Database Decoy, where the protein sequences are inverted and randomized. This operation allows the calculation of the false discovery rate (FDR) for each match, where all the proteins out of range of FDR between to 0.01 (strict) and 0.05 (relaxed) were rejected. For the localization of ALE/AGE-deriving modifications in the peptides arising from the pull-down and AGE-deriving modifications in the peptides coming from isolated HSA, the MS/MS spectra of modified peptides were manually inspected; for the confident mapping of the modification sites, spectra were requested to match the expected ions (b and/or y) neighboring the modified amino acid residue both at the N- and C-termini.

2.5. VC1 pull-down assay

VC1-His-Strep was expressed and purified from yeast *Pichia pastoris* culture supernatant as previously described [23]. The recombinant protein was immobilized on streptavidin-coated magnetic beads by exploiting the affinity of the Strep tag towards streptavidin. In order to obtain the VC1-resin, 51 µg of purified VC1-His-Strep in 170 µl of 20 mM HEPES pH 7.1, 100 mM NaCl (from now on referred to as buffer A) were added to 50 µl of homogenized streptavidin coated-beads 10% slurry, previously equilibrated with the same buffer.

To obtain the control resin a volume of 170 µl of buffer A was added to the same amount of beads in a different tube, thus, the control resin does not contain the VC1 recombinant protein. After 1 h of incubation at 4 °C on a rotary mixer, the unbound material was carefully removed and the magnetic beads were washed twice with 500 µl of buffer A. The VC1- and Control-resins were incubated for 2 h at 4 °C on a rotary mixer with 160 µl containing 800 µg of plasma proteins diluted in 20 mM HEPES pH 7.1, 100 mM NaCl, 10 mM $CaCl_2$, 0,5 % TritonX-100 (buffer B). The unbound material was carefully removed and the beads were washed twice with 500 µl of buffer B. The elution was performed by boiling the beads for 5 min in 15 µl of Laemmli Sample Buffer 4x mixed with 50 mM DTT (final), and then with other 10 µl of buffer A. The two eluates were pooled.

4-HNE		
PTM	**Residue Involved**	**ΔM**
Michael adduct (HNE-MA)	Cys His Lys Arg	+ 156.110502 Da
Schiff base (HNE-SB)	Lys Arg	+ 138.01446 Da
2-pentilpyrrole (PP)	Lys Arg	+ 120.0939 Da
Dehydropentylfuran (DHPF)	Cys His Lys Arg	+ 138.10446 Da
MDA		
PTM	**Residue Involved**	**ΔM**
N-propenal-lysine (NPK)	Lys	+ 54.01056 Da
Di-hydropyridine-lysine (DHPK)	Lys	+ 134.03678 Da
Malondialdehyde argpyrimidine(MDA-RP)	Arg	+ 36.0000 Da
ACR		
PTM	**Residue Involved**	**ΔM**
Michael adduct (propanal derivative) (ACR-MA)	Cys Lys His	+ 56.02621 Da
Hydroxy-tetra-hydropyrimidine (propane-arginine) (HTPR)	Arg	+ 56.02621 Da
Double Michael adduct (2ACR-KMA)	Lys	+ 112.05243 Da
Schiff base (ACR-SB)	Lys	+ 38.01565 Da
Formyl-dehydro-piperidyl-lysine (FDPK)	Lys	+ 94.04186 Da
Methylpyridine-lysine (MPK)	Lys	+ 77.03912 Da
GO		
PTM	**Residue Involved**	**ΔM**
Carboxymethyl derivative (GO_CM)	Lys Arg Cys	+ 58.00548 Da
Imidazolone (GO_IR)	Arg	+ 39.99492 Da
MGO		
PTM	**Residue Involved**	**ΔM**
Carboxyethyl derivative (MGO_CE)	Lys Cys Arg	+ 72.02113 Da
Methylimidazolone	Arg	+ 54.01056 Da
Argpyrimidine (RP)	Arg	+ 80.02622 Da
Tetrahydropyrimidine (THPR)	Arg	+ 144.04226 Da

Table 2. Known (literature based) covalent adducts induced by 4-HNE, MDA, ACR, GO and MGO set as variable modifications within the Proteome Discoverer parameters for the identification and localization of ALE/AGE-deriving adducts.

2.6. Electrophoretic procedures

The fractions obtained from pull-down experiments were analyzed by SDS PAGE. To 2 µl of input and unbound fractions, 2 µl of Laemmli Sample Buffer 4x mixed with 50 mM DTT (final) together with 6 µl of buffer A were added. The samples were denatured by incubation at 95 °C for 5 min. Input, unbound and elution samples from pooled plasma of HF patients or healthy subjects were separated by SDS-PAGE on Any KD ™ Mini Protean® TGX ™ precast gels and stained with Bio-Safe Coomassie blue (Bio-Rad). Images were acquired using the calibrated densitometer GS-800 and analyzed by the software Quantity one (Bio-Rad).

2.7. In-gel digestion of proteins subjected to the pull-down assay

Protein bands corresponding to the diluted pooled plasma samples (input), and those arising from the fraction retained by VC1- and control-resin, were excised from gels using a scalpel, finely chopped, and transferred to new and independent eppendorfs. An aliquot of 200 µl of destaining solution (25 mM ammonium bicarbonate (NH_4HCO_3)/ACN 1:1 (v/v)) was added to each gel portion and heated at 56 °C for 10 min in the thermomixer (1400 rpm); the destaining solution was then discarded. This step was repeated until destaining was completed. Then, destaining solution was replaced by pure acetonitrile (ACN 100%) under the same conditions. Afterwards, gel pieces were incubated with 150 µl of reducing solution (10 mM DTT in 50 mM NH_4HCO_3) at 56 °C for 1 h in the thermomixer (800 rpm), washed with 150 µl digestion buffer (50 mM NH_4HCO_3), and then with 150 µl of alkylating solution (55 mM iodoacetamide in 50 mM NH_4HCO_3) at room temperature for 45 min in the dark. Subsequently, gel pieces were washed with digestion buffer and finally dried with ACN 100%. In-gel digestion of gel spots was performed by overnight-incubation at 37 °C with 1 µg of sequencing-grade trypsin (Roche) dissolved in digestion buffer. The peptide mixtures were acidified with formic acid up to a final concentration of 1%. To guarantee better protein detection, peptide mixtures were extracted by a 10 min-incubation with 3% TFA/30% ACN in H_2O MilliQ (extraction solution) and by an additional 10 min-incubation with ACN 100%.

The two extracts were combined and dried in a vacuum concentrator (Martin Christ.). Digested peptide mixtures were then dissolved in an appropriate volume (20 µl) of 0.1% formic acid for MS analysis.

2.8. Mass spectrometry analyses of AGEs and ALEs in plasma

Peptides arising from digestion in-gel were separated by reversed-phase (RP) nanoscale capillary liquid chromatography (nanoLC) and analyzed by electrospray tandem mass spectrometry (ESI-MS/MS). For each analysis 5 µl of solubilized peptides were injected onto a C18HALO PicoFrit column (75 mM x 10 cm, 2.7 mM particles, pores 100 Å, New Objective, USA) by means of an autosampler. Samples were loaded onto the fused silica column at 400 nL/min of mobile phase

consisting of 99% of phase A and 1% of phase B (0.1% HCOOH in CH3CN) for 15 min. Peptide separation was performed with a 55 min linear gradient of phase B (1–35%). The separative gradient was followed by 5 min at 80% of phase B to rinse the column, and 15 min of 99% of phase A and 1% of phase B served to re-equilibrate the column to the initial conditions. The nano-chromatographic system, an UltiMate 3000 RSLCnano System (Dionex), was connected to an LTQ-Orbitrap XL mass spectrometer (Thermo Scientific Inc., Milan, Italy) equipped with a nanospray ion source (dynamic nanospray probe, Thermo Scientific Inc., Milan, Italy) set as follows: positive ion mode, spray voltage 1.8 Kv; capillary temperature 220 °C, capillary voltage 35 V; tube lens offset 120 V. The LTQ-Orbitrap XL mass spectrometer was operated in data-dependent acquisition mode (DDA) to acquire both the full MS spectra and the MS/MS spectra. Full MS spectra were acquired in "profile" mode, by the Orbitrap (FT) analyzer, in a scanning range between 300 and 1500 m/z, using a capillary temperature of 220 °C, AGC target = 5 × 105 and resolving power 60,000 (FWHM at 400 m/z).

Tandem mass spectra MS/MS were acquired by the Linear Ion Trap (LTQ) in CID mode, automatically set to fragment the nine most intense ions in each full MS spectrum (exceeding 1 ×104 counts) under the following conditions: centroid mode, isolation width of the precursor ion of 2.5 m/z, AGC target 1 × 104 and normalized collision energy of 35 eV. Dynamic exclusion was enabled (exclusion dynamics for 45 s for those ions observed 3 times in 30 s). Charge state screening and monoisotopic precursor selection were enabled, singly and unassigned charged ions were not fragmented. Xcalibur software (version 2.0.7, Thermo Scientific Inc., Milan, Italy) was used to control the mass spectrometer.

3. RESULTS

Human serum albumin (HSA) is the most abundant protein in plasma and, hence, it is highly susceptible to undergo oxidative post-translational modifications. Keeping in mind that we previously found raised plasma levels of early glycated albumin in severe HF patients (Chapter I), we decided to look for advanced glycation-HSA derivatives on isolated HSA.

To that end, we firstly separated HSA from the rest of plasma components, then HSA was digested and finally we proceeded to analyze the advanced glycation sites within the modified peptides by means of mass spectrometry.

Proteome Discoverer software was used for the identification of the adducted peptides arising from GO and MGO containing the mass increase reported in **Table 2**. Fragmentation spectra of some representative AGE-HSA peptides are showed in **Figure 2**. The relative extent of each modified residue was calculated by determining the peak area of the modified peptide with respect to the native one.

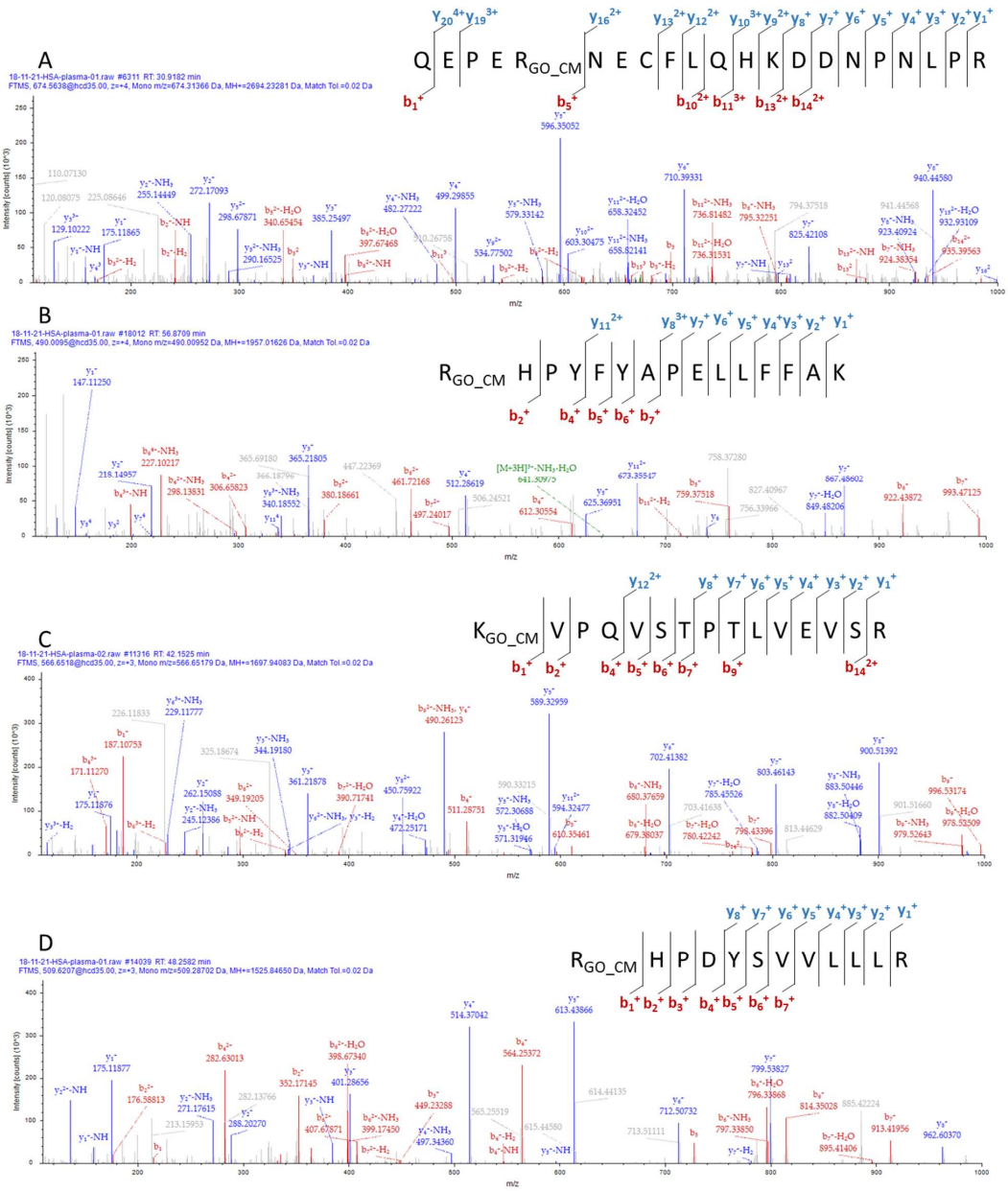

Figure 2. Fragmentation mass spectra (MS/MS) of four representative advanced glycated peptides present in the plasma of HF patients and the relevant fragments for their attribution. A) Spectrum corresponding to the peptide QEPERNECFLQHKDDNPNLPR (modified residue arg98), B) RHPYFYAPELLFFAK (modified residue arg145), C) KVPQVSTPTLVEVSR (modified residue lys414), and D) RHPDYSVVLLLR (modified residue arg337). The calculated fragment ions b^{+}, b^{2+}, b^{3+}, y^{+}, y^{2+}, $y^{3+}$and y^{4+} of the adducted peptides are highlighted by red (b series) and blue (y series) colors. GO_CM, carboxymethyl derivative.

After the analysis, 14 glycated residues were highlighted although we only detected covalent adducts induced by GO, specifically carboxymethyl derivatives (GO_CM) and imidazolone (GO_IR) adducts (**Table 3)**. In particular 8 carboxymethyl lysine, 6 carboxymethyl arginine and 1 imidazolone adducts were pointed out. The most abundant modified residues were lys20, arg98 and lys402 that accounted for roughly 50% of relative abundance, followed by a group of 5 residues (lys64, arg145, arg98, lys359 and arg445) that presented a relative abundance between the 23-8%. Conversely, the remaining identified residues showed a relative abundance below 1%. On the other hand, after pointing out the presence of AGE-HSA adducts in plasma, our next objective was to look for advanced glycation and lipoxidation end products (AGEs and ALEs) in other proteins than HSA. In other words, in the total protein content of HF plasma samples.

To reduce plasma complexity we took advantage of an enrichment system based on the capability of the VC1 domain of the RAGE receptor to bind AGEs and ALEs which are, presumably, natural ligands of the receptor. In this pull-down strategy, the VC1-His-Strep recombinant protein remains attached to streptavidin-coated magnetic beads acting as stationary phase (VC1-resin). A VC1-free coated resin (control-resin) was used as control to further discard the proteins that bound non-specifically to the streptavidin-coated magnetic beads. Therefore, we pooled separately the plasma of HF and healthy samples and performed the pull-down assay (n=3) as described in "material and methods" section. Then, the different fractions (input, unbound, and elution from either VC1- or control-resin) arising from each pool (HF pool 1, 2, and 3, as well as healthy pool 1, 2, and 3) were loaded in a SDS-PAGE to allow protein separation **(Figure 3)**. When comparing the pattern band from the VC1 elution fraction (VC1 E) with one coming from the control elution fraction (CTR E) observed in each HF gel (HF pool 1, 2, and 3) we did not detect the presence of different bands besides the signals that correspond the two glycovariants of the VC1 domain. The same trend was observed when comparing VC1 E and CTR E arising from each healthy pool gel. Additionally, the profile observed in all the pull-down fractions (input, unbound and elution from VC1- and control-resins) belonging to HF pool gels were substantially similar to the respective ones observed in the healthy pool gels.

Nevertheless, after protein separation by means of SDS-PAGE, we proceed to excise the bands. Proteins within each selected gel band were digested. Tryptic peptides were afterwards subjected to untargeted LC-MS/MS for the detection of adducts generated from reactive carbonyl species such as 4-HNE, MDA, ACR, GO or MGO and represented in **Table 2**. After the analysis with Proteome Discoverer, proteins that showed a non-specific binding towards the streptavidin-coated magnetic beads were discarded. Hence, common proteins identified both in the VC1- and in the control-resins were removed. Additionally, identified proteins in the VC1 fraction that appeared either in the patients or in the healthy subjects were deleted since we were looking only for specific modified proteins related to HF pathology. Unfortunately, after applying the previous criteria no reliable AGE- or ALE-adducted proteins were identified.

Annotated Sequence *	Modifications	Residue	Average Peak Area		Relative Abundance [%]
			unmodified peptide	modified peptide	
1	**K10(GO_CM)**; C24(Cam)	**Lys20**	1,33E+07	1,67E+07	**55,70**
2	**R5(GO_CM);** C8(Cam)	**Arg98**	1,38E+09	1,58E+09	**53,28**
3	C3(Cam); **K13(GO_CM)**	**Lys402**	4,71E+09	4,27E+09	**47,60**
4	C2(Cam); C11(Cam); **K13(GO_CM)**	**Lys64**	9,44E+08	2,79E+08	**22,78**
5	**R1(GO_CM)**	**Arg145**	1,17E+09	3,11E+08	**21,05**
6	**R5(GO_IR);** C8(Cam)	**Arg98**	1,38E+09	3,61E+08	**20,72**
7	**K8(GO_CM)**; C9(Cam); C10(Cam); C18(Cam)	**Lys359**	4,90E+07	6,96E+06	**12,43**
8	**R1(GO_CM);** C4(Cam); C17(Cam)	**Arg445**	8,88E+09	8,42E+08	**8,66**
9	**K9(GO_CM);** C11(Cam)	**Lys73**	6,86E+09	4,01E+07	**0,58**
10	**R1(GO_CM)**; C3(Cam)	**Arg485**	8,04E+09	3,44E+07	**0,43**
11	**K1(GO_CM)**	**Lys414**	1,34E+10	3,49E+07	**0,26**
12	**R1(GO_CM)**	**Arg337**	8,28E+09	1,98E+07	**0,24**
13	**K2(GO_CM)**	**Lys12**	9,76E+08	1,62E+06	**0,17**
14	**K6(GO_CM)**; C20(Cam)	**Lys378**	1,65E+10	1,04E+07	**0,06**

Table 3. List of carboxymethyl (GO_CM) and imidazole (GO_IR) derivatives identified in plasma HSA from heart failure patients. Cam, carbamidomethylation.

*1) FKDLGEENF**k**ALVLIAFAQYLQQcPFEDHVK, 2) QEPE**r**NEcFLQHKDDNPNLPR, 3) QNcELFEQLGEY**k**FQNALLVR, 4) TcVADESAENcD**k**SLHTLFGDK, 5) **r**HPYFYAPELLFFAK, 6) QEPE**r**NEcFLQHKDDNPNLPR, 7) TYETTLE**k**ccAAADPHEcYAK, 8) **r**MPcAEDYLSVVLNQLcVLHEKTPVSDR, 9) SLHTLFGD**k**LcTVATLR, 10) **r**PcFSALEVDETYVPK, 11) **k**VPQVSTPTLVEVSR, 12) **r**HPDYSVVLLLR, 13) F**k**DLGEENFK, 14) VFDEF**k**PLVEEPQNLIKQNcELFEQLGEYKFQNALLVR.

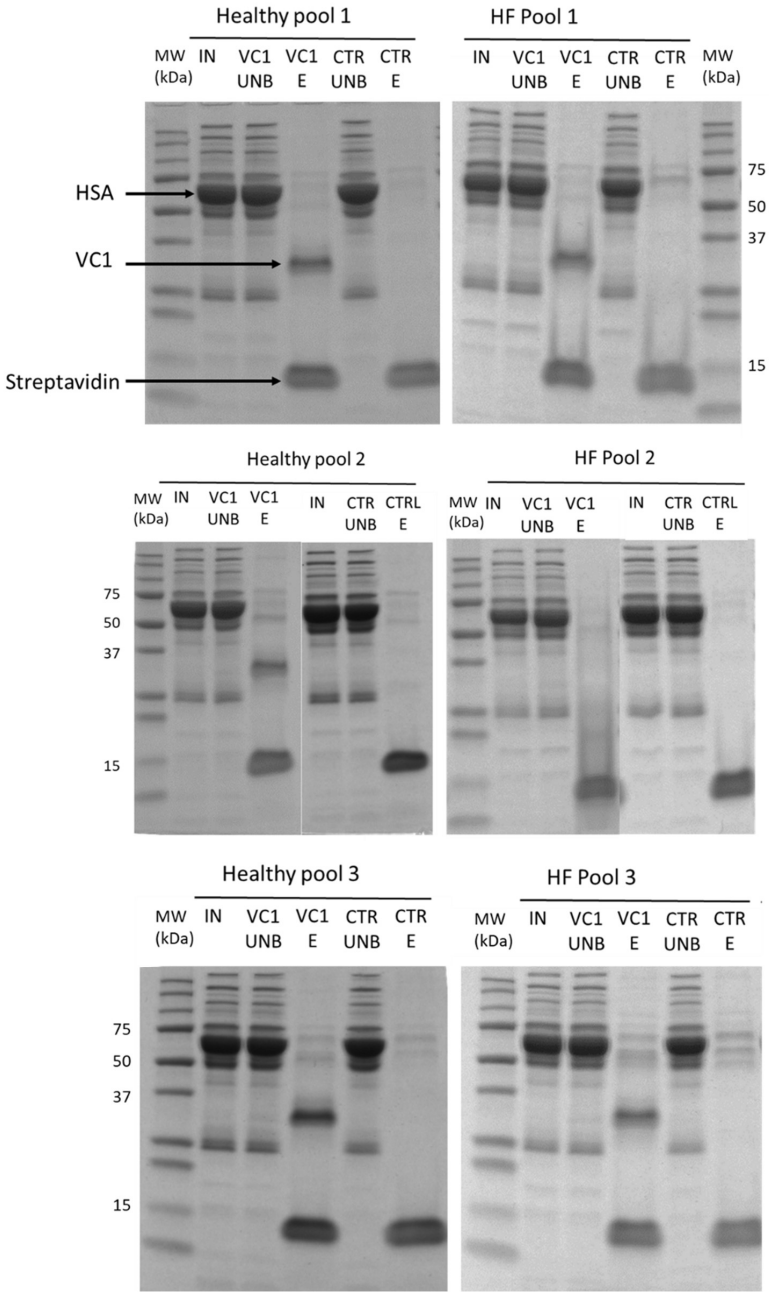

Figure 3. SDS PAGE analysis followed by Coomassie staining after VC1 pull-down assay with pooled plasma from healthy (left panel) or HF (right panel) subjects from the three independent pools from each condition. The gels show diluted plasma in buffer A used as input (IN), the unbound fractions (UNB) and eluates (E) both from VC1 and control (CTR) resins. Since the elution is performed in denaturing conditions, this step removes any associated molecule from the resin, including the two VC1 glycovariants (34 and 36 kDa) and streptavidin (14 kDa), indicated by arrows. HSA (66 kDa) is also pointed by an arrow.

4. DISCUSSION

The identification, characterization and quantification of AGEs and ALEs in pathological conditions have become of great interest in the last years because of their correlation with the onset and progression of diseases. Moreover, it helps to better understand the pathways underlying some pathological mechanisms associated to the disease.

It is likely that HSA undergo oxidative post-translational modifications owing to its abundance. Therefore, in this project we have investigated the presence of advanced glycation adducts on HSA. 14 different lysine and arginine adducts were identified and quantified, but the most abundant modified residues by glyoxal were lys20 and arg98. With respect to the results obtained in the Chapter I, AGE-HSA presented more glycomodified residues than GA and no relevant common residues were shared. Interestingly, in a very recent published article it was reported that advanced stage glycation modifications at lys536, lys573, and arg348 were observed only in the plasma of HF patients and not in healthy subjects [19]. The reason why we did not found these adducted residues in the present work could be due to differences in the clinical characteristics of the patients: patients enrolled in our study were slightly younger, exhibited a more severe degree of the pathology, and a higher LVEF value. By contrast, our results confirmed that one of the most modified residues, arg98, underwent only advanced glycation, as reported in the mentioned work [19]. One limitation of our study is that the analysis of advanced glycation residues in plasma of healthy subjects was not performed.

From a functional point of view, *in vivo* AGE-HSA isolated from HF patients induces the expression of both ICAM-1 and VCAM-1 in endothelial cells, contributing to inflammatory processes [19]. In addition, AGE-HSA derivatives can stimulate the RAGE receptor which in turn mediates its pathological effects via the activation of NADPH oxidase that may further induce an oxidative stress state through ROS production [20]. As a matter of fact, both inflammation and oxidative stress are involved in the onset of HF. Additionally, the identification, characterization and relative quantification of the advanced glycation-HSA pattern could be relevant for drug therapy design in order to avoid or reduce its pathological downstream effects associated to HF.

Due to these successful outcomes, we next decided to go one step further and to investigate the presence of AGE- and ALE-adducted proteins of low abundance in the total plasma protein content of HF patients in order to identify the modified proteins and to localize the targeted residues together with the type of modification. Because AGEs and ALEs are present at very low abundance in plasma, it is essential to reduce the complexity of the matrix. In this context, various strategies have been described to aid in the identification of low abundant molecules. For instance, the derivatization of the carbonyl groups with O-(biotinylcarbazoylmethyl)hydroxylamine or by means of 2,4-dinitrophenylhydrazine (DNPH) followed by avidin affinity chromatography enrichment or two-dimensional gel electrophoresis separation, respectively [21,22]. However, not

all AGEs and ALEs adducts contain a carbonyl group within their molecular entities. Hence, we took advantage of a pull-down strategy based on the ability of VC1 domain, a subdomain within the RAGE receptor, to bind AGE/ALE derivatives regardless the carbonyl moiety [23]. When comparing the stained SDS-PAGEs from the two conditions (healthy subjects and HF patients), we did not observe variations in the protein pattern band between the VC1- and the control-resins in any plasma pool. In addition, while the values of volume of O_2 uptake normalized by body mass (VO_2 peak/kg) gradually diminished from HF pool 1 to HF pool 3, no significant differences were observed when comparing the gels from HF pool 1, HF pool 2 and HF pool 3. Moreover, after MS spectra analysis no reliable AGEs or ALEs specific of HF were found, even though the enrichment of ALEs generated *in vitro* through this capture method was already successfully proved [24]. Unfortunately, we did not prosper in the attempt of enriching AGEs and ALEs in complex samples such as plasma. The fact that the identified carboxymethyl- and imidazolone-HSA adducts when HSA was isolated from the rest of plasma components were not enriched by means of the VC1 pull-down strategy which suggests that:

1) The surrounding moiety of the adducted residues is not able to bind the RAGE receptor either because it has been masked by other plasma components or because these AGEs/ALEs are not ligands of VC1 and therefore cannot be enriched. For AGEs/ALEs to bind the RAGE receptor, the covalent adducts should greatly reduce or abolish the basicity of the target amino acid, and the basic residues should be at the center of a set of carboxylic acids which, once the residue is modified, become available to freely contact the RAGE positive residues [24].

2) The concentration level of AGEs/ALEs present in HF plasma samples is so limited that protein-ligand complex affinity constant cannot be reached. Indeed, the binding affinity between RAGE and MGO-bovine serum albumin significantly increased when increasing molar rate of MGO-BSA [25]. A possible reason why ALEs generated *in vitro* were captured by the VC1 resin while endogenous plasma ALEs/AGEs did not bind to the receptor could be due the fact that the *in vitro* levels of reactive carbonyl precursors were considerably higher than the *in vivo* levels of the same precursors.

3) To detect low abundance products it is needed to use the newest ultra-high resolution MS instruments that present an improved sensitivity for extended coverage of low abundant proteins and a faster scanning MS detectors for increased throughput. Indeed, AGE-HSA adducts and modified residues have been detected by means of an Orbitrap Fusion Tribrid Mass Spectrometer.

In conclusion, in this study we have successfully characterized and relatively quantified the most susceptible amino acids of HSA associated to the pathology of HF target of undertaking advanced glycation. We attempt to investigate AGEs and ALEs in other plasma proteins of low abundance by applying the VC1 pull-down strategy, but unfortunately we were not able to enrich

AGEs/ALEs from HF patients, indicating the need for more sensitive enrichment methods or mass spectrometers.

5. REFERENCES

[1] K. Uchida, Role of reactive aldehyde in cardiovascular diseases, Free Radic. Biol. Med. (2000). doi:10.1016/S0891-5849(00)00226-4.

[2] E. Gianazza, M. Brioschi, A.M. Fernandez, C. Banfi, Lipoxidation in cardiovascular diseases, Redox Biol. (2019) 101119. doi:10.1016/j.redox.2019.101119.

[3] R.J. Henning, G.T. Johnson, J.P. Coyle, R.D. Harbison, Acrolein Can Cause Cardiovascular Disease: A Review, Cardiovasc. Toxicol. (2017). doi:10.1007/s12012-016-9396-5.

[4] C.M. Spickett, The lipid peroxidation product 4-hydroxy-2-nonenal: Advances in chemistry and analysis, Redox Biol. (2013). doi:10.1016/j.redox.2013.01.007.

[5] K. Uchida, Current status of acrolein as a lipid peroxidation product, Trends Cardiovasc. Med. (1999). doi:10.1016/S1050-1738(99)00016-X.

[6] V.R. Mali, S.S. Palaniyandi, Regulation and therapeutic strategies of 4-hydroxy-2-nonenal metabolism in heart disease, Free Radic. Res. (2014). doi:10.3109/10715762.2013.864761.

[7] H. Esterbauer, R.J. Schaur, H. Zollner, Chemistry and biochemistry of 4-hydroxynonenal, malonaldehyde and related aldehydes, Free Radic. Biol. Med. (1991). doi:10.1016/0891-5849(91)90192-6.

[8] K. Uchida, K. Sakai, K. Itakura, T. Osawa, S. Toyokuni, Protein modification by lipid peroxidation products: Formation of malondialdehyde-derived N(ε)(2-propenal)lysine in proteins, Arch. Biochem. Biophys. (1997). doi:10.1006/abbi.1997.0266.

[9] D.R. Janero, Malondialdehyde and thiobarbituric acid-reactivity as diagnostic indices of lipid peroxidation and peroxidative tissue injury, Free Radic. Biol. Med. (1990). doi:10.1016/0891-5849(90)90131-2.

[10] A. Ayala, M.F. Muñoz, S. Argüelles, Lipid peroxidation: Production, metabolism, and signaling mechanisms of malondialdehyde and 4-hydroxy-2-nonenal, Oxid. Med. Cell. Longev. (2014). doi:10.1155/2014/360438.

[11] D. V. Folden, A. Gupta, A.C. Sharma, S.Y. Li, J.T. Saari, J. Ren, Malondialdehyde inhibits cardiac contractile function in ventricular myocytes via a p38 mitogen-activated protein kinase-dependent mechanism, Br. J. Pharmacol. (2003). doi:10.1038/sj.bjp.0705384.

[12] C.R. Díaz-Vélez, S. García-Castiñeiras, E. Mendoza-Ramos, E. Hernández-López, Increased malondialdehyde in peripheral blood of patients with congestive heart failure, Am. Heart J. (1996). doi:10.1016/S0002-8703(96)90063-0.

[13] G. Vistoli, D. De Maddis, A. Cipak, N. Zarkovic, M. Carini, G. Aldini, Advanced glycoxidation and lipoxidation end products (AGEs and ALEs): An overview of their mechanisms of formation, Free Radic. Res. (2013). doi:10.3109/10715762.2013.815348.

[14] N.M.J. Hanssen, J. Westerink, J.L.J.M. Scheijen, Y. Van Der Graaf, C.D.A. Stehouwer, C.G.

Schalkwijk, Higher plasma methylglyoxal levels are associated with incident cardiovascular disease and mortality in individuals with type 2 diabetes, Diabetes Care. (2018). doi:10.2337/dc18-0159.

[15] C. Delgado-Andrade, Carboxymethyl-lysine: Thirty years of investigation in the field of AGE formation, Food Funct. (2016). doi:10.1039/c5fo00918a.

[16] S. Willemsen, J.W.L. Hartog, D.J. Van Veldhuisen, P. Van Der Meer, J.F. Roze, T. Jaarsma, C. Schalkwijk, I.C.C. Van Der Horst, H.L. Hillege, A.A. Voors, The role of advanced glycation end-products and their receptor on outcome in heart failure patients with preserved and reduced ejection fraction, Am. Heart J. (2012). doi:10.1016/j.ahj.2012.07.027.

[17] J.W.L. Hartog, A.A. Voors, C.G. Schalkwijk, J. Scheijen, T.D.J. Smilde, K. Damman, S.J.L. Bakker, A.J. Smit, D.J. Van Veldhuisen, Clinical and prognostic value of advanced glycation end-products in chronic heart failure, Eur. Heart J. (2007). doi:10.1093/eurheartj/ehm486.

[18] G. Degani, A.A. Altomare, M. Colzani, C. Martino, A. Mazzolari, G. Fritz, G. Vistoli, L. Popolo, G. Aldini, A capture method based on the VC1 domain reveals new binding properties of the human receptor for advanced glycation end products (RAGE), Redox Biol. (2017). doi:10.1016/j.redox.2016.12.017.

[19] B. Paradela-Dobarro, S.B. Bravo, A. Rozados-Luís, M. González-Peteiro, A. Varela-Román, J.R. González-Juanatey, J. García-Seara, E. Alvarez, Inflammatory effects of in vivo glycated albumin from cardiovascular patients, Biomed. Pharmacother. (2019). doi:10.1016/j.biopha.2019.108763.

[20] G. Daffu, C.H. del Pozo, K.M. O'Shea, R. Ananthakrishnan, R. Ramasamy, A.M. Schmidt, Radical roles for RAGE in the pathogenesis of oxidative stress in cardiovascular diseases and beyond, Int. J. Mol. Sci. (2013). doi:10.3390/ijms141019891.

[21] R.C. Bollineni, M. Fedorova, M. Blüher, R. Hoffmann, Carbonylated plasma proteins as potential biomarkers of obesity induced type 2 diabetes mellitus, J. Proteome Res. (2014). doi:10.1021/pr500324y.

[22] C. Banfi, M. Brioschi, S. Barcella, F. Veglia, P. Biglioli, E. Tremoli, P.G. Agostoni, Oxidized proteins in plasma of patients with heart failure: Role in endothelial damage, Eur. J. Heart Fail. (2008). doi:10.1016/j.ejheart.2008.01.016.

[23] G. Degani, M. Colzani, A. Tettamanzi, L. Sorrentino, A. Aliverti, G. Fritz, G. Aldini, L. Popolo, An improved expression system for the VC1 ligand binding domain of the receptor for advanced glycation end products in Pichia pastoris, Protein Expr. Purif. (2015). doi:10.1016/j.pep.2015.06.012.

[24] M. Mol, G. Degani, C. Coppa, G. Baron, L. Popolo, M. Carini, G. Aldini, G. Vistoli, A. Altomare, Advanced lipoxidation end products (ALEs) as RAGE binders: Mass spectrometric and computational studies to explain the reasons why, Redox Biol. (2018). doi:10.1016/j.redox.2018.101083.

[25] A. Syed, Q. Zhu, E.A. Smith, Ligand binding affinity and changes in the lateral diffusion of receptor for advanced glycation endproducts (RAGE), Biochim. Biophys. Acta - Biomembr. (2016).

CHAPTER IV:

Phospholipidome profile of heart failure patients

PHOSPHOLIPIDOME PROFILE OF HEART FAILURE PATIENTS

1. INTRODUCTION

Lipids are well known structural elements of biological membranes, which have also been found to mediate key signaling mechanisms, for instance via activation of a variety of receptors, including G protein-coupled and nuclear receptors, in several biological processes such as cell survival, proliferation or inflammation [1]. Additionally, lipids actively contribute to the onset and the development of cardiovascular diseases (CVD) such as atherosclerosis [2] or coronary artery disease (CAD) [3], which represent two antecedent causes of HF. Seeking the up- or down-regulation of certain lipid species in pathological contexts could lead to the discovery of novel biomarkers. Remarkably, recent advances in high-throughput mass spectrometry techniques have enabled the development of –omic analyses, and lipidomic profiling has emerged as a promising tool in the identification of novel biomarkers of CVD. For example, lipids belonging to lysophosphatidylcholines (LPC), sphingomyelins (SM), ceramides, and phosphatidylcholines (PC) subclasses are highly enriched in atherosclerotic plaque, while serum levels of LPC (18:2) were significantly lowered in CAD patients than in the control group [4]. In addition, decreased levels in LPC (16:0) and LPC (20:4) are related to the onset and progression of CVD [5]. Moreover, increased levels of triacylglyceride (54:2), cholesteryl ester (16:1), and phosphatidylethanolamine (PE) (36:5) are the most potent risk factor predictors of CVD [6]. The observation of different lipid signatures in diverse CVD suggests that lipid dysregulation could also occur upon HF. Altered lipid levels could serve as discriminators between healthy control subjects and patients with HF. Furthermore, such variations could shed light on the etiology of HF and facilitate the understanding of its mechanisms.

In this context, changes in the abundance of some phospholipids (PLs) belonging to the PC, SM or PE lipid subclasses have been observed in the plasma and in the erythrocytes of HF patients [7,8]. However, to the best of our knowledge, no previous works have studied the plasma phospholipidome of male and female HF patients.

In the present pilot study, we used hydrophilic interaction liquid chromatography-high resolution mass spectrometry (HILIC-MS/MS) for a comprehensive plasma phospholipidomic profiling of human HF, with the aim of defining the differences in circulating plasma phospholipids between healthy subjects and HF patients, and between age- and sex-matched male and female HF patients.

2. MATERIAL AND METHODS

2.1. Reagents/chemicals

Phospholipid internal standards 1,2-dimyristoyl-sn-glycero-3-phosphocholine (dMPC), 1,2-dimyristoyl-sn-glycero-3-phosphoethanolamine (dMPE), 1,2-dimyristoyl-sn-glycero-3-phospho-(10-rac-glycerol) (dMPG), were purchased from Avanti Polar Lipids, Inc. (Alabaster, AL). Phospholipid standards 1-palmitoyl-2-oleoyl-sn-glycero-3-phosphocholine (PC (34:1)) and 1-palmitoyl-2-linoleoyl-sn-glycero-3-phosphoethanolamine (PE (34:2)) were purchased from Cayman Chemical (Michigan, USA). Chloroform, methanol and acetonitrile were purchased from Fisher scientific (Leicestershire, UK); Water Milli-Q purity was purchased from Millipore (Synergy1, Millipore Corporation, Billerica, MA). All the solvents were of high-performance liquid chromatography (HPLC) grade and were used without further purification. All the other reagents and chemicals used were of the highest grade of purity commercially available.

2.2. Study population

10 patients with HF (5 females and 5 males) were enrolled in this study. Patients belong to a group of individuals regularly followed-up at our HF unit. Clinicopathological data included NYHA class, age at diagnosis, weight, height, BMI, glucose, triacylglycerides, HLD, LDL, and total cholesterol levels are listed in **Table 1**.

	Males		**Females**	
	Controls	**HF**	**Controls**	**HF**
n	5	5	5	5
Age	55.0 ± 1.4	55.8 ± 3.9	49.6 ± 2.6	52.6 ± 8.3
Weight (kg)	74.4 ± 9.2	81.0 ± 12.2	61.8 ± 6.6	55.8 ± 7.3
Height (cm)	174.0 ± 3.7	174.8 ± 3.4	167.0 ± 5.7	155.8 ± 3.8*
BMI (kg/m^2)	24.5 ± 2.3	26.7 ± 4.5	22.1 ± 1.7	23.1 ± 3.5
Glucose (mg/dL)	102.4 ± 12.8	126.8 ± 32.7	94.8 ± 4.9	99.2 ± 9.9
Triacylglycerides (mg/dL)	78.6 ± 23.8	111.0 ± 44.0	82.4 ± 49.4	186.4 ± 114.2
HDL-C (mg/dL)	59.4 ± 7.1	49.2 ± 8.0	70.4 ± 5.3	49.4 ± 22.7
LDL-C (mg/dL)	136.4 ± 32.9	101.6 ± 29.0	133.4 ± 15.8	124.0 ± 43.9
Total cholesterol (mg/dL)	211.4 ± 38.4	174.8 ± 37.9	220.4 ± 21.6	212.6 ± 66.4
NYHA class				
II		0		4
III		5		1

Table 1. Main biochemical parameters in plasma of control subjects and patients affected with heart failure (HF). Data are expressed as mean ± SD. BMI: body mass index; HDL-C: high-density lipoproteins cholesterol; LDL-C: low-density lipoproteins cholesterol; NYHA: New York Heart Association. * P-value < 0.05 calculated using a two-tailed Student's t-test.

Chronic HF patients enrolled in the study presented stable clinical conditions, left ventricular ejection fraction <40%, absence of a clinical history and/or documentation of pulmonary embolism or primary valvular heart disease, pericardial disease, severe obstructive lung disease, primitive or occupational lung disease, anemia (Hemoglobin <11 g/dL), renal failure (serum creatinine >2.0 mg/dL), significant peripheral vascular disease, exercise-induced angina, ST changes, or severe arrhythmias. All patients performed a cardiopulmonary exercise test (CPET). The investigation was approved by the local ethics committee and subjects signed a written informed consent before participating in the study. The control group was recruited from hospital staff and included 10 age-matched volunteer healthy subjects (5 females and 5 males).

2.3. Specimen handling and assays

Fresh blood (5 mL) was withdrawn into Vacutainer tubes containing citrate 0.129 mol/L as an anticoagulant. Complete blood was centrifuged at 3000 rpm for 10 minutes at 4 °C. Afterwards, plasma was immediately collected and aliquoted. Aliquots were frozen at −80°C until assayed.

2.4. Phospholipid extraction

The polar lipid fraction was isolated by using aminopropyl solid phase extraction (SPE) columns (HybridSPE-Phospholipid 30 mg, ref. 55261-U SUPELCO, Sigma-Aldrich). This step allows for rapid enrichment and recovery of PLs from the total human plasma. Briefly, 100 µL of plasma were mixed with 900 µL of acetonitrile:formic acid (99:1, v/v), vortexed for 30 seconds and centrifuged at 2000 rpm for 5 minutes for allowing protein precipitation. The supernatant was transferred to a HybridSPE column previously conditioned with 1 mL of acetonitrile (ACN). The columns were firstly washed with 1 mL of ACN:formic acid (99:1, v/v) followed by 1 mL of ACN. Lipids elution was carried out with 2 mL of ACN with 5% aqueous ammonia solution. The collected flow-through was dried (Thermo Savant SC110A Speed Vac Plus) and stored at -20 °C until analysis.

2.5. Phospholipid quantification

In order to determine the phospholipid amount in each lipid extract, the phosphorus measurement was performed [9]. Briefly, phosphate standards from 0.1 to 2 mg of phosphorus (P) were prepared from a sodium dihydrogen phosphate dihydrate ($NaH_2PO_4 \bullet 2H_2O$) stock solution (100 µg/mL of P). Dried PL pellets from samples were resuspended in 300 µL of chloroform of which 10 µL were added to 125 µL of perchloric acid (70%). Samples were incubated for 1h at 180 °C in a heating block (Stuart, U.K.) and then cooled to room temperature. Hereafter, 825 µL of Milli-Q water and 125 µL of ammonium molybdate (2.5% m/v) were added to samples and standards and were vortexed, followed by the addition of 125 µL of ascorbic acid (10% m/v). Samples and standards were vortexed thoroughly. Samples and standards were incubated in a water bath for

10 min at 100 °C and cooled down in a cold water bath. Finally, absorbance was measured at 797 nm in a microplate reader (Multiscan 90 Thermo Scientific).

2.6. HPLC-ESI-MS and MS/MS analysis

PLs were separated by hydrophilic interaction liquid chromatography (HILIC-LC-MS) using a high performance-LC (HPLC) system (Thermo scientific AccelaTM) with an autosampler coupled online to the Q-Exactive hybrid quadrupole Orbitrap mass spectrometer (Thermo Fisher Scientific, Bremen, Germany), according to Colombo et al. [10]. The solvent system consisted of two mobile phases as follows: mobile phase A [ACN:methanol:water 50:25:25 (v/v/v) with 1 mM ammonium acetate] and mobile phase B [ACN:methanol 60:40 (v/v) with 1 mM ammonium acetate]. Initially, 0% of mobile phase A was held isocratically for 8 min, followed by a linear increase to 60% of A within 7 min and a maintenance period of 15 min, returning to the initial conditions in 10 min. Before the analysis, each phospholipid extract was thawed on ice and dissolved in chloroform to the final concentration of 1 µg/µL. Then, 5 µL of this solution were diluted in glass vials containing 5 µL of each phospholipid standard (dMPC - 0.025 µg, dMPE - 0.025 µg, dMPG - 0.015 µg) and 80 µL of eluent B. 5 µL of this final solution were injected into the Ascentis Si column (15 cm × 1 mm, 3 µm, Sigma-Aldrich) with a flow rate of 40 µL min−1 and at 30 ºC. The mass spectrometer with Orbitrap® technology operated simultaneously in positive (electrospray voltage 3.0 kV) and negative (electrospray voltage -2.7 kV) modes with high resolution of 70,000 and AGC target of 1e6. The capillary temperature was 250 ºC and the sheath gas flow was 15 U. PC and LPC species were analyzed in the LC-MS spectra in the negative ion mode as acetate anions adducts [M + CH3COO]-. PE, PS and PI species were also analyzed in the LC-MS spectra in the negative ion mode, as [M-H]- ions. SM molecular species were analyzed in the LC-MS spectra in positive ion mode as [M+H]+ ions. In MS/MS experiments, a resolution of 17,500 and AGC target of 1E5 were used, and the cycles consisted of one full scan mass spectrum and ten data-dependent MS/MS scans that were repeated continuously throughout the experiments, with a dynamic exclusion of 60 seconds and an intensity threshold of 1E4. Normalized collision energy™ (CE) ranged between 25, 30 and 35 eV. At least one blank run was performed between different treatment samples to prevent cross-contamination, and samples where calibration standards were not within ±10% of the nominal value were re-injected. Data acquisition was carried out using the Xcalibur data system (V3.3, Thermo Fisher Scientific, USA). The quantitative analysis of PE (34:2) and PC (34:1) in human plasma was performed by LC-multiple reaction monitoring (MRM). For the optimization of the MS and MRM conditions, commercially available standards of PE (34:2) and PC (34:1) were diluted in methanol (0.1% formic acid) to the final concentration of 0.7 µM and were directly infused in a Xevo TQ-S micro triple quadrupole mass spectrometer equipped with an IonKey source (Waters, Milford, MI, USA), and the acquisition was performed in positive ion mode (cone

voltage, 26 V; capillary voltage, 4 kV; source temperature, 120 °C; desolvation gas flow rate, 2 L/h). The collision-induced dissociation of the [M+H]+ ions of the standards was optimized using different collision energies at Q2, and the optimal collision energy for the observation of the selected fragments was found to be 20 eV. The MRM transitions used to detect the phospholipid species included the protonated molecules [M+H]+ of PE (34:2) and PC (34:1) and their respective product ions. The selected transitions selected were m/z 716.6 → 575.7, m/z 716.6 → 436.4, m/z 716.6 → 454.4, monitored simultaneously for the quantification of PE (34:2), (dwell time, 80 ms); and m/z 760.7 → 184.1, m/z 760.7 → 496.5, m/z 760.7 → 504.8, monitored simultaneously for the quantification of PC (34:1) (dwell time, 110 ms).

For the quantification of the selected PE (34:2) and PC (34:1) molecular species in the plasma, each plasma extract prepared by SPE was dissolved to the final concentration of 3 µg/µL in isopropanol/ACN 50:50 (v/v). Then, 5 µL of each plasma extract (15 µg of phospholipids) were diluted in 120 µL of isopropanol/ACN 90/10 (v/v) with 0.1% formic acid and 0.01 mol/L ammonium formate (phase B) and 1.6 µL of this solution were injected on an Acquity C18 BEH column (150 µM x 100 mm; Waters, Milford, MI, USA), with a flow rate of 3 µL/min. The temperature of the column was maintained at 55°C. The mobile phases consisted of water/ACN 60/40 v/v with 0.1% formic acid and 10 mM ammonium formate (phase A), and isopropanol/ACN 90/10 v/v with 0.1% formic acid and 10 mM ammonium formate (phase B). The solvent gradient was set up with an initial increase from 45% B to 60% B at 3.5 min, followed by a linear increase to 99% B at 8 min, which was held isocratically until 14 min. The percentage of B was decreased to 45 % at minute 14.5 and maintained until the end of the run at 16.5 min. After the elution, PE (34:2) and PC (34:1) in the plasma extracts were individually detected by the Xevo TQ-S using MRM for the transitions of precursor ions to product ions reported above. All the other MS conditions were the same as those optimized during the direct infusion experiments.

Calibration curves were constructed using the peak areas of progressively diluted PE (34:2) and PC (34:1) standards. Concentrations of endogenous PE (34:2) and PC (34:1) were then calculated by interpolating their peak areas against the respective calibration curves and expressed as femtomoles per µmol of phospholipids in the plasma extract. The total phospholipid amount was calculated as lipid phosphorus/31.

2.7. Data and statistical analysis

Phospholipid peak integration and assignments were performed using MZmine 2.30. The software allows for filtering and smoothing, peak detection, peak processing, and assignment against an in-house database. During the processing of the raw data acquired in full MS mode, all the peaks with raw intensity lower than 1E4 were excluded. For all assignments, peaks within 6 ppm of the lipid exact mass were considered. Assigned PLs were further validated by manual analysis of the MS/MS data. Relative quantitation was performed by exporting integrated peak

areas values into a computer spreadsheet (Excel, Microsoft, Redmond, WA). For normalization of the data, the peak areas of the XICs of the PL precursors of each class were divided for the peak area of the IS selected for the class.

All statistical analyses were performed using R version 3.5.1 in RStudio version 1.1.456. Data were glog transformed and autoscaled using the R package Metaboanalyst R package. Lipidomic data were then analyzed by principal component analysis (PCA), with the R built-in function and ellipses were drawn using the R package ellipse, assuming a multivariate normal distribution and a level of 0.95. Partial least squares discriminant analysis (PLS-DA) was performed with the R package Metaboanalyst R and ellipses were drawn as described previously. Mann-Whitney U Test was performed with the R built-in function. Univariate statistical analysis of the PE (34:2) and PC (34:1) MRM datasets were performed using the Mann-Whitney U Test, using glog transformed data. All graphics and boxplots were created using the R package ggplot2. Other R packages used for data management and graphics included plyr, dplyr, and tidyr.

3. RESULTS

In this pilot study, we have evaluated differences in the plasma phospholipidome of male and female HF patients with respect to sex- and age-matched healthy subjects. There were no statistically significant differences between patients and controls neither in terms of age, BMI or weight, nor in levels of glucose, triacylglycerides, HDL-C, LDL-C, and total cholesterol (**Table 1**). Plasma phospholipids extracted from ten controls (5 males and 5 females) and ten HF patients (5 males and 5 females) were analyzed by HILIC-LC-MS and MS/MS analysis both in positive and negative ion modes, thus allowing identification and relative quantification of the lipid species at molecular level.

We performed the identification and the relative quantification of PL species belonging to 5 different classes: phosphatidylcholine (PC), lysophosphatidylcholine (LPC), sphingomyelin (SM), phosphatidylethanolamine (PE), and phosphatidylinositol (PI). A total of 136 phospholipid species, namely 53 PC, 17 LPC, 24 SM, 32 PE, and 10 PI, were identified and relatively quantified (**Table 2**). Then, the normalized datasets obtained from both patients affected with HF and controls were subjected to statistical analysis. Log-transformed data were autoscaled and then subjected to a projection to latent structures discriminant analysis (PLS-DA), commonly used for biomarker selection purposes, to sharpen the separation between the groups and to identify the differentiating lipids. When representing data from male and female together, the PLS-DA did not show different clusters between HF patients and healthy subjects (**Figure 1**),

Phospholipid species	Elemental composition				
PC	PC(30:0)	PC(32:0)	PC(32:1)	PC(32:2)	PC(34:0)
	PC(34:1)	PC(34:2)	PC(34:3)	PC(34:3)	PC(34:4)
	PC(34:5)	PC(36:0)	PC(36:1)	PC(36:2)	PC(36:3)
	PC(36:4)	PC(36:5)	PC(36:6)	PC(38:2)	PC(38:3)
	PC(38:4)	PC(38:5)	PC(38:6)	PC(38:7)	PC(38:8)
	PC(40:4)	PC(40:5)	PC(40:6)	PC(40:7)	PC(40:8)
	PC(40:9)	PC(42:10)	PC(42:2)	PC(42:6)	PC(42:7)
	PC(42:8)	PC(42:9)	PCo(32:0)	PCp(32:0)/PCo(32:1)	
	PCp(34:0)/PCo(34:1)		PCp(34:1)/PCo(34:2)	PCp(34:2)/PCo(34:3)	
	PCp(36:1)/PCo(36:2)		PCp(36:2)/PCo(36:3)	PCp(36:3)/PCo(36:4)	
	PCp(36:4)/PCo(36:5)		PCp(38:3)/PCo(38:4)	PCp(38:4)/PCo(38:5)	
	PCp(38:5)/PCo(38:6)		PCp(38:6)/PCo(38:7)	PCp(40:4)/PCo(40:5)	
	PCp(40:5)/PCo(40:6)		PCp(40:6)/PCo(40:7)		
LPC	LPC(14:0)	LPC(16:0)	LPC(16:1)	LPC(17:1)	LPC(18:0)
	LPC(18:1)	LPC(18:2)	LPC(18:3)	LPC(20:0)	LPC(20:1)
	LPC(20:2)	LPC(20:3)	LPC(20:4)	LPC(20:5)	LPC(22:4)
	LPC(22:5)	LPC(22:6)			
SM	SM(d34:0)	SM(d34:1)	SM(d34:2)	SM(d35:2)	SM(d36:0)
	SM(d36:1)	SM(d36:2)	SM(d36:3)	SM(d37:1)	SM(d37:2)
	SM(d38:1)	SM(d38:2)	SM(d38:3)	SM(d39:1)	SM(d39:1)
	SM(d39:2)	SM(d39:2)	SM(d40:0)	SM(d40:1)	SM(d40:2)
	SM(d41:2)	SM(d42:2)	SM(d42:3)	SM(d43:2)	
PE	PE(34:1)	PE(34:2)	PE(36:1)	PE(36:2)	PE(36:3)
	PE(36:5)	PE(38:3)	PE(38:4)	PE(38:5)	PE(38:6)
	PE(40:5)	PE(40:6)	PE(40:7)	PEo(34:2)/PEp(34:1)	
	PEo(34:3)/PEp(34:2)		PEo(36:2)/PEp(36:1)	PEo(36:3)/PEp(36:2)	
	PEo(36:4)/PEp(36:3)		PEo(36:5)/PEp(36:4)	PEo(36:6)/PEp(36:5)	
	PEo(38:4)/PEp(38:3)		PEo(38:5)/PEp(38:4)	PEo(38:6)/PEp(38:5)	
	PEo(38:7)/PEp(38:6)		PEo(38:8)/PEp(38:7)	PEo(40:5)/PEp(40:4)	
	PEo(40:6)/PEp(40:5)		PEo(40:7)/PEp(40:6)	PEo(40:8)/PEp(40:7)	
	PEo(40:9)/PEp(40:8)		PEo(42:7)/PEp(42:6)	PEp(34:5)	
PI	PI(34:1)	PI(34:2)	PI(36:1)	PI(36:2)	PI(36:3)
	PI(36:4)	PI(38:3)	PI(38:4)	PI(38:5)	PI(40:6)

Table 2. Elemental composition for the PLs proposed by MZmine tool. Lipid nomenclature is based on the LIPID MAPS consortium recommendations. For instance, the shorthand notation PC 36:4 represents a phosphatidylcholine lipid containing 36 carbons and four double bonds. PC, phosphatidylcholine; LPC, lysophosphatidylcholine; SM, sphingomyelin; PE, phosphatidylethanolamine; PI, phosphatidylinositol; PCp, plasmalogen phosphatidylcholine; PCo, ether phosphatidylcholine; PEo, ether phosphatidylethanolamine ; PEp plasmalogen phosphatidylethanolamine.

We wondered whether intrinsic differences between male and female plasma lipidomes could hamper the identification of species significantly up- or down-regulated in HF patients versus controls. Thus, datasets were clustered by gender, reaching the final number of 4 groups (female HF, male HF, female control and male control) and were subjected to PLS-DA according to the gender. In the case of females (female HF VS female control), the PLS-DA analysis showed

clustering trends corresponding to the two groups (**Figure 2A**), although the overfitting of the model should be considered. The score plots described 19.3% of the variance for Component 1 and 31.6% of cumulative variance in Component 2.

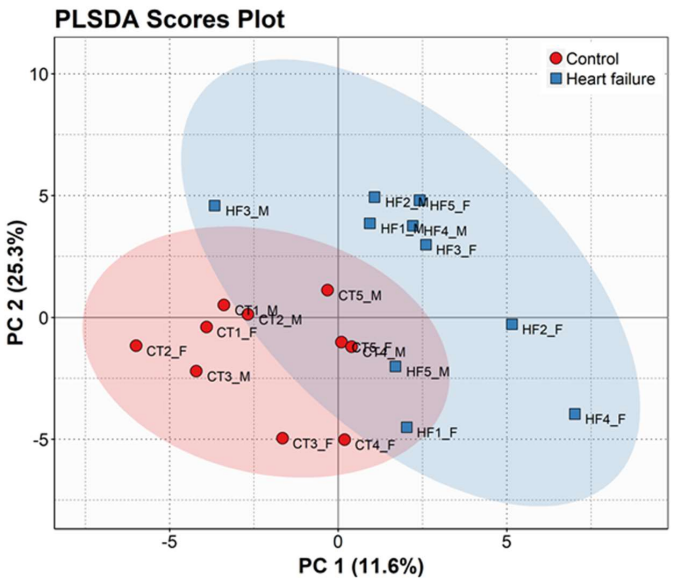

Figure 1. Projection to latent structures discriminant analysis (PLS-DA) score plot of plasma lipid profiles obtained from female and male HF (squares) and female and male control (circles) groups. Sample names were labelled accordingly to the gender. M, males; F, females; CT, control; HF, heart failure.

Along the chart, the female controls were plotted at the bottom on the left region while the female HF subjects were scattered at the diagonal of the plot. The top 16 variable importance in projection (VIP) lipids that were differentially regulated between the two female groups are shown in **Figure 2B**. These species include several plasma PE species, namely PE (34:1), PE (34:2), PE (36:1), PE (36:2), PE (36:3), PE (36:5), PE (38:3), PE (38:4), PE (38:5), PE (38:6), PE (40:5), and PE (40:6), which were increased in females with HF, along with decreased levels of one LPC (22:6), one plasmalogen phosphatidylethanolamine (PEp 40:5), and one ether phosphatidylcholine (PCo, 40:6), in the plasma of female HF with respect to the female control group. The PLS-DA score plot of the males cluster described Component 1 with a variance percentage of 22.2% and a cumulative variance of 31.1% in Component 2 (**Figure 2C**), although the overfitting of this model should be considered. The male control group was scattered at the left on the bottom, whereas the male HF group was scattered at the diagonal of the plot.

Hereafter, univariate statistical analysis was performed to screen out the significantly different PL species between the two groups, HF patients and healthy subjects, considering the gender, thus in males and females separately.

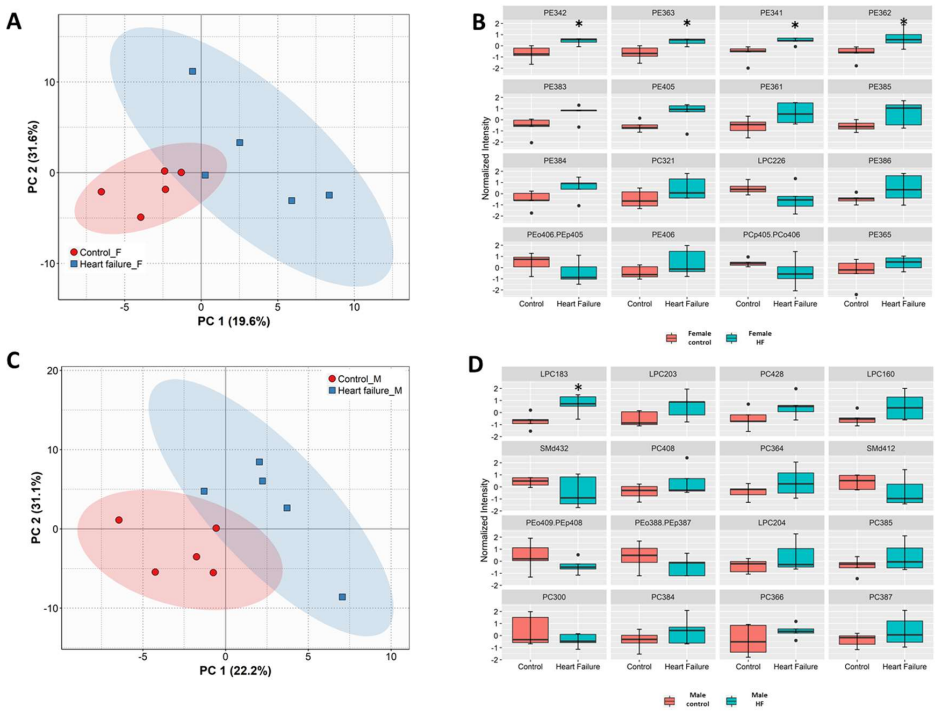

Figure 2. Projection to latent structures discriminant analysis (PLS-DA) score plot of plasma lipid profiles obtained from A) female HF and female controls (R2X = 0.59542, R2Y = 0.75903, Q2X = -1.0797 and Q2Y = -0.96486) and C) male HF and male controls (R2X = 0.54747, R2Y = 0.79761, Q2X = -1.6635, Q2Y = -1.5682). B) Boxplot of the levels of the top 16 variable importance in projection (VIP) lipids differentially regulated between female HF and female control groups and D) between male HF and male control groups. The relative abundances of four PEs (34:1, 34:2, 36:2, and 36:3) were significantly differentially regulated ((*), $p < 0.05$ (Mann-Whitney U test)) when comparing the two female groups (female HF patients and female controls). Likewise, the relative abundance of LPC (18:3) obtained from male HF patients and male controls was significantly differentially regulated. * $p < 0.05$ (Mann-Whitney U test) for the two male groups. In the box-and-whisker plots, the outlying values are depicted by black dots, the box signifies the 75th and 25thr quartiles, the short horizontal lines represent the minimum and maximum values and the median is represented by a short black line within the box for each phospholipid species. PEp, plasmalogen phosphatidylethanolamine; PCo, etherphosphatidylcholines.

Results from the Mann-Whitney U test, that was ran to compare the distribution of each PL species in the female HF VS female control groups, revealed that 4 PE species - PE (34:1), PE (34:2), PE (36:2), and PE (36:3) - were significantly more abundant in female HF than in the female control groups (p-value < 0.05) with a fold change of 1.3, 1.39, 1.35, and 1.32, respectively. Results from each PE molecular species were annotated in **Figure 2B** and summarized in **Table 3**.

The same statistical procedure was applied for males and, in this case, one LPC species, LPC (18:3), was two times significantly more abundant in male HF than in male controls ($p < 0.05$, fold change = 2.17) (**Figure 2D and Table 3**).

Class	Species (C:N)	Adaptation	Fold change	*p-value	Groups
PE	34:1	↑	1.3	0.0079365	Female HF vs. Control
	34:2	↑	1.39	0.015873	
	36:2	↑	1.35	0.015873	
	36:3	↑	1.32	0.031746	
LPC	18:3	↑	2.17	0.015873	Male HF vs. Control

Table 3. Summary of the phospholipid species significantly differentially regulated among the observed groups (female HF VS female control or male HF vs. male controls). * Significant when $p < 0.05$ (Mann-Whitney U test).

With the aim of validating the trends observed during the semi-quantitative phospholipidomics profiling, we performed a multiple reaction monitoring (MRM) targeted approach to quantitate PE (34:2) levels in plasma of HF and control subjects. Hence, we tested whether the concentration of this species was significantly increased in the plasma of females affected with HF. By contrast, PC (34:1) was selected as negative control. The MRM transitions used to detect the chosen PLs were determined on the basis of the principal fragmentation products (**Figure 3**).

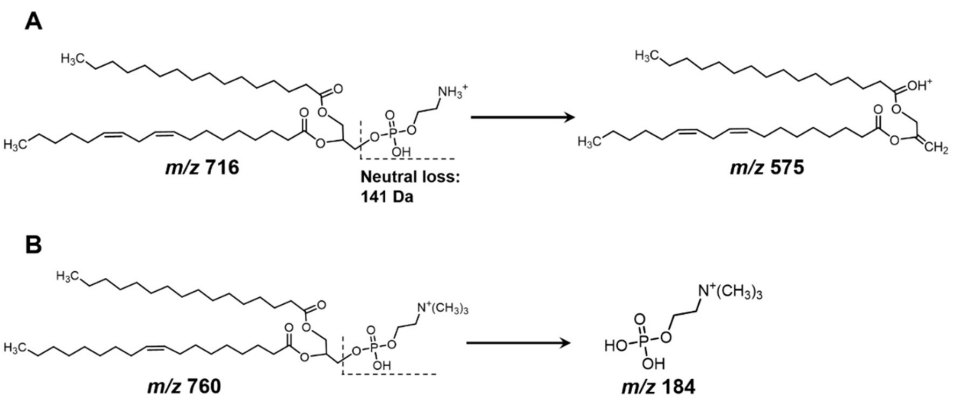

Figure 3. Main MS/MS transitions chosen for A) PE (34:2) and B) PC (34:1) during the development of the MRM method.

In the case of female HF, the average concentration of PE (34:2) measured in plasma was 13.6 ± 1.3 pmol/µmol$_{Phospholipid\ (PL)}$, while the average concentration of PE (34:2) measured in plasma of female controls was 5.2 ± 2.3 pmol/µmol$_{PL}$; the distributions in the two groups differed significantly (Mann–Whitney U = 1.0, $p < 0.027$ two-tailed), confirming that the plasma concentration of PE (34:2) was significantly higher in female HF when compared to female controls (Figure 4, Table 3). For male HF, the average concentration of PE (34:2) measured in plasma was 5.6 ± 2.0 pmol/µmol$_{PL}$ while the average concentration of PE (34:2) measured for male controls was 8.0 ± 2.3 pmol/µmol$_{PL}$. Therefore, no significant differences in the abundance of PE (34:2) were observed between the two male groups (**Figure 4 and Table 3**).

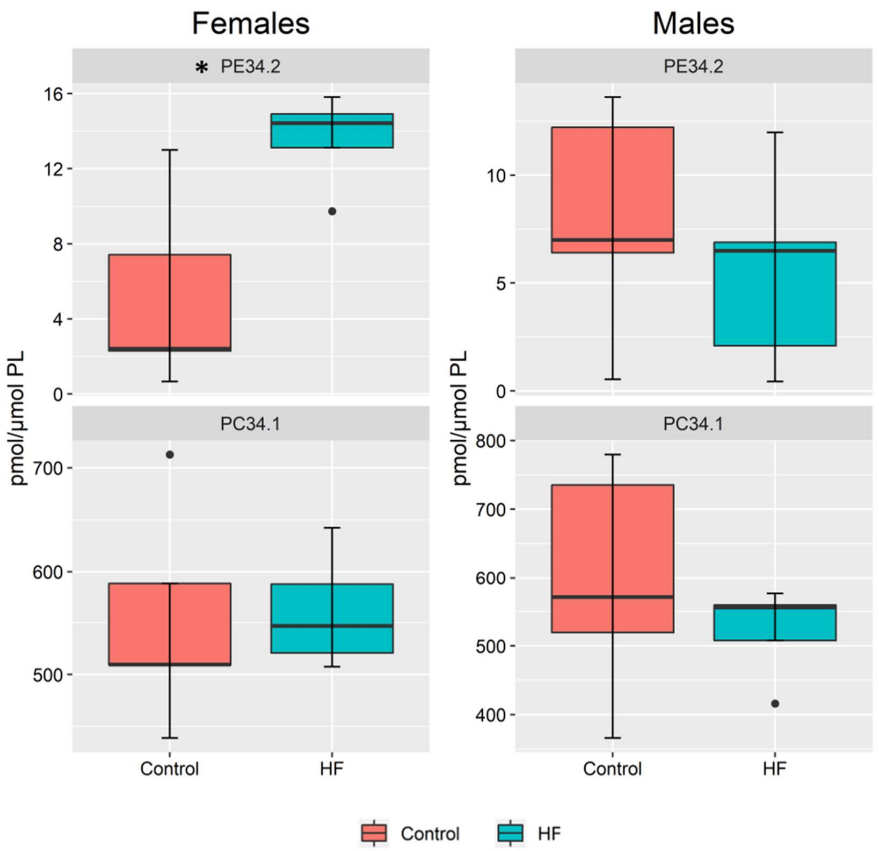

Figure 4. Box-and-whisker plots comparing for females and males subjects the plasma concentrations of PE (34:2) and PC (34:1) in female HF, female controls, and male HF and male controls. (*), significant when $p < 0.05$ (Mann-Whitney U test). In the box-and-whisker plots, the outlying values are depicted by black dots, the box signifies the 75th and 25thr quartiles, the short horizontal lines represent the minimum and maximum values and the median is represented by a short black line within the box for each phospholipid species.

As a test of negative control used to validate our targeted method, we also quantitated PC (34:1) whose concentration, based on the previous phospholipidomics analysis, was not expected to change between HF patients and control volunteers. Both for females and for males with HF compared with control subjects, the average concentration of PC (34:1) in plasma did not show statistical differences (**Figure 4 and Table 3**).

	Females		**Males**	
	Controls	**HF**	**Controls**	**HF**
PE (34:2) [pmol/μmol$_{PL}$]	$\bar{x}$ 5.2 ± 2.3 Md 2.4	$\bar{x}$ 13.6 ± 1.3 (*) Md 14.4	$\bar{x}$ 8.0 ± 2.3 Md 7.0	$\bar{x}$ 5.6 ± 2.0 Md 6.5
PC (34:1) [pmol/μmol$_{PL}$]	$\bar{x}$ 551.7 ± 46.7 Md 509.8	$\bar{x}$ 621.2 ± 64.6 Md 568.7	$\bar{x}$ 594.3 ± 75.0 Md 571.1	$\bar{x}$ 523.0 ± 29.0 Md 555.9

Table 3. Average mean and median of plasma concentrations (pmol/μmolPL) of PE (34:2) and PC (34:1) in female HF, female controls, and male HF and male controls. * P-value < 0.05 (Mann-Whitney U test). Md, sample median; $\bar{x}$, sample mean ± SEM.

4. DISCUSSION

The knowledge of phospholipidome changes associated with HF could provide evidence at the molecular level of the mechanisms underlying the development and progression of the disease, and may help to the identification of promising diagnostic, risk stratification or prognostic biomarkers. Importantly, the elucidation of the gender-specific plasma phospholipidome of HF may contribute to the application of personalized medicine. Although the overall prevalence of HF in males and females is quite similar [11], some limitations do exist when studying gender differences in CVD. Firstly, many major clinical trials do not include a gender analysis [11]. Secondly, research studies involving women with CVD are still a lot less compared to that of men, so that women are under-represented in most of the HF studies [12]. However, clinical manifestations of HF differ between these two groups [13]. Furthermore, only 28% of the specific predictors of mortality were common to male and female hospitalized HF patients [14]. Nevertheless, to the best of our knowledge, besides the present study, no other published works have reported the adaptation of the phospholipid profile of HF patients with respect to the gender.

In this pilot study, we carried out a plasma phospholipidome profiling of male and female HF patients looking for modulations associated either to the pathology or to the sex. Since lipidomes of males and females are compositionally heterogeneous [15], we decided to cluster the groups according to the gender for further statistical analysis. Multivariate and univariate analysis (PLS-

DA and Mann-Whitney U test, respectively) unveiled that PE species were more abundant in female HF patients while LPC species (specifically LPC (18:3)) was more abundant in the plasma of male patients (**Figure 5**).

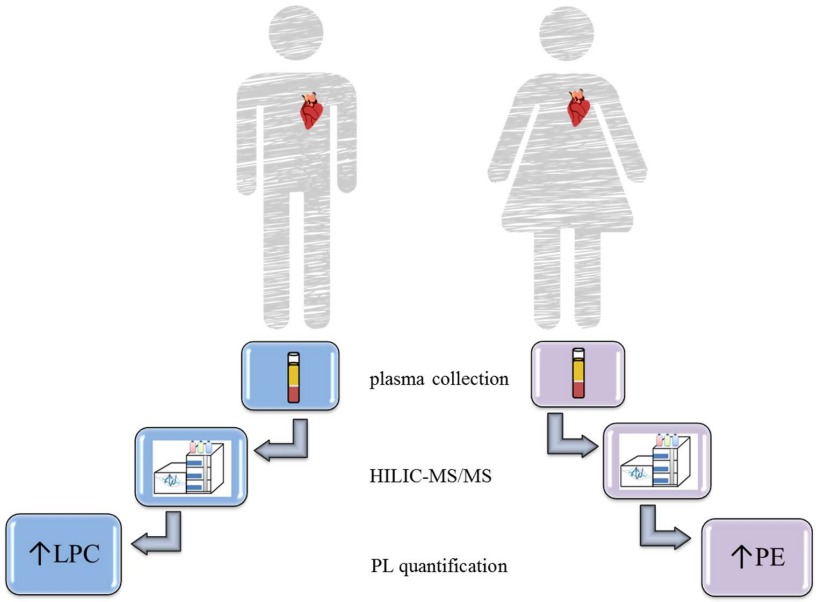

Figure 5. Schematic representation of the preliminary differences found in the plasma phospholipidome profile of male and female heart failure subjects. LPC, lysophosphatidylcholine; PE, phosphatidylethanolamine; PL, phospholipid.

Additionally, regarding the female HF group, the semi-quantitative trend unveiled in the HILIC-LC-MS/MS analysis was consolidated for PE (34:2) by means of MRM.

PE is the second most abundant phospholipid class in the in the inner cell and mitochondrial membrane and participates in cellular membrane integrity, mediates signaling pathways, and regulates membrane fluidity [16]. In comparison with other tissues, the heart muscle contains a raised number of mitochondria, its primary energy source, responsible for the ATP production needed by the heart to contract and keep functioning. Interestingly, van der Veen et al. demonstrated that an increase of mitochondrial PE positively correlates with ATP levels *in vitro* [17]. In addition, our results pinpointed raised levels of several PEs with mono- and polyunsaturated fatty acyl moieties in the plasma of female HF patients. In this context, many works have addressed that excess of polyunsaturated PE species under oxidative stress could trigger the formation of PE hydroperoxides that may intensify membrane curvature which in turn promotes higher accessibility to oxidants causing membrane destruction and, eventually, cellular death via the ferroptosis pathway [18,19].

On the other hand, PE is thought to be crucial in autophagy processes. Indeed, PE serves as an anchor for LC3 to bind autophagosomal membranes through LC3-PE lipidation. LC3-PE conjugation is involved in autophagosome maturation owing to its contribution to cargo recognition, membrane extension, and closure of the autophagosome membrane [20]. Conflicting results have been reported with respect to the role of raised autophagy in the failing heart. Some studies indicated that elevated autophagy appears to be a sign of the repair of failed cardiomyocytes as an adaptive response for protecting cells from hemodynamic stress [21]. Conversely, excessive autophagy can rise to maladaptive loss of cardiomyocytes, contributing to the worsening of HF [22].

In view of our results regarding females, we can consider two hypotheses for the role of PEs:

1) PE may function in a protective manner, increasing the levels of ATP needed by the failing heart for performing a proper cardiac function. In addition, PE is required in autophagy and raised levels of PE could provide cardiomyocyte protection from stress processes in failing hearts, thus improving HF prognosis for female patients. In fact, women have shown increased short and long-term survival rates after the diagnosis of HF [23].

2) PE species can be related to cellular death via ferroptosis pathway through the formation of PE hydroperoxides, although oxidized PE species have not been detected in this work, or via autophagy, with the subsequent excessive loss of cardiomyocytes, thus leading to the death of cardiac cells contributing to the pathological cardiac remodeling characteristic of HF.

In terms of male HF patients, only LPC (18:3) was observed to be significantly up-regulated in comparison with the male control group. LPCs are considered important cell signaling molecules. LPCs, a major lipid component of oxidized LDL, are thought to be important mediators of inflammation and atherosclerosis contributing to the development of the atherosclerotic lesion [24]. As such, LPCs have been detected in human plasma and atherosclerotic tissue from patients with atherosclerotic lesions. Remarkably, persistent inflammation is a feature of chronic HF [25], and atherosclerotic coronary arteries are one of the most common antecedent causes of HF. LPC abundance seems to be increased downstream of caspase activation. LPC is considered to be a chemoattractant of phagocytes in the clearance of dead cells. After induction of apoptosis and caspase activation, the apoptotic cells secrete LPC for promoting the migration of macrophages to apoptotic cells [26], and expose LPC in the outer leaflet of the membrane facilitating the binding to the G-protein-coupled receptor G2A on macrophages for the destruction of apoptotic cells [27]. Interestingly, cell death via the apoptotic pathway of cardiac muscle cells has been identified as an essential process in the progression to HF [28]. Considering our results, we could speculate that the increase of LPC (18:3) observed in male HF patients could be the product of the increased apoptotic activity carried out in the heart. Indeed, myocyte apoptosis has been found to be enhanced in men compared with women [29].

A possible confounding factor in this study is the non-identical HF severity distribution between males and females. However, in previous metabolomic studies, neither PE or LPC species were found to contribute to the discrimination of patients belonging to different NYHA [30], which suggest that a specific phospholipidome fingerprint of HF is independent of the NYHA classification.

In conclusion, our pilot study points out a gender-dependent adaptation of the plasma phospholipidome occurring in the HF pathology. We support that gender is a major and often underestimated factor that should be carefully considered when screening lipidomes of pathological processes. Although further studies increasing the number of samples are needed to validate these preliminary data, our results reveal for the first time phospholipid disturbances between HF patients and controls together with specific HF phospholipid signatures associated with the gender. These results could contribute to a better understanding of the pathology and open a window for a more in-depth investigation of the impact of those lipid species in the development and progression of HF according to the gender.

5. REFERENCES

[1] G. Van Meer, D.R. Voelker, G.W. Feigenson, Membrane lipids: Where they are and how they behave, Nat. Rev. Mol. Cell Biol. (2008). doi:10.1038/nrm2330.

[2] I. Tabas, Lipids and atherosclerosis, in: Biochem. Lipids, Lipoproteins Membr., 2008. doi:10.1016/B978-044453219-0.50023-4.

[3] A.H. Ellims, G. Wong, J.M. Weir, P. Lew, P.J. Meikle, A.J. Taylor, Plasma lipidomic analysis predicts non-calcified coronary artery plaque in asymptomatic patients at intermediate risk of coronary artery disease, Eur. Heart J. Cardiovasc. Imaging. (2014). doi:10.1093/ehjci/jeu033.

[4] K. Paapstel, J. Kals, J. Eha, K. Tootsi, A. Ottas, A. Piir, M. Zilmer, Metabolomic profiles of lipid metabolism, arterial stiffness and hemodynamics in male coronary artery disease patients, IJC Metab. Endocr. (2016). doi:10.1016/j.ijcme.2016.05.001.

[5] S. Rai, S. Bhatnagar, Novel Lipidomic Biomarkers in Hyperlipidemia and Cardiovascular Diseases: An Integrative Biology Analysis, Omi. A J. Integr. Biol. (2017). doi:10.1089/omi.2016.0178.

[6] C. Stegemann, R. Pechlaner, P. Willeit, S.R. Langley, M. Mangino, U. Mayr, C. Menni, A. Moayyeri, P. Santer, G. Rungger, T.D. Spector, J. Willeit, S. Kiechl, M. Mayr, Lipidomics profiling and risk of cardiovascular disease in the prospective population-based bruneck study, Circulation. (2014). doi:10.1161/CIRCULATIONAHA.113.002500.

[7] M.L. Cheng, C.H. Wang, M.S. Shiao, M.H. Liu, Y.Y. Huang, C.Y. Huang, C.T. Mao, J.F. Lin, H.Y. Ho, N.I. Yang, Metabolic disturbances identified in plasma are associated with outcomes in patients with heart failure: Diagnostic and prognostic value of metabolomics, J. Am. Coll. Cardiol. (2015). doi:10.1016/j.jacc.2015.02.018.

[8] H.Y. Tang, C.H. Wang, H.Y. Ho, P.T. Wu, C.L. Hung, C.Y. Huang, P.R. Wu, Y.H. Yeh, M.L. Cheng, Lipidomics reveals accumulation of the oxidized cholesterol in erythrocytes of heart failure patients, Redox Biol. (2018). doi:10.1016/j.redox.2017.10.020.

[9] B. Sousa, T. Melo, A. Campos, A.S.P. Moreira, E. Maciel, P. Domingues, R.P. Carvalho, T.R. Rodrigues, H. Girão, M.R.M. Domingues, Alteration in Phospholipidome Profile of Myoblast H9c2 Cell Line in a Model of Myocardium Starvation and Ischemia, J. Cell. Physiol. 231 (2016) 2266–2274. doi:10.1002/jcp.25344.

[10] S. Colombo, T. Melo, M. Martínez-López, M.J. Carrasco, M.R. Domingues, D. Pérez-Sala, P. Domingues, Phospholipidome of endothelial cells shows a different adaptation response upon oxidative, glycative and lipoxidative stress, Sci. Rep. 8 (2018) 12365. doi:10.1038/s41598-018-30695-0.

[11] N. Azad, A. Kathiravelu, S. Minoosepeher, P. Hebert, D. Fergusson, Gender differences in the etiology of heart failure: A systematic review, J. Geriatr. Cardiol. (2011). doi:10.3724/SP.J.1263.2011.00015.

[12] R. Baetta, M. Pontremoli, A. Martinez Fernandez, C.M. Spickett, C. Banfi, Proteomics in cardiovascular diseases: Unveiling sex and gender differences in the era of precision medicine, J. Proteomics. 173 (2018). doi:10.1016/j.jprot.2017.11.012.

[13] F. Duca, C. Zotter-Tufaro, A.A. Kammerlander, S. Aschauer, C. Binder, J. Mascherbauer, D. Bonderman, Gender-related differences in heart failure with preserved ejection fraction, Sci. Rep. (2018). doi:10.1038/s41598-018-19507-7.

[14] G.Y. Stein, T. Ben-Gal, A. Kremer, T. Bental, D. Alon, R. Korenfeld, I. Yedidia, A. Porter, E. Abramson, A. Sagie, S. Fuchs, Gender-related differences in hospitalized heart failure patients, Eur. J. Heart Fail. (2013). doi:10.1093/eurjhf/hft024.

[15] S. Sales, J. Graessler, S. Ciucci, R. Al-Atrib, T. Vihervaara, K. Schuhmann, D. Kauhanen, M. Sysi-Aho, S.R. Bornstein, M. Bickle, C. V. Cannistraci, K. Ekroos, A. Shevchenko, Gender, Contraceptives and Individual Metabolic Predisposition Shape a Healthy Plasma Lipidome, Sci. Rep. (2016). doi:10.1038/srep27710.

[16] J.E. Vance, Phosphatidylserine and phosphatidylethanolamine in mammalian cells: Two metabolically related aminophospholipids, J. Lipid Res. (2008). doi:10.1194/jlr.R700020-JLR200.

[17] J.N. Van Der Veen, S. Lingrell, R.P. Da Silva, R.L. Jacobs, D.E. Vance, The concentration of phosphatidylethanolamine in mitochondria can modulate ATP production and Glucose Metabolism in Mice, Diabetes. (2014). doi:10.2337/db13-0993.

[18] D. Patel, S.N. Witt, Ethanolamine and Phosphatidylethanolamine: Partners in Health and Disease, Oxid. Med. Cell. Longev. (2017). doi:10.1155/2017/4829180.

[19] E. Agmon, J. Solon, P. Bassereau, B.R. Stockwell, Modeling the effects of lipid peroxidation during ferroptosis on membrane properties, Sci. Rep. (2018). doi:10.1038/s41598-018-23408-0.

[20] S. Martens, No ATG8s, no problem? How LC3/GAB ARAP proteins contribute to autophagy, J. Cell Biol. (2016). doi:10.1083/jcb.201611116.

[21] A. Nakai, O. Yamaguchi, T. Takeda, Y. Higuchi, S. Hikoso, M. Taniike, S. Omiya, I. Mizote, Y. Matsumura, M. Asahi, K. Nishida, M. Hori, N. Mizushima, K. Otsu, The role of autophagy in

cardiomyocytes in the basal state and in response to hemodynamic stress, Nat. Med. (2007). doi:10.1038/nm1574.

[22] G.R.Y. De Meyer, G.W. De Keulenaer, W. Martinet, Role of autophagy in heart failure associated with aging, Heart Fail. Rev. (2010). doi:10.1007/s10741-010-9166-6.

[23] A. Strömberg, J. Mårtensson, Gender differences in patients with heart failure, Eur. J. Cardiovasc. Nurs. (2003). doi:10.1016/S1474-5151(03)00002-1.

[24] T. Matsumoto, T. Kobayashi, K. Kamata, Role of Lysophosphatidylcholine (LPC) in Atherosclerosis, Curr. Med. Chem. (2007). doi:10.2174/092986707782793899.

[25] S.D. Anker, S. Von Haehling, Inflammatory mediators in chronic heart failure: An overview, Heart. (2004).

[26] S.Y. Park, I.S. Kim, Engulfment signals and the phagocytic machinery for apoptotic cell clearance, Exp. Mol. Med. (2017). doi:10.1038/emm.2017.52.

[27] K. Lauber, E. Bohn, S.M. Kröber, Y.J. Xiao, S.G. Blumenthal, R.K. Lindemann, P. Marini, C. Wiedig, A. Zobywalski, S. Baksh, Y. Xu, I.B. Autenrieth, K. Schulze-Osthoff, C. Belka, G. Stuhler, S. Wesselborg, Apoptotic cells induce migration of phagocytes via caspase-3-mediated release of a lipid attraction signal, Cell. (2003). doi:10.1016/S0092-8674(03)00422-7.

[28] V.P.M. Van Empel, A.T.A. Bertrand, L. Hofstra, H.J. Crijns, P.A. Doevendans, L.J. De Windt, Myocyte apoptosis in heart failure, Cardiovasc. Res. (2005). doi:10.1016/j.cardiores.2005.04.012.

[29] S. Guerra, A. Leri, X. Wang, N. Finato, C. Di Loreto, C.A. Beltrami, J. Kajstura, P. Anversa, Myocyte death in the failing human heart is gender dependent, Circ. Res. (1999). doi:10.1161/01.RES.85.9.856.

[30] L. Tenori, X. Hu, P. Pantaleo, B. Alterini, G. Castelli, I. Olivotto, I. Bertini, C. Luchinat, G.F. Gensini, Metabolomic fingerprint of heart failure in humans: A nuclear magnetic resonance spectroscopy analysis, Int. J. Cardiol. (2013). doi:10.1016/j.ijcard.2013.08.042.

CHAPTER V:

Long- and short-chain lipid peroxidation products in heart failure plasma samples

LONG- AND SHORT-CHAIN LIPID PEROXIDATION PRODUCTS IN HEART FAILURE PLASMA SAMPLES

1. INTRODUCTION

Lipid peroxidation is an endogenous chain reaction that consists in the oxidative degradation of lipids. It involves the formation and propagation of lipid radicals where double bonds within unsaturated lipids further rearrange upon oxygen uptake leading to the production of a variety of breakdown products, including alcohols, ketones, alkanes, aldehydes and ethers [1].

Lipid hydroperoxides are the primary peroxidation products and can be structurally rearranged and converted into secondary highly reactive peroxidation products, known as reactive carbonyl species (RCS) [2]. RCS are a heterogeneous group with different chain lengths, numbers and locations of double bonds, and substituents, that can be classified into long-, short-chain (or truncated) carbonyl derivatives and small lipid peroxidation products. All groups can covalently react with proteins generating Michael adducts or Schiff bases, early products that are reversible or can further rearrange forming additional specific reaction compounds [2].

From a biological point of view, lipid peroxidation causes a decrease in membrane fluidity, might induce molecular damage and damaging cellular responses based on: inflammatory responses, changes in gene expression, apoptosis and ferroptosis, protein synthesis inhibition, and alteration in the activity of a wide range of enzymes [1,3].

To date, much more research has been carried out on small aldehyde breakdown products of lipid peroxidation (for instance 4-hydroxynonenal (4-HNE), malondialdehyde (MDA), acrolein (ACR) or glyoxal) than on their esterified counterparts, such as truncated phospholipid products. Furthermore, studies focused on cholesteryl ester oxidation products are even fewer than those on oxidized phospholipids (oxPLs), especially in the context of atherosclerosis and CVDs, although in the past few years the interest has grown and the number of reports is increasing [4].

Despite the fact that natural lipidomes are characterized by extremely high complexity and dynamic range, several works have identified and quantified some small lipid breakdown products of peroxidation in the circulatory system associated to HF [5,6], partly thanks to the development of commercial kits based on the reaction of chromogenic reagents with specific RCS, such as MDA or 4-HNE, that turn into more stable and measurable chromophores facilitating their study.

However, these methods have limitations with respect to the long-chain and fragmented-chain lipid peroxidation products (LPPs) in terms of identification, characterization and quantification. Lipidomics approaches can provide powerful tools to analyze complex biological samples with a high throughput rate, offering an extremely useful and versatile analytical tool for biomedical research [7]. Additionally, the development of sophisticated analytic platforms, i.e. LipidHunter

[8] or LppTiger [9], to handle complex data enables the analysis of phospholipids and oxidized lipids.

Even though the identification of oxidized phospholipids (oxPLs) have been carried out in plasma of patients with cardiovascular diseases [10,11], to the best of our knowledge, no previous works have characterized long-chain and truncated oxidized lipids in the plasma of HF patients.

In this chapter we took advantage of untargeted and targeted mass spectrometry approaches together with analytical platforms aiming to detect long-chain oxidized phospholipids and oxidized cholesteryl esters as well as truncated species in plasma samples from HF patients.

2. MATERIAL AND METHODS

2.1. Study population

Plasma samples collected at Centro Cardiologico Monzino were selected from a subset of healthy subjects (controls) and HF patients according to their age, sex, and clinical characteristics. A detailed summary of the clinical characteristics is reported in **Table 1**.

	Healthy subjects	**HF (VO_2 peak/kg)**		
		<12	12-16	>16
n	10	13	14	13
Age	53 ± 1	61 ± 2	57 ± 2	54 ± 2
Gender (m/f)	5/5	3/10	4/10	4/9
Weight (kg)	68.1 ± 3.2	81.7 ± 6.5	87.1 ± 6.5	79.2 ± 5.9
Height (cm)	170.5 ± 1.8	168.5 ± 2.7	171.9 ± 3.1	172.8 ± 2.5
BMI	23.3 ± 0.7	28.6 ± 1.9	29.1 ± 1.5	26.3 ± 1.7
Total cholesterol (mg/dL)	214.9 ± 10.5	158.2 ± 9.7*	187.8 ± 11.8	173.7 ± 11.6
EF%		31.6 ± 4.9	30.6 ± 3.1	34.1 ± 1.4
VO_2 peak/kg (ml/min/kg)		10.1 ± 0.4	13.5 ± 0.4**	19.4 ± 1.1****

Table 1. Clinical characteristics of subjects categorized in healthy subjects and HF patients grouped in three groups (VO_2 peak/kg<12, 12<VO_2 peak/kg<16, VO_2 peak/kg>16). Data are expressed as mean ± SEM. BMI, body mass index; EF, ejection fraction; VO_2 peak, maximum oxygen uptake during intense exercise; m, male; f, female. Data are presented as mean ± SEM. *P-value < 0.05 *, **p-value < 0.01, ****p-value < 0.0001.

The study was approved by the Ethical Committee European Institute of Oncology and Centro Cardiologico Monzino (registration number R205-CCFM S208/412). All subjects belonged to a cohort of HF patients regularly followed at our HF Unit and underwent our standard HF assessment which included full clinical evaluation, standard laboratory tests, echocardiography, spirometry, and alveolar capillary diffusion, as well as cardiopulmonary exercise test. Patients were classified according to VO_2 peak/kg value, which has been previously associated with the severity of HF (**Table 2**).

VO_2 peak/kg	HF severity
<12	Severe
12-16	Moderated
>16	Mild

Table 2. Classification of HF patients according to VO_2 peak/kg value

2.2. Lipid extraction

375 µL of methanol (MeOH) containing 0.1% butylated hydroxytoluene (BHT) were added to 50 µL of plasma and vortexed. Then, 1,25 mL of methyl tert-butyl ether (MTBE) was added and the mixture was incubated for 1 h at 4 ºC in a shaker. Phase separation was induced by adding 315 µL of MS-grade water containing 0.1% BHT. Upon 10 min of incubation at 4 ºC in a shaker, the samples were centrifuged at 4,500 rpm for 10 min. The upper (organic) phase was collected and dried in a vacuum centrifuge. Lipid extracts were stored at -20 ºC until their use. Before MS analysis, pellets were dissolved in 300 µL of MeOH and incubated at room temperature in a shaker and the supernatant was collected after centrifugation at 10,000 rpm for 5 min.

2.3. LC-MS/MS untargeted analysis and Parallel reaction monitoring targeted analysis

Chromatography method: Lipid UHPLC separations were performed on C18 reverse phase column. The solvent system consisted of two mobile phases in which eluent A consisted of acetonitrile:water, (50:50, v/v) and eluent B of isopropanol:acetonitrile:water, (85:10:5, v/v/v), both containing ammonium formate (5 mmol/L) and formic acid (0.1%, v/v). UHPLC separation was performed on a Vanquish Horizon UHPLC System equipped with a binary pump, an autosampler and a column compartment. Lipid pellets were dissolved in MeOH and 2 µL were loaded onto a C18 reverse phase column (150 × 2.1 mm, 2.6 µm particle size, and 150 Å pore size) at 10% B and eluted using several gradient steps: ramp from 10% to 86% B (20 min; non-linear slope, curve 4), then to 95% (2 min), followed by isocratic elution at 95% (4 min) before returning to the initial conditions and equilibration for 8 min. The column temperature was set to 50 °C and the flow rate to 300 µL/min.

Tandem Mass Spectrometry: A Thermo Scientific™ Q Exactive™ Plus hybrid quadrupole-Orbitrap mass spectrometer (Thermo Fisher Scientific, Bremen, Germany) was operated in positive (source voltage 3.5 kV) and negative (source voltage -2.5 kV) in data dependent acquisition (DDA) mode. Ion source parameters were the following: ion transfer tube temperature 300°C, sheath gas 40 arbitrary units, aux gas 10 arbitrary units, sweep gas 1 arbitrary unit, vaporizer temperature 370°C. The S-Lens RF level was set to 35%. The Orbitrap mass analyzer was operated at a resolution setting of 140,000 at m/z 100 in full-scan mode (scan range: m/z 350–1200; automatic gain control target: 1e6; max. injection time: 100 ms). For MS/MS mode a resolution of 17,500 at m/z 200 in Top 15 data-dependent mode (HCD, stepped normalized collision energy: 15, 20 and 30; isolation width: 1.2 m/z; automatic gain control target: 1e5; max. injection time: 60 ms; automatic gain control target: 1e5; Profile product spectra were collected. For parallel reaction monitoring (PRM), the peptides were separated using the same column and gradient (0–10% in 2 min, 10–86% in 20 min, and 86–95% in 2 min followed by isocratic elution at 95% of solvent B). The Q Exactive was operated in the targeted MS/MS mode, resolution of 17,500, stepped normalized collision energy: 10, 20 and 30; isolation width: 1.2 m/z; automatic gain control target: 2e5. Only selected m/z values at a specific rt were fragmented. Profile product spectra were collected and were analyzed with Xcalibur software. At least one blank run was performed between different treatment samples to prevent cross-contamination.

2.4. Automated identification of lipid peroxidation products (LPPs)

LPPtiger software source code version was used for oxPLs identification (https://bitbucket.org/SysMedOs/lpptiger). The list of modifications included hydroperoxy, hydroxy, epoxy, and keto groups with the maximum number equal to the number of bis-allylic and allylic sites in the structure. The oxidative cleavage products with aldehyde and carboxylic acid on the terminal carbon were included. All raw spectra were converted into mzML format using ProteoWizard MSconvert (Version 3.0.9134 64bit) and the following parameters were used for all files: m/z range 400–1000, isotope score filter 80, and overall score filter 40 and mass tolerance of 10 ppm on MS and MS2 levels was applied.

2.5. Nomenclature

Nomenclature rules were applied as previously described [12]. Lipid nomenclature is based on the LIPID MAPS consortium recommendations [13]. For instance, the shorthand notation PC 36:4 represents a phosphatidylcholine lipid containing 36 carbons and four double bonds. When the fatty acid identities and sn-position are known, as in our case, the slash separator is used (e.g., PC 16:0/20:4). Since no unified nomenclature is available for oxidized lipids, the short hand notations provided by LPPtiger tool were used [28]. Short chain oxidized lipids were indicated

by the corresponding terminal enclosed in angular brackets (e.g. "<" and ">"), with the truncation site indicated by the carbon atom number (e.g., <COOH@C9> and <CHO@C12). For long chain products our recommendation is to indicate the number of oxygen addition after the fully identified parent lipid (e.g. PC 16:0/20:4 + 1O) when the type of addition is not known, or in parenthesis for known functional groups (e.g. PC 16:0/20:4[1xOH@C11]).

3. RESULTS

The objective of this work was to investigate the presence of long- and shortened-chain oxidized lipids in plasma of HF patients with respect to healthy subjects. To that end, plasma samples from 40 HF patients (classified in 3 groups according to the degree severity, see **Table 2**) and 10 controls age- and sex-matched were collected upon informed consent. Plasma lipids were extracted applying the methyl-tert-butyl ether (MTBE)/methanol method. Then, lipid extracts were subjected to LC-MS/MS data dependent acquisition mode (DDA) in positive and negative mode using a high resolution Orbitrap mass spectrometer (**Figure 1**). Once conditions were set, acquired data were analyzed by LipidHunter [8] for phospholipid composition elucidation. As result, 54 PC, 9 LPC, 9 PE and 6 PI species were identified (**Table 3**).

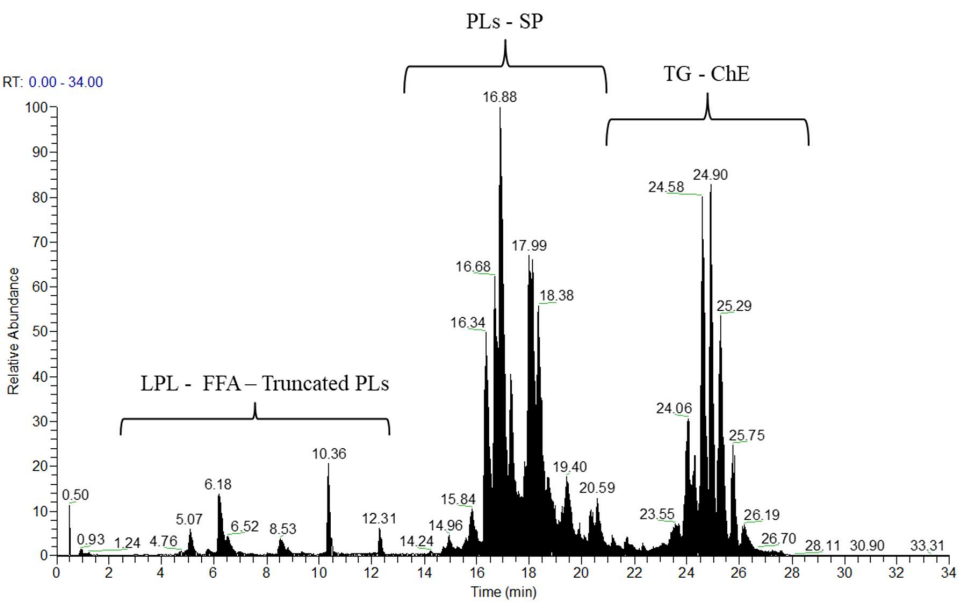

Figure 1. Total ion chromatogram (TIC) of pooled plasma samples from HF patients. LPL, Lysophospholipids; FFA, free fatty acid; PLs, phospholipids; SP, sphingolipids; TG, triacylglycerol species; ChE, cholesteryl ester species.

Phospholipid species	Elemental composition
PC	PC(14:0/14:0) PC(12:0/16:0) PC(14:0/16:0) PC(14:0/16:1) PC(16:0/16:0) PC(16:0/16:1) PC(14:0/18:1) PC(16:1/16:1) PC(14:0/18:2) PC(16:0/18:0) PC(16:0/18:1) PC(16:0/18:2) PC(16:1/18:1) PC(16:1/18:2) PC(16:0/18:3) PC(14:0/20:4) PC(18:0/18:1) PC(16:0/20:1) PC(18:1/18:1) PC(18:0/18:2) PC(16:0/20:2) PC(18:1/18:2) PC(16:0/20:3) PC(18:0/18:3) PC(18:2/18:2) PC(16:0/20:4) PC(16:1/20:3) PC(18:1/18:3) PC(16:1/20:4) PC(18:0/20:2) PC(18:0/20:3) PC(18:0/20:4) PC(16:0/22:4) PC(18:1/20:3) PC(16:0/22:5) PC(18:1/20:4) PC(18:2/20:3) PC(18:0/20:5) PC(16:0/22:6) PC(18:2/20:4) PC(18:1/20:5) PC(18:0/22:4) PC(18:0/22:5) PC(18:0/22:6) PC(18:1/22:5) PC(18:1/22:6) PC(20:4/20:4) PC(O-16:0/20:4) PC(O-18:0/20:4) PC(O-18:0/22:6) PC(P-16:0/18:1) PC(P-16:0/18:2) PC(P-16:0/20:4) PC(P-18:0/20:4)
PE	PE(18:0/18:1) PE(18:0/18:2) PE(18:1/18:1) PE(18:1/18:2) PE(16:0/20:4) PE(18:2/20:0) PE(18:0/20:3) PE(18:0/20:4) PE(18:0/22:6)
PI	PI(16:1/18:0) PI(18:0/18:1) PI(18:1/18:1) PI(18:0/18:2) PI(18:0/20:3) PI(18:0/22:6)
LPC	LPC(14:0) LPC(16:1) LPC(18:0) LPC(18:1) LPC(18:2) LPC(18:3) LPC(20:3) LPC(20:5) LPC(22:6)

Table 3. Elemental composition for the PLs proposed by LipidHunter and manually checked with Xcalibur software. PC, phosphatidylcholine; PE, phosphatidylethanolamine; PI, phosphatidylinositol; LPC, lysophosphatidylcholine; PCp, plasmalogen phosphatidylcholine; PCo, ether phosphatidylcholines.

Data generated by LipidHunter were used in LppTiger, a software capable of predicting *in silico* the oxidized phospholipidome and their fragmentation spectra on the basis of the plasma lipid composition identified by LipidHunter. LppTiger compares the *in silico* oxidized lipid fragmentation spectra with the observed ones in the sample, to identify oxidized species.
Unfortunately, LppTiger did not point out any reliable match due to the lack of fragmentation spectra (MS2) from the suspected oxidized species.

To overcome this limitation, PRM targeted analysis was performed aiming to increase the MS2 peak intensity. In a PRM analysis, only selected precursor ions will undergo fragmentation. To pick the oxidized phospholipids of interest 1,624 potential candidates previously suggested by LppTiger and several cholesteryl esters found in other cardiovascular diseases [11] were carefully

checked manually using the Xcalibur software. Those that presented a retention time (rt) and a m/z values compatible with an oxidized lipid were included in the targeted fragmentation list. The final list accounted for 146 species. After manual spectra analysis, so far we identified the long- and short-chain oxidized lipids that appear in **Table 4**.

Oxidized lipid	Positive mode		Negative Mode		Adducted species	RT
	Parent ion (m/z)	Precursor ion (m/z)	Parent ion (m/z)	Precursor ion (m/z)		
PC(16:0/4:0<CHO@C4)	624.3512	101, 255	580.3614	184	+ HCOO	6.43
PC(16:0/5:0<CHO@C5)	638.3669	115, 255	594.3770	184	+ HCOO	6
PC(16:0/9:0<CHO@C9)	694.4295	171, 255	650.4396	184	+ HCOO	8
PC(18:0/9:0<CHO@C9)	722.4608	171, 283	678.4709	184	+ HCOO	10
PC(16:0/18:2[2xDB,1xKETO])	816.5390	255, 291	772.5492	184	-H	15.05
PC(18:1/16:0[1xDB,1xOH])	820.5703	281, 271	776.5805	184	-H	15.5
ChE9:0<CHO@C9>			558.4886	369.25	+ NH4	18.62
ChE9:0<CHO@C9>			563.444	NL 368.36	+ Na	19.02
ChE18:2[2xDB,1xKETO]			685.5535	NL 368.34	+ Na	23.19
ChE18:2[2xDB,1xOH,1xOOH]			714.6036	369.35	+ NH4	23.18

Table 4. Elemental composition for the oxidized lipids manually checked with Xcalibur software after PRM analysis. PC, phosphatidylcholine; ChE, cholesteryl ester; NL, neutral loss; CHO, aldehyde moiety; DB, double bond.

The totality of the identified phospholipid- or cholesteryl ester-truncated forms contained a terminal aldehyde (CHO) moiety. Representative spectra of some oxidized species are depicted in **Figure 2 and 3**. With respect to the long-chain oxidized species, it was not possible to determine the exact carbon that held a keto, hydroxyl (OH), or hydroperoxy (OOH) group within the chain.

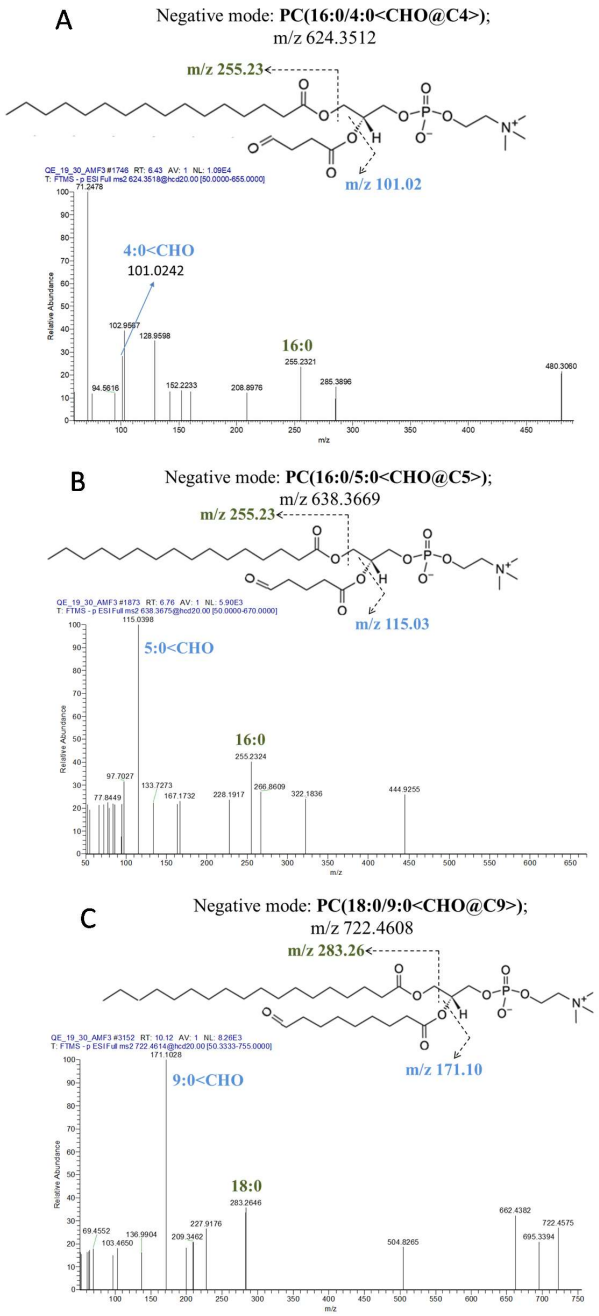

Figure 2. Higher-energy collisional dissociation (HCD) tandem mass spectra in negative ion mode and proposed structures of A) PC(16:0/4:0<CHO@C4), B) PC(16:0/5:0<CHO@C5) and C) PC(18:0/9:0<CHO@C9). Blue-coding of structure-related signals in the negative mode MS/MS spectra corresponds to the anion of oxidized or truncated fatty acid while green-coding corresponds to the unmodified fatty acid anion.

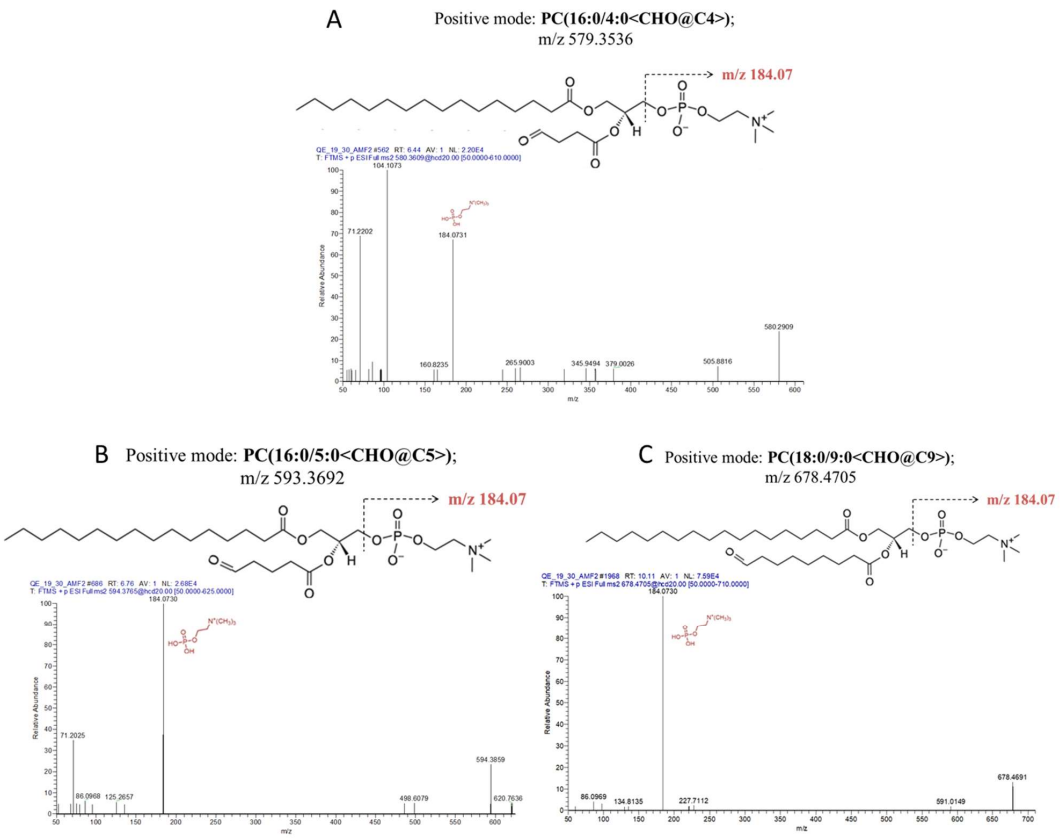

Figure 3. Higher-energy collisional dissociation (HCD) tandem mass spectra in positive ion mode and proposed structures of A) PC(16:0/4:0<CHO@C4), B) PC(16:0/5:0<CHO@C5) and C) PC(18:0/9:0<CHO@C9). Red-coding of structure-related signals in the positive mode MS/MS spectra corresponds to the characteristic fragment of phosphocholine at m/z 184.0727.

4. DISCUSSION

In this study, we performed a human plasma lipidomic analysis to investigate disturbed lipid features associated to oxidative stress in healthy controls and HF patients, a challenging task owing to the limited extent of oxPLs in plasma and to the lack of standard methods for their detection. To reach our objective, we performed both untargeted and targeted MS strategies.

For the detection and identification of oxPLs in the discovery phase we took advantage of the LppTiger analytical software for spectra analysis and oxPL matching, although no oxidized lipids were identified due to the low fragmentation intensity or even the absence of MS2 spectra from the parent ions of the suspected oxidized species. The most probable cause of the lack of MS2

spectra associated to oxidized lipids is their low abundance in plasma, highlighting the need of enrichment strategies or targeted MS analysis.

To increase the fragmentation peak intensity a PRM analysis was performed. PRM uses targeted tandem MS to simultaneously monitor product ions of specific m/z values with high resolution and mass accuracy [14]. The precursor ions of interest are then isolated at a specific retention time by the quadrupole and fragmented in the high-energy collisional dissociation (HCD) cell and the fragmented ions are then analyzed with an Orbitrap mass analyzer. So far, 9 oxidized lipids (6 PCs and 3 ChE) were successfully pointed out for the first time in the plasma of HF patients. PC species were the major oxidized lipids identified in this work, together with cholesteryl esters. Considering that PCs accounts for 40–50% of total phospholipids in mammalian cells or lipoproteins [2], it is not surprising the fact that all oxidized phospholipids found up to now belong to this class.

Lipid peroxidation occurs in a number of pathologies. Indeed, oxidation of cholesteryl esters and phospholipids have been shown to play a crucial role in the onset and development of cardiovascular disorders, especially those involving inflammation such as atherosclerosis, where oxidized lipids are actively involved in the inflammatory responses by interacting with immune cells (such as macrophages) and endothelial cells [11].

From a biological point of view, peroxidation of PLs not only generates a wide spectrum of reactive molecules that can modify endogenous structures, including proteins and other lipids, but also phosphocholine-containing OxPLs have been identified as important antigens that can be recognized by soluble and cell-associated pattern-recognition receptors of innate immunity [15]. For example, the binding of OxPLs to CD36 promotes formation of foam cells characteristic of atherosclerosis [2]. In human aortic endothelial cells, oxPLs modulate the expression of genes related to angiogenesis, atherosclerosis, inflammation and wound healing [16]. OxPLs also activate the electrophilic stress response and stimulate several types of signal-transducing receptors on the cell surface or in the nucleus, including G protein-coupled receptors, receptor tyrosine kinases, Toll-like receptors, receptors coupled to endocytosis, and nuclear ligand-activated transcription factors [15]. Besides, oxidation of PLs can have drastic effects on cellular functions via altering biophysical properties of the plasma and mitochondrial membranes, such as membrane rigidity increase or reorientation of the modified side chains [17]. OxChE are the major component of oxidized low density proteins and might induce atherogenic and inflammatory responses such as monocyte adhesion to endothelial cells, CD36 expression, production of ROS, expression of inflammatory cytokines, and macrophage lipid accumulation [18].

Taking into account that, besides small peroxidation products (4-HNE, MDA, ACR, etc.), no previous works have characterized long lipid peroxidation products in HF plasma samples, the

results presented in this chapter contribute to expand the knowledge about plasma lipid changes associated to HF induced under oxidative stress conditions, such as changes at functional group level and their position within the carbon chain, which might be essential to understand differences in the biological and in physiopathological activity of oxidized lipids.

Despite the positive preliminary results, a higher number of identified oxidized lipids was expected. Indeed, we pursue to quantify the abundance of those lipid peroxidation products to understand if their concentration levels in plasma of HF patients are raised with respect to the controls, as presumed. It is also our objective to associate an oxidative pattern to the severity degree of HF. Consequently, each individual sample together with internal standards will be subjected to an optimized PRM analysis to be able to quantify and raise the number of detected oxidized lipids. This work is still ongoing in collaboration with the University of Leipzig (Germany) and therefore the results will not be discussed in this thesis.

To summarize, we have contributed with this study to identify for the first time nine long- and short-chain oxidized PCs and ChE, products of oxidative stress, in the plasma of HF patients by applying a parallel reaction monitoring (PRM) on a Q Exactive Plus mass spectrometer. This promising results will be further quantified and the current protocol used here will be optimized aiming to detect a larger number of oxPLs and oxChE. Additionally, the final list of oxidized lipids along with their abundances will be confronted to those arising from the healthy group in order to highlight the modified lipids present solely in HF patients.

5. REFERENCES

[1] M. Repetto, J. Semprine, A. Boveris, Lipid Peroxidation: Chemical Mechanism, Biological Implications and Analytical Determination, in: Lipid Peroxidation, 2012. doi:10.5772/45943.

[2] E. Gianazza, M. Brioschi, A.M. Fernandez, C. Banfi, Lipoxidation in cardiovascular diseases, Redox Biol. (2019). doi:10.1016/j.redox.2019.101119.

[3] A. Naud, M. Jov, V. Ayala, O. Ramrez, R. Cabr, J. Prat, M. Portero-Otin, I. Ferrer, R. Pamplo, Region Specific Vulnerability to Lipid Peroxidation in the Human Central Nervous System, in: Lipid Peroxidation, 2012. doi:10.5772/46022.

[4] R.M. Domingues, P. Domingues, T. Melo, D. Pérez-Sala, A. Reis, C.M. Spickett, Lipoxidation adducts with peptides and proteins: Deleterious modifications or signaling mechanisms?, J. Proteomics. (2013). doi:10.1016/j.jprot.2013.06.004.

[5] C.R. Díaz-Vélez, S. García-Castiñeiras, E. Mendoza-Ramos, E. Hernández-López, Increased malondialdehyde in peripheral blood of patients with congestive heart failure, Am. Heart J. (1996). doi:10.1016/S0002-8703(96)90063-0.

[6] S. Mak, D.C. Lehotay, M. Yazdanpanah, E.R. Azevedo, P.P. Liu, G.E. Newton, Unsaturated

aldehydes including 4-OH-nonenal are elevated in patients with congestive heart failure, J. Card. Fail. (2000). doi:10.1054/jcaf.2000.7272.

[7] R. Baetta, M. Pontremoli, A. Martinez Fernandez, C.M. Spickett, C. Banfi, Proteomics in cardiovascular diseases: Unveiling sex and gender differences in the era of precision medicine, J. Proteomics. 173 (2018). doi:10.1016/j.jprot.2017.11.012.

[8] Z. Ni, G. Angelidou, M. Lange, R. Hoffmann, M. Fedorova, LipidHunter Identifies Phospholipids by High-Throughput Processing of LC-MS and Shotgun Lipidomics Datasets, Anal. Chem. (2017). doi:10.1021/acs.analchem.7b01126.

[9] Z. Ni, G. Angelidou, R. Hoffmann, M. Fedorova, LPPtiger software for lipidome-specific prediction and identification of oxidized phospholipids from LC-MS datasets, Sci. Rep. (2017). doi:10.1038/s41598-017-15363-z.

[10] J. Lu, B. Chen, T. Chen, S. Guo, X. Xue, Q. Chen, M. Zhao, L. Xia, Z. Zhu, L. Zheng, H. Yin, Comprehensive metabolomics identified lipid peroxidation as a prominent feature in human plasma of patients with coronary heart diseases, Redox Biol. (2017). doi:10.1016/j.redox.2017.04.032.

[11] S. Zhong, L. Li, X. Shen, Q. Li, W. Xu, X. Wang, Y. Tao, H. Yin, An update on lipid oxidation and inflammation in cardiovascular diseases, Free Radic. Biol. Med. (2019). doi:10.1016/j.freeradbiomed.2019.03.036.

[12] Z. Ni, B. Sousa, S. Colombo, C. Afonso, T. Melo, A. Pitt, C. Spickett, P. Domingues, M. Domingues, M. Fedorova, A. Criscuolo, Evaluation of air oxidized PAPC: A multi laboratory study by LC-MS/MS, Free Radic. Biol. Med. (2019). doi:10.1016/j.freeradbiomed.2019.06.013.

[13] E. Fahy, S. Subramaniam, R.C. Murphy, M. Nishijima, C.R.H. Raetz, T. Shimizu, F. Spener, G. Van Meer, M.J.O. Wakelam, E.A. Dennis, Update of the LIPID MAPS comprehensive classification system for lipids, J. Lipid Res. (2009). doi:10.1194/jlr.R800095-JLR200.

[14] G.E. Ronsein, N. Pamir, P.D. von Haller, D.S. Kim, M.N. Oda, G.P. Jarvik, T. Vaisar, J.W. Heinecke, Parallel reaction monitoring (PRM) and selected reaction monitoring (SRM) exhibit comparable linearity, dynamic range and precision for targeted quantitative HDL proteomics, J. Proteomics. (2015). doi:10.1016/j.jprot.2014.10.017.

[15] V.N. Bochkov, O. V. Oskolkova, K.G. Birukov, A.L. Levonen, C.J. Binder, J. Stöckl, Generation and biological activities of oxidized phospholipids, Antioxidants Redox Signal. (2010). doi:10.1089/ars.2009.2597.

[16] M.Z. Ashraf, N.S. Kar, E.A. Podrez, Oxidized phospholipids: Biomarker for cardiovascular diseases, Int. J. Biochem. Cell Biol. (2009). doi:10.1016/j.biocel.2008.11.002.

[17] J.W. Borst, N. V. Visser, O. Kouptsova, A.J.W.G. Visser, Oxidation of unsaturated phospholipids in membrane bilayer mixtures is accompanied by membrane fluidity changes, Biochim. Biophys. Acta - Mol. Cell Biol. Lipids. (2000). doi:10.1016/S1388-1981(00)00084-6.

[18] S.H. Choi, D. Sviridov, Y.I. Miller, Oxidized cholesteryl esters and inflammation, Biochim. Biophys. Acta - Mol. Cell Biol. Lipids. (2017). doi:10.1016/j.bbalip.2016.06.020.

Concluding remarks and future perspectives

CONCLUDING REMARKS AND FUTURE PERSPECTIVES

CONCLUDING REMARKS

Products of oxidative stress contribute to the onset of a number of inflammatory diseases, including HF. They might be used as biomarkers providing information about the pathological pathway of HF development, the disease progression, and the clinical outcome [1]. However, the classic biomarkers of oxidative stress identified in HF do not provide thoroughly information but report about a general oxidative stress status. For a better understanding of the pathology of HF it is needed to unveil not only protein and lipid targets of oxidative damage but also the residues undergoing the modification within the protein and the structure of the oxidation products. Analysis of all of these oxPTMs and lipid peroxidation products by mass spectrometry is extremely challenging, and this is specially true for glycation and lipoxidation [2]. Indeed, oxPTMs tend to occur randomly on a number of susceptible residues and proteins, making it extremely difficult to define all protein species.

Along this project, plasma samples from HF patients belonging to different NYHA groups (from class I to class IV) have been collected for the establishment of a biobank of HF biological samples (**Table 1**). All patients underwent cardiopulmonary exercise tests, echocardiographic evaluation or spirometry tests, once signed a written informed consent, and those that showed an ejection fraction lower than 40% were enrolled. Blood was withdrawn in tubes containing EDTA or citrate as anticoagulants to further collect the plasma fraction.

	Male	**Female**
n	101	22
Age	65.0 ± 10.8	62.4 ± 13.0
NYHA (I/II/III/IV)	24/50/24/3	5/13/4/0
VO_2 peak/kg (ml/min/kg)	14.8 ± 5.7	13.9 ± 3.4
EF (%)	29.7 ± 6.9	29.8 ± 5.2

Table 1. Number of patients recruited and enrolled in the biobank along this project.
NYHA, New York Heart Association; VO_2 peak/kg, oxygen uptake; EF, ejection fraction.

These plasma samples were therefore used to identify oxidized biomolecules as potential biomarkers of HF taking advantage of different plasma prefractionation strategies combined with high-throughput untargeted and targeted mass spectrometry techniques. Consequently, part of this project has been focused on the study of oxidative modifications in human serum albumin (HSA), the most abundant protein in the circulatory system, associated to HF. HSA is involved in a wide

range of biological functions. However, due to its long half-life and high concentration in plasma compared to other proteins, HSA is highly sensitive to undergo oxPTMs that may lead to its functional loss contributing to the progression of HF [3].

Taking advantage of the high abundance of HSA, we relatively quantified for the first time plasma levels of cysteinylated HSA (cys-HSA) and also the levels of early glycated HSA (GA) in HF patients, and we observed a significant increase in the patients with respect to the healthy subjects. Additionally, a positive correlation between the levels of both isoforms and the severity of HF was highlighted whereas the abundance of total HSA showed a tendency to decrease when raising the severity degree of HF.

For a deeper characterization of GA, we elucidated for the first time the early glycation pattern of HSA associated to HF by means of the newest generation of Tribrid MS instruments. Lys233 and lys525 were observed as the two most abundant glycated amino acids (79% and 13% respectively) [3]. Considering that further modifications of GA, such as rearrangement, oxidation, polymerization, and cleavage give rise to irreversible conjugates, called advanced glycation end products (AGEs), we also aimed to unveil the plasma advanced glycation pattern associated to HF. In this case, lys20, arg98 and lys402 emerged as the three most abundant carboxymethylated residues. Therefore, the results suggested that, on one hand lys233 and lys525, and on the other lys20, arg98 and lys402, might represent the main potential therapeutic targets to reduce GA and AGE-HSA levels in HF patients, respectively. Therefore, MS offers the potential advantage of providing both structural and qualitative information to clarify the regions that are being modified during the glycation process along with the form of these modifications.

Along this Ph.D. project, we have also evaluated the potential causal role of GA in the etiopathogenesis of HF. While the pathological role of AGE-HSA has been widely studied (i.e. AGEs bind with endothelial RAGE resulting in endothelial dysfunction, cross linking myocardial collagen with AGEs cause myocardial stiffness affecting tissue mechanical properties, physiological functions and diastolic dysfunction [4]), the possible effects of Amadori products such as GA in cardiovascular diseases are less studied with respect to AGE-HSA. Hence, we pursued to evaluate the biological effects of GA on cardiac myocytes. Results highlighted that *in vitro* GA modulates the cardiomyocyte expression of inflammatory cytokines such as IL-6 or TNF-α. Interestingly, it has been reported that HSA synthesis is suppressed by pro-inflammatory cytokines, including interleukin 6 (IL-6) and TNF-α, in the context of the acute phase response, leading to hypoalbuminemia [5], a condition that has also been highlighted in HF patients in this Thesis. Furthermore, we reported that GA induces oxidative stress and oxidative modifications of a multitude of cellular proteins within cardiac myocytes. In addition, GA modulates the secretion of several cardiac proteins involved in response to stress biological process. In conclusion, the present work has contributed to expand the current knowledge of GA [3].

Besides the study of oxidized isoforms of HSA, we also tried to identify other less abundant advanced glycation and lipoxidation end products (AGEs and ALEs) in plasma by means of an enrichment strategy based on the ability of RAGE receptor to bind AGEs and ALEs [6]. Unfortunately, we did not succeed in this attempt. Different reasons could explain the negative results: 1) AGEs and ALEs in HF plasma samples are not structurally able to bind the RAGE receptor, and therefore cannot be enriched [7]. 2) The concentration level of AGEs/ALEs present in HF plasma samples is so low that protein-ligand complex affinity constant cannot be reached. 3) To detect low abundance products it is needed the use of ultra-high resolution MS instruments to improve sensitivity of low abundant proteins.

On the other hand, lipids play a crucial role in physiological processes and phospholipid disruption may participate in cardiovascular disease events, therefore the phospholipidome profiling has emerged as a powerful tool to explore novel biomarkers and mechanisms in several pathologies. Hence, we have also studied for the first time the plasma phospholipidome of HF patients. In this pilot study we have applied both untargeted and targeted (MRM) tools together with fractionating methods to separate the phospholipid content from the rest of plasma components, in order to decrease the heterogeneity and complexity of this biological matrix. The results suggested that the plasma phospholipid profiles of male and female HF patients were significantly altered when compared to their respective control groups. Furthermore, HF plasma phospholipid signatures were gender-specific. In the case of females, several PE species were more abundant in HF than in the control group. By the contrary, male HF patients mainly showed a higher abundance of LPC species when compared to the male control group. Additionally, lipidomic approaches (LC-MS/MS and PRM) have been carried out to define for the first time a circulating oxidative lipid pattern associated to HF. In this case, we have focused on long- and short-chain products of lipid peroxidation since their identification and characterization in the pathology of HF were still lacking. Promising results have been pinpointed so far: we have detected 9 lipid peroxidation products (full-chain oxidized lipids together with fragmented species). Nevertheless, this study is still ongoing.

In conclusion, the results gathered along this Ph.D. project provide evidence at the molecular level of the mechanisms associated to oxidative stress and oxidative damage underlying the development and progression of HF, thus contributing to a better understanding of the pathology. Indeed, the elucidation of specific modified residues within key circulating proteins such as HSA, or the characterization of long-chain oxidized lipids present in HF plasma samples reported in this thesis may pave the way to new therapies to reduce and treat HF. We have also contributed

to expand the awareness of the biological effects of GA in the cardiac context. Additionally, this project has pointed out a gender-dependent adaptation of the plasma phospholipidome occurring in the pathology of HF, highlighting that gender is a major and often underestimated factor that should be carefully considered when screening lipidomes or proteomes of pathological processes. Finally, we have demonstrated that either proteomic or lipidomic technologies can provide deep biological insight into human health and disease.

OUTLOOK

Although very exciting and novel results have been elucidated in this work, other parts of the project have potential to be further developed.

1. It would be of interest to investigate the effects of cys-HSA on cardiomyocytes in order to find a causal role in the etiopathogenesis of HF. Unlike GA, cys-HSA cannot be commercially purchased. Therefore, cys-HSA *in vitro* synthesis or isolation from biological sources is required.
2. It would be attractive to test whether different antioxidants are capable of reducing the plasma levels of cys-HSA and GA.
3. Since HSA has an established role as a blood stream carrier, it will be exciting to test how these modifications can affect drug delivery of various pharmacological treatments in HF.
4. It should be also investigated the presence of other than glycated-, carboxymethylated- or cysteinylated-HSA adducts in the plasma of HF subjects by means of MS after isolation of HSA. It would be beneficial to analyze the samples according to the NYHA classification and/or according to the gender to obtain a relation between the degree of oxidative damage and the disease severity as well as to understand if there is a HSA oxidation pattern linked to the gender. Additionally, it would be strongly recommended to analyze the adducts in the plasma of the healthy group
5. With respect to the pilot study about disturbances in the plasma phospholipidome of male and female HF patients, it is essential to raise significantly the number of enrolled HF patient, at least three or four times, in order to confirm the preliminary results and aiming to get more solid and sustainable data.
6. In the case of the identification of lipid peroxidation products, we still pursue to identify more oxidized species as well as to quantify them in order to correlate the levels of lipid peroxidation products with the disease severity and to compare them with those present in the healthy group.

REFERENCES

[1] E. Gianazza, M. Brioschi, A.M. Fernandez, C. Banfi, Lipoxidation in cardiovascular diseases, Redox Biol. (2019). doi:10.1016/j.redox.2019.101119.

[2] R. Baetta, M. Pontremoli, A. Martinez Fernandez, C.M. Spickett, C. Banfi, Proteomics in cardiovascular diseases: Unveiling sex and gender differences in the era of precision medicine, J. Proteomics. 173 (2018). doi:10.1016/j.jprot.2017.11.012.

[3] A. Martinez Fernandez, L. Regazzoni, M. Brioschi, E. Gianazza, P. Agostoni, G. Aldini, C. Banfi, Pro-oxidant and pro-inflammatory effects of glycated albumin on cardiomyocytes, Free Radic. Biol. Med. (2019). doi:0.1016/j.freeradbiomed.2019.06.023.

[4] Z. Hegab, Role of advanced glycation end products in cardiovascular disease, World J. Cardiol. (2012). doi:10.4330/wjc.v4.i4.90.

[5] C. Valerio, E. Theocharidou, A. Davenport, B. Agarwal, Human albumin solution for patients with cirrhosis and acute on chronic liver failure: Beyond simple volume expansion, World J. Hepatol. (2016). doi:10.4254/wjh.v8.i7.345.

[6] G. Degani, A.A. Altomare, M. Colzani, C. Martino, A. Mazzolari, G. Fritz, G. Vistoli, L. Popolo, G. Aldini, A capture method based on the VC1 domain reveals new binding properties of the human receptor for advanced glycation end products (RAGE), Redox Biol. (2017). doi:10.1016/j.redox.2016.12.017.

[7] M. Mol, G. Degani, C. Coppa, G. Baron, L. Popolo, M. Carini, G. Aldini, G. Vistoli, A. Altomare, Advanced lipoxidation end products (ALEs) as RAGE binders: Mass spectrometric and computational studies to explain the reasons why, Redox Biol. (2018). doi:10.1016/j.redox.2018.101083

Acknowledgements

ACKNOWLEDGEMENTS

Firstly, I would like to express my gratitude to my supervisor Dr. Banfi, who provided me the opportunity to join her team as a Ph.D. Student, for all the things I have learned and for introducing me into the proteomics field. I would also like to thank the former and current members of the Proteomic Unit at CCM: Dr. Brioschi, Dr. Baetta, Dr. Gianazza, Stefania Ghilardi, Federica Casalnuovo, Marta Pontremoli, and Valeria Mastrullo, for their comments and assistance.

Thanks to Prof. Aldini for his co-supervision, guidance, assistance, and for allowing me to perform part of my research in his department. Also, I would like to acknowledge his team members, in particular Alessandra, Genny, Luca, and Marco, for the time they spent helping me.

My sincere gratitude to the people involved in the MASSTRPLAN programme who hardly worked to get a successful outcome, in particular to Prof. Spickett for her support at personal and scientific levels. A warm thanks to Prof. Rosario Domingues, Prof. Pedro Domingues, Dr. Maria Fedorova, and their respective collaborators, for the wonderful and fruitful time I spent in their labs during my secondments. A big thanks to Dr. Pérez-Sala, who introduced me the MASSTRPLAN project, for her motivation, role model, and guidance along my first research stages as a Bachelor and Master Student, which incented me to continue my career in the scientific field. Finally, thanks to all the ESRs, for their partnership and friendship.

Thanks to Vale, Fede, Marta, Chiara, Giacomo, Donato, Patty, Marta Z. and Yuri, among many others, for their priceless friendship, immense support along these 3 years, for making me feel at home, and for understanding me even when I was not speaking any understandable language.

Last but not least, I would like to thank all members of my big family, my parents and brothers, because everything is easier when they are by my side. Specially, thank you Mamá and Pablo for your absolute support and encouragement throughout this thesis and in my life in general. But most of all, thank you Álvaro for the countless tips to carry out this thesis, for your unconditional help, care, patience, and love, and for always being there for me. I have learned and I am still learning so much from you.

APPENDIX:
Scientific contributions

SCIENTIFIC CONTRIBUTIONS

CONFERENCE PARTICIPATION

1. Advances in the study of lipid and protein oxidation: from methods to targets. March 2019 (Ghent, Belgium)
   Oral presentation: Biological effects of glycated albumin on cardiomyocytes: possible implications in the development and progression of heart failure
   Poster: Phospholipid profile of male and female heart failure patients: a pilot study

2. FEBS Advanced Lecture Course: Redox-omic Technologies and their Applications in Health&Disease. September 2018 (Spetses, Greece)
   Poster: Phospholipid profile of male and female heart failure patients: a pilot study (Highly commended poster award)

3. International HNE Club Meeting "Reactive Oxygen Species and Lipid Peroxidation in Human Health and Disease" September 2017 (Graz, Austria).
   Poster: Cysteinylated and glycated human serum albumin levels are increased in human heart failure.

4. Annual meeting Ricerca Monzino: Who we are, What we do, Where we are going. March 2017 (Milan, Italy)
   Oral presentation: H2020 & MASS Spectrometry TRaining network for Protein Lipid adduct ANalysis: fostering new skills.

PUBLICATIONS

1. **Alma Martinez Fernandez**, Luca Regazzoni, Maura Brioschi, Erica Gianazza, Piergiuseppe
   Agostoni, Giancarlo Aldini, Cristina Banfi. Pro-oxidant and pro-inflammatory effects of glycated albumin on cardiomyocytes. Free Radical Biology and Medicine. Jun 2019
   DOI: 10.1016/j.freeradbiomed.2019.06.023

2. Erica Gianazza, Maura Brioschi**, Alma Martinez Fernandez**, Cristina Banfi. Lipoxidation in cardiovascular diseases. Redox Biology, 2019; 25:101119. DOI: 10.1016/j.redox.2019.101119

3. Roberta Baetta, Marta Pontremoli, **Alma Martinez Fernandez**, Corinne M Spickett, Cristina Banfi. Proteomics in cardiovascular diseases: unveiling sex and gender differences in the era of precision medicine**.** *Journal of Proteomics,* 2018; 173:62-76. DOI: 10.1016/j.jprot.2017.11.012

4. Cristina Banfi, **Alma Martinez Fernandez**, Maura Brioschi. Exploring the biochemistry of prenylome and its role in disease through proteomics: progress and potential. Expert Review of Proteomics*,* 2017; 14(6):515-528. DOI: 10.1080/14789450.2017.1332998

Free Radical Biology and Medicine xxx (xxxx) xxx–xxx

Contents lists available at ScienceDirect

Free Radical Biology and Medicine

journal homepage: www.elsevier.com/locate/freeradbiomed

Pro-oxidant and pro-inflammatory effects of glycated albumin on cardiomyocytes

Alma Martinez Fernandez[a], Luca Regazzoni[b], Maura Brioschi[a,*], Erica Gianazza[a], Piergiuseppe Agostoni[a,c], Giancarlo Aldini[b], Cristina Banfi[a]

[a] Centro Cardiologico Monzino, IRCCS, Milan, Italy
[b] Department of Pharmaceutical Sciences, University of Milan, Milan, Italy
[c] Department of Clinical Sciences and Community Health, Cardiovascular Section, University of Milan, Milan, Italy

ARTICLE INFO

Keywords:
Glycated albumin
Cardiomyocytes
Oxidative stress
Inflammatory response

ABSTRACT

Human serum albumin (HSA) is the most abundant circulating protein in the body and presents an extensive range of biological functions. As such, it is prone to undergo post-translational modifications (PTMs). The non-enzymatic early glycation of HSA, one of the several PTMs undergone by HSA, arises from the addition of reducing sugars to amine group residues, thus modifying the structure of HSA. These changes may affect HSA functions impairing its biological activity, finally leading to cell damage.

The aim of this study was to quantitate glycated-HSA (GA) levels in the plasma of heart failure (HF) patients and to evaluate the biological effects of GA on HL-1 cardiomyocytes.

Plasma GA content from HF patients and healthy subjects was measured by direct infusion electrospray ionization mass spectrometry (ESI-MS). Results pointed out a significant increase of GA in HF patients with respect to the control group ($p < 0.05$). Additionally, after stimulation with GA, proteomic analysis of HL-1 secreted proteins showed the modulation of several proteins involved, among other processes, in the response to stress. Further, stimulated cells showed a rapid increase in ROS generation, higher mRNA levels of the inflammatory cytokine interleukin-6 (IL-6) and tumor necrosis factor alpha (TNF-α), and higher levels of the oxidative 4-HNE-protein adducts and carbonylated proteins.

Our findings show that plasma GA is increased in HF patients. Further, GA exerts pro-inflammatory and pro-oxidant effects on cardiomyocytes, which suggest a causal role in the etiopathogenesis of HF.

1. Introduction

Human serum albumin (HSA) is the most abundant circulating protein in the body. Besides its well-known oncotic function, it has an extensive range of physiological and pharmacological functions that may be relevant under physiological circumstances and in disease [1].

It plays an important defensive role in oxidative stress, exerts immunomodulatory, anti-inflammatory, and anti-coagulant effects; it is a crucial part of the endothelial surface, and contributes to the maintenance of the normal capillary permeability and endothelial stabilization (reviewed in Ref. [1]). Further, a plethora of drugs has been determined to bind in specific sites of albumin, so that albumin has a fundamental drug-carrier role which interferes with drugs efficacy and availability at target organs [2].

Because of its long half-life (about 21 days) compared with other proteins and its high concentration in the circulatory system, serum

Abbreviations: **4-HNE**, 4-hydroxy-2-nonenal; **ACN**, acetonitrile; **AGEs**, advanced glycation end products; **CML**, carboxymethyl lysine; **CVD**, cardiovascular diseases; **DMSO**, dimethyl sulfoxide; **DNP**, dinitrophenol; **DNPH**, 2,4-dinitrophenylhydrazine; **ELISA**, enzyme-linked immunosorbent assay; **eNOS**, endothelial nitric oxide synthase; **ESI**, electrospray ionization; **FA**, formic acid; **GADPH**, glyceraldehyde 3-phosphate dehydrogenase; **GA**, glycated human serum albumin; **GLM**, general linear model; **HF**, heart failure; **HSA**, human serum albumin; **HSA-SH**, mercaptoalbumin; **HSP**, heat shock protein; **IL-6**, interleukin-6; **LC**, liquid chromatography; **MS**, mass spectrometry; **MTT**, 3-(4,5-dimethylthiazol-2-yl)-2,5-diphenyltetrazolium bromide; **NADPH**, nicotinamide adenine dinucleotide phosphate; **NF-κB**, nuclear factor kappa-light-chain-enhancer of activated B cells; **Nrf2**, nuclear factor (erythroid-derived 2)-like 2; **NYHA**, New York Heart Association; **PCR**, polymerase chain reaction; **PGC1**, peroxisome proliferator-activated receptor gamma coactivator 1; **PTMs**, post-translational modifications; **qRT-PCR**, real-time quantitative PCR; **ROS**, reactive oxygen species; **SDS-PAGE**, sodium dodecyl sulfate polyacrylamide gel electrophoresis; **TNF-α**, tumor nrecrosis factor alpha; **UPLC**, Ultra performance liquid chromatography

* Corresponding author. Monzino Cardiologic Center IRCCS, 20138, via Parea, 4, Milan, Italy.
E-mail address: maura.brioschi@ccfm.it (M. Brioschi).

https://doi.org/10.1016/j.freeradbiomed.2019.06.023
Received 19 December 2018; Received in revised form 13 June 2019; Accepted 19 June 2019

albumin is a plasmatic protein that is highly sensitive to post-translational modifications (PTMs), such as glycation.

Non-enzymatic glycation is indeed one of the underlying modifications that can modify its native secondary and tertiary structure [3]. In this process, also known as the Maillard reaction, free amine groups of albumin are initially attached by glucose or derivatives to reversibly form a Schiff base product, followed by the formation of a stable fructosamine residue by Amadori rearrangement. This is the early glycation process: Schiff's base and fructosamine (Amadori product) have been called early glycation adducts. Further modifications in these early stage glycation products, such as rearrangement, oxidation, polymerization, and cleavage give rise to irreversible conjugates, called advanced glycation end products (AGEs) [4].

Non-enzymatic glycation occurs in normal conditions, but HSA is typically 2–3 times more glycated than the rest of the serum proteins in hyperglycaemic condition [3].

Several *in vitro* studies have shown the implication of glycated albumin, mainly AGE-albumin, in cardiovascular diseases (CVD): for example, platelets are activated by both irreversibly and reversibly glycated albumin, thus promoting CVD development [5]; in endothelial cells glycated albumin enhanced ROS production by activating multiple signaling pathways [6]. Glycated albumin can also trigger damaging effects *in vitro* and *in vivo* on hepatic cells [7], all features that contribute to the increased mortality of diabetic patients [8]. Finally, bovine glycated albumin stimulates cardiomyocyte ROS production, which results in NF-κB activation and upregulation of atrial natriuretic factor mRNA suggesting that glycated albumin may play a role in the development of diabetic heart disease [9].

The relationship between AGEs and cardiovascular diseases is well known [10]. Elevated levels of AGEs were first associated with diabetes, where it was thought that AGEs formation was exclusively the result of increased blood sugar concentrations [11]. However, recent studies have extended this view and have shown that AGEs accumulation occurs also in pathological situations such as cardiac dysfunction, and renal failure, independent of diabetes [12–15].

Further, through decreased compliance of the heart and the vasculature, AGE accumulation is considered to be related to the onset and progression of heart failure (HF) [14,16].

However, the possible effects of early glycation products, such as the Amadori product, in the cardiovascular system have been less studied than the effects of the irreversible AGEs.

In this study we analyzed the levels of the Amadori product glycated-albumin (GA) in non-diabetic patients with HF and the effects of this modified protein on cardiomyocytes *in vitro*.

2. Materials and methods

2.1. Study population

Plasma samples were obtained from a subset of healthy subjects (controls) and HF patients matched according to their age, sex, and clinical characteristics, from a previously enrolled population [17]. The study was approved by the Ethical Committee European Institute of Oncology and Monzino Cardiologic Center (registration number R205-CCFM S208/412) [17]. All patients belong to a cohort of HF patients regularly followed at our HF Unit and underwent our standard HF assessment which included full clinical evaluation, standard laboratory tests, echocardiography, spirometry, and alveolar capillary diffusion, as well as cardiopulmonary exercise test. All patients had severe HF, being in New York Heart Association (NYHA) class III and IV, but were in stable clinical conditions. Patients with an established diagnosis of diabetes mellitus or under diabetes treatment were excluded. A detailed summary of the clinical characteristics, obtained as previously described [17], is reported in Table 1.

Table 1
Clinical characteristics of subjects categorized in healthy subjects, HF patients (NYHA class III), and HF patients (NYHA class IV).

	Healthy subjects (n = 10)	HF patients NYHA III (n = 7)	HF patients NYHA IV (n = 7)
Age	56.27 ± 4.69	67 ± 12.14	67.43 ± 6.24
Gender (m/f)	7/3	5/2	6/1
Hypertension	0/10	5/7	5/7
Dyslipidemia	0/10	4/7	4/7
Smoke	1/10	1/7	3/7
BMI	25.66 ± 3.42	26.68 ± 3.38	27.11 ± 4.81
Glycemia (mg/dL)	102.4 ± 12.76	105 ± 12.39	120.2 ± 12.01
GA (%)	6.53 ± 0.54	7.38 ± 1.47	8.13 ± 0.77
EF (%)	–	39.9 ± 6.57	26.86 ± 11.31
BNP (pg/mL)	–	265.14 ± 310.15	967.8 ± 668.6
DLCO (% predicted)	94.21 ± 21.06	72.09 ± 17.43	65.87 ± 12.21
VO_2 peak/Kg (mL/min/Kg)	34.58 ± 8.46	15.39 ± 8.95	11.05 ± 2.09

Data are expressed as mean ± SD. BMI, body mass index; GA, glycated human serum albumin; EF, ejection fraction; BNP, Brain natriuretic peptide; DLCO, carbon monoxide lung diffusion; VO_2, oxygen consumption; m, male; f, female.

2.2. Quantitation of glycated albumin (GA) by mass spectrometry

The relative composition of albumin isoforms in human plasma samples was evaluated, as previously described [18], by direct infusion using the Xevo TQS micro triple quadrupole mass spectrometer coupled with the M-Class UPLC system (Waters Corporation, Milford, USA). Briefly, centrifuged plasma samples at 3000 × *g* for 10 min at 4 °C were diluted 200 folds in 50% ACN containing 0.1% FA. After centrifugation at 14 000 × *g* for 10 min at 4 °C, 5 µl were injected at 5 µl/min and the spectra were acquired for 6 min with the following parameters: positive ESI mode; mass range 1100–1350 *m/z*; capillary voltage, 3 kV; cone, 90 V; desolvation temperature 350 °C; source temperature 150 °C. Data processing for deconvolution was performed with the MaxEnt1 function on the Masslynx software (Waters Corporation, Milford, USA). Mercaptoalbumin (native HSA) and GA (+160 ± 2 Da) were detected and their intensities were used to calculate the relative abundances as previously described [18] and detailed in Supplementary information.

2.3. Carboxymethyl lysine assay

Plasma levels of carboxymethyl lysine (CML) were measured with a commercially available ELISA kit (Biosite, Taby, Sweden) according to the manufacturer's instruction.

2.4. Cell culture and treatment

The HL-1 cardiomyocytes, a kind gift of Prof. W.C. Claycomb, (LSU Health Sciences Center, New Orleans, LA, USA), were cultured in complete Claycomb medium supplemented with 10% FBS (Sigma-Aldrich, Milan, Italy), 2 mmol/L L-glutamine (Thermo Fisher Scientific, Milan, Italy), and 100 µmol/L norepinephrine (Sigma-Aldrich, Milan, Italy) according to Prof. Claycomb's instructions [19]. HL-1 cells (1×10^5) were seeded onto a 6-well plate and were grown for 48 h in complete media. Before stimulation, cells were washed with PBS and then were incubated with vehicle (control cells), GA (A8301, Sigma, Milan, Italy, at 100 or 250 µg/mL corresponding to ~1.5 µmol/L or ~3.7 µmol/L, respectively), and non-glycated recombinant albumin (HSA, A9731, Sigma, Milan, Italy, at 250 µg/mL corresponding to ~3.7 µmol/L) for 8 or 16 h in Claycomb serum free medium. For secretome analysis, the treatment of the cells for 8 h and 16 h with vehicle or human albumin (GA or non-glycated) was prolonged for additional 24 h after changing the medium with serum- and phenol-free medium

[20].

2.5. MTT assay

The methylthiazolyldiphenyl-tetrazolium bromide (MTT) assay was based on the protocol first described by Mosmann [21]. Briefly, after treatment for 16 h with GA (100–250 μg/mL) or vehicle in Claycomb serum-free media as specified above, the cells were washed with PBS and incubated in serum-free and phenol-free medium for 24 h. Afterward, cells were incubated for 30 min at 37 °C with 0.1 mg/mL of MTT (Sigma-Aldrich, Milan, Italy), dissolved in serum- and phenol-free medium. At the end of the incubation, cells were dissolved in DMSO. Absorbance was recorded at 550 nm using the microplate spectrophotometer system (Mithras LB940, Berthold Technologies, Bad Wildbad, Germany). Data are expressed as absorbance values/μg of proteins.

2.6. Cell death analysis

Cytoplasmic histone-complexed DNA fragments (mono- and oligonucleosomes) were quantified as described [22] by using a one-step sandwich immunoassay (Cell death detection ELISA, Roche Diagnostics, Mannheim, Germany), according to the manufacturer's instructions. The data are expressed as absorbance at 405 nm (reference wavelength 490 nm)/μg of proteins.

2.7. Label-free mass spectrometry analysis

Secretome samples for proteomic analysis were desalted, concentrated and digested as previously described [20] with minor variations. Briefly, the cell culture media from each condition were collected and cell debris was removed by centrifugation. Then, samples were dialyzed at 4 °C using a 3500 molecular weight cut-off dialysis tubing (Spectrum Laboratories, Rancho Dominguez, CA, USA) against 5 mmol/L NH_4HCO_3 containing 0.01% EDTA, followed by dialysis against water. After lyophilization, the secreted protein pellets were dissolved in 25 mmol/L NH_4HCO_3 containing 0.1% RapiGest (Waters Corporation, Milford, MA, USA), sonicated, and centrifuged at 13 000 × *g* for 10 min. Samples (25 μg of protein) were then incubated 15 min at 80 °C and reduced with 5 mmol/L DTT at 60 °C for 15 min, followed by carbamidomethylation with 10 mmol/L iodoacetamide for 30 min at room temperature in the darkness. Then, 2 μg of sequencing grade trypsin (Promega, Milan, Italy) were added to each sample and incubated overnight at 37 °C. After digestion, 2% TFA was added to hydrolyze RapiGest and inactivate trypsin. Tryptic peptides were used for label-free mass spectrometry analysis. Label-free mass spectrometry analysis, LC-MS^E, was performed on a hybrid quadrupole-time of flight mass spectrometer coupled with a nanoUPLC system and equipped with a Trizaic source, as previously detailed [20,23].

2.8. Gene ontology analysis

Data were analyzed with the Search Tool for the Retrieval of Interacting Genes/Proteins (STRING 10.5) database [24] as previously described [25], to identify enriched gene ontology (GO) terms in the biological process, molecular function or cellular component categories.

2.9. Intracellular reactive oxygen species (ROS) formation

Generation of intracellular ROS was measured by the oxidative-sensitive fluorescent probe 2′,7′-dichlorofluorescein diacetate (DCF-DA). HL-1 cells were grown in complete media for two days on 96 black-wall clear bottom plates followed by 24 h of starvation in serum-free and phenol-free media. Cells were incubated with 10 μmol/L DCFH-DA (Sigma-Aldrich, Milan, Italy) in serum-free and phenol-free media for 1 h at 37 °C in the presence of 100 μmol/L ascorbic acid. At the end of the incubation, cells were washed in PBS and exposed to GA 250 μg/mL, HSA 250 μg/mL or vehicle for the indicated time. The production of ROS was measured by the intensity of DCF emission at 525 nm (excitation 485 nm), in a multifunctional microplate reader Tecan Infinite 200 PRO (TECAN, Milan, Italy). Results are expressed as absolute fluorescence (arbitrary units) of DCF after subtracting blank readings from all measurements.

2.10. Western blotting

Cell monolayers were harvested in Laemmli buffer (2% SDS, 10% glycerol and 62.5 mmol/L Tris, pH 6.8) containing a protease inhibitor cocktail (Sigma-Aldrich, Milan, Italy). Cell protein content was measured using the DC Protein Assay (Biorad Laboratories, Milan, Italy). Equal amounts of proteins (specifically 35 μg for the detection of HNE-adducts, 15 μg for the detection of carbonylated proteins, and 10 μg for the detection of HSP90 beta), from each condition, were separated on 12% SDS-polyacrylamide gel under reducing conditions in running buffer (25 mmol/L Tris, 3.5 mmol/L SDS, 192 mmol/L glycine) and transferred to nitrocellulose membranes in Transfer buffer with SDS (25 mmol/L Tris, 192 mmol/L glycine, 20% methanol, and 0.02% SDS) as previously described [26]. Transferred proteins were stained with MEMCode staining kit (Thermo Fisher Scientific, Milan, Italy) for loading control. The membranes were incubated with primary antibodies against 4-HNE-adducts (1:3000, Abcam, Cambridge, UK) or HSP90 beta (1:5000, Thermo Fisher Scientific, Milan, Italy), and subsequently with anti-rabbit horseradish peroxidase-conjugated secondary antibody (1:5000, Bio-Rad, Milan, Italy).

For the detection of carbonylated proteins, lyophilized pellets were suspended in 6% SDS and extracted proteins were derivatized with 20 mmol/L DNPH (in TFA 20%) for 15 min at room temperature. The DNPH-derivatized samples were then neutralized with 2 mol/L Trizma buffer containing 30% glycerol and 10% 2-β-mercaptoethanol, and the proteins were separated by SDS-PAGE and blotted to nitrocellulose membranes. Immunodetection was carried out using biotinylated anti-DNP antibody (1:5000, Invitrogen, Milan, Italy) and conjugated avidin-HRP (1:1000, Biorad, Milan, Italy) [27].

The bands were visualized by means of enhanced chemiluminescence (GE Healthcare, Milan, Italy) and analyzed with the QuantityOne software (Bio-Rad Laboratories, Milan, Italy) for densitometric analysis including normalization for total protein loading.

2.11. RNA extraction and real-time reverse transcription polymerase chain reaction (RT-PCR)

Total cellular RNA was extracted using the Total RNA purification plus kit (Norgen BioTek, Ontario, Canada) and reverse transcribed at 42 °C for 50 min, and at 70 °C for 15 min (Bio-Rad Laboratories, Milan, Italy). For 1 μg of total cellular RNA, we used 200 units of reverse transcriptase (RT; SuperScript III, Invitrogen, Life Technologies, Monza, Italy), 3 μg random hexamer primers, 1 mmol/L dNTPs, and 40 units Rnase inhibitor.

Real-time quantitative PCR (qRT-PCR) was carried out to detect Nrf2, IL-6, TNF-α, IL-10, PGC1α, and PGC1β mRNA, with GAPDH mRNA being used for sample normalization. Primers were purchased from Integrated DNA Technologies (Leuven, Belgium) and the primer sequences were: mouse GAPDH sense 5′ CGTGCCGCCTGαAACC 3’; mouse GAPDH antisense: 5′ TGGAAGAGTGGGAGTTGCTGTTG 3’; mouse Nrf2 sense 5′ GATGCTCATGAAATTTGCCTGC 3′ and mouse Nrf2 antisense: 5′ ACAAGCTTCGGTCTGGATCCA 3’. Primers for IL-6 (QT00098875), TNF-α (QT00104006), IL-10 (QT00106169), PGC1α (QT02524242), and PGC1β (QT00125272), were purchased from Qiagen (Milan, Italy). qRT-PCR was carried out as previously described on the iCycler optical system (Bio-Rad Laboratories, Milan, Italy) [28].

2.12. Statistical analysis

Clinical data from healthy subjects (control) and HF patients were analyzed using SAS v9.4 (SAS Institute, Cary, NC, USA) and are expressed as mean ± standard deviation (SD), subdividing HF patients according to NYHA class (III vs IV). Univariate analysis was performed by ANOVA to identify statistically different variables among groups while Pearson correlation was used to identify a possible correlation between GA and clinical variables. General linear model (GLM) was used to highlight the trend of increase of GA with the gravity of the disease, both as univariate analysis and as multivariate analysis taking into consideration differences of age and presence of hypertension.

Data obtained from *in vitro* experiments were expressed as mean values ± SEM and analyzed with GraphPad Prism v5.03 using ANOVA for repeated measures, followed by Tukey's test (n = the number of individual experiments performed in duplicate or triplicate), after normality assessment by Kolmogorov-Smirnov tests. p values of < 0.05 were considered significant.

3. Results

3.1. Analysis of glycated albumin in heart failure patients

Mass spectrometry analysis of albumin in human plasma samples allowed us to calculate the fraction of GA with respect to all the albumin isoforms (Fig. 1A). Comparing the percentage of GA between healthy subjects and HF patients, subdivided according to HF severity as inferable from the NYHA class (III *vs* IV), we observed an increase of GA in the plasma of the patients with respect to the healthy subjects (6.53 ± 0.54% for healthy subjects, 7.38 ± 1.47% for HF class III, and 8.13 ± 0.77% for HF class IV, Table 1). The statistical analysis demonstrated that the percentage of GA was significantly higher in the patients' group with the higher degree of HF severity (Fig. 1B), according to a univariate ANOVA analysis ($p = 0.0075$) and GLM analysis ($p = 0.0022$). Considering that age and presence of hypertension correlate with GA and are significantly different among groups, a multivariate GLM analysis was also performed after adjustment for age and hypertension revealing a significant association of GA with HF severity ($p = 0.0391$). Of note, we detected an inverse correlation between GA and peak VO_2/Kg (Fig. 1C), a known index of oxygen consumption previously associated with HF severity [17].

Analysis of CML levels on the plasma of HF patients and controls did not reveal any significant changes (Supplementary Fig. 1), thus indicating that in our samples early glycation, not advanced glycation, was present (data not shown).

3.2. Proteomic analysis of the secretome from HL-1 treated with GA

In order to investigate the effects of GA on HL-1 cardiomyocytes, we stimulated the cells with the purified commercially available GA. To this purpose, we first characterized the glycation sites present in the purified commercially available GA and in the one isolated from plasma of HF patients by means of mass spectrometry (details are available in the Supplementary Material). Results showed that 8 out of 9 glycated residues found in the human albumin from HF patients were also present in the purified commercially available GA (Supplementary Fig. 2 and Supplementary Table S1). Additional modified residues were detected only in the purified commercially available GA, although the majority at a low relative abundance (Supplementary Table S1).

Aiming to elucidate the biological impact of GA on HL-1 cardiomyocytes, we first determined the influence of GA on cell viability and apoptosis. The cells were stimulated with GA (100 or 250 μg/mL) for 16 h and then subjected to MTT assay. As reported in Fig. 2A, cells treated with GA (250 μg/mL) exhibited a slightly decreased in proliferation (−10%, $p < 0.05$) compared to the control cells. Further, apoptosis was assessed by means of Cell Death Detection ELISA assay, which measures cytosolic histone-associated DNA fragments present in the cell lysates. Results indicated that cell apoptotic responses remained unchanged after GA treatment (Fig. 2B).

For the proteomic analysis, HL-1 cells were pre-treated for 8 h or 16 h with GA (100 or 250 μg/mL) in serum-free Claycomb medium and then incubated for 24 h, in serum-free phenol-free medium in the absence of GA, in order to collect secreted proteins without the contamination of the exogenously added GA. Then, employing a label-free mass spectrometry based method (LC-MS^E) [20], we compared the secretome after GA treatment at the two different time points (8 h and 16 h) and identified those proteins that were differently abundant.

This approach allowed us to identify a total of 216 and 246 proteins in cells incubated for 8 h or 16 h, respectively, as reported in Supplementary Tables S2 and S3. After treatment with GA for 8 h, eight proteins were less abundant after treatment with 250 μg/mL GA, and only one was released at higher extent (Table 2). At 16 h, six proteins were more abundant after treatment with 250 μg/mL GA, while eight were more abundant in the secretome of control cells (Table 3).

The lists of differentially abundant proteins were analyzed with STRING for evaluation of protein-protein interactions and gene ontology analysis in order to find out the enriched biological processes. As shown in Fig. 3, considering only the proteins that were modulated after 8 h, no significantly enriched biological process was detected, while among proteins modulated after 16 h of treatment some biological processes, including response to organic substance and response to stress, were significantly enriched.

Of note, three proteins (Heat shock protein HSP90 beta, Nucleolin and Heat shock protein HSP90 alpha) belonging to these biological processes were commonly modulated at 8 h and 16 h, as shown in the Venn diagram in Fig. 4.

Thus, in order to verify the proteomic results, we confirmed by immunoblotting that treatment with GA significantly reduced the release of Heat shock protein HSP90 beta (Fig. 5). This modulation was not observed when cells were stimulated with non-glycated HSA (250 μg/mL) (Supplementary Fig. 3A).

3.3. Effects of GA on protein oxidation and lipoxidation

In view of the statistically significant enrichment of the GO term related to response to stress, we next assessed the capacity of GA to cause oxidative damage.

Exposure of HL-1 cells to GA resulted in the rapid intracellular generation of ROS, assessed by DCF fluorescence (Fig. 6). When cells were in presence of non-glycated HSA no increase in ROS levels was observed (Supplementary Fig. 3B).

Subsequently, we investigated whether GA mediated downstream oxidative damage to proteins. We evaluated, by means of western blot, intracellular 4-hydroxynonenal-protein adducts and carbonylated protein levels, both biomarkers of protein oxidation and lipoxidation. Levels of adducted proteins with 4-hydroxynonenal (4-HNE) after 8 h and 16 h of cell treatment with GA are shown in Fig. 7A and C, and Supplementary Figs. 4B and 4C. Densitometric analysis revealed that 4-HNE-protein adduct levels increased dose-dependently at 8 h, being statistically significant when the cells were incubated with GA (250 μg/mL) (Fig. 7B). 4-HNE-protein adducts formation after 16 h of cell treatment with GA did not change with respect to the control cells (Fig. 7D).

Carbonylated protein levels of cells treated with GA were detected after DNPH derivatization of the carbonyl groups using an anti-DNP antibody (Fig. 8A and C, Supplementary Figs. 4D and 4E). Densitometric analysis unveiled that cells treated with GA showed a significant increase in protein carbonylation in comparison with control cells at 16 h (Fig. 8B and D). Cells treatment with non-glycated HSA (250 μg/mL) did not show differences in the levels of carbonylated proteins with respect to the control cells (Supplementary Figs. 3C and 3D).

Additionally, it was also investigated if GA could modulate mRNA

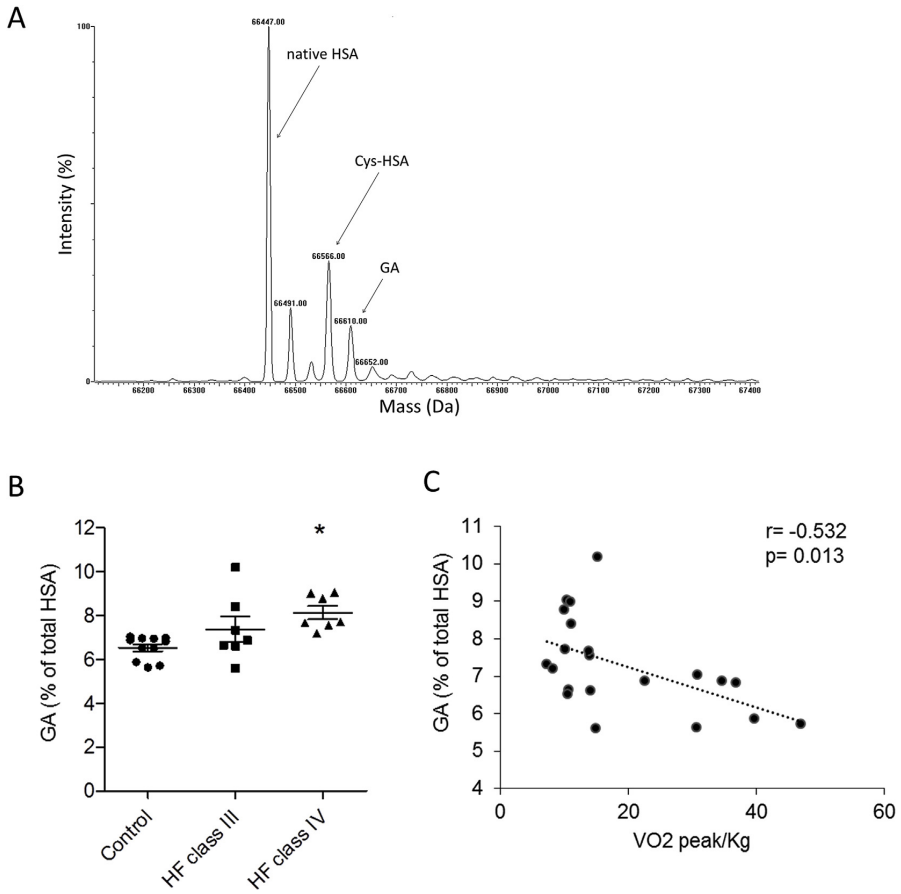

Fig. 1. Glycated albumin (GA) in heart failure patients. A) Representative deconvoluted ESI-MS spectrum of albumin from plasma of a HF patient. Arrows indicate the mercaptoalbumin (native HSA), the cysteinylated (Cys-HSA), and the glycated (GA) albumin isoforms characterized by a mass shift of 119 ± 2 and 162 ± 2 Da with respect to the native HSA, respectively. ESI-MS spectra were acquired in positive ion mode and setting a scan range of *m/z* 1100–1350. B) The percentage of GA with respect to the total amount of albumin has been analyzed by mass spectrometry in healthy subjects (controls) and HF patients divided in NYHA class III and class IV. Observed GA percentage values were 6.53 ± 0.54%, 7.38 ± 1.47%, and 8.13 ± 0.77% for healthy subjects, HF class III, and HF class IV, respectively. Values are represented as mean ± SEM. *p < 0.05 *vs* controls. C) Correlation between the percentage of GA and peak VO_2/Kg. HSA, human serum albumin.

expression levels of nuclear factor (erythroid-derived 2)-like 2 (Nrf2). Our results showed a significant increase of Nrf2 mRNA when the cells were treated with 250 μg/mL GA, either after 8 h and 16 h (Fig. 9). This effect was not observed when the cells were treated with non-glycated HSA (Supplementary Fig. 3E).

3.4. Effects of GA on inflammation and mitochondrial biogenesis mediators

Further, our results highlighted a significantly enhanced IL-6 mRNA production only after 8 h of treatment with GA (100 or 250 μg/mL) (Fig. 10A and E). The levels of IL-6 mRNA were not significantly

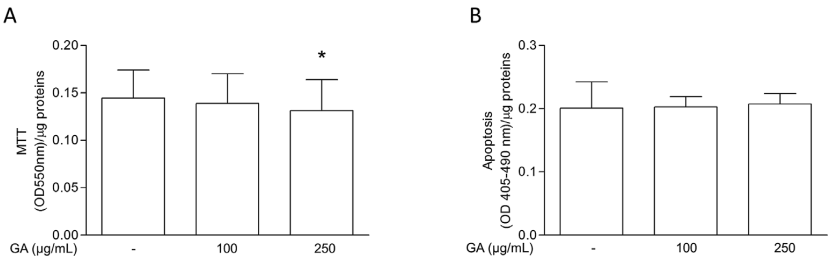

Fig. 2. Effects of GA on HL-1 cell proliferation and apoptosis. A) HL-1 cells were stimulated with GA (100 or 250 μg/mL) for 16 h and then cultured in serum-free phenol-free medium for additional 24 h. Cell proliferation assay was performed employing the MTT colorimetric method. Data are expressed as the means ± SEM of absorbance values/μg of proteins from 3 independent experiments. *p < 0.05 compared to control cells. B) Analysis of apoptosis. Cells were stimulated with GA for 16 h. Cell lysates were collected to measure apoptosis after 24 h of incubation in serum-free and phenol-free by means of Cell Death Detection ELISA Plus assay. Data are expressed as the means ± SEM of absorbance values/μg of proteins from 3 independent experiments.

Table 2
List of differentially abundant proteins in the secretome of HL-1 cells treated with GA for 8 h identified by LC-MS^E and analyzed with Progenesis QIP.

Accession	Description	Peptide count/Unique peptides	Score[a]	Anova (p)	Max fold change	Highest mean condition	Lowest mean condition
P14869	60S acidic ribosomal protein P0	6/3	32.6	2.67E-06	1.422	CTRL	250
P09405	Nucleolin	7/5	38.4	1.55E-13	1.413	CTRL	250
P26350	Prothymosin alpha	3/2	25.4	2.86E-05	1.397	CTRL	250
P14131	40S ribosomal protein S16	4/3	26.0	0.000763	1.312	CTRL	250
P11499	Heat shock protein HSP90 beta	37/18	266.4	5.77E-09	1.263	CTRL	250
P02301	Histone H3.3C	14/10	79.3	0.243 836	1.239	CTRL	250
Q03265	ATP synthase subunit alpha, mitochondrial	13/6	70.4	6.63E-06	1.236	CTRL	250
P07901	Heat shock protein HSP90 alpha	25/7	160.9	1.73E-06	1.205	CTRL	250
P68037	Ubiquitin-conjugating enzyme E2 L3	3/3	19.6	0.077 822	1.258	250	CTRL

[a] Confidence score for protein identification from Progenesis QIP; CTRL, control; 250, GA concentration (μg/mL).

Table 3
List of differentially abundant proteins in the secretome of HL-1 cells treated with GA for 16 h identified by LC-MS^E and analyzed with Progenesis QIP.

Accession	Description	Peptide count/Unique peptides	Score[a]	Anova (p)	Max fold change	Highest mean condition	Lowest mean condition
P51881	ADP/ATP translocase 2	5/2	30.1	0.0298	2.029	CTRL	100
P09405	Nucleolin	11/5	65.6	0.0049	1.764	CTRL	250
P11499	Heat shock protein HSP90 beta	37/13	297.9	0.0006	1.678	CTRL	250
P63158	High mobility group protein B1	4/2	21.7	0.0233	1.511	CTRL	250
P08113	Endoplasmin	11/2	57.6	0.0044	1.403	CTRL	250
P07901	Heat shock protein HSP90 alpha	31/10	218.6	0.0500	1.301	CTRL	250
Q9CS84	Neurexin-1	2/2	8.9	0.0035	1.247	CTRL	250
P14211	Calreticulin	11/6	89.2	0.0399	1.222	CTRL	250
O89086	RNA-binding protein 3	5/2	39.6	0.0001	1.467	250	CTRL
Q8CGC7	Bifunctional glutamate/proline–tRNA ligase	18/8	96.4	0.0013	1.336	250	CTRL
Q7TMK9	Heterogeneous nuclear ribonucleoprotein Q	9/4	48.1	0.0017	1.243	250	CTRL
P05201	Aspartate aminotransferase, cytoplasmic	25/17	196.7	0.0000	1.234	250	CTRL
P63017	Heat shock cognate 71 kDa protein	44/20	449.6	0.0007	1.223	250	CTRL
Q99JF5	Diphosphomevalonate decarboxylase	2/2	10.9	0.0425	1.204	250	CTRL

[a] Confidence score for protein identification from Progenesis QIP; CTRL, control; 100 or 250, GA concentration.

affected when the cells were treated for 8 h with non-glycated HSA (250 μg/mL) (Supplementary Fig. 3F). Additionally, a significant increase of TNF-α mRNA levels was observed in cells treated with GA (250 μg/mL), but not with non-glycated HSA, for 8 h (Fig. 10B and Supplementary Fig. 3G). The anti-inflammatory cytokine interleukin-10 (IL-10) mRNA was not detectable even after stimulation with GA (data not shown).

We next investigated the effects of GA on the expression of peroxisome proliferator-activated receptor gamma coactivator 1-alpha and beta (PGC1α and PGC1β respectively), two genes involved in the mitochondrial biogenesis. As regards PGC1α, no significant modulations were observed either after 8 h or 16 h of treatment (Fig. 10C and F). By the contrary, PGC1β mRNA levels raised after 8 h of treatment with GA (Fig. 10D and G).

4. Discussion

In this study, we found an increased amount of glycated albumin, measured by quantitative mass spectrometry, in the plasma of HF patients, and we took advantage of a proteomics-based approach to assess the effects of GA in *in vitro* cultured cardiomyocytes. Further, a functional interpretation of the identified proteins, obtained by searching the Gene Ontology (GO) annotations for over-represented terms, revealed that GA is a potential mediator of the response to stress.

Among proteins decreased after GA treatment, we found HSP90, one of the most abundant cellular HSPs that contributes intracellularly to

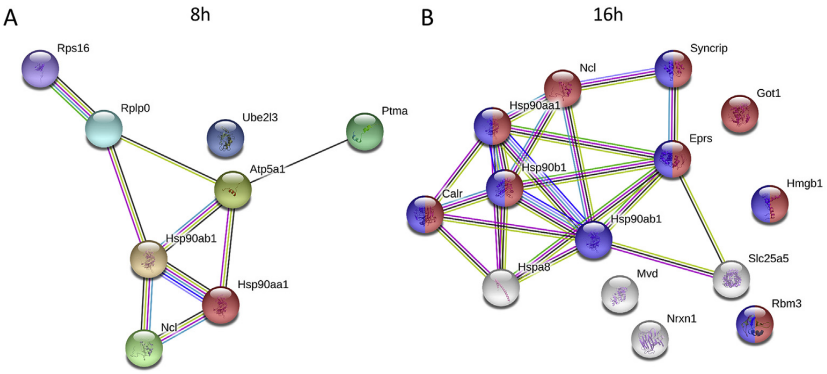

Fig. 3. Gene ontology analysis of secreted proteins modulated by GA visualized with STRING. A) Protein network obtained with proteins modulated after 8 h of treatment with GA. B) Protein network obtained with proteins modulated after 16 h of treatment with GA in which enriched biological processes are highlighted. In B, proteins associated with the GO term response to stress are colored in blue (p = 0.0229), while proteins associated with the response to organic substances are colored in red (p = 0.000222).

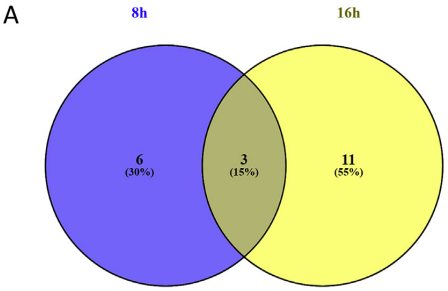

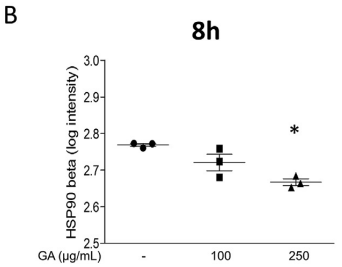

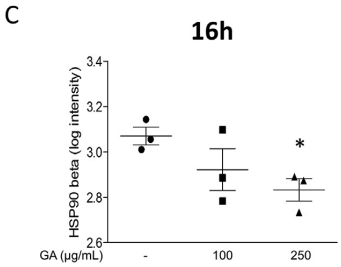

Fig. 4. Proteomic analysis of HL-1 secretome after treatment with GA. A) Venn diagram of the modulated proteins after 8 h and 16 h of incubation with GA. B–C) Graphical representation of the intensity of one of the 3 proteins that are modulated at both time points, Heat shock protein 90 beta (HSP90 beta), obtained by label free MS analysis after treatment with GA for 8 h (B) or 16 h (C). *p value $<$ 0.05 *vs* control cells.

cell survival and protection by regulating the folding and stability of a wide range of key cellular proteins, including survival and apoptotic factors [29]. HSP90 efficiently ameliorates myocardial IR-induce myocardial dysfunction in ischemic condition [30] and exerts an anti-apoptotic effect on cardiomyocytes subjected to hypoxia [31], whereas the inhibition of HSP90 markedly diminishes the protective effects of hypoxic pre-conditioning against prolonged hypoxia/reoxygenation-induced injury in H9C2 cardiac cells [32]. On the other hand, extracellular HSP90 predisposes vascular smooth muscle cells to a pro-inflammatory phenotype by IL-8 elevation in the stressed vasculature [33]. Additionally, the association of extracellular HSP90 with transforming growth factor β receptor I (TGCβRI) at the surface of cardiac fibroblast plasma membrane is critical in collagen production during fibrotic processes [34].

The role of HSPs in the glycated bovine serum albumin mediated effects has been previously observed in cultured β-cells in which a HSP60-correlated signaling pathway was hypothesized to contribute to the AGEs-RAGE axis-induced β-cell hypertrophy and dysfunction under diabetic hyperglycemia [35].

Nevertheless, there is still limited information with respect to the HSPs extracellular role on cardiomyocytes and their relationship with the pathogenesis of HF.

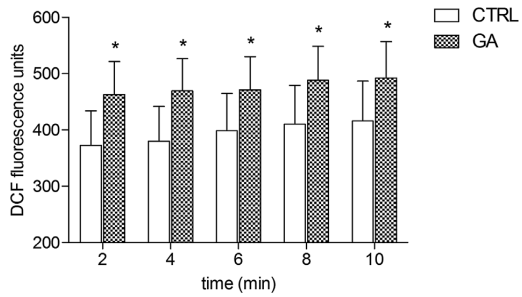

Fig. 6. Intracellular generation of reactive oxygen species (ROS) mediated by GA. HL-1 cells were loaded with 10 μmol/L DCF-DA and stimulated with GA (250 μg/mL) for different times. Data shown represent the averages of three independent experiments (mean ± SEM). *p $<$ 0.05 *vs* untreated cells.

Moreover, we found that exposure of cardiomyocytes to GA resulted in oxidative modifications, in terms of carbonylation or lipoxidation adducts, of a multitude of cellular proteins. We indeed observed that GA significantly enhances ROS production, which is in agreement with

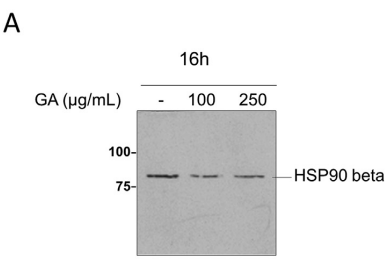

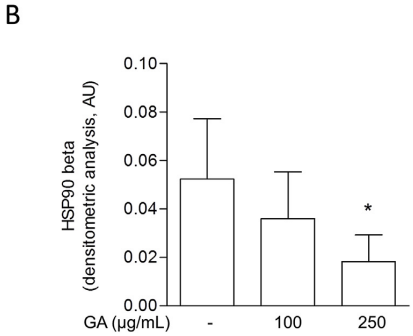

Fig. 5. Immunoblotting analysis of HSP90 beta in HL-1 secretome after treatment with GA. A) Representative image of immunoblotting analysis of HSP90 beta in the secretome from HL-1 cells treated with GA for 16 h. B) Densitometric analysis of HSP90 beta from 3 independent experiments. Data were normalized for total protein loading visualized with the MEMcode staining (Supplementary Fig. 4A). *p $<$ 0.05 *vs* untreated cells.

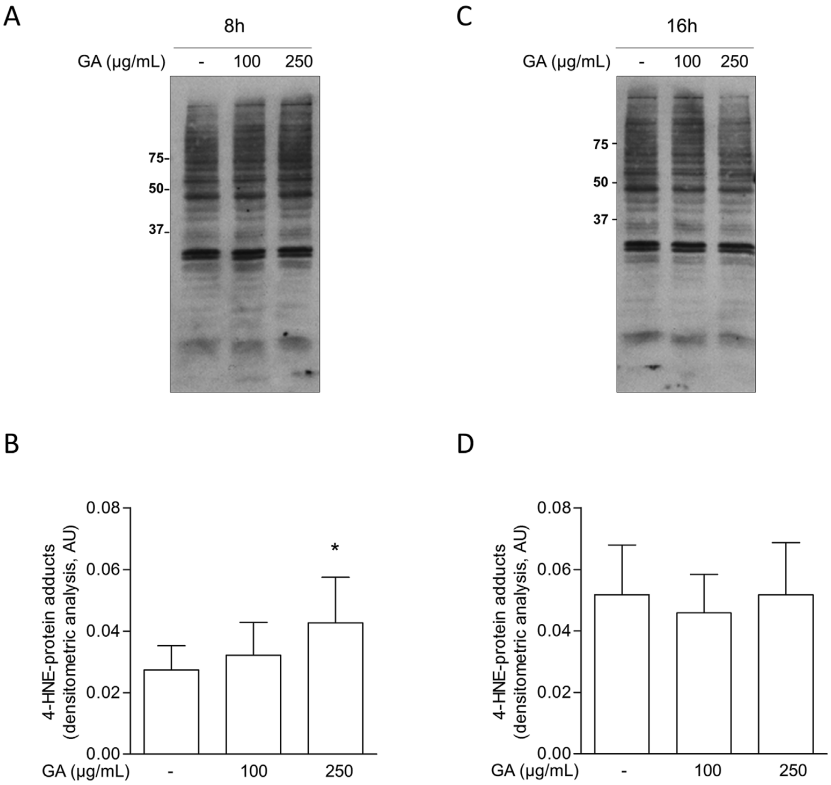

Fig. 7. Effect of GA on protein lipoxidation. Immunoblotting were performed using antibody against 4-HNE for the detection of 4-HNE-protein adducts. A) Representative western blot showing 4-HNE-protein adducts after treatment with 100 or 250 μg/mL GA for 8 h, and C) for 16 h. B) Densitometric analysis of western blots corresponding to 4-HNE immunoreactivity after 8 h and D) 16 h of treatment with GA. Data were normalized for total protein loading visualized with the MEMcode staining. Values are representative of 8 experiments and are expressed as mean ± SEM. *p < 0.05 compared to control cells.

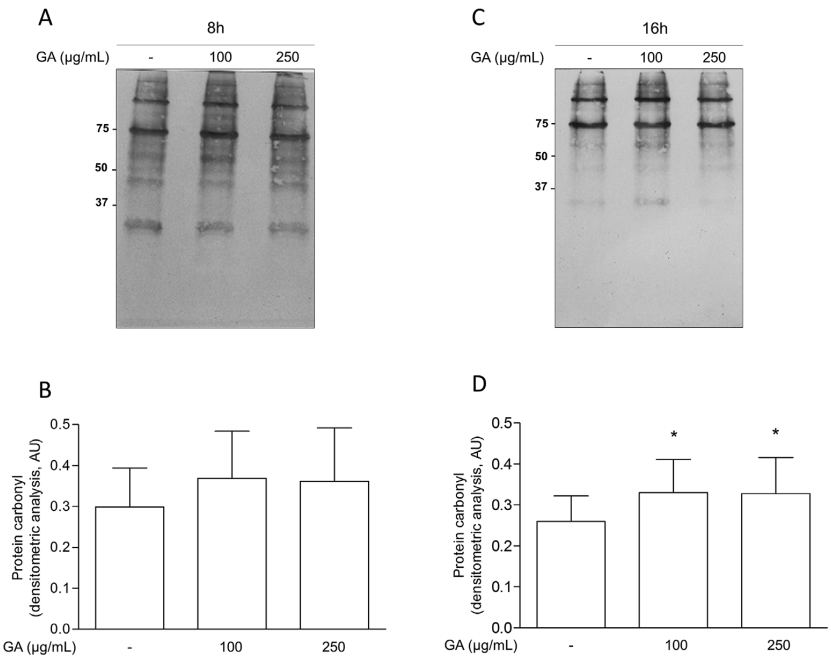

Fig. 8. Effect of GA on protein oxidation. Immunoblotting were performed using antibody against DNP for the detection of carbonylated proteins. A) Representative western blot showing carbonylated protein signal after treatment with 100 or 250 μg/mL GA for 8 h and C) 16 h. B) Densitometric analysis relative to carbonylated protein levels after 8 h and D) 16 h of incubation with GA. Values are representative of at least 8 experiments and are expressed as mean ± SEM. *p < 0.05 compared to control cells.

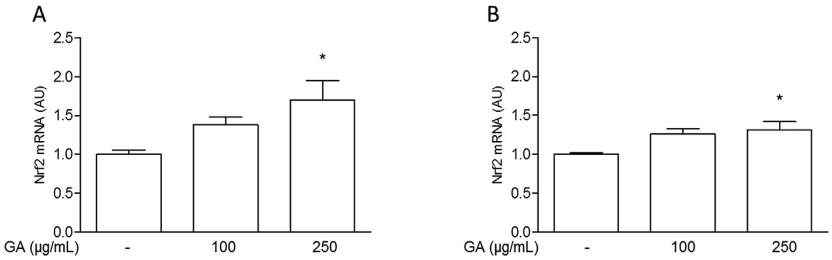

Fig. 9. Effect of GA on Nrf2 at mRNA level. Transcript expression levels analyzed by RT-qPCR were measured after A) 8 h and B) 16 h of treatment with 100 or 250 μg/mL GA. Gene expression was normalized relative to the expression of the glyceraldehyde-3-phosphate dehydrogenase (GAPDH). Results are based on 3 independent analysis and data are presented as mean ± SEM. *p < 0.05 *vs* control.

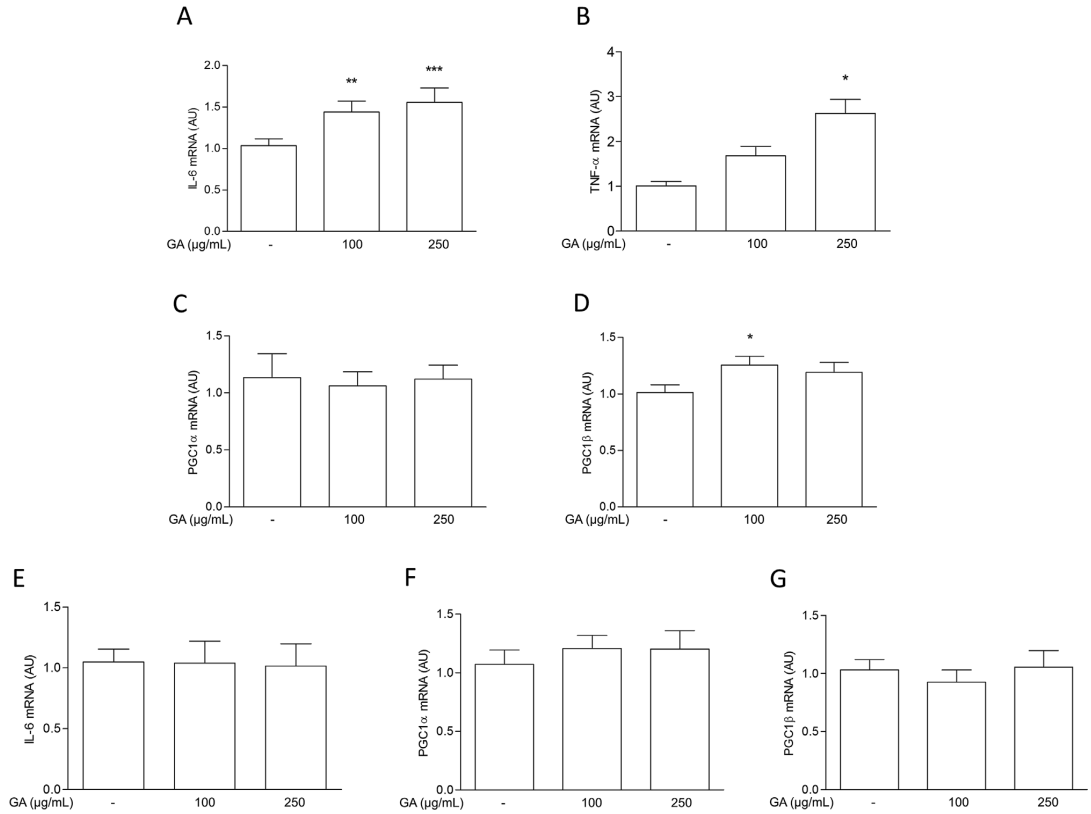

Fig. 10. Effect of GA on the mRNA levels of IL-6, TNF-α, PGC1α, and PGC1β. mRNA levels of A) IL-6, B) TNF-α, C) PGC1α, and D) PGC1β after 8 h of treatment with 100 or 250 μg/mL of GA were analyzed by RT-qPCR. mRNA levels of E) IL-6, F) PGC1α, and G) PGC1β were evaluated after 16 h or treatment with 100 or 250 μg/mL GA. Gene expression was normalized relative to the expression of the glyceraldehyde-3-phosphate dehydrogenase (GAPDH). Results are based on 10 independent experiments for IL-6, PGC1α, and PGC1β genes and on 3 independent experiments for TNF-α. Data are presented as mean ± SEM. *p < 0.05 *vs* control cells, **p < 0.01 *vs* control cells, ***p < 0.001 *vs* control cells.

previous works [36], and modulates the expression of Nrf2, a master transcription factor that becomes upregulated in response to oxidative stress [37]. The observed increase in protein carbonylation and 4-HNE-protein adduct formation can be a downstream effect of the oxidative stress mediated by GA, where excessive ROS may either oxidize proteins directly or modify them indirectly through the adduction of small breakdown products of lipid peroxidation such as 4-HNE [38]. The increase in the levels of 4-HNE modified proteins at 8 h, but not later, is suggestive of their removal by the proteasomal system, as reported by Griesser et al. [39].

The first evidence of a connection between GA and oxidative stress was the suppression of GA-induced cell apoptosis by antioxidants in bovine retinal pericytes [40]. In macrophages, GA activates ERK-dependent increases in TGF-β1 production, through oxidative stress and NF-κB induction [41]. An accumulation of oxidatively modified proteins, mainly structural proteins (i.e. ACTB and Annexin A2), was observed in human mature adipocytes incubated with GA [42]. Further, GA induces lipid infiltration in mice aorta independently of diabetes and of renin-angiotensin system local modulation by inducing lipid peroxidation and inflammation [43].

We also analyzed the expression levels of the transcriptional coactivator peroxisome proliferator-activated receptor γ coactivator-1 α (PGC-1α) and β (PGC-1 β), which, beyond their role as 'master regulator' of mitochondrial biogenesis, have been identified as inducer of

many antioxidant-detoxifying enzymes [44–46]. Downregulation of PGC-1α causes indeed an increase of intracellular ROS levels and carbonylated proteins and a decrease of antioxidant enzymes [47]. Additionally, mitochondrial activity and ROS scavenging in skeletal muscles of PGC-1β deficient mice can be enhanced by PGC-1β [46]. In our study we observed an early increase in the expression of PGC-1β but not of PGC-1α, suggesting that they cannot completely counteract the pro-oxidant effects of GA.

We also found that GA increased the expression of the pro-inflammatory cytokines IL-6 and TNF-α. Previous studies have indeed shown that GA upregulates several inflammatory mediators through the NF-κB and AP-1 signaling pathways in smooth muscle cells and endothelial cells [48,49]. Of interest, GA stimulates cell growth and migration in smooth muscle cells and fibroblasts [48,50], suggesting that GA may play a role in atherogenesis by inducing both inflammatory mediators in the vessel wall, as well as proliferative and migratory effects. By contrast, in cardiomyocytes GA slightly reduced cell viability thus supporting the hypothesis that GA plays a role in cardiac dysfunction [51].

In conclusion, this study shows that GA, measured by mass spectrometry, is elevated in the plasma of patients with HF, and it is highest in subjects with the most severe HF, thus expanding previous observations obtained by means of an enzymatic assay [52]. Specifically, Selvin et al. found a significant association of GA with cardiovascular outcomes (new cases of coronary heart disease, ischemic stroke, HF, and deaths), even after adjustment for traditional cardiovascular risk factors, in 11 104 participants with and without diabetes, during two decades of follow-up of in the community-based Atherosclerosis Risk in Communities (ARIC) Study.

Further, the findings that GA exerts pro-inflammatory and pro-oxidant effects on murine HL-1 cardiomyocytes, highlight a causal role in the etiopathogenesis of HF. However, some limitations need to be acknowledged. Indeed, other factors rather than only HF may contribute to increase the GA levels in this population studied. Further, due to the small sample size, we did not study patients with moderate HF or patients at high risk of HF, so that the progressive role of GA in the development of HF is still unknown, albeit the correlation between GA levels and peak VO_2 suggests it. Finally, our results could provide a mechanistic base for a possible use of the new antidiabetic drugs (DPP-4 inhibitors) in non-diabetic HF patients due to their favourable effect in reducing glycated proteins, specifically haemoglobin [53].

This study also highlights the role of mass spectrometry for the detection and quantitation of specific protein modifications, and contributes to strengthen the value of GA measurement over that of HbA1c which has important limitations: it does not change rapidly in response to changes in treatment, and a number of conditions affect the validity of the test result (eg, anemia, altered red cell lifespan, transfusion, kidney disease, liver disease, and abnormal forms of hemoglobin).

Declarations of interest

None.

Funding

This work was supported by the European Union's Horizon 2020 research and innovation programme under the Marie Sklodowska-Curie (grant agreement number 675132) and by the Italian Ministry of Health, Rome, Italy (Ricerca Corrente 2017 BIO 18, ID 2631209).

Aknowledgement

The Authors thank Prof William Claycomb, (LSU Health Sciences Center, New Orleans, LA, USA) for the kind gift of the HL-1 cells; Dr Alice Bonomi (Centro Cardiologico Monzino, IRCCS, Milano, Italy) for her excellent assistance in the statistical analysis; and Dr Alessandra Altomare (Department of Pharmaceutical Sciences, Università degli Studi di Milano, Milano, Italy) for the analysis of albumin modifications.

Appendix A. Supplementary data

Supplementary data to this article can be found online at https://doi.org/10.1016/j.freeradbiomed.2019.06.023.

References

[1] R. Ferrer, X. Mateu, E. Maseda, J.C. Yebenes, C. Aldecoa, C. De Haro, J.C. Ruiz-Rodriguez, J. Garnacho-Montero, Non-oncotic properties of albumin. A multidisciplinary vision about the implications for critically ill patients, Expert Rev. Clin. Pharmacol. 11 (2) (2018) 125–137, https://doi.org/10.1080/17512433.2018.1412827.

[2] F. Zsila, Subdomain IB is the third major drug binding region of human serum albumin: toward the three-sites model, Mol. Pharm. 10 (5) (2013) 1668–1682, https://doi.org/10.1021/mp400027q.

[3] P. Rondeau, E. Bourdon, The glycation of albumin: structural and functional impacts, Biochimie 93 (4) (2011) 645–658, https://doi.org/10.1016/j.biochi.2010.12.003.

[4] M.P. Cohen, Clinical, pathophysiological and structure/function consequences of modification of albumin by Amadori-glucose adducts, Biochim. Biophys. Acta 1830 (12) (2013) 5480–5485, https://doi.org/10.1016/j.bbagen.2013.04.024.

[5] I. Soaita, W. Yin, D.A. Rubenstein, Glycated albumin modifies platelet adhesion and aggregation responses, Platelets 28 (7) (2017) 682–690, https://doi.org/10.1080/09537104.2016.1260703.

[6] B.K. Rodino-Janeiro, B. Paradela-Dobarro, S. Raposeiras-Roubin, M. Gonzalez-Peteiro, J.R. Gonzalez-Juanatey, E. Alvarez, Glycated human serum albumin induces NF-kappaB activation and endothelial nitric oxide synthase uncoupling in human umbilical vein endothelial cells, J. Diabet. Complicat. 29 (8) (2015) 984–992, https://doi.org/10.1016/j.jdiacomp.2015.07.016.

[7] J. Patche, D. Girard, A. Catan, F. Boyer, A. Dobi, C. Planesse, N. Diotel, A. Guerin-Dubourg, P. Baret, S.B. Bravo, B. Paradela-Dobarro, E. Alvarez, M.F. Essop, O. Meilhac, E. Bourdon, P. Rondeau, Diabetes-induced hepatic oxidative stress: a new pathogenic role for glycated albumin, Free Radic. Biol. Med. 102 (2017) 133–148, https://doi.org/10.1016/j.freeradbiomed.2016.11.026.

[8] S.A. Harrison, Liver disease in patients with diabetes mellitus, J. Clin. Gastroenterol. 40 (1) (2006) 68–76 https://doi.org/10.1097/01.mcg.0000190774.91875.d2.

[9] M. Zhang, A.L. Kho, N. Anilkumar, R. Chibber, P.J. Pagano, A.M. Shah, A.C. Cave, Glycated proteins stimulate reactive oxygen species production in cardiac myocytes: involvement of Nox2 (gp91phox)-containing NADPH oxidase, Circulation 113 (9) (2006) 1235–1243, https://doi.org/10.1161/CIRCULATIONAHA.105.581397.

[10] D. Deluyker, L. Evens, V. Bito, Advanced glycation end products (AGEs) and cardiovascular dysfunction: focus on high molecular weight AGEs, Amino Acids 49 (9) (2017) 1535–1541, https://doi.org/10.1007/s00726-017-2464-8.

[11] M. Brownlee, Advanced protein glycosylation in diabetes and aging, Annu. Rev. Med. 46 (1995) 223–234, https://doi.org/10.1146/annurev.med.46.1.223.

[12] E.D. McNair, C.R. Wells, A.M. Qureshi, R.S. Basran, C. Pearce, J. Orvold, J. Devilliers, K. Prasad, Low levels of soluble receptor for advanced glycation end products in non-ST elevation myocardial infarction patients, Int. J. Angiol. 18 (4) (2009) 187–192 https://doi.org/10.1055/s-0031-1278352.

[13] S. Willemsen, J.W. Hartog, M.R. Heiner-Fokkema, D.J. van Veldhuisen, A.A. Voors, Advanced glycation end-products, a pathophysiological pathway in the cardiorenal syndrome, Heart Fail. Rev. 17 (2) (2012) 221–228, https://doi.org/10.1007/s10741-010-9225-z.

[14] S. Willemsen, J.W. Hartog, D.J. van Veldhuisen, P. van der Meer, J.F. Roze, T. Jaarsma, C. Schalkwijk, I.C. van der Horst, H.L. Hillege, A.A. Voors, The role of advanced glycation end-products and their receptor on outcome in heart failure patients with preserved and reduced ejection fraction, Am. Heart J. 164 (5) (2012) 742–749, https://doi.org/10.1016/j.ahj.2012.07.027 e3.

[15] G. Misciagna, G. De Michele, M. Trevisan, Non enzymatic glycated proteins in the blood and cardiovascular disease, Curr. Pharmaceut. Des. 13 (36) (2007) 3688–3695 https://doi.org/10.2174/138161207783018545.

[16] J.W. Hartog, A.A. Voors, S.J. Bakker, A.J. Smit, D.J. van Veldhuisen, Advanced glycation end-products (AGEs) and heart failure: pathophysiology and clinical implications, Eur. J. Heart Fail. 9 (12) (2007) 1146–1155, https://doi.org/10.1016/j.ejheart.2007.09.009.

[17] P. Gargiulo, C. Banfi, S. Ghilardi, D. Magri, M. Giovannardi, A. Bonomi, E. Salvioni, E. Battaia, P.P. Filardi, E. Tremoli, P. Agostoni, Surfactant-derived proteins as markers of alveolar membrane damage in heart failure, PLoS One 9 (12) (2014) e115030, , https://doi.org/10.1371/journal.pone.0115030.

[18] L. Regazzoni, L. Del Vecchio, A. Altomare, K.J. Yeum, D. Cusi, F. Locatelli, M. Carini, G. Aldini, Human serum albumin cysteinylation is increased in end stage renal disease patients and reduced by hemodialysis: mass spectrometry studies, Free Radic. Res. 47 (3) (2013) 172–180, https://doi.org/10.3109/10715762.2012.756139.

[19] W.C. Claycomb, N.A. Lanson Jr., B.S. Stallworth, D.B. Egeland, J.B. Delcarpio, A. Bahinski, N.J. Izzo Jr., HL-1 cells: a cardiac muscle cell line that contracts and

retains phenotypic characteristics of the adult cardiomyocyte, Proc. Natl. Acad. Sci. U. S. A. 95 (6) (1998) 2979–2984 https://doi.org/10.1073/pnas.95.6.2979.
[20] M. Brioschi, S. Lento, E. Tremoli, C. Banfi, Proteomic analysis of endothelial cell secretome: a means of studying the pleiotropic effects of Hmg-CoA reductase inhibitors, J Proteomics 78 (2013) 346–361, https://doi.org/10.1016/j.jprot.2012.10.003.
[21] T. Mosmann, Rapid colorimetric assay for cellular growth and survival: application to proliferation and cytotoxicity assays, J. Immunol. Methods 65 (1–2) (1983) 55–63 https://doi.org/10.1016/0022-1759(83)90303-4.
[22] S. Cosentino, C. Banfi, J.C. Burbiel, H. Luo, E. Tremoli, M.P. Abbracchio, Cardiomyocyte death induced by ischaemic/hypoxic stress is differentially affected by distinct purinergic P2 receptors, J. Cell Mol. Med. 16 (5) (2012) 1074–1084, https://doi.org/10.1111/j.1582-4934.2011.01382.x.
[23] M. Roverso, M. Brioschi, C. Banfi, S. Visentin, S. Burlina, R. Seraglia, P. Traldi, A. Lapolla, A preliminary study on human placental tissue impaired by gestational diabetes: a comparison of gel-based versus gel-free proteomics approaches, Eur. J. Mass Spectrom. (Chichester) 22 (2) (2016) 71–82, https://doi.org/10.1255/ejms.1412.
[24] A. Franceschini, D. Szklarczyk, S. Frankild, M. Kuhn, M. Simonovic, A. Roth, J. Lin, P. Minguez, P. Bork, C. von Mering, L.J. Jensen, STRING v9.1: protein-protein interaction networks, with increased coverage and integration, Nucleic Acids Res. 41 (2013) D808–D815, https://doi.org/10.1093/nar/gks1094 (Database issue).
[25] M. Pontremoli, M. Brioschi, R. Baetta, S. Ghilardi, C. Banfi, Identification of DKK-1 as a novel mediator of statin effects in human endothelial cells, Sci. Rep. 8 (1) (2018) 16671, https://doi.org/10.1038/s41598-018-35119-7.
[26] C. Banfi, M. Brioschi, S.S. Barbieri, S. Eligini, S. Barcella, E. Tremoli, S. Colli, L. Mussoni, Mitochondrial reactive oxygen species: a common pathway for PAR1- and PAR2-mediated tissue factor induction in human endothelial cells, J. Thromb. Haemost. 7 (1) (2009) 206–216, https://doi.org/10.1111/j.1538-7836.2008.03204.x.
[27] M. Brioschi, G. Polvani, P. Fratto, A. Parolari, P. Agostoni, E. Tremoli, C. Banfi, Redox proteomics identification of oxidatively modified myocardial proteins in human heart failure: implications for protein function, PLoS One 7 (5) (2012) e35841, , https://doi.org/10.1371/journal.pone.0035841.
[28] S. Lento, M. Brioschi, S. Barcella, M.T. Nasim, S. Ghilardi, S.S. Barbieri, E. Tremoli, C. Banfi, Proteomics of tissue factor silencing in cardiomyocytic cells reveals a new role for this coagulation factor in splicing machinery control, J Proteomics 119 (2015) 75–89, https://doi.org/10.1016/j.jprot.2015.01.021.
[29] K. Terasawa, M. Minami, Y. Minami, Constantly updated knowledge of Hsp90, J. Biochem. 137 (4) (2005) 443–447, https://doi.org/10.1093/jb/mvi056.
[30] C. Kupatt, C. Dessy, R. Hinkel, P. Raake, G. Daneau, C. Bouzin, P. Boekstegers, O. Feron, Heat shock protein 90 transfection reduces ischemia-reperfusion-induced myocardial dysfunction via reciprocal endothelial NO synthase serine 1177 phosphorylation and threonine 495 dephosphorylation, Arterioscler. Thromb. Vasc. Biol. 24 (8) (2004) 1435–1441, https://doi.org/10.1161/01.ATV.0000134300.87476.d1.
[31] W. Wang, Y. Peng, Y. Wang, X. Zhao, Z. Yuan, Anti-apoptotic effect of heat shock protein 90 on hypoxia-mediated cardiomyocyte damage is mediated via the phosphatidylinositol 3-kinase/AKT pathway, Clin. Exp. Pharmacol. Physiol. 36 (9) (2009) 899–903, https://doi.org/10.1111/j.1440-1681.2009.05167.x.
[32] J.D. Jiao, V. Garg, B. Yang, K. Hu, Novel functional role of heat shock protein 90 in ATP-sensitive K+ channel-mediated hypoxic preconditioning, Cardiovasc. Res. 77 (1) (2008) 126–133, https://doi.org/10.1093/cvr/cvm028.
[33] S.W. Chung, J.H. Lee, K.H. Choi, Y.C. Park, S.K. Eo, B.Y. Rhim, K. Kim, Extracellular heat shock protein 90 induces interleukin-8 in vascular smooth muscle cells, Biochem. Biophys. Res. Commun. 378 (3) (2009) 444–449, https://doi.org/10.1016/j.bbrc.2008.11.063.
[34] R. Garcia, D. Merino, J.M. Gomez, J.F. Nistal, M.A. Hurle, A.L. Cortajarena, A.V. Villar, Extracellular heat shock protein 90 binding to TGFbeta receptor I participates in TGFbeta-mediated collagen production in myocardial fibroblasts, Cell. Signal. 28 (10) (2016) 1563–1579, https://doi.org/10.1016/j.cellsig.2016.07.003.
[35] S.S. Guan, M.L. Sheu, R.S. Yang, D.C. Chan, C.T. Wu, T.H. Yang, C.K. Chiang, S.H. Liu, The pathological role of advanced glycation end products-downregulated heat shock protein 60 in islet beta-cell hypertrophy and dysfunction, Oncotarget 7 (17) (2016) 23072–23087, https://doi.org/10.18632/oncotarget.8604.
[36] B.K. Rodino-Janeiro, M. Gonzalez-Peteiro, R. Ucieda-Somoza, J.R. Gonzalez-Juanatey, E. Alvarez, Glycated albumin, a precursor of advanced glycation end-products, up-regulates NADPH oxidase and enhances oxidative stress in human endothelial cells: molecular correlate of diabetic vasculopathy, Diabetes Metab. Res. Rev. 26 (7) (2010) 550–558, https://doi.org/10.1002/dmrr.1117.
[37] C. Ma-On, A. Sanpavat, P. Whongsiri, S. Suwannasin, N. Hirankarn, P. Tangkijvanich, C. Boonla, Oxidative stress indicated by elevated expression of Nrf2 and 8-OHdG promotes hepatocellular carcinoma progression, Med. Oncol. 34 (4) (2017) 57, https://doi.org/10.1007/s12032-017-0914-5.
[38] E. Gianazza, M. Brioschi, A.M. Fernandez, C. Banfi, Lipoxidation in cardiovascular diseases, Redox Biol. (2019) 101119, https://doi.org/10.1016/j.redox.2019.101119.
[39] E. Griesser, V. Vemula, N. Raulien, U. Wagner, S. Reeg, T. Grune, M. Fedorova, Cross-talk between lipid and protein carbonylation in a dynamic cardiomyocyte model of mild nitroxidative stress, Redox Biol. 11 (2017) 438–455, https://doi.org/10.1016/j.redox.2016.12.028.
[40] J. Kim, K.S. Kim, J.W. Shinn, Y.S. Oh, H.T. Kim, I. Jo, S.H. Shinn, The effect of antioxidants on glycated albumin-induced cytotoxicity in bovine retinal pericytes, Biochem. Biophys. Res. Commun. 292 (4) (2002) 1010–1016, https://doi.org/10.1006/bbrc.2002.6751.
[41] M.P. Cohen, E. Shea, S. Chen, C.W. Shearman, Glycated albumin increases oxidative stress, activates NF-kappa B and extracellular signal-regulated kinase (ERK), and stimulates ERK-dependent transforming growth factor-beta 1 production in macrophage RAW cells, J. Lab. Clin. Med. 141 (4) (2003) 242–249, https://doi.org/10.1067/mlc.2003.27.
[42] N.R. Singh, P. Rondeau, L. Hoareau, E. Bourdon, Identification of preferential protein targets for carbonylation in human mature adipocytes treated with native or glycated albumin, Free Radic. Res. 41 (10) (2007) 1078–1088, https://doi.org/10.1080/10715760701487674.
[43] D.J. Gomes, A.P. Velosa, L.S. Okuda, F.B. Fusco, K.S. da Silva, P.R. Pinto, E.R. Nakandakare, M.L. Correa-Giannella, T. Woods, M.A. Brimble, R. Pickford, K.A. Rye, W.R. Teodoro, S. Catanozi, M. Passarelli, Glycated albumin induces lipid infiltration in mice aorta independently of DM and RAS local modulation by inducing lipid peroxidation and inflammation, J. Diabet. Complicat. 30 (8) (2016) 1614–1621, https://doi.org/10.1016/j.jdiacomp.2016.07.001.
[44] K. Aquilano, P. Vigilanza, S. Baldelli, B. Pagliei, G. Rotilio, M.R. Ciriolo, Peroxisome proliferator-activated receptor gamma co-activator 1alpha (PGC-1alpha) and sirtuin 1 (SIRT1) reside in mitochondria: possible direct function in mitochondrial biogenesis, J. Biol. Chem. 285 (28) (2010) 21590–21599, https://doi.org/10.1074/jbc.M109.070169.
[45] J. St-Pierre, S. Drori, M. Uldry, J.M. Silvaggi, J. Rhee, S. Jager, C. Handschin, K. Zheng, J. Lin, W. Yang, D.K. Simon, R. Bachoo, B.M. Spiegelman, Suppression of reactive oxygen species and neurodegeneration by the PGC-1 transcriptional coactivators, Cell 127 (2) (2006) 397–408, https://doi.org/10.1016/j.cell.2006.09.024.
[46] T. Gali Ramamoorthy, G. Laverny, A.I. Schlagowski, J. Zoll, N. Messaddeq, J.M. Bornert, S. Panza, A. Ferry, B. Geny, D. Metzger, The transcriptional coregulator PGC-1beta controls mitochondrial function and anti-oxidant defence in skeletal muscles, Nat. Commun. 6 (2015) 10210, https://doi.org/10.1038/ncomms10210.
[47] S. Baldelli, K. Aquilano, M.R. Ciriolo, PGC-1alpha buffers ROS-mediated removal of mitochondria during myogenesis, Cell Death Dis. 5 (2014) e1515, https://doi.org/10.1038/cddis.2014.458.
[48] Y. Hattori, M. Suzuki, S. Hattori, K. Kasai, Vascular smooth muscle cell activation by glycated albumin (Amadori adducts), Hypertension 39 (1) (2002) 22–28.
[49] H.J. Wang, W.Y. Lo, L.J. Lin, Angiotensin-(1-7) decreases glycated albumin-induced endothelial interleukin-6 expression via modulation of miR-146a, Biochem. Biophys. Res. Commun. 430 (3) (2013) 1157–1163, https://doi.org/10.1016/j.bbrc.2012.12.018.
[50] Y. Liu, C. Liang, X. Liu, B. Liao, X. Pan, Y. Ren, M. Fan, M. Li, Z. He, J. Wu, Z. Wu, AGEs increased migration and inflammatory responses of adventitial fibroblasts via RAGE, MAPK and NF-kappaB pathways, Atherosclerosis 208 (1) (2010) 34–42, https://doi.org/10.1016/j.atherosclerosis.2009.06.007.
[51] Z. Hegab, S. Gibbons, L. Neyses, M.A. Mamas, Role of advanced glycation end products in cardiovascular disease, World J. Cardiol. 4 (4) (2012) 90–102, https://doi.org/10.4330/wjc.v4.i4.90.
[52] E. Selvin, A.M. Rawlings, P.L. Lutsey, N. Maruthur, J.S. Pankow, M. Steffes, J. Coresh, Fructosamine and glycated albumin and the risk of cardiovascular outcomes and death, Circulation 132 (4) (2015) 269–277, https://doi.org/10.1161/CIRCULATIONAHA.115.015415.
[53] K. Esposito, P. Chiodini, M.I. Maiorino, G. Bellastella, A. Capuano, D. Giugliano, Glycaemic durability with dipeptidyl peptidase-4 inhibitors in type 2 diabetes: a systematic review and meta-analysis of long-term randomised controlled trials, BMJ Open 4 (6) (2014) e005442, , https://doi.org/10.1136/bmjopen-2014-005442.

SUPPLEMENTARY MATERIALS AND METHODS

QUANTITATION OF TOTAL GLYCATED ALBUMIN (GA) BY MASS SPECTROMETRY

The relative composition of albumin isoforms in human plasma samples was evaluated, as previously described [1], by direct infusion using the Xevo TQS micro triple quadrupole mass spectrometer coupled with the M-Class UPLC system (Waters Corporation, Milford, USA). Briefly, centrifuged plasma samples at 3000 x g for 10 min at 4°C were diluted 200 folds in 50% ACN containing 0.1% FA. After centrifugation at 14000 x g for 10 min at 4°C, 5 µl were injected at 5 µl/min and the spectra were acquired for 6 minutes with the following parameters: positive ESI mode; mass range 1100-1350 m/z; capillary voltage, 3kV; cone, 90V; desolvation temperature 350°C; source temperature 150°C. Data processing for deconvolution was performed with the MaxEnt1 function on the Masslynx software (Waters Corporation, Milford, USA). Mercaptoalbumin (native HSA) and GA (+160 ± 2 Da) were detected and their intensities were used to calculate the relative abundances as previously described [1]. For the relative quantitation of glycated HSA in the plasma of HF patients we performed the intact protein MS analysis as described by Regazzoni et al [1]. After deconvolution of the spectra we identified a peak that corresponds to the Mercaptoalbumin HSA (approximately 66446 Da) and a peak with a mass increase of 162 Da with respect to the previous one, which is the mass shift characteristic after the addition of one molecule of glucose per molecule of albumin. Hence, in this step, we considered the intensity of the Mercaptoalbumin HSA and the intensity of the peak that presented a mass shift of 162 to calculate the % of glycated-HSA.

ANALYSIS OF PURIFIED COMMERCIALLY AVAILABLE GA AND PLASMA HSA GLYCATION SITES

a) **Sample preparation: In solution digestion of purified commercially available GA and plasma HSA from HF patients**

HSA from HF patients was removed from plasma (Pierce Albumin depletion kit (Thermo Fisher Scientific, Milan, Italy)). HSA from HF patients and purified commercially available GA (Sigma, Milan, Italy) concentrations were determined by means of Bradford's method. 10 µg of each sample were reduced with 10 mmol/L DTT at 56 °C for 30 min, and carbamidomethylated with 55 mmol/L iodoacetamide for 20 min at room temperature in the darkness. In solution digestion was performed incubating 0.5 µg trypsin (Roche, Monza, Italy) overnight at 37 °C. 2 µg of tryptic peptides from each sample were purified by use of ZipTip C18 pipette tip (Merck Millipore, Milan, Italy). The purified peptides were eluted with 0.1% formic acid (FA) in water/acetonitrile 2/8 (vol/vol) respectively. Afterwards, eluted tryptic peptides were dried and stored at -20 °C until further analysis.

b) Mass spectrometry analyses

Tryptic peptides were analyzed at UNITECH OMICs (University of Milano, Italy) using a Dionex Ultimate 3000 nano-LC system (Sunnyvale CA, USA) connected to an Orbitrap Fusion™ Tribrid™ Mass Spectrometer (Thermo Scientific, Bremen, Germany) equipped with a nano-electrospray ion source. Peptide mixtures were pre-concentrated onto an Acclaim PepMap 100 - 100µm x 2cm C18 and separated on EASY-Spray column, 15 cm x 75 µm ID packed with Thermo Scientific Acclaim PepMap RSLC C18, 3 µm, 100 Å. The temperature was setting to 35 °C and the flow rate was 300 nL min−1. Mobile phases were the following: 0.1% formic acid (FA) in water (solvent A); 0.1% FA in water/acetonitrile (solvent B) with 2/8 ratio. Peptides were eluted from the column with the following gradient: 4% to 28% of B for 90 min and then 28% to 40% of B in 10 min, and to 95% within the following 6 min to rinse the column. Column was re-equilibrated for 20 min. Total run time was 130 min. One blank was run between replicates to prevent sample carryover. MS spectra were collected over an m/z range of 375-1500 Da at 120,000 resolutions, operating in the data dependent mode (DDA), cycle time 3 sec between master scans. HCD was performed with collision energy set at 35 eV. Each sample was analyzed in two technical replicates.

c) Identification and localization of protein adducts

The software Proteome Discoverer (version 1.3.0.339, Thermo Scientific, USA), implemented with the algorithm SEQUEST, was used to compare the experimental full and tandem mass spectra with the theoretical ones obtained by the in silico digestion of the HSA sequence (Uniprot P02768). Trypsin was selected as the cleaving protease, allowing a maximum of 2 missed cleavages. Peptide and fragment ion tolerances were set to 5 ppm and 10 mmu, respectively. Cysteine carbamidomethylation was set as fix modification (+57.02147); methionine oxidation was allowed as a variable modification in addition to the known glycation-derived modifications as listed in Table below.

Table S4. Glycation-derived PTMs and their corresponding mass shift.

Glycation-derived PTMs	**Δm shift (Da)**	**AA residue**
Deoxy-fructosyl-derivative	+162.05282	Lys, Arg
3-deoxyglucosone-derived imidazolone	+144.04226	Arg
Pyrraline	+108.17230	Lys

As a quality filter, only peptides with an Xcore value grater then 2.2 were considered as genuine peptide identifications. To ensure the lowest number of false positives, the mass values experimentally recorded were further processed through a combined search with the Database Decoy, where the protein sequences are inverted and randomized. This operation allows the calculation of the false discovery rate (FDR) for each match, so that all the proteins out of range of FDR between to 0.01 (strict) and 0.05 (relaxed) were rejected.

For the localization of glycation-derived modifications, the MS/MS spectra of modified peptides were manually inspected; for the confident mapping of the modification sites, spectra were requested to match the expected ions (b and/or y) neighboring the modified amino acid residue both

at the N- and C-termini. Representative spectra of the peptides containing the modification are represented in **Supplementary Figure 5 and 6**.

d) Semi-quantitative analysis of PTMs in purified commercially available GA and plasma HSA from HF patients

The relative extent of each protein modification has been calculated by determining the amount of the modified peptide in respect to the native one, by assuming that the ionization efficiency of the native and the modified peptides are equal. In particular, the single ion traces (SIC) of the native and modified peptides were firstly reconstituted by setting as filter ion the m/z values of the corresponding precursor protonated peptides. The peak areas were then automatically calculated by the Qual Browser tool of the Xcalibur data system (version 2.0.7, Thermo Scientific Inc., Milan, Italy) and then the relative abundance calculated by using the eq. 1.

Eq. 1 $$\text{Relative Abundance \%} = \frac{\text{Modified Peptide Peak Area}}{(\text{Modified Peptide Peak Area} + \text{Nativ Peptide Peak Area})} * 100$$

The relative abundance of each modified peptide was determined in both the purified commercially available GA and plasma HSA from HF patients.

LEGENDS TO SUPPLEMENTARY FIGURES

Supplementary Figure 1. Levels of carboxymethyl lysine (CML) in plasma from healthy subjects and HF patients. Plasma levels of CML were analyzed by ELISA assay and are expressed as mean±SD. No statistically significant differences were detected.

Supplementary Figure 2. Venn diagram of the glycated residues found in plasma from HF patients and in the purified commercially available GA.

Supplementary Figure 3. Effects of 250 μg/mL HSA (non-modified HSA) on HL-1 cardiomyocyte cells. A) Densitometric analysis relative to Hsp90 beta after 16 hours of treatment with HSA. B) Intracellular generation of reactive oxygen species (ROS) mediated by HSA. HL-1 cells were loaded with 10 μmol/L DCF-DA and stimulated for different times. C) Densitometric analysis relative to carbonyl protein levels after 8 hours and D) 16 hours of incubation with HSA. E) mRNA expression of Nrf2, F) IL-6, and G) TNFα after 8 hours of treatment with 250 μg/mL HSA.. Immunoblotting were performed using antibody against HSP90 beta or DNP for detecting carbonylated protein levels, and signal intensity were normalized relative to the total protein staining. Gene expression was normalized relative to the expression of the glyceraldehyde-3-phosphate dehydrogenase (GAPDH). Results are based on at least 3 independent experiments and data are presented as mean±SD.

Supplementary Figure 4. Total protein loading control of representative western blot membranes stained with MemCode™. Blots were subsequently used for incubation with antibodies against: A) HSP90 beta after 16 hours of treatment with 100 and 250 μg/mL GA; B) 4-HNE after 8 hours and C) 16 hours of treatment with 100 and 250 μg/mL GA; and DNP after D) 8 hours and E) 16 hours of treatment with 100 and 250 μg/mL GA.

Supplementary Figure 5: Fragmentation mass spectra (MS/MS) of the two most abundant glycated peptides present in the plasma of HF patients and the relevant fragments for their attribution. A) Spectrum from the peptide AEFAEVSkLVTDLTK (glycated residue Lys 233). B) Spectrum corresponding to the peptide kQTALVELVK (modified residue Lys 525). The calculated fragment ions b+, b2+, y+, y2+ of the adducted peptides are reported in the tables and those identified in the MS/MS spectra are highlighted by red (b series) and blue (y series) colors. The y and b fragment ions which are matched in the MS/MS spectra are highlighted by red and blue color and also labeled. DF, deoxy-fructosyl.

Supplementary Figure 6: Fragmentation mass spectra (MS/MS) of the two most abundant glycated peptides present in the purified commercially available glycated-HSA and the relevant fragments for their attribution. A) Spectrum from the peptide AEFAEVSkLVTDLTK (glycated residue Lys 233). B) Spectrum corresponding to the peptide kQTALVELVK (modified residue Lys 525). The calculated fragment ions b+, b2+, b3+, y+, y2+ of the adducted peptides are reported in the tables and those identified in the MS/MS spectra are highlighted by red (b series) and blue (y series) colors. The y and b fragment ions which are matched in the MS/MS spectra are highlighted by red and blue color and also labeled. DF, deoxy-fructosyl.

REFERENCES

[1] L. Regazzoni, L. Del Vecchio, A. Altomare, K.J. Yeum, D. Cusi, F. Locatelli, M. Carini, G. Aldini, Human serum albumin cysteinylation is increased in end stage renal disease patients and reduced by hemodialysis: mass spectrometry studies, Free Radic Res 47(3) (2013) 172-80.DOI: 10.3109/10715762.2012.756139.

Supplementary Figure 1

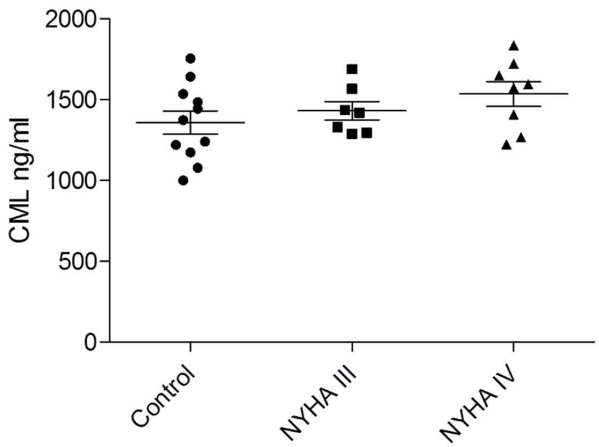

Supplementary Figure 2

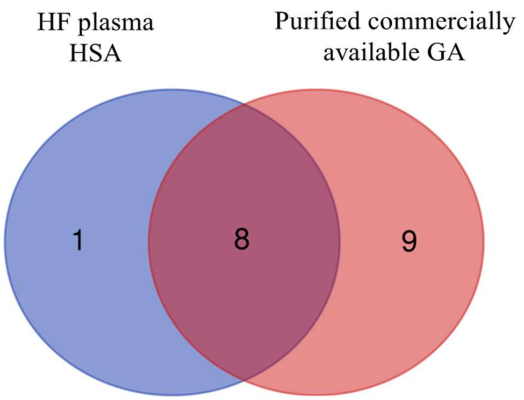

Supplementary Figure 3

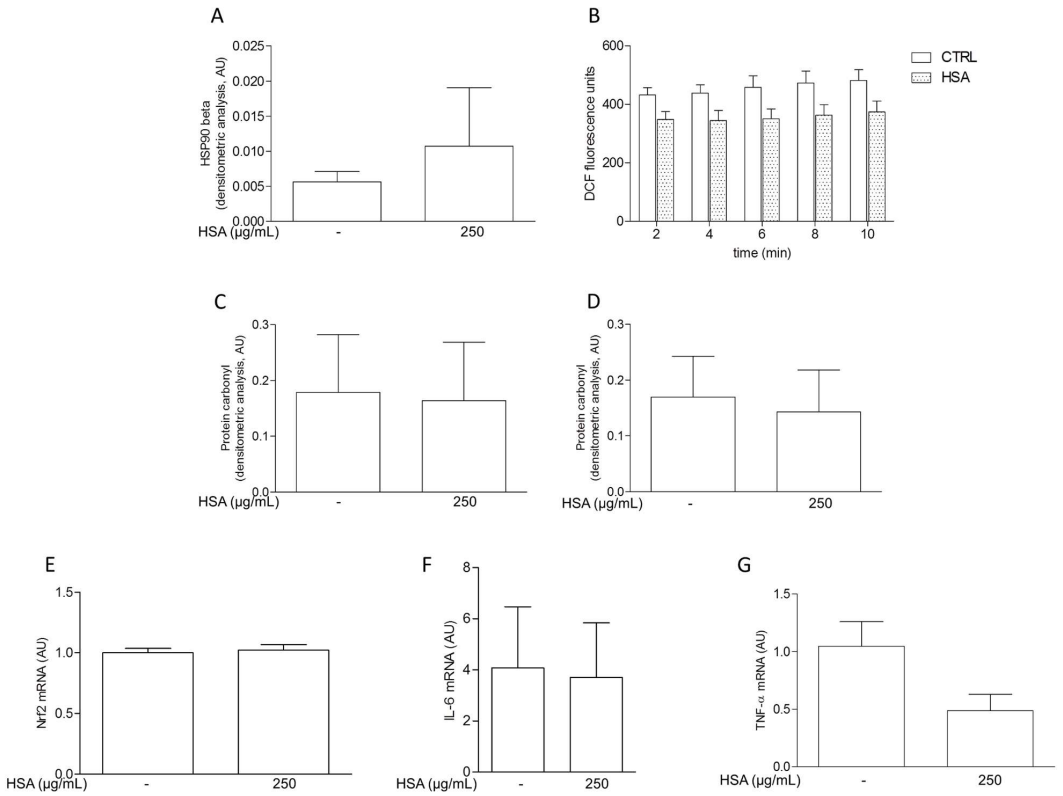

Supplementary Figure 4

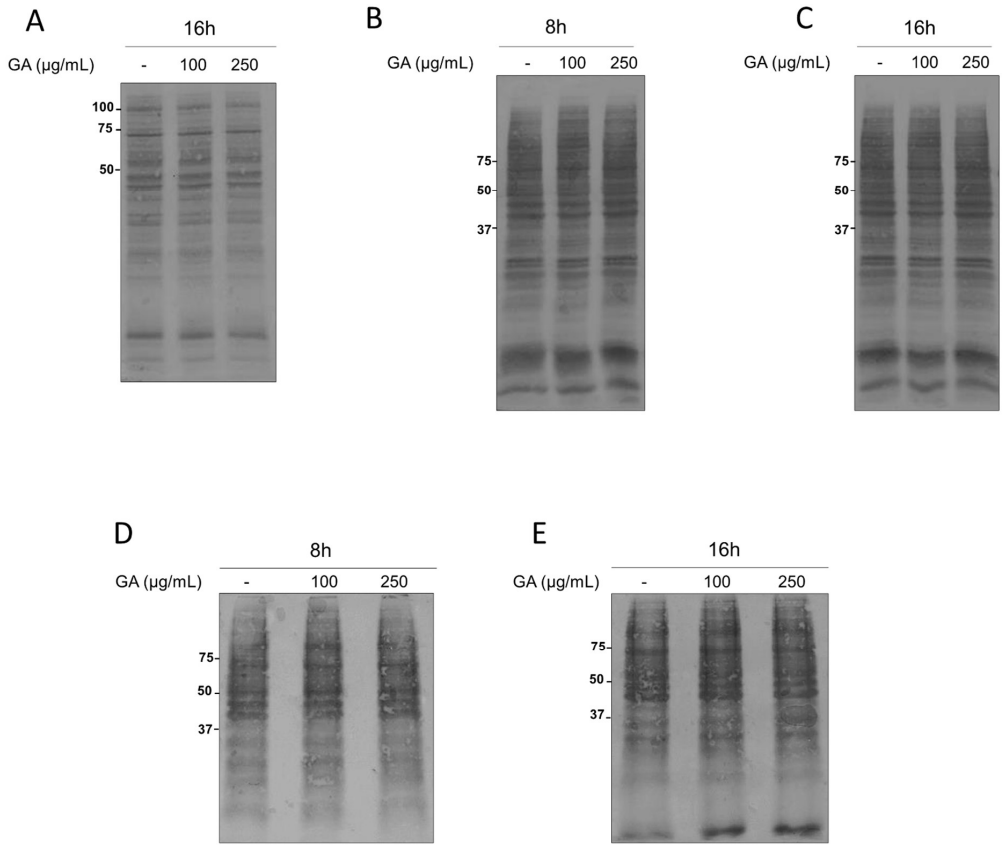

Supplementary Figure 5

A

z1	b+	b2+	Seq.	y+	y2+	z2
1	72.04439	36.52583	A			15
2	201.08698	101.04713	E	1741.91058	871.45893	14
3	348.15540	174.58134	F	1612.86799	806.93763	13
4	419.19251	210.09989	A	1465.79958	733.40343	12
5	548.23510	274.62119	E	1394.76246	697.88487	11
6	647.30352	324.15540	V	1265.71987	633.36357	10
7	734.33555	367.67141	S	1166.65146	583.82937	9
8	1024.48333	512.74530	K-Glu_deo..	1079.61943	540.31335	8
9	1137.56739	569.28733	L	789.47165	395.23946	7
10	1236.63581	618.82154	V	676.38758	338.69743	6
11	1337.68349	669.34538	T	577.31917	289.16322	5
12	1452.71043	726.85585	D	476.27149	238.63938	4
13	1565.79449	783.40088	L	361.24455	181.12591	3
14	1666.84217	833.92472	T	248.16048	124.58388	2
15			K	147.11280	74.06004	1

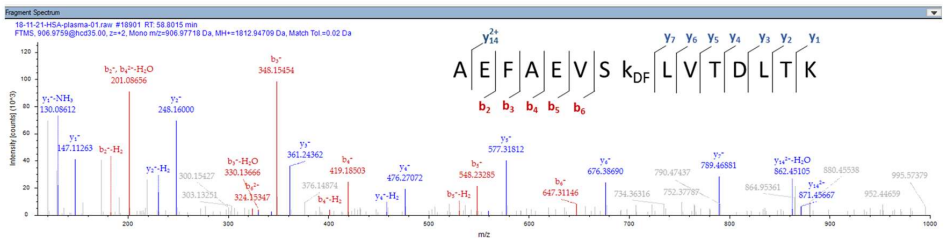

B

z1	b+	b2+	Seq.	y+	y2+	z2
1	291.15506	146.08117	K-Glu_deo..			10
2	419.21364	210.11046	Q	1000.60372	500.80550	9
3	520.26132	260.63430	T	872.54515	436.77621	8
4	591.29843	296.15285	A	771.49747	386.25237	7
5	704.38249	352.69488	L	700.46035	350.73381	6
6	803.45091	402.22909	V	587.37629	294.19178	5
7	932.49360	466.76039	E	488.30788	244.65758	4
8	1046.67766	523.39243	L	359.26628	180.13628	3
9	1144.64598	572.82663	V	246.18122	123.59425	2
10			K	147.11280	74.06004	1

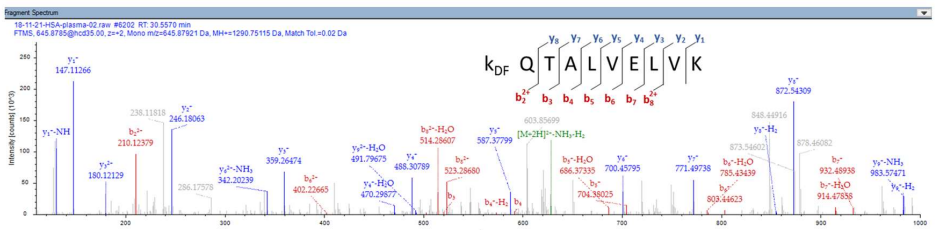

Supplementary Figure 6

A

#1	b+	b2+	b3+	Seq.	y+	y2+	y3+	#2
1	72.04439	36.52583	24.68631	A				15
2	201.08698	101.04713	67.70051	E	1741.91058	871.45893	581.30838	14
3	348.15540	174.58134	116.72332	F	1612.86799	806.93763	538.29418	13
4	419.19251	210.09989	140.40235	A	1465.79958	733.40343	489.27138	12
5	548.23510	274.62119	183.41655	E	1394.76246	697.88487	465.59234	11
6	647.30352	324.15540	216.43936	V	1265.71987	633.36357	422.57814	10
7	734.33555	367.67141	245.45003	S	1166.65146	583.82937	389.55534	9
8	1024.48333	512.74530	342.16596	K-Glu_deo..	1079.61943	540.31335	360.54466	8
9	1137.56739	569.28733	379.86065	L	789.47165	395.23946	263.82873	7
10	1236.63581	618.82154	412.88345	V	676.38758	338.69743	226.13405	6
11	1337.68349	669.34538	446.56601	T	577.31917	289.16322	193.11124	5
12	1452.71043	726.85885	484.90833	D	476.27149	238.63938	159.42868	4
13	1565.79449	783.40088	522.60302	L	361.24455	181.12591	121.08637	3
14	1666.84217	833.92472	556.28557	T	248.16048	124.58388	83.39168	2
15				K	147.11280	74.06004	49.70912	1

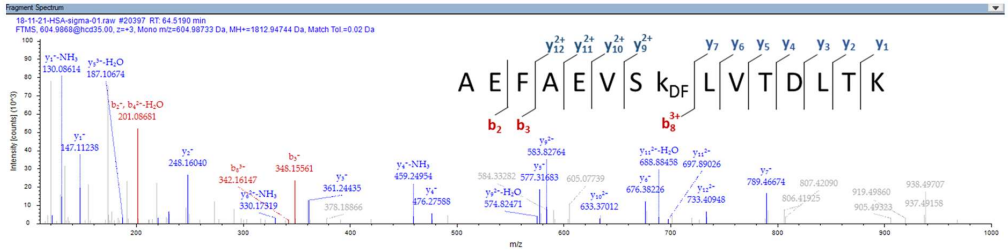

B

#1	b+	b2+	Seq.	y+	y2+	#2
1	291.15506	146.08117	K-Glu_deo..			10
2	419.21364	210.11046	Q	1000.60372	500.80550	9
3	520.26132	260.63430	T	872.54515	436.77621	8
4	591.29843	296.15285	A	771.49747	386.25237	7
5	704.38249	352.69488	L	700.46035	350.73381	6
6	803.45091	402.22909	V	587.37629	294.19178	5
7	932.49350	466.75039	E	488.30788	244.65756	4
8	1045.57756	523.29242	L	359.26528	180.13628	3
9	1144.64598	572.82663	V	246.18122	123.59425	2
10			K	147.11280	74.06004	1

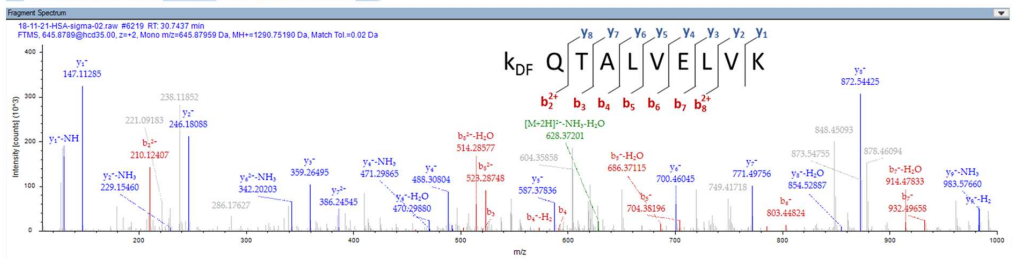

Suplementary Table S1. List of deoxy-fructosyl-lysine (DFK) and deoxy-fructosyl-arginine (DFR) residues identified in purified commercially available GA and in plasma HSA from heart failure patients.

				PLASMA			PURIFIED COMMERCIALLY AVAILABLE		
Annotated Sequence	**Modifications**	**# Missed Cleavages**	**AA Residue**	**Average Peak Area Unmodified peptide**	**Average Peak Area modified peptide**	**Relative Abundance [%]**	**Average Peak Area Unmodified peptide**	**Average Peak Area modified peptide**	**Relative Abundance [%]**
AEFAEVSkLVTDLTK	K8(DFK)	1	Lys 233	87533668,78	336518601,4	**79,36**	14591207,42	155096027	**91,40**
kQTALVELVK	K1(DFK)	1	Lys 525	332178442,9	52545037,88	**13,66**	429189524,8	82564518,31	**16,13**
TcVADESAENcDkSLHTLFGDK / TcVADESAENcDkSLHTLFGDKLcTVATLR	C2(Carbamidomethyl); C11(Carbamidomethyl); K13(DFK); C24(Carbamidomethyl)	1 or 2	Lys 64	944213327,9	29860991,33	**3,07**	88722865, 35	69942639,63	**44,08**
kLVAASQAALGL	K1(DFK)	1	Lys 574	775927938,6	11877099,95	**1,51**	1107741375	220465903,4	**16,60**
ALVLIAFAQYLQQcPFEDHVkLVNEVTEFAK	C14(Carbamidomethyl); K21(DFK)	1	Lys 41	1337349004	13703767,57	**1,01**			
VHTEccHGDLLEcADDrADLAk / VHTEccHGDLLEcADDrADLAkYIcENQDSISSK	C5(Carbamidomethyl); C6(Carbamidomethyl); C13(Carbamidomethyl); R17 OR K22(DFK_DFR); C25(Carbamidomethyl)	1 or 2	Arg 257 OR Lys 262	1568640168	13545550,8	**0,86**	2675906803	14790229,88	**0,55**
QNcELFEQLGEYkFQNALLVR	C3(Carbamidomethyl); K13(DFK)	1	Lys 402	4707999157	23446626,1	**0,50**	16108999545	280585892,4	**1,71**
VFDEFkPLVEEPQNLIk / VFDEFkPLVEEPQNLIkQNcELFEQLGEYK	K6 or K17 (DFK); C20(Carbamidomethyl)	1 or 2	Lys 378 OR Lys 389	16674357678	44019798,39	**0,26**	16805658341	139093027,5	**0,82**
SLHTLFGDkLcTVATLR	K9(DFK); C11(Carbamidomethyl)	1	Lys 73	6749065665	9251368,872	**0,14**	6310983942	312173317,7	**4,71**
TcVADESAENcDkSLHTLFGDkLcTVATLR	C2(Carbamidomethyl); C11(Carbamidomethyl); K13(DFK); K22(DFK); C24(Carbamidomethyl)	2	Lys 64 AND Lys 73				122086061,9	3206647,941	**2,56**
VFDEFkPLVEEPQNLIK	K6(DFK)	1	Lys 378				16805658341	415874807,5	**2,41**
FkDLGEENFK	K2(DFK)	1	Lys 12				1691360402	9306601,216	**0,55**
kVPQVSTPTLVEVSR	K1(DFK)	1	Lys 414				12194130891	34573292,05	**0,28**
FPkAEFAEVSK	K3(DFK)	1	Lys 225				1668328,142	32782100,66	**95,16**
LVRPEVDVMcTAFHDNEETFLkK	C10(Carbamidomethyl); K22(DFK)	1	Lys 136				7586455,517	2130030,712	**21,92**
LDELRDEGkASSAK	K9(DFK)	2	Lys 190				63259796,32	3267171,605	**4,91**
LVNEVTEFAkTcVADESAENcDK	K10(DFK); C12(Carbamidomethyl); C21(Carbamidomethyl)	1	Lys 51				8072274908	242194919,9	**2,91**
QEPErNEcFLQHKDDNPNLPR	R5(DFR); C8(Carbamidomethyl)	2	Arg 98				540614084,4	5266906,633	**0,96**

Redox Biology xxx (xxxx) xxxx

Contents lists available at ScienceDirect

Redox Biology

journal homepage: www.elsevier.com/locate/redox

Review article

Lipoxidation in cardiovascular diseases

Erica Gianazza, Maura Brioschi, Alma Martinez Fernandez, Cristina Banfi*

Centro Cardiologico Monzino, IRCCS, Milano, Italy

ARTICLE INFO

Keywords:
Lipoxidation
Mass spectrometry
Cardiovascular diseases
4-Hydroxy-2-nonenal
Lipoprotein
Advanced lipoxidation end-products

ABSTRACT

Lipids can go through lipid peroxidation, an endogenous chain reaction that consists in the oxidative degradation of lipids leading to the generation of a wide variety of highly reactive carbonyl species (RCS), such as short-chain carbonyl derivatives and oxidized truncated phospholipids. RCS exert a wide range of biological effects due to their ability to interact and covalently bind to nucleophilic groups on other macromolecules, such as nucleic acids, phospholipids, and proteins, forming reversible and/or irreversible modifications and generating the so-called advanced lipoxidation end-products (ALEs).

Lipoxidation plays a relevant role in the onset of cardiovascular diseases (CVD), mainly in the atherosclerosis-based diseases in which oxidized lipids and their adducts have been extensively characterized and associated with several processes responsible for the onset and development of atherosclerosis, such as endothelial dysfunction and inflammation.

Herein we will review the current knowledge on the sources of lipids that undergo oxidation in the context of cardiovascular diseases, both from the bloodstream and tissues, and the methods for detection, characterization, and quantitation of their oxidative products and protein adducts.

Moreover, lipoxidation and ALEs have been associated with many oxidative-based diseases, including CVD, not only as potential biomarkers but also as therapeutic targets. Indeed, several therapeutic strategies, acting at different levels of the ALEs cascade, have been proposed, essentially blocking ALEs formation, but also their catabolism or the resulting biological responses they induce. However, a deeper understanding of the mechanisms of formation and targets of ALEs could expand the available therapeutic strategies.

1. Lipid peroxidation and formation of advanced lipoxidation end-products (ALEs)

Lipid peroxidation is an endogenous chain reaction that consists in the oxidative degradation of lipids; free radicals or non-radical species attack lipids containing carbon-carbon double bonds, with the hydrogen abstraction from a carbon and oxygen insertion that results in lipid peroxyl radicals and hydroperoxides [1].

Lipid peroxidation generates a wide variety of oxidation products, among which the main primary products are lipid hydroperoxides (LOOH) [2]. Lipid hydroperoxides are non-radical intermediates that originate from phospholipids, unsaturated fatty acids, glycolipids, cholesterol and cholesterol esters.

Both enzymatic and non-enzymatic pathways are involved in lipid hydroperoxides formation [3]. Indeed, lipids can be oxidized by several enzymes like cyclooxygenases, lipoxygenases and cytochrome P450 [4].

On the other hand, non-enzymatic lipid peroxidation involves the generation of free radicals (mainly reactive oxygen species (ROS), such as hydroxyl radical ($HO^{\bullet}$), hydroperoxyl ($HOO^{\bullet}$) and peroxynitrite ($ONOO^-$)) that attack lipids containing carbon-carbon double bonds, like polyunsaturated fatty acids (PUFAs) in cell membranes [2]. PUFAs have multiple double bonds between which there are methylene bridges ($-CH_2-$) that contain reactive hydrogen atoms, and they can be classified in omega-3 (n-3) and omega-6 (n-6) fatty acids. Mitochondria, plasma membrane, endoplasmic reticulum, and peroxisomes are the main sources of ROS; $HO^{\bullet}$ and $HOO^{\bullet}$ are the principal ROS that affect lipids. Lipid peroxidation is propagated in a process that is called "chain reaction mechanism", which usually terminates when an antioxidant molecule reacts with the lipid peroxide radical, as summarized in Fig. 1.

Lipid hydroperoxides are the primary peroxidation products and give rise to the generation of short-chain unesterified aldehydes and a second class of aldehydes still esterified to the parent lipid [1]. Moreover, lipid hydroperoxides can be structurally rearranged and converted into secondary peroxidation products that are highly reactive, known as reactive carbonyl species (RCS). RCS are a heterogeneous group and can be classified into short-chain carbonyl derivatives and oxidized truncated phospholipids [5]. The first group includes α,β-unsaturated aldehydes (e.g. 4-hydroxy-2-nonenal (4-HNE), 4-hydroxy-2-

* Corresponding author. Monzino Cardiologic Center IRCCS, Unit of Proteomics, 20138, Via Parea, 4, Italy.
E-mail address: cristina.banfi@ccfm.it (C. Banfi).

https://doi.org/10.1016/j.redox.2019.101119
Received 2 October 2018; Received in revised form 9 January 2019; Accepted 21 January 2019

Abbreviations

15d-PGJ2	15-deoxy-Δ12,14-prostaglandin J2
15-LOX	15-lipoxygenases
2,5-DBA	2,5-dihydroxy-benzaldehyde
2DE	two-dimensional electrophoresis
4-APC	4-(2-(trimethylammonio)ethoxy)benzenaminium halide
4-HBA	4-hydroxybenzaldehyde
4-HNE	4-hydroxy-2-nonenal
8-epi-PGF2a	15(S)-8-iso-prostaglandin F2alpha
AA	arachidonic acid
ACE	angiotensin-converting enzyme
ACR	acrolein
AGE	advanced glycation end-products
AIDA	alternate isotope-coded derivatization assay
ALEs	advanced lipoxidation end-products
ApoB	apolipoprotein B
ApoE	apolipoprotein E
ATP	adenosine triphosphate
BHT	butylated hydroxytoluene
CE	capillary electrophoresis
CHD	1,3-cyclohexandione
CoA	coenzyme A
COX	cyclooxygenase
CPT1	carnitine palmitoyl transferase 1
CVD	cardiovascular diseases
CyPG	cyclopentenone prostaglandin
DAG	diacylglycerol
DDB	1,2-diamino-4,5-dimethoxybenzen
DHA	docosahexaenoic acid
DNPH	2,4-dinitrophenylhydrazine
DPPP	diphenyl-1-pyrenylphosphine
EAT	epicardial adipose tissue
EGFR	epidermal growth factor receptor
ELISA	enzyme-linked immunosorbent assay
eNOS	endothelial nitric oxide synthase
EPA	eicosapentaenoic acid
ER	endoplasmic reticulum
ESR	electron spin resonance
F2-IsoPs	F2-isoprostanes
FABP	fatty acid binding proteins
FACS	fatty acyl-CoA synthetase
$FADH_2$	flavin adenine dinucleotide
FATP	fatty acid transport proteins
FFAs	free fatty acids
FOX	ferrous oxidation-xylenol orange
GC	gas chromatography
G-PC	glutaric acid ester of 1-acyl-*sn*-glycero-3-phosphocholine
GSH	glutathione or γ-L-glutamyl-L-cysteinylglycine
HDL	high-density lipoprotein
HLB	hydrophilic lipophilic balanced
HOCl	hypochlorous acid
HPLC	high performance liquid chromatography
HSP60	heat shock 60 kDa protein
IDL	intermediate-density lipoprotein
IKKβ	IkB kinase β
IR	ischemia/reperfusion
IsoPs	isoprostanes
LC	liquid chromatography
LC-FD	LC-fluorescence detection
LC-UV	LC-ultraviolet
LDLs	low-density lipoproteins
LLE	liquid-liquid extraction
Lp(a)	lipoprotein(a)
LPL	lipoprotein lipase
LV	left ventricular
MALDI-TOF	matrix assisted laser-desorption ionization-time of flight
MAPK	mitogen-activated protein kinase
MDA	malondialdehyde
MRM	multiple reaction monitoring
MS	mass spectrometry
NAC	N-acetyl cysteine
NADH	nicotinamide adenine dinucleotide
NADPH	nicotinamide adenine dinucleotide phosphate
NF-kB	nuclear factor kappa-light-chain-enhancer of activated B cells
NO	nitric oxide
OFL	ofloxacin
ONE	4-oxo-nonenal
OV-PC	5-oxovaleric acid ester of 1-acyl-*sn*-glycero-3-phosphocholine
oxLDL	oxidized low-density lipoproteins
oxPL	oxidized phospholipid
PCs	phosphatidylcholines
PDGFR	platelet-derived growth factor receptor
PDGFβ	platelet-derived growth factor receptor-β
PFB-Br	pentafluorobenzyl bromide
PGC-1α	peroxisome proliferator-activated receptor γ coactivator-1α
PM	pyridoxamine
POBN	α-(4-pyridyl-1-oxide)-N-*tert*-butyl nitrone
PPAR	peroxisome proliferator-activated receptor
PTB	N-phenacylthiazolium bromide
PUFAs	polyunsaturated fatty acids
RCS	reactive carbonyl species
RNS	reactive nitrogen species
ROS	reactive oxygen species
SC	subcutaneous
SPE	solid-phase extraction
SRM	selected reaction monitoring
TAG	triacylglycerol
TBA	thiobarbituric acid
TBARS	thiobarbituric acid reactive substances
TLC	thin-layer chromatography
TLR	Toll like receptors
UCPs	uncoupling proteins
VLDL	very low-density lipoprotein

hexenal, nonenal and acrolein (ACR)), di-aldehydes (e.g. malondialdehyde (MDA) and glyoxal) and ketoaldehydes (e.g. methylglyoxal, 4-oxo-nonenal (ONE) and isoketals also called levuglandins). In the second class, the electrophilic moiety remains covalently linked to the phospholipid. Electrophilic prostaglandin metabolites are an additional class of RCS that are characterized by a cyclopentenone. The cyclopentenone prostaglandins are structurally and functionally related to a subset of isoprostanes (IsoPs), a series of prostaglandin-like compounds produced via a non-enzymatic mechanism involving the free radical-mediated peroxidation of PUFAs, mostly arachidonic acid (AA) [6].

RCS exert a wide range of biological effects due to their ability to interact and covalently react with nucleophilic groups on other macromolecules, such as nucleic acids, phospholipids, and proteins, to form irreversible modifications, generating the so-called advanced lipoxidation end-products (Fig. 2) [7].

Covalent adducts of lipid peroxidation products with DNA have been described both at nuclear and mitochondrial DNA level with

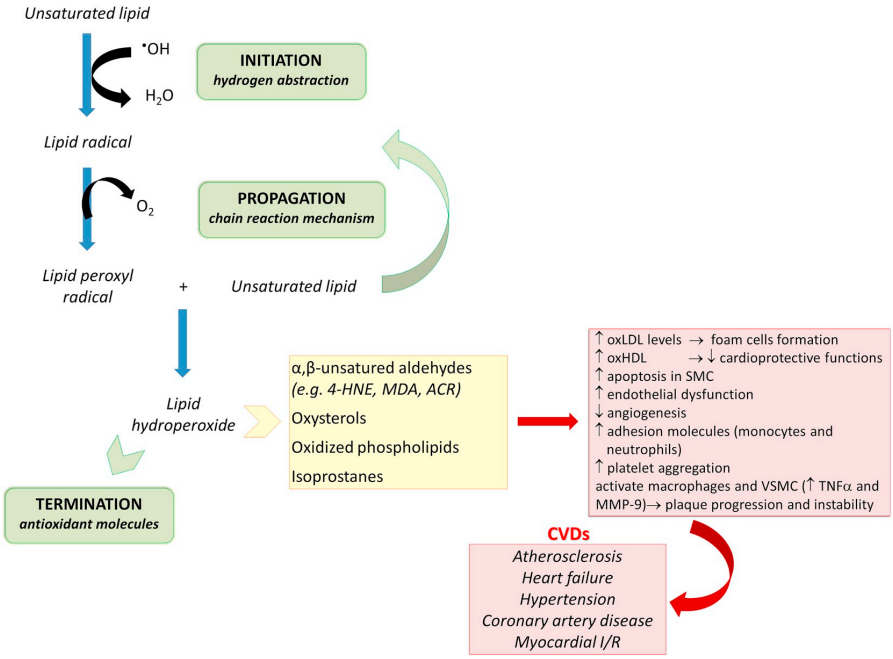

Fig. 1. Scheme of the lipid peroxidation reaction and its effects in the development and progression of CVDs. 4-HNE, 4-hydroxy-2-nonenal; ACR, acrolein; HDL, high-density lipoprotein; I/R, ischemia/reperfusion; LDL, low-density lipoproteins; MDA, malondialdehyde; MMPs, metalloproteinases; TNFα, tumor necrosis factor α; VSMC, vascular smooth muscle cells.

potential mutagenic and carcinogenic effects [2,8]. Additionally, RCS can interact with aminophospholipids, generating covalent adducts such as carboxymethyl-phosphatidylethanolamine or MDA-phosphatidylethanolamine, and starting the reactions occurring in DNA and proteins [7,9].

Finally, both short-chain RCS and oxidized phospholipids can covalently react with proteins generating Michael adducts or Schiff bases, early products that are reversible or can further rearrange forming additional specific reaction compounds [10,11]. However, the protein targets could be different for the two classes, because the short-chain RCS or RCS bound to phospholipids have diverse cellular distribution. The carbonyl group reacts with the nucleophilic side chains on amino acid residues of proteins, such as the imidazole nitrogen of histidine, the thiol group of cysteine, the epsilon amino group of lysine or the guanidine of arginine [5,10]. An example of ALE is represented by carboxymethyl-lysine (CML), a product of the reaction with glyoxal, which derives by both lipid and sugar oxidation pathway and is considered a general marker of oxidative stress and protein damage in cardiovascular diseases and aging [5,12].

Further, bifunctional α,β-unsaturated aldehydes, such as 4-HNE, can act as small crosslinkers between or within proteins leading to the formation of aggregates, besides their effects on protein function [13]. The formation of MDA adducts on proteins generates highly cross-linked undegradable aggregates, such as the fluorescent pigment lipofuscin, which can compromise cell viability [14].

Additionally, prostaglandins present an electrophilic carbon that can interact with the nucleophilic amino acids generating, with a pathway similar to that described for α,β-unsaturated aldehydes, a Michael adduct with effects on cell signaling pathways [10].

1.1. Electrophilic lipid species detectable in cardiovascular diseases

1.1.1. Lipid peroxidation-derived aldehydes

4-hydroxy-2-nonenal (4-HNE) is produced by the oxidation of PUFAs containing n-6 acyl groups, such as AA and linoleic acid, and it is the most abundant lipid-derived RCS. 4-HNE can be produced by the decomposition of lipid peroxidation products that are generated both by enzymatic reactions triggered by 15-lipoxygenases (15-LOX) or from several non-enzymatic oxidative pathways through mechanisms involving the reactions of free radicals and their products [2].

Nowadays 4-HNE is considered one of the major toxic products due to its rapid reaction with thiols and amino groups [15]. 4-HNE usually forms Michael adducts with His, Cys, and Lys residues and the preference for the amino acid modification is Cys ≫ His > Lys.

The degradation of n-6-PUFAs also generates 4-oxo-nonenal (ONE), which derives from the peroxidation of linoleoyl chains of fatty acids. ONE is a more reactive product than 4-HNE and modifies the nucleophilic side chains of Lys, Cys, Arg and His on proteins. ONE can form, at C3 and C2, 4-ketoaldehyde Michael adducts that are relatively unstable and can eventually produce furan derivatives or more stable compounds, such as dihydropyrroles and isomeric 4-ketoamide derivatives [16]. ONE also reacts with Lys forming a Schiff base, which can give the fluorophore pyrrolium Lys-Lys crosslink and Lys-derived pyrrolinone. Unlike 4-HNE, ONE reacts also with Arg residues to yield stable covalent adducts, but this reaction is less favorable than the other amino acid nucleophiles (i.e. preference order is Cys > His > Lys > Arg).

Acrolein (ACR) arises not only by peroxidation of PUFAs but also from the metabolism of amino acids, polyamines, and drugs. Under oxidative stress and inflammation, the endogenous production of acrolein is also controlled by myeloperoxidase-mediated degradation of threonine and the amine oxidase-mediated degradation of spermine and spermidine [5]. Compared to all α,β-unsaturated aldehydes, ACR has the highest reactivity with protein nucleophiles (i.e. the order of

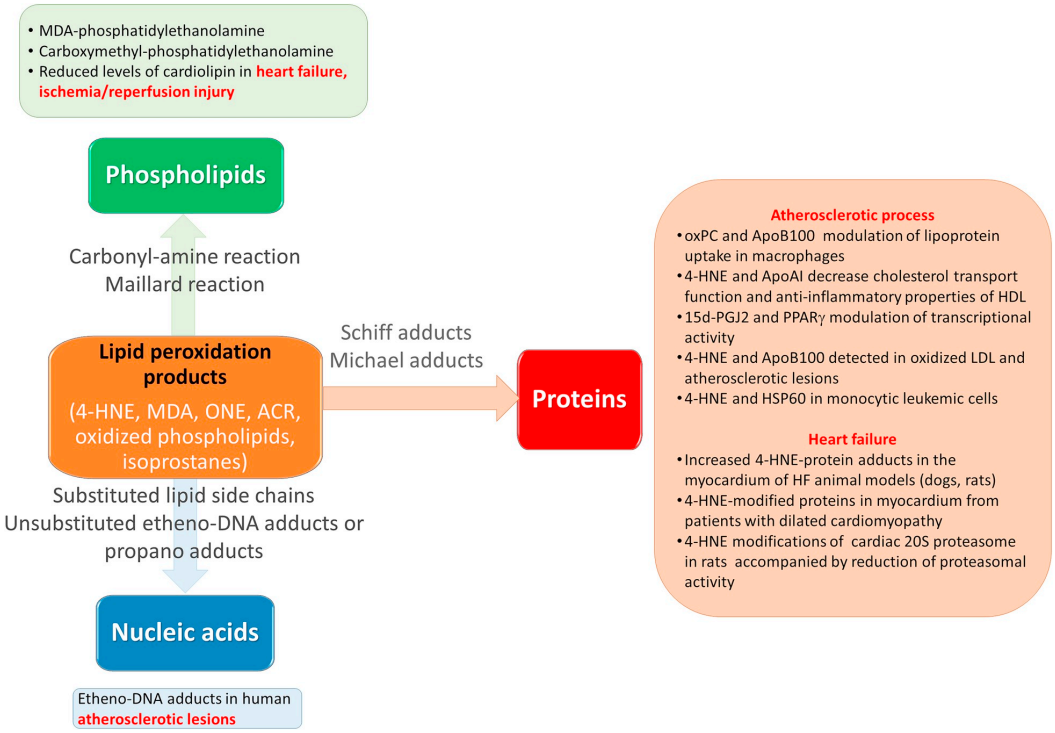

Fig. 2. Mechanisms involved in the formation of advanced lipoxidation end-products. Relevant targets and their involvements in cardiovascular diseases are highlighted. On nucleic acids, the exocyclic amino group of deoxyguanosine, deoxyadenosine, and deoxycytosine can react with α,β-unsaturated aldehyde generating two types of adducts: substituted lipid side chains (for example with MDA, ACR or 4-HNE) and unsubstituted etheno-DNA adducts (for example with 2,3-epoxy-4-hydroxynonanal). On proteins, the reaction of aldehydes with the free amino group of lysine or arginine generates a Schiff base, while the reaction of the electrophilic carbon of α,β-unsaturated aldehydes with the nitrogen lone pair of lysine and histidine or the -SH of cysteine generates a Michael adduct, which is more stable even if both these adducts are reversible.

reactivity is Cys > His > Lys). The formation of ACR adducts on Cys residues is the principal way, but ACR forms additional ALEs with His and Lys, as detected in the oxidized low-density lipoproteins (oxLDL) [17].

Malondialdehyde (MDA) results from lipid peroxidation of PUFAs with two or more methylene-interrupted double bonds. It is a reactive aldehyde that forms interactions with nucleic acids and covalent protein adducts inducing toxic stress in cells [18]. MDA is a highly toxic molecule and it is usually considered a biomarker of oxidative stress in the organism. The most important precursors of MDA are monocyclic peroxides obtained from fatty acids with three or more double bonds. MDA can be also derived by enzymatic processes from prostaglandins during the biosynthesis of thromboxane A2 and 12-l-hydroxy-5,8,10-heptadecatrienoic acid [18]. MDA is able to form adducts with several proteins, introducing cross-links that can alter their biochemical properties. MDA reactivity is pH-dependent: at physiological pH, it can rapidly form the enolate salt, which is of low reactivity; at lower pH, MDA exists as β-hydroxyacrolein, the reactivity increases, and reacts with Lys forming N-propenal-Lys.

1.1.2. Prostaglandin-like compounds: isoprostanes

The IsoPs are a class of prostaglandin-like compounds that are generated *in vivo* from the non-enzymatic free radical-catalyzed peroxidation of essential fatty acids (mainly AA) [19,20]. They are produced in cell membranes at the site of free radical attack, from which they are removed by phospholipases, get into the circulation and then are excreted in urine. They have been found also in other fluids, such as pericardial fluid [21] and cerebrospinal fluid [22,23]. The F2-isoprostanes (F2-IsoPs) are a class of stable molecules that are generated *in vivo* under conditions of oxidative stress, so they can be used as an effective measure of endogenous oxidative stress. Other classes of IsoPs from AA have been described and these classes differ based on the functional groups on the prostane ring. In particular, E2/D2-IsoPs are not terminal products of the IsoPs pathway, but they can rearrange to form A2/J2-IsoPs, also known as cyclopentenone IsoPs, that contain α,β-unsaturated cyclopentenone ring structure [24]. A2/J2-IsoPs react with cellular thiols to form Michael adducts [25], that are metabolized *in vivo* by glutathione transferase enzymes to water-soluble modified glutathione conjugates. Isoprostanes can be also produced from the PUFAs, such as EPA, DHA, adrenic acid, and α-linolenic acid [26,27]. Moreover, the compounds known as isoketals or isolevuglandins are produced *in vivo* by lipid peroxidation and rearrangement of endoperoxide intermediates of the isoprostane pathway [28], and they covalently form adducts with Lys residues on proteins inducing a biological dysfunction. Oxidation of AA can also yield to cyclic peroxides and isofurans, when the intermediate undergoes a 5-exo cyclization reaction with molecular oxygen [29,30].

1.1.3. Oxidized phospholipids (oxPLs)

oxPLs, found in oxidized lipoproteins or in membranes of apoptotic cells, include hundreds of different structures and can be generated both enzymatically, by lipoxygenases, myeloperoxidase and nicotinamide adenine dinucleotide phosphate (NADPH) oxidase, and non-enzymatically [31]. Oxidized forms of phosphatidylserine and

phosphatidylethanolamine have been described but the most oxidized phospholipid is phosphatidylcholine, which accounts for 40–50% of phospholipids in mammalian cells or lipoproteins.

Alkyl peroxyl radicals or singlet oxygen directly oxidize phospholipid-bound PUFAs to generate fatty acyl derivatives, such as fatty acid hydroperoxides, which are compounds that subsequently and easily undergo decomposition to various reactive products. A common reaction, involving the reduction of fatty acid hydroperoxides, leads also to the generation of truncated phospholipids, such as γ-hydroxyalkenal phosphatidylcholines (PCs). These molecules can undergo another step of fragmentation to the 5-oxovaleric acid ester of 1-acyl-*sn*-glycero-3-phosphocholine (OV-PC) or glutaric acid ester of 1-acyl-*sn*-glycero-3-phosphocholine (G-PC) that have been described in atherosclerotic lesions. Additionally, phospholipid-bound PUFAs are prone to non-enzymatic formation of IsoPs, while they are not a target of cyclooxygenases, and several IsoP-PCs have been described also in atherosclerotic regions [31].

2. Lipid sources in the cardiovascular system

Lipids, with a relevant role in the onset of cardiovascular diseases and susceptible to oxidation, can be originated from many sources, both in the bloodstream as in tissues (Fig. 3).

2.1. Circulating lipoproteins and lipids

Lipoproteins, the major carrier of water insoluble lipids in the blood, are complex particles with a central core of cholesterol esters and triglycerides surrounded by free cholesterol, phospholipids, and apolipoproteins. They are divided into classes according to their size, lipid compositions and apolipoproteins (chylomicrons, chylomicron remnants, very low-density lipoprotein (VLDL), intermediate-density lipoprotein (IDL), LDL, high-density lipoprotein (HDL), and lipoprotein (a) (Lp(a))). Lipoproteins play a role in the adsorption and transport of dietary lipids from the intestine and endogenous lipids from the liver. HDL are involved in the so-called reverse cholesterol transport from the peripheral tissues to the liver and intestine, thus exerting a protective role. LDL, being the main player in cholesterol transport to the cells, are instead considered a well-established cardiovascular risk factor. This lipoprotein class is responsible for the development of atherosclerosis as a consequence of its modification (oxidation, acetylation, and aggregation) in the sub-endothelial space. Following these modifications, LDL provoke endothelial injury, promote inflammatory cells adhesion and their differentiation to macrophages [32]. Further, a plethora of effects, relevant to the disease progression, is induced, such as endothelial dysfunction, endothelial nitric oxide synthase (eNOS) inhibition, inflammatory cytokines release, and platelet aggregation. Vascular endothelium is a dynamic structure that has many important functions, including regulation of vascular tone, hemostasis, molecular exchange between blood and tissues, and signaling for the immune response and

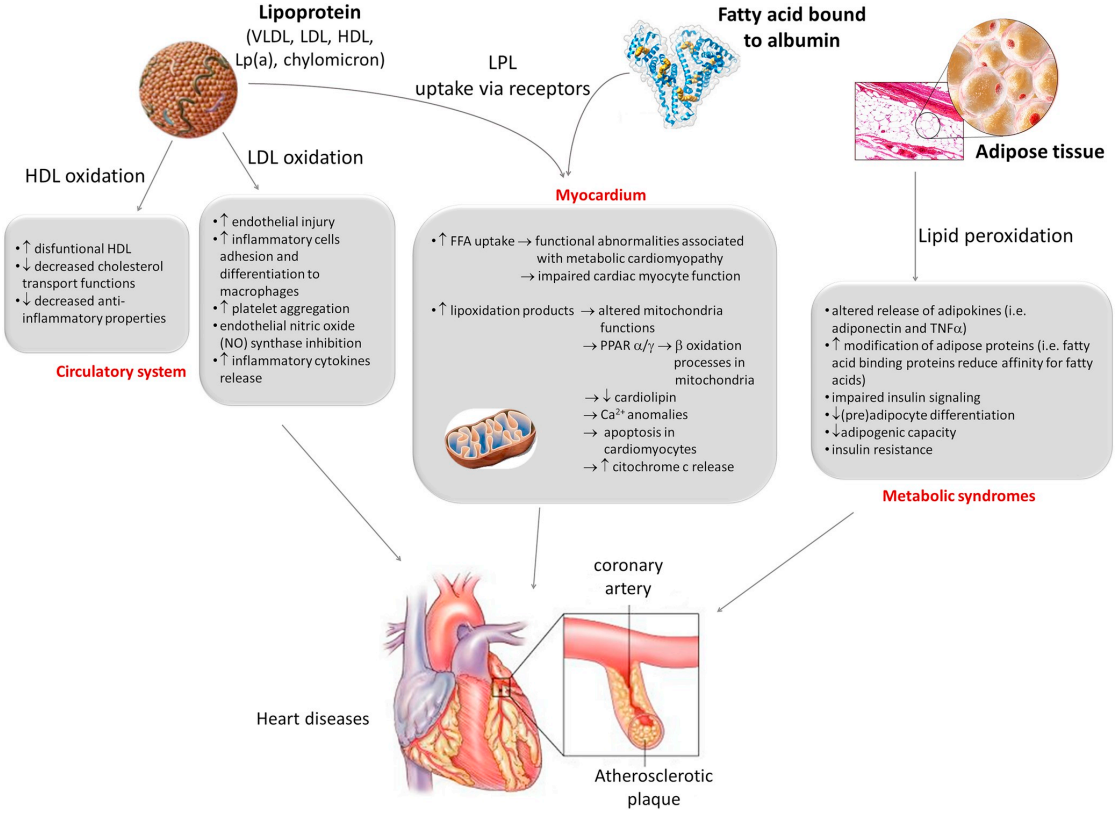

Fig. 3. Relevance of circulating and tissue lipids in the development of cardiovascular diseases. VLDL, very low-density lipoprotein; LDL, low-density lipoproteins; HDL, high-density lipoprotein; Lp(a), lipoprotein(a); LPL, lipoprotein lipase; FFA, free fatty acids; PPAR, peroxisome proliferator-activated receptor; TNFα, tumor necrosis factor α.

inflammation [33,34]. The endothelium maintains vascular tone through the synthesis of vascular dilatory and constricting molecules and controls lipid modification. Alterations of these normal functions lead to atherogenesis. Endothelial dysfunction is clinically characterized by impaired endothelium-dependent vasorelaxation due to a reduced nitric oxide (NO) bioavailability, which is considered an independent factor used for prognosis of patients with cardiovascular disease [35,36]. Endothelial dysfunction has a key role in the development of several cardiovascular diseases and their complications, including atherosclerosis, coronary artery disease, heart failure, as well as diabetes and obesity, which are known risk factors for cardiovascular diseases. The endothelial injury causes the infiltration of LDL-cholesterol into the vessel wall and the oxidation of cholesterol that is a key step in the atherosclerosis development. Cholesterol oxidation products are significantly accumulated in atherosclerotic lesions, such as oxysterols and core-aldehydes. OxLDL uptake and foam cells formation are facilitated by the presence of endothelial scavenger receptors, which have a significant role in promoting atherogenesis. For example, lectin-like oxidized low-density lipoprotein receptor 1 (LOX-1) is one of the major endothelial receptor for oxLDL and promotes apoptosis of endothelial cells, increases the expression of monocyte chemotactic protein 1 (MCP-1) and transforming growth factor β1 (TGFβ1), decreases eNOS activity, and induces matrix metalloproteinases production in vascular smooth muscle cells [37,38].

Although the oxidative hypothesis of atherosclerosis was mostly investigated on LDL, there is also evidence that oxidation on other lipoproteins, such as on HDL, can take place in atherogenesis leading to their conversion from atheroprotective, anti-inflammatory, and antioxidant particles to deleterious ones [39]. This HDL remodeling paves the way to the concept that the quality and functionality, instead of the quantity of HDL plasma level, is more relevant, in light of the observations that HDL-raising therapies did not result in cardiovascular risk reduction [40].

Several processes have been involved in the oxidation of lipoproteins, including transition metals, lipoxygenases, hemoglobin, and ROS (reviewed in Ref. [41]). Of note, hypochlorous acid (HOCl) can modify the lipid and protein components of LDL *in vitro* and/or *in vivo* [42] and MDA reacts with the positively charged ε amino group of lysyl residues present in the LDL apolipoprotein ApoB-100, leading to increased uptake by macrophages [43]. ApoAI, the main apolipoprotein of HDL, could be oxidatively modified, leading to dysfunctional HDL and increasing cardiovascular risk [44].

Antibodies against oxidized phospholipids have also been used to detect oxPL-protein adducts in human plasma proteins and LDL. For example, the use of the E0-series of monoclonal auto-antibodies to detect the occurrence of adducts of oxidized phosphatidylcholines, such as 1-palmitoyl2-(5′-oxo)valeroyl-*sn*-glycero-3-phosphocholine, with ApoB-100, showed that the adducts were crucial in inducing uptake of modified lipoproteins by scavenger receptors into foam cells [45].

Very recently, Que et al. suggested that therapies inactivating oxidized phospholipids might be beneficial for reducing a generalized inflammation, including the progression of atherosclerosis, aortic stenosis and hepatic steatosis [46].

Additionally, endothelial cells are highly predisposed to 4-HNE induced damage, which includes increment of proinflammatory factors and failure of the endothelial barrier function. Increased 4-HNE reduces NO bioavailability associated with a decrease in dimethylarginine dimethylamine hydrolase (DDAH) activity [47], which leads to high methylarginine levels, reduction of eNOS-derived NO production, and consequently endothelial dysfunction.

The endothelium expresses also other important targets of lipoxidation, such as soluble epoxide hydrolase (sEH), whose major function is to metabolize the epoxides of AA and linoleic acid. sEH rapidly hydrolyzes epoxyeicosatrienoic acids (EETs), which have been demonstrated to be endothelium-derived hyperpolarizing factors, to dihydroxyeicosatrienoic acids (DHETs) [48]. EETs are vasodilators independent of NO that have protective effects on the vasculature and the heart. Thus, inhibitors of sEH reduce inflammation and prevent the development of atherosclerotic plaques [49].

It has been demonstrated that n-3 PUFAs decrease sEH protein expression in rat aortic strips and endothelial cells [48]. Moreover, 4-hydroxy hexenal (4-HHE), which is a lipid peroxidation product of n-3 PUFAs and a potential activator of the Nrf2 pathway [50], also decreased sEH protein expression increasing the EETs concentration. The antioxidant N-acetyl-L-cysteine (NAC) pretreatment inhibits the reduction in sEH protein induced by n-3 PUFAs or 4-HHE. Oxidative stress induces p38 kinase activation in vascular endothelial cells, thus the inhibition of p38 kinase diminishes the effect of n-3 PUFAs and 4-HHE on sEH protein expression.

Oxysterols, oxidized phospholipids, free and core-aldehydes promote the inflammatory process underlying atherosclerosis, extracellular matrix deposition and arterial wall remodeling [51]. Advanced lipoxidation end-products, such as MDA- and 4-HNE-protein adducts, can promote monocyte activation and vascular complications via induction of inflammatory pathways and networks [52]. In monocytes, ALEs can lead to cellular dysfunction, adhesion to the endothelium, and transmigration into the subendothelial space, through several monocyte-macrophage inflammatory cytokines and chemokines. All these events are important in the pathogenesis of atherosclerosis. Oxidized LDL promotes macrophage proinflammatory gene expression, such as TNFα, IL-1β, and IL-6, through ligand activation of peroxisome proliferator-activated receptor gamma (PPARγ) [53]. Lipid peroxidation products increase the expression of MCP-1, interferon-γ–inducible protein-10, and cyclooxygenase-2 (COX-2), as well as facilitate transcription of nuclear factor (NF)-κB that is a redox-sensitive gene regulatory factor activated by modified LDL internalization.

Leukotrienes, derived from the oxidation of AA, are themselves a family of eicosanoid inflammatory mediators that stimulate the activation of endothelial cells and foam cells.

Acrolein, for example, increased macrophages expression of the atherogenic factors 5-lipoxygenase, leukotriene B4 and matrix metalloproteinase [54,55], and induced mast cell degranulation that can increase inflammatory injury [56].

Additionally, 4-HNE induced the synthesis of metalloproteinases MMP-9 in macrophages [57] and MMP-2 in vascular smooth muscle cells [58], thus contributing to the instability of the atherosclerotic plaque consequently leading to the thrombus formation in atherosclerosis.

Indeed, in smooth muscle cells, 4-HNE stimulates the activity of extracellular matrix-degrading matrix metalloproteinases-1 and -2 [59], protein kinase B (Akt) [58], p38 mitogen-activated protein kinase (MAPK) [60] and induces the phosphorylation of c-jun N-terminal kinase (JNK) [61].

Of note, the balance between ROS and endogenous antioxidants has different effects in different vascular beds, due to the evident differences between arteries and veins in term of cellular composition. ROS regulate multiple cellular functions, among which endothelial and smooth muscle cells growth, proliferation, migration and apoptosis, angiogenesis, vascular tone, and genomic activity through several transcription factors [62].

NAD(P)H oxidase (i.e. Nox enzymes) activity is the major source of ROS in the vasculature, both in human veins and arteries, and it has an important role in the disease development. It has been demonstrated that NAD(P)H oxidase system is the greater source of superoxide in veins, whereas in addition, xanthine oxidase seems to largely contribute to superoxide production in arteries [63]. NAD(P)H oxidase is present both in vascular smooth muscle cells and in endothelial cells, but there are some differences in the component distribution of NAD(P)H oxidases in specific vascular cells, in the extent of superoxide anion radicals production and in the stimuli of NAD(P)H oxidases activation [64]. The molecular composition of vascular NAD(P)H oxidases seems to be different in the vascular cell types and at different phases of

atherosclerotic plaques progression [63]. Moreover, NAD(P)H oxidase is Nox2-based in saphenous veins, while it is proportionally mostly Nox4-based in arteries. The relative contribution of the individual vascular wall segments to the total superoxide production was evaluated, and in human veins, the major contribution comes from the endothelium and adventitia, while in arteries the smooth muscle cells have a key role [63].

Recently, it has been reported that 4-HNE-adducts accumulate mainly in smooth muscle cells in human aorta, and their content increases with the age in the intima and the adventitia, and at a lower amount in the media [65]. The accumulation of 4-HNE-adducts is very high in the intimal aorta and predominantly in patients with high atherosclerosis grade. The 4-HNE expression is also increased in the adventitia, probably associated with the vasa vasorum and microcapillaries in atherosclerotic lesion [66]. Aortic elastin is not modified by 4-HNE, indicating that elastin is not a target of 4-HNE in the vascular wall, but 4-HNE contributes to its degradation and impaired regeneration [67,68].

Myeloperoxidase, lipoxygenases, mitochondria and uncoupled eNOS are other sources of oxidants in the vessel wall that are usually expressed in human atherosclerotic lesions [64].

2.2. Lipids in the myocardium

To sustain its intense metabolism, the myocardium must continually generate, at a high rate, adenosine triphosphate (ATP), which is produced in the mitochondrion utilizing all classes of energy substrates, such as lipids, carbohydrates, amino acids, and ketone bodies (for details see review [69]). In the normal heart, mitochondria are mainly fueled by fatty acyl-coenzyme A (CoA) and pyruvate, which are the primary metabolites of fatty acids and carbohydrates, respectively.

Fatty acids are supplied to the myocardium either attached to the blood albumin or covalently bound to circulating lipoproteins in the form of triacylglycerol. Triglyceride rich lipoproteins (chylomicron and VLDL) are indeed an important source of fatty acids, being chylomicrons the major contributor. The enzyme lipoprotein lipase (LPL) is responsible for the hydrolysis of free fatty acids (FFAs) from chylomicrons, whereas the uptake of VLDL by the VLDL/apolipoprotein E (ApoE) receptors, expressed by the heart, represents an alternative route (reviewed in Ref. [70]). The supply of FFAs to the heart is dependent from alterations in the synthesis, secretion, and transport to the capillary lumen of LPL. Usually, increased activity of LPL, as occurs in fasting conditions, is associated with an increase in fatty acid oxidation.

After dissociation from albumin or lipoproteins, fatty acids are transported to the cardiac muscle through the capillary endothelium, and, after crossing the sarcolemma and cytoplasm, are converted to fatty acyl-CoA at the mitochondrial outer membrane or the sarcoplasmic reticulum. In details, fatty acids enter the cells via transporters (fatty acid transport proteins, FATP) on the cell membrane, such as CD36/FAT and fatty acid binding proteins (FABP) [70]. To allow entry into the mitochondria, a CoA group is added to the fatty acid by fatty acyl-CoA synthetase (FACS) and, subsequently, the conversion to acyl carnitine by carnitine palmitoyl transferase 1 (CPT1) is necessary. Carnitine translocase mediates the entrance into the inner membrane of mitochondria where the long-chain fatty acyl carnitine is then converted back to a fatty acyl-CoA by the CPT2, which finally enters the fatty acid oxidation process [71]. Part of the long-chain acyl CoA can also be used for the synthesis of lipid intermediates such as triacylglycerol (TAG), diacylglycerol (DAG) and ceramides, which have all received considerable interest as implicated in the development of diabetes and cardiovascular diseases. The heart has indeed labile stores of TAG that can undergo dynamic turnover; for example, intramyocardial TAG is accelerated by adrenergic stimulation whilst their synthesis is increased with elevated plasma FFA, as occurs in diabetes or fasting (discussed in Ref. [70]). The production of these intracellular intermediates (TAG, DAG, and ceramides) depends on the FFA supply. In mice over-expressing FATP1, the increased FFA uptake and metabolism resulted in functional abnormalities consistent with metabolic cardiomyopathy, which, rather than inducing cell death, manifests as impaired cardiac myocyte dysfunction [72]. An open question is related to the lipotoxicity induced by a defect of long-chain acyl-CoA removal by the fatty acid oxidation process.

An in-depth description of all steps and factors influencing the fatty acid metabolism in the heart is present in the review by Lopashuk [70]. The metabolism of long-chain acyl-CoA in the mitochondrial matrix occurs via the β-oxidation pathway, which involves sequential metabolism of acyl-CoAs by four enzymes: acyl-CoA dehydrogenase, enoyl-CoA hydratase, L-3-hydroxyacyl-CoA dehydrogenase, and 3-ketoacyl CoA thiolase. These enzymes are susceptible to feedback inhibition by the same products of the process, that is acetyl CoA, flavin adenine dinucleotide ($FADH_2$), and nicotinamide adenine dinucleotide (NADH). The enzymes involved in the fatty acid β-oxidation are under a tight transcriptional control mainly mediated by the nuclear receptor transcription factors peroxisome proliferator-activated receptor α (PPARα) and peroxisome proliferator-activated receptor γ coactivator-1α (PGC-1α). PPARα is abundantly expressed in the heart and regulates genes involved in all aspects of the fatty acid metabolism, from the uptake, binding, and oxidation [73,74]. PPARβ/δ and PPARγ are also expressed in the heart and appear as important regulator of the fatty acid metabolism even if "loss-of-function" and "gain-of-function" studies result in phenotypic differences in comparison with PPARα, likely due to the fact that they do not regulate all the genes involved in fatty acid metabolism as PPARα [75]. Of note, PPARγ is known to be activated by several natural occurring lipid metabolites, including PUFAs, phospholipids, and also oxidized fatty acids [76–78]. 15d-PGJ2 is one of the lipid peroxidation products that is able to covalently bind through a Michael addition to cysteine residues on several proteins (i.e. H-Ras, NF-kB, IkB, AP1) including PPARγ. It has been demonstrated that the formation of an ALE between α,β-unsaturated aldehydes (i.e. 15d-PGJ2, hydroxyeicosatetraenoic acid, hydroxyeicosadecaenoic acid, 4-HNE) and PPARγ can modulate its transcriptional activity and the expression of several genes activated by PPARγ *in vivo* [76,78]. The actions of the nuclear transcription factors are supported by the transcriptional activators PGC-1α and PGC-1β; for example, their upregulation by physiological (i.e. exercise) or pathophysiological (i.e. fasting, diabetes) stimuli results in increased mitochondrial biogenesis, fatty acid β-oxidation, and oxidative phosphorylation. *Vice versa,* in conditions like cardiac hypertrophy, heart failure or in the fetal heart, where the expression of PGC-1 is decreased, also fatty acid β-oxidation and mitochondrial biogenesis are impaired [79].

Because of its immense requirement for nutrients and oxygen, the heart contains a very high content of mitochondria in comparison with other organs. Mitochondria are at the same time the main source of energy and the largest source of intracellular ROS in cardiomyocytes, as superoxide is continuously formed at sites within the electron transport system during oxidative phosphorylation [80]. Thus, due to these characteristics mitochondria are presumably the largest endogenous source of lipid peroxidation in the heart. Although these organelles have robust antioxidant and detoxification systems, ensuring that lipid peroxidation and levels of reactive aldehydes are kept at sub-toxic levels, over time, and under various pathological states, these antioxidant and aldehyde detoxification systems become compromised (reviewed in Ref. [81]). Thus, the resulting accumulation of lipid peroxidation products has profound consequences for the function of mitochondria, the cardiomyocytes, and the heart.

The molecular targets of lipid oxidation are firstly the membrane of mitochondria, which are particularly enriched of cardiolipin, a highly unsaturated phospholipid specifically localized to this compartment, constituting ~20% of the local lipids [82]. Cardiolipin that ensures the efficient function of the electron transport chain complexes, diminishes dramatically in robust lipid peroxidation conditions [82], and decreased levels of cardiolipin have been observed in many pathological

conditions including aging, Barth syndrome, heart failure, ischemia/reperfusion injury, diabetes, and neurodegenerative diseases [82].

Lipid peroxidation products exert many effects on cardiomyocytes, usually detrimental [81]. For example, ACR, the simplest unsaturated aldehyde, that is produced widely in different tissues and is found ubiquitously in the environment as a pollutant, induces contractile dysfunction, Ca^{2+} anomalies, and apoptosis in *in vitro* cultured cardiomyocytes [83,84].

Similarly to ACR, trans-2-hexenal is an endogenous product of lipid peroxidation [85–87], as well as a ubiquitous pollutant, which has potent effects on cardiac function [88]. Trans-2-hexenal exposure results in direct cardiac toxicity through, at least in part, induction of mitochondrial cytochrome c release-mediated apoptosis in murine cardiomyocytes [88].

Interestingly, 4-HNE has been widely accepted as an inducer and mediator of oxidative stress [89], but it is also able, depending on its concentration, to elicit an adaptive response and to protect cells against the oxidative stress through signaling pathways activation and modulation of transcriptional activity (reviewed in Ref. [90]). For example, 4-HNE protects rat neonatal ventricular myocytes against cardiac ischemia/reperfusion (IR) injury via the Nrf2-dependent pathway [91,92].

2.3. The epicardial adipose tissue

Recent studies renewed the importance of ectopic myocardial lipids as the result of the rapid development in the field of non-invasive imaging, which has made possible the quantitation of cardiac fat deposit with high accuracy. The epicardial adipose tissue (EAT), localized between the myocardial surface and the visceral layer of the pericardium, originates from mesodermal cells and is similar to the visceral fat; conversely, the pericardial fat, which has an ectodermal origin, is similar to the subcutaneous fat. This distinction is of great clinical importance [93]. EAT functions span from a mechanical protection role with attenuation of the torsion developed by the myocardium during the contraction, to a role as energy provider [93]. Further, EAT can potentially protect the heart from the cardiotoxic effect of the large amount of FFA due to its capacity to rapidly uptake them; additionally, it represents a paracrine and vasocrine source of inflammatory mediators and adipokines. Adiponectin secreted by EAT improves endothelial function through stimulation of nitrogen monoxide synthase, and reduces oxidative stress and inflammatory cytokines [94]. These properties, and the close proximity to coronary arteries, raised the hypothesis for a direct role of EAT in the development and progression of coronary atherosclerosis [95]. Indeed, a number of cardiovascular diseases, such as coronary artery disease, atrial fibrillation, type 2 diabetes or insulin resistance syndrome, are all associated with an increased amount of epicardial fat (reviewed in Ref. [93]). In this regard, epicardial adipose tissue can contribute increasing oxidative stress. Indeed, it has been shown that the epicardial adipose tissue has more oxidative stress markers than the subcutaneous (SC) adipose tissue in a study conducted with proteomic analysis [96]. Further, EAT may cause an increased risk of cardiovascular diseases by leading to increased oxidative stress in patients with metabolic syndrome [97].

2.4. Adipose tissue

The adipose tissue has recently been reconsidered from a relatively inert organ with a primary role as a storage depot for excess energy, in the form of triglycerides, to a metabolically active organ involved in cross-talk between various systems [98]. Indeed, recently, the term “adiposopathy” has been coined [98]. The central dogma of adiposopathy is based on a shift to visceral adipose tissue distribution (intraperitoneal and retroperitoneal spaces), an onset of ectopic fat deposition (fat store in the liver, pancreas, heart, and skeletal muscle), a dysregulation of the inflammatory and adipokine system, and an insulin resistance.

The adipose tissue, which represents one of the largest body compartments, is classified according to its anatomical location and related functions, and still, an accepted taxonomy is lacking. For example, SC adipose tissue, which mostly contains white adipocytes enriched in triglycerides, stores lipids at a variety of anatomical sites that differ in metabolic and physiological characteristics [99]. On the other hand, visceral adipose tissue is a smaller storage compartment for lipids and it is mechanistically linked to many of the metabolic disturbances and adverse outcomes associated with obesity [100].

The perturbation of the adipose tissue results in a pathological response that directly or indirectly contributes to cardiovascular and metabolic diseases. Cardiovascular disease mortality and morbidity have been shown to be high in individuals who are overweight, mainly with central deposition of adipose tissues [101]. Obesity could be associated with dyslipidemia, hypertension, diabetes, or insulin resistance, and high levels of fibrinogen and C-reactive protein, all of which increase the risk of CVD events [102]. The distribution and the amount of adipose tissue can influence the synthesis and secretion of adipokines and hormones provoking an inflammatory state, and the hydrolysis of triglycerides present in the adipocytes releases free fatty acids which are poured into the plasma. An excessive adiposity causes an increase in the size of liposomes in hepatocytes (steatosis), which leads to a series of pathological states, including nonalcoholic fatty liver disease, steatohepatitis, and cirrhosis, and it can also cause an accumulation of lipid intermediates (e.g., ceramides) in some non-adipose tissues, with cellular dysfunction and apoptosis, due to lipotoxicity (reviewed in Ref. [100]).

Oxidative stress in human and murine adipose tissue, as well as in cultured 3T3-L1 adipocytes, alters the release of adipokines, such as adiponectin and tumor necrosis factor α [103,104]. Further, the modification of adipose proteins by lipid peroxidation products could be one of the contributing factors linking oxidative stress to insulin resistance. Among lipid peroxidation products, oxysterols and 4-HNE received most attention since cross-sectional studies and experimental data indicate their mechanistic implication in the pathophysiology of obesity-linked metabolic diseases (reviewed in Ref. [105]).

In animal models, adipose 4-HNE accumulation *per se* was shown either to promote the obese state or to induce the development of insulin resistance, through carbonylation of key adipocytes proteins involved in lipid metabolism [106]. For example, the adipocyte fatty acid-binding protein, a protein implicated in the regulation of insulin resistance, after modification, reduces its affinity for fatty acids, approximately 10-fold [107]. Furthermore, the exposure of adipose cells to 4-HNE led to a dysfunctional phenotype characterized by an impairment of the insulin signaling, increased lactate and reduced adiponectin production, all features typical of insulin resistance developing [104].

Finally, in differentiating (pre)adipocytes, oxidative stress can induce intracellular 4-HNE production, which, in turn, by activating the MAPK pathway, inhibits adipocyte differentiation, fostering the noxious effect of 4-HNE on adipose homeostasis [108].

Recently, it has been shown that long-term treatment of human primary pre-adipocytes, isolated from SC adipose tissues of obese subjects with physiological concentrations of 4-HNE (up to 10 μM) causes increased oxidative stress, inhibition of cell growth, loss of adipogenic capacity and induction of insulin resistance, thus highlighting the crucial role of 4-HNE in the progression obesity-associated metabolic syndrome [109].

3. Molecular and cellular effects of lipid peroxidation products

Lipid peroxidation products are involved in inflammatory processes, cell proliferation, and viability, and have specific roles in signaling cascades that activate an adaptive response to oxidative damage in order to improve the physiological antioxidant defenses. Shreds of

evidence suggest that 4-HNE is able to activate uncoupling proteins (UCPs) in the mitochondria, inducing negative feedback to lower proton motive forces and to protect the cells from oxidative damage [7,110]. Moreover, lipid peroxidation products can also activate transcription factors, such as Nrf2, through the modification of its inhibitory protein Keap1, inducing genes that modulate the antioxidant response of the cell [7,111].

It has been demonstrated, however, that the effects of lipid peroxidation products are finely tuned and concentration-dependent. Indeed, at a lower concentration, they could have beneficial effects, inducing for example cell growth through epidermal growth factor receptor (EGFR) or platelet-derived growth factor receptor (PDGFR), while, at higher concentration, they can inhibit proliferation and even induce apoptosis [112,113].

Further, oxPLs can exert a variety of biological effects that are different from those of free fatty acids derived from their degradation and are concentration- and cell-type-dependent [114]. They can alter the physical properties of the cell membrane, due to the different chemical-physical characteristics (polarity and shape) in comparison with the corresponding native phospholipids, influencing also the functions of the membrane-bound protein involved, for example, in ion transport [31].

OxPL can be recognized by cell surface receptors, including the scavenger receptor for recognition and uptake of oxLDL, CD36, or toll-like receptors (TLRs), or with circulating LPS binding protein or CD14 [31], activating a cascade of events. These interactions can partially explain their involvement in complex processes ranging from inflammation to apoptosis, affecting endothelial cells, smooth muscle cells and macrophages, as summarized by Fruhwirth et al. [31,115].

However, the ability of lipid peroxidation products to interact with different types of macromolecules, including DNA, phospholipids, and proteins, gives rise to a plethora of biological effects, due to molecular damages.

DNA modification induced by lipid peroxidation products could be repaired by the cells through a nucleotide excision repair pathway, as described for etheno-DNA adducts with 4-HNE [116]. However, these adducts can cause DNA damage associated with carcinogenic effects and profound alterations of the signal transduction pathways involved in particular, in the control of the cell cycle and gene expression [8]. In the context of cardiovascular diseases, oxidative DNA damage could induce apoptosis and regulate angiogenesis [117] and it has been demonstrated that lipid peroxidation-derived etheno-DNA adducts are present in human atherosclerotic lesions [118].

Phospholipids modifications can result in changes of their physical properties and turnover, leading to an altered distribution of aminophospholipids among the cellular or subcellular membranes with potential effects on the activity of proteins that interact with phospholipids [7]. Further, oxidized phospholipids are also involved in protein modifications, as demonstrated by Horkko et al. who showed that adducts of oxidized phosphatidylcholine with ApoB-100, the major protein of LDL, modulate the lipoprotein uptake by macrophages [45].

Protein lipoxidation can occur on different proteins in relation to the presence of residues susceptible to the formation of adducts with lipid peroxidation products, but also to their molecular conformation and the presence of metal binding sites. These modifications can alter both the structure and the function of the modified proteins influencing their physico-chemical characteristics, their degradation and trafficking introducing crosslinking or even stimulating an autoimmune response [7], as described in details for 4-HNE-modified proteins by Schaur et al. [119].

One of the most studied targets of lipoxidation is represented by LDLs considering the role of oxLDL in several pathological processes including atherosclerosis. Several adducts have been identified with MDA, 4-HNE, glyoxal or acrolein leading to a variety of biological and atherogenic processes [112]. Additionally, protein oxidation by 4-HNE on ApoAI, the principal protein component of HDL, has been associated with a decrease in cholesterol transport function and anti-inflammatory properties of these lipoproteins [120].

Of note, one of the mechanisms of degradation of 4-HNE-modified proteins is mediated by the proteasome, but some protein components of the proteasome have been identified as specific targets of these modifications with a consequent loss of function of the entire proteasome system and accumulation of modified proteins [13].

Regarding the protein modifications due to the formation of adducts with oxidized phospholipids, the literature is sparse, especially regarding the mapping of these adducts *in vivo*, even if the role of phospholipid oxidation products in several diseases, including atherothrombosis, has been extensively documented, mainly using antibodies against oxidized phospholipid adducts [11].

Protein adducts can also be formed with prostaglandins, mainly the cyclopentenone prostaglandin (CyPG), a molecule involved in the response to oxidative stress and in the resolution of inflammatory processes. It covalently reacts with proteins generating irreversible adducts, as demonstrated for various proteins involved in the NF-kB signaling cascade, including IkB kinase β (IKKβ), p65 and p50 subunits of NF-kB [121–123] or PPARγ, whose modification is necessary for the conformational changes of the receptors and the binding with the coactivator [10,124].

4. Involvement of lipid peroxidation in cardiovascular complications of systemic diseases

Obesity, metabolic syndrome, and diabetes are the major cardiovascular disease risk factors, including coronary heart disease, atrial fibrillation, ventricular arrhythmias and heart failure.

The association between obesity and different cardiovascular diseases is complex, but it is well known that obesity can cause coronary atherosclerosis through dyslipidemia, hypertension, and diabetes mellitus 2, as well as other factors like subclinical inflammation, increased free fatty acid turnover, intramyocardial and subepicardial fat deposition, elevated leptin and insulin concentrations [125]. Systemic alterations involved in obesity are increased oxidative damage to proteins and lipids, and severe inflammation as indicated by elevated levels of TNF, interleukin-1β and other pro-inflammatory cytokines [126]. Oxidative stress and inflammation are concurrent processes in many tissues that are affected because oxidative stress induces inflammatory cytokines production that in turn promote ROS generation [127]. Levels of 4-HNE are increased in the blood and muscle tissue of obese subjects in comparison to normal weight subjects [127,128]. Enhanced levels of 4-HNE are also present in adipocytes in obese subjects, where they impair the function of proteins responsible for lipid synthesis and suppression of inflammation [107]. Moreover, it has been demonstrated that high intracellular 4-HNE in adipocyte causes enhanced lipolysis through multifactorial mechanisms, which is the major feature in obesity-related metabolic disorders [129].

Oxidative stress is closely related to glycation: free radical oxidation of glycated residues in proteins generates a permanent and irreversible modification. This process is known as glycoxidation and it is involved in the complications associated with several disorders including diabetes, cardiovascular disease and other several forms of cancer [130].

Both glycoxidation and lipoxidation of vascular wall structural proteins are also implicated in diabetes. Hyperglycemia-induced increase in the production of oxidants and other reactive intermediates is a key mechanism for the development and progression of endothelial dysfunction in diabetic patients [126]. Although oxidative stress has a known important role in diabetic complications and atherosclerosis, it is not clear whether oxidative stress is a primary event that is present at early disease stage or whether it represents a secondary event that is a consequence of the end-stage tissue damage. Glycoxidation products in collagen have been demonstrated to minimize the NO activity, which alters vascular tone and perfusion, and contribute to hypertension. High aortic stiffness has been reported in diabetic patients and it is associated

Table 1
Most common methods for detecting and analyzing the principal lipoperoxidation products and their protein adducts. 4-APC, 4-(2-(trimethylammonio)ethoxy)benzenaminium halide; 4-HNE, 4-hydroxy-2-nonenal; ACR, acrolein; AIDA, alternate isotope-coded derivatization assay; CE, capillary electrophoresis; CVDs, cardiovascular diseases; DNPH, 2,4-dinitrophenylhydrazine; ESR, electron spin resonance; GC, gas chromatography; HLB, hydrophilic-lipophilic balanced; LC, liquid chromatography; LC-FD, LC-fluorescence detection; LC-UV, LC-ultraviolet; LDLs, low-density lipoproteins; LLE, liquid-liquid extraction; MALDI-TOF, matrix assisted laser-desorption ionization-time of flight; MDA, malondialdehyde; MRM, multiple reaction monitoring; MS, mass spectrometry; oxPC, oxidized phosphatidylcholine; SPE, solid-phase extraction; SRM, selected reaction monitoring; TBA, thiobarbituric acid; TLC, thin-layer chromatography.

Electrophilic lipid species	Name	Detection methods	CVDs	Cardiovascular targets
Lipid peroxidation-derived aldehydes	4-HNE	**Free 4-HNE:** – **Spectrophotometric methods** (carbonyl-reactive reagents, e.g. DNPH, biotin-containing probes, fluorescence probes and tritiated sodium borohydride) [137,138] – **LC-MS/MS** [142,143] – **GC-MS/MS** (sample derivatization) [139,140] **4-HNE-protein adducts:** – **Immunochemical methods** (immunocytochemistry and immunohistochemistry, ELISA, Western blotting) [146,147,153,156,304] – **MALDI-TOF MS/MS, LC-MS/MS** and **GC-MS/MS** (enrichment strategies, e.g. biotin hydrazide, immuno-based, click chemistry) [154,158–161,166,305]	– Atherosclerosis [112,151,154,272] – Coronary and peripheral artery disease [196] – Dilated cardiomyopathy [165] – Heart failure [166,295] – Myocardial ischemia and reperfusion injury [306,307]	– Apolipoprotein B-100 (LDLs) [148] – Apolipoprotein AI (HDLs) [120] – Heart fatty acid-binding protein [308] – Mitochondrial proteins (e.g. cytochrome c oxidase subunit I) [161,305] – Platelet-derived – growth factor receptor beta [272] – Carnosine [283,286,288] – Serine/threonine-protein kinase STK11 [309] – Glutathione [260] – Ether-a-go-go-related channels [310]
Lipid peroxidation-derived aldehydes	MDA	**Free MDA:** – **Spectrophotometric methods** (sample derivatization with TBA) [170,172–174] **MDA-protein adducts:** – **Spectrophotometric methods** (sample derivatization with TBA, strong acids, hydrazine-based or non-hydrazine-based reagents) [171,180,183] – **LC-UV** or **LC-FD** [176,177,180] – **LC-MS/MS** (e.g. **SRM/MRM MS** or **label-free**; sample derivatization with AIDA assay, 4-APC) [186–188,194,195] – **GC-MS/MS** (sample derivatization with hydrazine-based or non-hydrazine-based reagents) [178,179,190,191,196] – **CE-UV** [193]	– Atherosclerosis [112] – Coronary and peripheral artery disease [196,311] – Aortic stenosis [265] – Heart failure [312]	– Apolipoprotein B-100 (LDLs) [43] – Apolipoprotein AI (HDLs) [313] – Mitochondrial proteins [314] – Carnosine [282,285]
Lipid peroxidation-derived aldehydes	ACR	**Free ACR:** – Fluorescence methods (e.g. Skraup reaction with m-aminophenol, lanthanide probe) [202,204,205] – LC-FD [206,208] – LC-MS/MS (sample derivatization) [214] **ACR-protein adducts:** – Immunochemical methods [209,211] – GC-MS/MS and LC-MS/MS (e.g. SRM/MRM MS; enrichment strategies, e.g. hydrazide-based reagents, non-hydrazine-based reagents, immuno-based) [212,213,216] – LC with electrochemical detection [215]	– Atherosclerosis [112] – Myocardial dysfunction [83]	– Apolipoprotein B-100 (LDLs) [315] – Mitochondrial proteins [160,216] – Carnosine [284]
Prostaglandin-like compounds	Isoprostanes	– Immunochemical methods (ELISA) [223,225] – GC-MS/MS and LC-MS/MS (e.g. SRM/MRM MS; extraction strategies, e.g. SPE, LLE, affinity column, TLC, silica and HLB cartridges) [219,226–228,230,232–236,239]	– Atherosclerosis [228,316] – Coronary heart disease [317–319] – Acute coronary syndrome [320]	– Thrombomodulin [321] – Thromboxane A2 prostanoid receptor [228,322]
Oxidized phospholipids	oxPC	– Spectroscopy methods (e.g. ESR) [241] – Immunoassays [31,46] – Colorimetric and fluorimetric assays (e.g. iodometric titration, ferrous oxidation-xylenol orange assay, isoluminol-dependent assay, diphenyl-1-pyrenylphosphine and hydrazine-based reagents) [242,243] – MALDI-TOF MS/MS, GC-MS/MS and LC-MS/MS (e.g. SRM/MRM MS; extraction strategies, e.g. SPE and TLC) [114,244–247,251]	– Atherosclerosis and aortic stenosis [31,46] – Atherothrombosis [11] – Familial combined hyperlipidemia and familial hypercholesterolemia [246]	– Apolipoprotein B-100 (LDLs) [45] – Apolipoprotein AI (HDLs) [44]

with increased cross-linking of connective tissue proteins. Glycated collagen specifically binds LDL compared to control collagen, and this increased LDL trapping by AGEs accelerates the atherosclerosis development in patients with diabetes mellitus [131]. Dyslipidemia is a common feature in diabetic patients and elevated levels of plasma lipoproteins might contribute to lipoxidation. AGE lipids have been detected in diabetic plasma lipoproteins and isoprostanes levels are high in diabetic patients [132,133].

5. Methods for identification and quantitation of lipid peroxidation products: strategies and challenges

Lipid peroxidation products can be identified in the free form, but they are more likely to be present in biological samples as covalent adducts with proteins, DNA or aminophospholipids.

Methods for the detection and quantification of free lipid peroxidation products include spectrophotometric methods and gas or liquid chromatography (GC and LC, respectively) coupled to mass spectrometry (MS). However, most attention has been focused in recent years on detecting and quantifying adducts with proteins by employing two main approaches: antibody-dependent techniques and proteomic methods based on MS. Currently, MS is the method of choice for the identification of protein-lipid adducts, because it is possible to detect the mass shift caused by the adducts and to acquire fragmentation spectra that can be used for the identification of specific fragment ions (i.e. reporter ions) for each modified amino acid within the protein sequence [134]. Of course, a method for enriching adducted proteins over non-adducted proteins prior to LC-MS/MS analysis would enhance the overall identification of lower abundance protein compounds.

Many pre-analytical factors can influence the analysis of lipid peroxidation products in plasma, serum, and tissue [135]. Lipid peroxidation product concentrations can be higher than the real physiological amounts, due to their artefactual formation that depends on storage time/conditions. The use of antioxidants, such as butylated hydroxytoluene (BHT), or the use of COX inhibitors to block the enzymatic formation, can be possible strategies to avoid/minimize *ex vivo* formation. Accurate and standardized protocols are essential to control the adverse effects of pre-analytical issues on lipid peroxidation product measurements.

Most common technologies for detecting and quantifying the principal lipid peroxidation products and their protein adducts are summarized in Table 1.

5.1. 4-Hydroxy-2-nonenal analysis

Several methods are available to detect and study both free 4-HNE and 4-HNE-protein adducts (Table 1). Methods for detection and quantitation of free 4-HNE include spectrophotometric methods and mass spectrometry analysis [136]. 4-HNE can be separated from other aldehydes by high performance liquid chromatography (HPCL) and quantified by spectrophotometrically monitoring. Anyway, in complex biological samples, specific carbonyl-reactive probes are commonly used, such as 2,4-dinitrophenylhydrazine (DNPH), biotin-containing probes, fluorescence probes (e.g. 1,3-cyclohexandione (CHD)) [137] and tritiated sodium borohydride [138].

Instead of UV, MS can be applied for the identification of the compound based on its fragmentation pattern. In particular, GC-MS analysis is able to detect and quantify derivatized 4-HNE in negative ion chemical ionization mode using a deuterated 4-HNE as internal standard [139]. In order to avoid losses during sample preparation, many isotopic internal standards have been used till now, such as 2,5-dihydroxy-benzaldehyde (2,5-DBA) [140], 4-hydroxybenzaldehyde (4-HBA) [141] and pentafluorobenzylhydroxylamine-HCl [139]. Instead, LC-MS analysis does not necessarily require derivatization, so the sample preparation is less complex and prone to pre-analytical errors during the manipulation [142,143].

However, the majority of 4-HNE is present as adducts of a variety of biomolecules and many reviews reported the main analytical approaches used to detect them (e.g. Refs. [10,144,145]). The two possible approaches to detect 4-HNE adducts are immunochemical techniques and MS analysis. Sometimes, a reduction step with borohydride is required to stabilize the Schiff bases or Michael adducts before the analysis.

Immunohistochemistry/immunocytochemistry approaches detect 4-HNE bound to histidine and the distribution of the 4-HNE-histidine adducts in cells and tissues using antibodies [146]. The advantage of immunohistochemistry is to evaluate the distribution of 4-HNE-protein conjugates, but their quantitation can be estimated only semi-quantitatively [147].

Several antibodies for the 4-HNE adducts identification have been developed over the years [136,146]. In 1990, Palinski et al. developed polyvalent and monoclonal antibodies against sodium cyanoborohydride-reduced 4-HNE-treated LDL and these antibodies were able to recognize 4-HNE-lysine adducts on apolipoprotein B (ApoB) that were produced during copper-induced oxidation of LDL *in vitro* [148]. A few years later [149], a polyvalent antiserum to human 4-HNE-LDL modified under non-reducing conditions, also showed *in vivo* the recognition of copper-oxidized LDL and cross-reactivity with 4-HNE-albumin and a lower extent 4-HNE-HDL. Uchida et al. produced monoclonal antibodies that reacted strongly with 4-HNE-treated proteins and immunohistochemical analysis of atherosclerotic lesions of human aorta demonstrated their specific reactivity with epitopes present in the foam cells [150]. Later, Itakura's group developed a monoclonal antibody directed to a fluorescent derivative of 4-HNE with Lys residue [151] and reported the presence of the fluorophore in atherosclerotic lesions from the human aorta and in the oxidatively modified LDL. However, another study demonstrated that the majority of the epitopes on the oxidatively modified LDL were 4-HNE-histidine adducts [152]; this is also the case of other 4-HNE adducts on various proteins analyzed, suggesting that 4-HNE-histidine adducts could be the major bioactive form of 4-HNE interactions with proteins and peptides.

Another antibody-based approach to estimate the amounts of 4-HNE-protein conjugates is the Western-blot method, which, being a semi-quantitative immunochemical analysis [153,154], is not a standardized and precise method, and provides only an approximate quantitation [155].

Over the years, the enzyme-linked immunosorbent assay (ELISA) technique has given rise to great interest for the analysis of 4-HNE-protein adducts. An ELISA method was developed to detect 4-HNE-histidine adducts in human lysates of cells subjected to slight or severe oxidative stress [147], and it was also adapted to a commercial antibody for the analysis of human plasma samples [156].

Labelling approaches have been used to determine the 4-HNE-protein conjugates in several studies, combined with MS techniques that were required for the identification of the tagged 4-HNE-protein adducts. While the use of 4-HNE-antibodies in ELISAs and immunostaining allows only the detection and quantitation of adducts, the MS provides also a characterization of 4-HNE adducts. Matrix assisted laser-desorption ionization-time of flight (MALDI-TOF) MS has been used for 4-HNE-adducts detection in biological samples by the increase in mass to charge (m/z) ratio of the peptide compared to the native form (i.e. an increased mass of 138 Da by Schiff's base formation or 156 Da by Michael addition [145,157]). Additionally, MS/MS analysis allows sequencing of proteins and identification of the modification sites [136]. However, the analysis is more complicated when reduced products of the sample, due to the treatment with sodium borohydride or cyanoborohydride, or structural rearrangements occur, and a further increase of the mass should be considered. As an example, Arcaro et al. observed by two-dimensional electrophoresis (2DE) and MALDI-TOF MS that the exposure of human promyelocytic HL-60 cells to non-toxic doses of 4-HNE resulted in a heat shock 60 kDa protein 1 (HSP60) modification by 4-HNE, and suggested a possible involvement of the

HSP60 modification with 4-HNE in the pathogenesis of atherosclerosis [154].

Several proteomic studies on the 4-HNE-protein adducts have been also performed by LC-MS/MS. Methods for enriching 4-HNE-adducted proteins over non-adducted proteins prior to LC-MS/MS analysis often enhance the overall identification of lower abundance protein adducts in biological samples. The use of azido and alkynyl derivatives in combination with click chemistry has been proven to be an efficient approach for the identification of the protein targets of 4-HNE prior to LC-MS/MS analysis [158]. Some years later, a study demonstrated the possibility to use stable-isotope tagging followed by enrichment of 4-HNE-modified peptides by solid-phase hydrazide chemistry and combined with LC-MS/MS analysis for quantitation of 4-HNE-modified proteins in plasma samples [159]. In the same year, Chavez et al. reported the identification of endogenous protein targets of several electrophilic 2-alkenals, among which 4-HNE, in cardiac mitochondria by using a chemical aldehyde/keto specific labeling and affinity strategy in combination with LC-MS/MS [160]. In addition, 2DE followed by LC-ESI-MS/MS has been successfully applied to identify 4-HNE modified [161,162]. Increased levels of 4-HNE-modified proteins have been detected both in animal models and patients with heart failure (HF). For example, 4-HNE-protein adducts were significantly increased in the left ventricular myocardium of HF dogs [163] or in the myocardium from rats with HF [164]. In humans, 4-HNE-modified proteins have been found in the myocardium from patients with dilated cardiomyopathy [165]. Moreover, significantly higher 4-HNE plasma levels have been observed in HF patients with respect to healthy subjects. Increased 4-HNE levels correlated with higher heart rate and impaired left ventricular contractility [166].

5.2. Malondialdehyde analysis

The analytical strategies to analyze MDA, free or bound to proteins, can be divided into derivatization-based and label-free methods (Table 1). In particular, these strategies have been implemented with separation techniques such as LC or GC, in order to facilitate MDA measurement [167]. Methods which require an acidic or basic sample pre-treatment, or the use of strong acids to precipitate the protein fraction, are able to hydrolyze the bound MDA and provide an assessment of the total MDA.

Many derivatization-based assays have been developed for the detection of MDA, among which the most frequently used and simplest is TBARS assay (thiobarbituric acid reactive substances assay) in which thiobarbituric acid (TBA) reacts with MDA to obtain a colored chromogen fluorescent red adduct [18,168]. However, TBARS assay is unspecific which has led to important controversy over its use for quantification of MDA from *in vivo* samples [2]. Indeed, TBA may react with many other compounds in addition to MDA [169] and the condensation process may generate further oxidation of the matrix with consequently an overestimation of the quantitative results. Aimed to reduce the matrix oxidation, the precipitation of protein prior to the TBA reaction is often applied as a pre-treatment of the sample [18].

Over the years, different methods based on TBA derivatization have been proposed, in order to improve specificity, selectivity and to obtain accurate quantification of MDA [170–172]. An interesting on-line analytical system that involves the use of microdialysis perfusion, on-line derivatization, and HPLC analysis was developed for the continuous monitoring of MDA [173], and similarly, an on-line microdialysis sampling system coupled with an HPLC system was also proposed for the simultaneous determination of ofloxacin (OFL) and MDA in whole blood [174]. Cooley et al. described a capillary electrophoresis (CE)-fluorescence method combined with *in vivo* microdialysis sampling [170] to quantify MDA in rat heart, muscle, liver, and brain dialysate.

Since TBARS assay failed to distinguish free and bound MDA and it is intrinsically unspecific, several alternative approaches have been proposed [175]. Hydrazine-based derivatization reagents, such as DNPH [176–179], FMOC-hydrazine [180] or dansylhydrazine [181], have been used in the analysis of MDA by LC- or GC-MS. Non-hydrazine-based reagents have been also employed for the measurement of MDA: 1-methyl-2-phenylindole [182,183], diaminonaphthalene [184] and 2-aminoacridone [185].

Besides the use of LC-ultraviolet (LC-UV) and LC-fluorescence detection (LC-FD) for the MDA derivatives analysis, also LC-MS/MS-based strategies have been reported in several studies. For example, alternate isotope-coded derivatization assay (AIDA) and the reagent 4-(2-(trimethylammonio)ethoxy)benzenaminium halide (4-APC) have been proposed for the quantitative analysis of MDA and other aldehydes using LC-MS/MS [186–188]. Other hydrazine labels, such as 2,4,6-trichlorophenylhydrazine [189] and 2,2,2-trifluoroethylhydrazine [190], have been widely used also for the GC-based methodologies. Similarly, the analysis of MDA by GC-MS and GC-MS/MS has been reported using non-hydrazine-based reagents [175,191].

On the other hand, label-free analysis of free MDA is possible and ranges from UV-based methodologies to LC-MS/MS technique. However, the UV detection of MDA has poor sensitivity and selectivity when the analysis of complex biological matrices is performed and, thus, a separation technique by LC [192] or CE [193] is required in order to simplify the UV-absorbance.

LC-MS/MS technique using selected reaction monitoring/multiple reaction monitoring (SRM/MRM) has been applied in several studies for precise quantitation of MDA in biological fluids, coupled with a SPE for a pre-treatment of the biological fluids before SRM [194] or using 3-nitrophenylhydrazine chemical derivatization and isotope-labeling [195]. Recently, Tsikas et al. applied GC-MS/MS technique to analyze simultaneously MDA and 4-HNE in human serum and plasma, from patients with coronary or peripheral artery disease, after administration of L-arginine [196].

In the cardiac context, *in vitro* studies with isolated adult rat ventricular myocytes demonstrated that MDA impairs cardiac contraction and maximal velocity of cardiac contraction and relaxation [197]. Moreover, plasma MDA levels have been found to be significantly elevated in HF patients [198,199]. HF patients with raised MDA plasma levels presented reduced left ventricular ejection fraction [199] and a higher NYHA functional class [200]. Additionally, high plasma MDA levels were a significant independent predictor of mortality in HF patients [201].

5.3. Acrolein analysis

To date, several methods have been developed for the estimation of ACR levels in biological samples, as reported in Table 1. The conventional method for detecting free ACR in biological samples is the fluorescence analysis based on the Skraup reaction with m-aminophenol [202,203] or using a lanthanide probe [204]. A less expensive and practical fluorescence-based method, using a two-step tethering strategy, for the detection of ACR in human plasma under mild conditions without the use of HPLC, has been also developed [205]. In other studies, HPLC-fluorescence detection in combination with a derivatization reaction was used for the accurate quantification of ACR in human serum and plasma samples [206–208].

ACR-protein adducts or -DNA adducts can be detected using monoclonal antibodies [209–211], which allow the detection of conjugates using gel-based approaches. However, the method is time-consuming and site-specific characterization of oxidative modifications is often not possible with gel-based techniques.

MS-based methods were successfully applied to determine ACR using GC-MS [212] or LC-MS/MS [134,213] and mostly DNPH as a derivatization reagent [214]. However, Imazato et al. developed a method for ACR analysis by HPLC with fluorescence detection after pre-column derivatization using 1,2-diamino-4,5-dimethoxybenzen (DDB) [208], which is not a hydrazine reagent and does not have intrinsic fluorescence itself that can interfere with the detection of ACR

derivative.

Alternatively, HPLC with electrochemical detection method allowed the determination of ACR without any derivatization step [215].

Finally, in 2011, Wu et al. developed an analytical approach that combines the identification and relative quantification of ACR-modified proteins in cardiac mitochondrial proteome samples by nanoLC-MS/MS SRM analysis [216].

5.4. Isoprostanes analysis

The measurement of IsoPs is considered the most reliable index for the assessment of lipid peroxidation in humans [217,218]. In humans, F2-IsoPs are usually measured in plasma and urine, but they can be also measured in other biological fluids (e.g. exhaled breath condensate, amniotic fluid, and saliva) or tissue homogenate [219]. Particular care must be taken during plasma collection and storage for F2-IsoPs analysis because isoprostanes can be also produced in plasma from *ex vivo* oxidation of AA [220]. Indeed, in order to minimize artefactual elevation of plasma F2-IsoPs, Barden et al. recommended blood collection into EDTA tubes containing the antioxidants BHT and reduced glutathione (GSH), in addition to storage at −80 °C [221]. Several other factors are important to consider when measuring F2-IsoPs and include the timing of sample collection, the optimal sample matrix and some key issues regarding their hydrolysis, excretion, and metabolism [222].

Commercially available ELISA kits [223–225] or mass spectrometry combined with gas [226,227] or liquid chromatography [228] are employed for the measurement of F2-IsoPs (Table 1).

Anyway, the comparison between commercially available ELISA kits provided very poor correlation and different results compared to LC/LC-MS/MS approach [218]. GC-MS/MS and LC-MS/MS provide indeed more accurate measurements [229], but often require multiple extraction and purification methods before the analysis. Moreover, the GC-MS approach involves derivatization steps to facilitate the following MS detection.

The extraction from biological samples is very important and several approaches are available including solid phase extraction (SPE) [230], liquid-liquid extraction (LLE) [219,231], affinity column [232], thin-layer chromatography (TLC) [233], silica cartridges [234] and hydrophilic-lipophilic balanced (HLB) cartridges [235]. In 2010, Taylor et al. developed and validated a reproducible and sensitive method for the extraction of 15-series F2-IsoPs from plasma samples, applying a combination of SPE and LLE to obtain a cleaner and more easily concentrated extract and reducing the HPLC separation time, before MRM analysis [236]. Some years later, a LLE method using negative chemical ionization GC-MS/MS have been proposed for the measurement of total isoprostanes in plasma and tissue homogenates, allowing the quantification of both free and esterified isoprostanes in order to have a correct estimation of the oxidative status [219].

In general, a known amount of deuterated internal standards is commonly added in sample preparation, before the purification steps, in order to obtain absolute quantification of the isoprostanes [237], and LC-MS/MS using MRM can yield an accurate measurement monitoring multiple pairs of transition mass ions [238–240].

5.5. oxPLs analysis

As shown in Table 1, analytical approaches to measure oxPLs include spectroscopy methods, immunoassays, colorimetric assays, and mass spectrometry, mainly coupled with different separation techniques [114].

When oxPLs are initially generated by radical attack they can be analyzed by electron spin resonance (ESR) [241], but due to the difficulties of this approach, colorimetric or fluorimetric assays are preferred for complex biological samples. Hydroperoxy groups can be evaluated with iodometric titration, ferrous oxidation-xylenol orange (FOX) assay or isoluminol-dependent assay. Alternatively, DNPH or pentafluorobenzyl hydroxylamine can be employed for the detection of aldehydes or ketones on phospholipids [114]. Of note, these methods can be coupled with tissue imaging as demonstrated for diphenyl-1-pyrenylphosphine (DPPP), a suitable fluorescent probe to monitor lipid peroxidation within cell membranes specifically [242]. In particular, lipid peroxidation was evidenced by DPPP fluorescence with microscopy techniques in isolated ischemic rat lungs perfused with DPPP, evaluating also its co-localization with an endothelial cell marker, DiI-acetylated LDL [243].

In order to improve the specificity of these assays, especially in complex samples, separation steps have been also introduced based on TLC, GC or HPLC interfaced with different detectors [114].

Immunoassays have been extensively applied for the analysis of oxidized phospholipids in biological samples since the introduction of the E0 series of antibodies against oxidized phosphatidylcholine, generated from apoE-deficient mice. In particular, the E06 antibody has been used to detect oxPLs both in their free or protein-bound forms [31] and has been extensively employed in the field of atherosclerosis. Further, it has also been suggested as a potential therapy to counteract the *in vivo* effects of oxPLs, not only in atherosclerosis but also in aortic stenosis or hepatic steatosis [46].

MS-based methods, such as MALDI-TOF or LC-ESI-MS/MS, offer the advantages of less handling artifacts and more structural information. Despite some studies have been performed by MALDI-TOF to identify oxidized phospholipids [244], the lack of the possibility to separate lipids before MS reduces their applicability to complex samples. However, it is worth noting the possibility to couple MALDI with imaging techniques allowing also the precise localization of the specific species [245].

Interestingly, Stubiger et al. used a MALDI-TOF-MS/MS approach to profile atherogenic phospholipids in human plasma and lipoproteins of hyperlipidemic patients and evidenced a positive correlation between oxPCs and markers of CVD, such as the intimal medial thickness that is considered an early marker in this young population [246].

Recently, Gao et al. presented the first systematic investigation of HDL apolipoproteins modifications by exposure to endogenous oxPLs *in vitro* [247]. They made a comparison of oxPLs with short-chain aldehyde 4-HNE using MALDI-TOF MS and demonstrated the high selectivity and efficiency of oxPLs in the modification of HDL apoproteins, providing novel insights into the mechanisms of the loss of HDL atheroprotective capacity.

On the other hand, ESI-MS can be easily coupled to HPLC separation at least to separate different classes of lipids, even if it does not resolve oxidation products from their precursors, and it is still the most convenient method in phospholipidomics [248]. Indeed, oxPLs have been analyzed both with shotgun approaches, to have a global analysis of phospholipids and oxPLs, and targeted MS approaches. These latter are the most preferred approaches to deal with the low concentration of oxPLs *in vivo*, thanks to their selectivity and sensitivity, even if they do not provide a comprehensive analysis of all the species [248]. The main reason for the failure of shotgun analysis has been the lack of bioinformatics tools for the identification of oxPLs. Novel bioinformatics solutions have been recently proposed, for example, with the development of the prediction software, LPPtiger, which can provide a system view of oxidized forms of phospholipids for untargeted analysis [249].

On the other hand, targeted approaches are largely used and are mainly based on a precursor ion acquisition of *m/z* 184 Da (phosphocholine headgroup) for the detection of PC and sphingomyelins, and the neutral loss of water (−18 Da) for hydroxides and hydrogen peroxide (−34 Da) for hydroperoxides derivatives [114]. Additionally, MRM approaches have been applied to evaluate oxPE induced by lipoxygenases, or the presence of oxPS, through the detection of the typical neutral loss of the phosphoserine headgroup (−87 Da) [114]. Novel strategies have been also developed to enrich oxidized LDL before MS analysis [250] or to introduce labeling of PE to increase the

signal intensity and allow a relative comparison of multiple samples using deuterated forms [251].

6. Molecular strategies to prevent ALEs formation in the cardiovascular system

Lipoxidation and, more specifically, ALEs are now considered not only indexes of oxidative damage, but also potential drug targets, due to their involvement in pathogenic mechanisms of oxidative-based diseases, including diabetes, atherosclerosis, and neurological disorders.

Identification of the products and sources of lipid peroxidation and its enzymatic or non-enzymatic nature have been essential for the design of mechanism-based therapies. Indeed, several therapeutic strategies, acting at different levels of the ALEs cascade, have been proposed essentially blocking ALEs formation, but also their catabolism or the resulting biological responses they induce (Fig. 4) [252].

6.1. Inhibition of ALEs formation

As described above, ALEs are generated through the covalent addition to specific nucleophilic amino acids of RCS, which are generated by lipid peroxidation; thus, several approaches have been proposed to reduce ALEs modulating RCS levels in different manners. Inhibition of ALEs formation can be obtained both with indirect strategies, mainly with antioxidants or metal ion chelators, or directly through RCS quenching.

6.1.1. Antioxidants

Antioxidants are molecules that are able to prevent undesired oxidation through their reaction with oxidants or oxidation intermediates. In this category are included xenobiotics that potentiate the endogenous detoxification machinery, which is composed of different enzymes involved in the inactivation of RCS [252], such as natural flavonoids and antioxidant micronutrients (i.e. β-carotene, retinol, vitamin E, and vitamin C). Vitamin E is, indeed, able to scavenge lipid peroxyl radicals, generating a tocopherol radical recycled to vitamin E by lipoic acid and ascorbic acid, while vitamin C is more effective in trapping oxygen, nitrogen and sulfhydryl radical reducing the generation of lipid hydroperoxide.

Among the antioxidant compounds able to inhibit lipid peroxidation, pyridoindole stobadine was proposed due to its ability to not only scavenge oxygen radicals but also to quench singlet oxygen, to repair oxidized bases and to maintain oxidation of SH groups by one-electron donation [253]. It has been demonstrated that stobadine is able to reduce both lipid peroxidation (i.e. conjugated dyene or MDA) [254] and the consequent protein modifications induced by oxidative stress, and it has been postulated as a novel cardioprotectant [253,255,256]. *In vitro* studies demonstrated that stobadine decreased oxidation of LDL, both at lipid and protein level, suggesting a role in atherosclerosis [255]. Moreover, studies performed *in vitro* or in animal models demonstrated that stobadine could reduce the myocardium impairment attributable to oxidative stress (e.g. myocardial infarction, hypoxia/reoxygenation, catecholamine overexposure) [253] and is able to correct hypertriglyceridemia and hypercholesterolemia in diabetic rats [254]. Of note, it has been demonstrated that the effects of stobadine can be

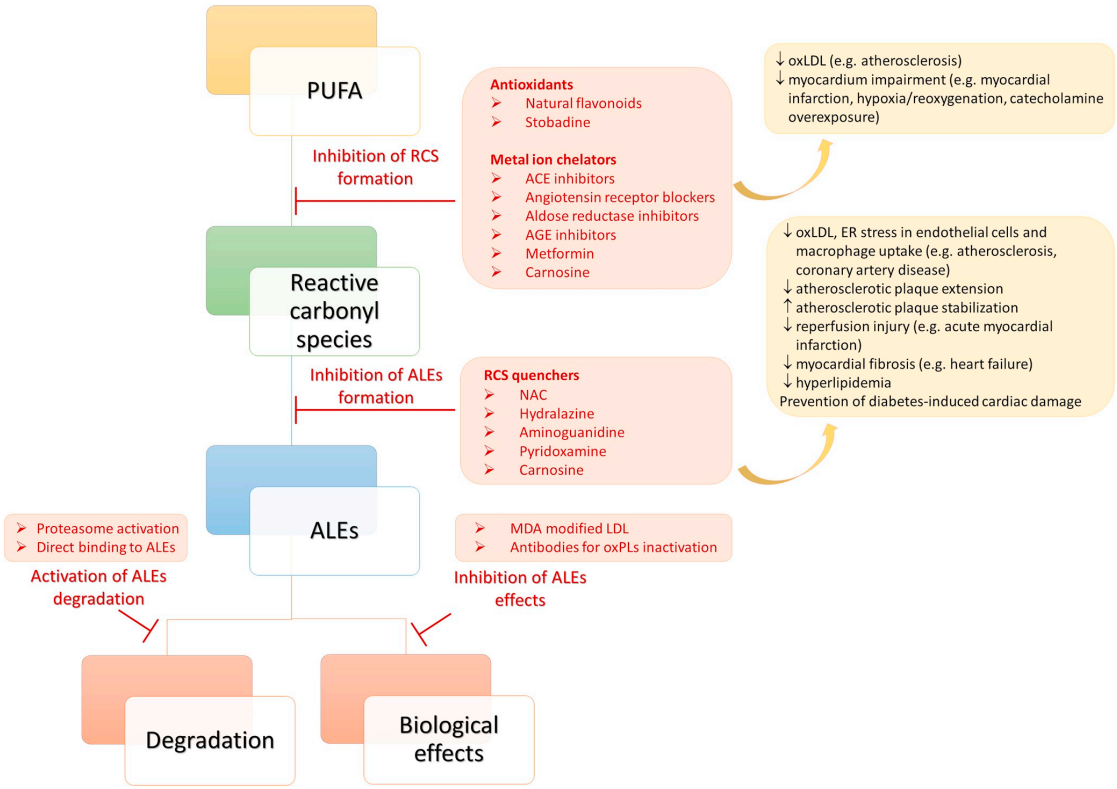

Fig. 4. Strategies to prevent lipoxidation effects and their implication in cardiovascular diseases. ER, endoplasmic reticulum; LDL, low-density lipoproteins; PUFA, polyunsaturated fatty acids; RCS, reactive carbonyl species; ALEs, advanced lipoxidation end-products.

ameliorated by concomitant administration of other antioxidants, such as vitamin E [256], and this is in line with the observation that *in vivo* interactions of antioxidants with endogenous vitamins may contribute to increasing the final antioxidant capacity [252,254]. Other antioxidant compounds include BHT, or Trolox, a soluble analog of alpha-tocopherol that has been shown also to contribute to the recycle of stobadine [257].

Notwithstanding the protective effects of these antioxidant compounds have been *in vitro* and *in vivo* demonstrated, a definitive conclusion regarding their clinical benefits is still lacking.

6.1.2. Metal ion chelators

ALE formation can also be inhibited by metal ion chelators or by multifunctional agents that possess this ability to chelate metal ions, which are the promoter of RCS formation, taking into consideration that complete elimination of all metal ions should not be achieved.

Of note, chelation is one of the most common mechanism to inhibit lipoxidation reactions utilized by many drugs employed to treat cardiovascular diseases, such as angiotensin-converting enzyme (ACE) inhibitors, angiotensin receptor blockers, aldose reductase inhibitors, hydralazine, and other advanced glycation end-products (AGE) inhibitors, including pyridoxamine, carnosine or metformin [252,258]. However, regarding AGE breakers, N-phenacylthiazolium bromide (PTB) and its analogs, it has been demonstrated that chelating activity could be prevalent at high concentrations, such as those used in *in vitro* studies, but not at therapeutic concentrations in which the carbonyl trapping activity resulted to be more important [259].

6.1.3. RCS quenchers

ALE formation could also be reduced by RCS quenchers, strong reactive nucleophilic molecules that form covalent adducts with electrophilic carbonyl derivatives, including dialdehydes, keto-aldehydes, and α,β-unsaturated carbonyls. Classification of RCS quenchers is essentially based on the number of functional groups and their chemical nature: monoreactive quenchers include thiol-containing compounds, β-dicarbonyl analogs, guanidine and hydrazine derivatives; polyreactive compounds are amino derivatives, heterocycle-based compounds, phenols, and polyphenols. In general, monoreactive compounds are characterized by a lower selectivity than polyreactive molecules, which, on the other hand, display softer reactivity and do not act against physiological carbonyls [252].

The most important example of thiol-containing carbonyl scavenger is represented by the endogenous tripeptide γ-L-glutamyl-L-cysteinylglycine (GSH), a known antioxidant characterized also by a marked sulfur nucleophilicity that allows the formation of covalent adducts with electrophilic compounds [260]. The detoxifying activity is exerted by the mercapturic acid, which is generated after the loss of GSH terminal residues and makes the quenched molecules more hydrophilic, facilitating its secretion. GSH quenching activity could be spontaneous or catalyzed by specific enzymes, glutathione-S-transferases, that are upregulated by oxidative stress to improve detoxification of α,β-unsaturated aldehydes, such as 4-HNE.

A similar quenching activity has also been demonstrated by free cysteine and N-acetyl cysteine (NAC) [137]. NAC is known as a precursor of GSH as well as a direct antioxidant for some oxidant species, such as NO_2 and HOX. It is also able to break disulfides, thus releasing free thiols as well as reduced proteins [261], besides its activity in preventing ALEs accumulation [262].

NAC is employed in several branches of medicine including cardiology, where it has been increasingly used over the past decades, especially to reduce reperfusion injury in the treatment of acute myocardial infarction as demonstrated in several animal models [263]. Indeed, a recent systematic review highlighted the ameliorative properties of NAC in preventing diabetes-induced cardiac damage through inhibition of oxidative stress [264], together with several preclinical studies supporting this effect. Reyes et al. demonstrated in a rat model of long-term ascending aortic stenosis NAC treatment resulted in a reduction of myocardial fibrosis during the transition from compensated left ventricular (LV) hypertrophy to heart failure, paralleled by reduced oxidative stress due to restored glutathione levels and reduced MDA [265]. Giam et al. demonstrated that NAC could blunt cardiac fibrosis and related remodeling in the setting of heart failure, in mice with cardiomyopathy secondary to the cardiac-specific overexpression of mammalian sterile 20-like kinase 1, and this effect was ascribed to reduced oxidative stress [266].

In addition, NAC has also been proposed for the treatment of atherosclerosis. In *in vitro* studies, NAC inhibits lipoxidation- and oxidized LDL-induced endoplasmic reticulum (ER) stress in human endothelial cells implicated in atherogenesis [267]. Moreover, Cui et al. demonstrated that NAC attenuates atherosclerosis and reduces LDL oxidation in a mouse model of atherosclerosis represented by LDL receptor knockout mice. This effect was also evidenced *in vivo* in patients with coronary artery disease in which oxidized LDL, and not native LDL, were reduced by NAC [268]. Moreover, in ApoE deficient mice, NAC was able to induce atherosclerotic plaque stabilization [269].

Among the monoreactive nitrogen-containing compounds, an important role is played by the hydrazine derivatives, which react both with α,β-unsaturated aldehydes and dicarbonyls, even if with low selectivity. This category includes several well-established vasodilators, such as hydralazine, used as antihypertensive drugs, all with an excellent scavenging activity. Thus, several studies have been designed to evaluate the effects of their scavenging activity in oxidative stress-based diseases; for example, many hydrazine derivatives can reduce atherosclerotic lesion development through the carbonyl stress inhibition [270,271]. In particular, Vindis et al. demonstrated that hydralazine traps 4-HNE and reduces the formation of 4-HNE adducts on the platelet-derived growth factor receptor-β (PDGFβ) in smooth muscle cells treated *in vitro* with oxidized LDL. Moreover, this effect was also evidenced *in vivo* in hypercholesterolemic rabbits. Indeed, accumulation of 4-HNE-adducts on PDGFβ was increased in the aorta of hypercholesterolemic rabbits in comparison with normocholesterolemic rabbits, but hydralazine was able to reduce them, mainly in the intima, with a concomitant reduction of the extension of the atherosclerotic plaque [272].

Similarly, aminoguanidine reduces modifications of LDL induced by MDA, thereby preventing macrophage uptake and degradation of oxidized LDL [273], even if this protective effect could be also ascribed to the antioxidant properties of aminoguanidine, not only to its activity as RCS quencher [112].

Pyridoxamine (PM), one of the three natural forms of vitamin B6, is another carbonyl quencher known to prevent the formation of both ALEs and AGEs in various biological systems [112]. Several studies reported that PM can trap lipid peroxidation intermediates, thus reducing the chemical modifications of proteins exerted by peroxidizing agents, *in vitro* but also *in vivo* [274–276]. It has been demonstrated that PM can react with products of lipid peroxidation via its benzoyl amino group, and completely prevented the modifications of lysine residues on the RNase treated with arachidonic acid, and on LDL in a model of copper-catalyzed oxidation [275]. These effects have been ascribed to the ability of PM to intercept early lipid peroxidation products, precursors of reactive carbonyl groups involved in the formation of ALEs [275,276]. In addition, Kang et al. showed that PM interferes with the lipid peroxidation damage directly trapping MDA, under physiological conditions, as demonstrated by its ability to reduce the generation of lipofuscin-like fluorescence resulting from the incubation of MDA with bovine serum albumin [274]. More recently, Lee et al. compared the reaction of PM with ONE and 4-HNE and its effects on lysine modifications on human serum albumin exerted by the two lipid hydroperoxide-derived aldehydes. They demonstrated that the formation of adducts of PM with ONE is preferred, and that albumin modified by ONE, but not by 4-HNE, was decreased by treatment with PM [277]. Protective effects of PM have also been demonstrated in insulin-

secreting cells exposed *in vitro* to NO, where PM was able to inhibit NO-induced apoptosis through the inhibition of ALEs formation and carbonylation of poly (ADP-ribose) polymerase [278]. Finally, PM could also reduce AGE/ALEs formation *in vivo,* in streptozotocin-diabetic rats and in non-diabetic Zucker obese rats, with a consequent reduction of hyperlipidemia and protection against renal and vascular complications [279,280].

Carnosine, a polyreactive quencher, is a dipeptide of β-alanine and His, characterized by a strong antioxidant capacity due to metal ion chelation and RCS scavenging properties. These effects were demonstrated *in vitro* and *in vivo*, both in physiological conditions and in animal models of oxidative stress [281]. Several studies report the ability of carnosine to prevent ALEs formation induced by different precursors, including MDA [282]. It has been demonstrated that carnosine can directly bind to α,β-unsaturated aldehydes, such as 4-HNE [283], acrolein [284] and MDA [285]. Recently, Vistoli et al. evaluated also the quenching activity of carnosine and some of its derivatives towards MDA and methylglyoxal, and demonstrated that derivatives are more reactive with MDA than with methylglyoxal [285]. The quenching activity of carnosine towards 4-HNE have also been demonstrated *in vivo* in Zucker obese rat [286]. Therapeutic use of carnosine and its analogs have been tested in several pathological states, from cancer to Alzheimer's and cardiovascular disease, ischemia or diabetic complications, as previously summarized in the review by Boldyrev et al. [281].

Of note, a recent paper demonstrated the therapeutic value of a carnosinase-resistant analog, carnosinol, which displayed a higher potency and selectivity toward α,β-unsaturated aldehydes (e.g. 4-HNE, ACR) and reduced 4-HNE adduct formation in rodent models of obesity and metabolic syndrome [287]. Of note, Menini et al. showed that D-carnosine was able to protect, *in vitro,* smooth muscle cells from 4-HNE-induced injury and, to reduce, *in vivo*, atherosclerosis, in a mouse model of ApoE null mice fed with a Western diet [288].

6.2. Other therapeutic strategies

Once ALEs are formed, alternative strategies could be employed to reduce their effects, by enhancing, for example, their catabolism or by acting on ALE-induced biological responses, as already widely demonstrated for AGEs [252].

Degradation of ALEs and, in particular, of 4-HNE-modified proteins, has been mainly ascribed to a proteasome-dependent process, even if 4-HNE-protein adducts could form cross-linked aggregates able to inhibit the proteasome system, thus impairing their cellular turnover [289]. Few studies reported alternative ways of degradation based on lysosomal degradation or protease activity [13]. Of note, the above-described RCS quencher carnosine has been shown to react directly with ALEs leading to the formation of carbonyl-carnosine adducts and, thus, reducing crosslinking of oxidized proteins with other unmodified proteins, such as the proteasome components [281,282]. Proteasome activation could also be linked to the ability of carnosine to modulate release, metabolism, and activity of nitric oxide, a known activator of proteasome activity [281].

On the other hand, concerning the possibility of acting on the biological responses raised by ALEs, the extensive knowledge on the role of LDL oxidation in the atherosclerotic process led to the development of MDA-modified homologous LDL (MDA-LDL), able to exert atheroprotective effects in rabbits and mice [148]. More recently, Gonen et al. demonstrated that also small immunogens generated from the condensation of two or more MDA molecules with lysine could lead to atheroprotective responses; therefore, they have been proposed to generate a vaccine to retard or even prevent the development of atherosclerosis [290]. Recent studies suggest also that inactivation of oxPLs with modified forms of E06 antibody could reduce the inflammatory state associated with atherosclerosis [46].

7. Lipid peroxidation in clinical studies

Several oxidative biomarkers are currently measured in research laboratories, but they are not yet used as routine assays in clinical laboratories because of their uncertain diagnostic value [291,292]. The clinical applicability of several oxidative stress markers is influenced by the fact that some protein modifications by excessive ROS have a direct effect on the function of target molecules, while other modifications just reflect the general local degree of oxidative stress [293]. Venous blood and urinary samples are the most commonly used in clinical practice, but sometimes the measurement in specific tissue or cell samples may give more precise information. Measurement of lipid peroxidation products may be a reliable marker, as long as it is characterized by high sensitivity, specificity, and reproducibility.

However, several clinical studies focused on the detection and quantitation of the main lipid peroxidation products are actually reported in the literature. One of the most important clinical studies that evaluated the predictive value of lipid hydroperoxides levels for adverse cardiovascular outcomes in patients with stable CAD was PREVENT (Prospective Randomized Evaluation of the Vascular Effects of Norvasc) Trial [294]. Circulating levels of 4-HNE bound to proteins, for example, were measured by GC-MS in ambulatory symptomatic heart failure patients and control subjects, along with other clinically- and biochemically-relevant parameters, such as other oxidative stress markers, total levels of fatty acids from all classes [295]. Few clinical studies documented also circulating plasma levels of MDA using the highly criticized TBARS method [198,200,296]. Urinary and plasma isoprostanes have been mostly promoted for the *in vivo* estimation of oxidative stress for human studies. Urinary and plasma 8-isoprostane levels were measured in patients scheduled for coronary angiography, in order to investigate their association with the presence and severity of CAD [297,298]. Moreover, a case-control study was performed to measure by LC-MS/MS systemic levels of multiple specific fatty acid oxidation products including F2-isoprostanes in CAD patients and subjects without CAD [299]. A larger case-control study also investigated the association between lipoprotein-associated phospholipase A(2) (Lp-PLA(2)) activity and CAD in relation to oxidative stress markers, in particular urinary 8-iso-PGF2α, in patients with angiographically confirmed CAD versus healthy controls [300]. Indexes of redox status have been also proposed evaluating the oxidative stress by using more than one criterion [301,302]. The OXY-SCORE is a global oxidative stress index, computed by subtracting the protection score (GSH, alpha- and gamma-tocopherol levels, and antioxidant capacity) from the damage score (plasma free and total MDA, GSSG/GSH ratio, and urine F2-IsoPs). Its good performance was demonstrated in CAD patients versus healthy subjects, and the OXY-SCORE was significantly higher in CAD after adjusting for age, gender and smoking [303]. Similarly, Oxidative-INDEX reflects both oxidative and antioxidant counterparts [302].

8. Conclusions

Lipid peroxidation products represent a broad category of highly reactive compounds that exert many biological effects due to direct activation of signaling pathways or modification of other macromolecules, including nucleic acids, phospholipids or proteins.

Their involvement in the context of cardiovascular diseases has been mainly associated with the oxidation of circulating lipoprotein and the role of oxidized LDL in atherosclerosis. However, the heart is a highly oxidative organ in which cardiomyocyte turnover is virtually absent, making it particularly vulnerable to the accumulation of lipid peroxidation products formed as a result of oxidative damage.

Technological advances, mainly in the field of mass spectrometry, allowed overcoming the challenges in the detection, characterization, and quantitation of such complex heterogeneous class of lipid modifications.

Thanks to the expanding knowledge of the products and sources of lipid peroxidation and ALEs formation, several therapeutic strategies have been proposed and successfully applied to different oxidative-based diseases. However, a deeper understanding of the mechanisms of formation and targets of ALEs could expand the available therapeutic strategies. Indeed, it is clear that antioxidants can be used to reduce ALEs formation, but cannot neutralize the effects of ALEs when adducts are already formed, and this aspect could explain why *in vitro* or pre-clinical efficacy of antioxidant treatment is not always confirmed *in vivo,* in human patients.

Declaration of interest

None.

Funding

This work was supported by the European Union's Horizon 2020 research and innovation programme under the Marie Sklodowska-Curie (grant agreement number 675132) and by the Italian Ministry of Health, Rome, Italy (Ricerca Corrente 2018 ID 2634609).

Appendix A. Supplementary data

Supplementary data to this article can be found online at https://doi.org/10.1016/j.redox.2019.101119.

References

[1] T. Shibata, K. Shimizu, K. Hirano, et al., Adductome-based identification of biomarkers for lipid peroxidation, J. Biol. Chem. 292 (2017) 8223–8235.
[2] A. Ayala, M.F. Munoz, S. Arguelles, Lipid peroxidation: production, metabolism, and signaling mechanisms of malondialdehyde and 4-hydroxy-2-nonenal, Oxid. Med. Cell Longev. 2014 (2014) 360438.
[3] S.H. Lee, I.A. Blair, Characterization of 4-oxo-2-nonenal as a novel product of lipid peroxidation, Chem. Res. Toxicol. 13 (2000) 698–702.
[4] K.A. Massey, A. Nicolaou, Lipidomics of oxidized polyunsaturated fatty acids, Free Radic. Biol. Med. 59 (2013) 45–55.
[5] G. Vistoli, D. De Maddis, A. Cipak, et al., Advanced glycoxidation and lipoxidation end products (AGEs and ALEs): an overview of their mechanisms of formation, Free Radic. Res. 47 (Suppl 1) (2013) 3–27.
[6] E. Miller, A. Morel, L. Saso, et al., Isoprostanes and neuroprostanes as biomarkers of oxidative stress in neurodegenerative diseases, Oxid. Med. Cell Longev. 2014 (2014) 572491.
[7] R. Pamplona, Advanced lipoxidation end-products, Chem. Biol. Interact. 192 (2011) 14–20.
[8] X. Wei, H. Yin, Covalent modification of DNA by alpha, beta-unsaturated aldehydes derived from lipid peroxidation: recent progress and challenges, Free Radic. Res. 49 (2015) 905–917.
[9] A. Naudi, M. Jove, V. Ayala, et al., Non-enzymatic modification of aminophospholipids by carbonyl-amine reactions, Int. J. Mol. Sci. 14 (2013) 3285–3313.
[10] R.M. Domingues, P. Domingues, T. Melo, et al., Lipoxidation adducts with peptides and proteins: deleterious modifications or signaling mechanisms? J. Proteom. 92 (2013) 110–131.
[11] S. Lee, K.G. Birukov, C.E. Romanoski, et al., Role of phospholipid oxidation products in atherosclerosis, Circ. Res. 111 (2012) 778–799.
[12] M.X. Fu, J.R. Requena, A.J. Jenkins, et al., The advanced glycation end product, Nepsilon-(carboxymethyl)lysine, is a product of both lipid peroxidation and glycoxidation reactions, J. Biol. Chem. 271 (1996) 9982–9986.
[13] J.P. Castro, T. Jung, T. Grune, et al., 4-Hydroxynonenal (HNE) modified proteins in metabolic diseases, Free Radic. Biol. Med. 111 (2017) 309–315.
[14] A. Hohn, T. Grune, Lipofuscin: formation, effects and role of macroautophagy, Redox Biol. 1 (2013) 140–144.
[15] R.J. Schaur, Basic aspects of the biochemical reactivity of 4-hydroxynonenal, Mol. Aspect. Med. 24 (2003) 149–159.
[16] W.H. Zhang, J. Liu, G. Xu, et al., Model studies on protein side chain modification by 4-oxo-2-nonenal, Chem. Res. Toxicol. 16 (2003) 512–523.
[17] T. Maeshima, K. Honda, M. Chikazawa, et al., Quantitative analysis of acrolein-specific adducts generated during lipid peroxidation-modification of proteins in vitro: identification of N(tau)-(3-propanal)histidine as the major adduct, Chem. Res. Toxicol. 25 (2012) 1384–1392.
[18] D. Del Rio, A.J. Stewart, N. Pellegrini, A review of recent studies on malondialdehyde as toxic molecule and biological marker of oxidative stress, Nutr. Metabol. Cardiovasc. Dis. 15 (2005) 316–328.
[19] L.J. Roberts 2nd, G.L. Milne, Isoprostanes, J. Lipid Res. 50 (Suppl) (2009) S219–S223.
[20] J.D. Morrow, K.E. Hill, R.F. Burk, et al., A series of prostaglandin F2-like compounds are produced in vivo in humans by a non-cyclooxygenase, free radical-catalyzed mechanism, Proc. Natl. Acad. Sci. U. S. A. 87 (1990) 9383–9387.
[21] Z. Mallat, I. Philip, M. Lebret, et al., Elevated levels of 8-iso-prostaglandin F2alpha in pericardial fluid of patients with heart failure: a potential role for in vivo oxidant stress in ventricular dilatation and progression to heart failure, Circulation 97 (1998) 1536–1539.
[22] H.C. Yen, T.W. Chen, T.C. Yang, et al., Levels of F2-isoprostanes, F4-neuroprostanes, and total nitrate/nitrite in plasma and cerebrospinal fluid of patients with traumatic brain injury, Free Radic. Res. 49 (2015) 1419–1430.
[23] R. Bartova, D. Petrlenicova, K. Oresanska, et al., Changes in levels of oxidative stress markers and some neuronal enzyme activities in cerebrospinal fluid of multiple sclerosis patients, Neuroendocrinol. Lett. 37 (2016) 102–106.
[24] Y. Chen, J.D. Morrow, L.J. Roberts 2nd, Formation of reactive cyclopentenone compounds in vivo as products of the isoprostane pathway, J. Biol. Chem. 274 (1999) 10863–10868.
[25] G.L. Milne, G. Zanoni, A. Porta, et al., The cyclopentenone product of lipid peroxidation, 15-A2t-isoprostane, is efficiently metabolized by HepG2 cells via conjugation with glutathione, Chem. Res. Toxicol. 17 (2004) 17–25.
[26] J.M. Galano, J.C. Lee, C. Gladine, et al., Non-enzymatic cyclic oxygenated metabolites of adrenic, docosahexaenoic, eicosapentaenoic and alpha-linolenic acids; bioactivities and potential use as biomarkers, Biochim. Biophys. Acta 1851 (2015) 446–455.
[27] M. VanRollins, R.L. Woltjer, H. Yin, et al., F2-dihomo-isoprostanes arise from free radical attack on adrenic acid, J. Lipid Res. 49 (2008) 995–1005.
[28] R.G. Salomon, E. Batyreva, K. Kaur, et al., Isolevuglandin-protein adducts in humans: products of free radical-induced lipid oxidation through the isoprostane pathway, Biochim. Biophys. Acta 1485 (2000) 225–235.
[29] H. Yin, N.A. Porter, New insights regarding the autoxidation of polyunsaturated fatty acids, Antioxidants Redox Signal. 7 (2005) 170–184.
[30] J.P. Fessel, L. Jackson Roberts, Isofurans: novel products of lipid peroxidation that define the occurrence of oxidant injury in settings of elevated oxygen tension, Antioxidants Redox Signal. 7 (2005) 202–209.
[31] G.O. Fruhwirth, A. Loidl, A. Hermetter, Oxidized phospholipids: from molecular properties to disease, Biochim. Biophys. Acta 1772 (2007) 718–736.
[32] S. Parthasarathy, D. Steinberg, J.L. Witztum, The role of oxidized low-density lipoproteins in the pathogenesis of atherosclerosis, Annu. Rev. Med. 43 (1992) 219–225.
[33] M. Khazaei, F. Moien-Afshari, I. Laher, Vascular endothelial function in health and diseases, Pathophysiology 15 (2008) 49–67.
[34] A. Sandoo, J.J. van Zanten, G.S. Metsios, et al., The endothelium and its role in regulating vascular tone, Open Cardiovasc. Med. J. 4 (2010) 302–312.
[35] K.H. Park, W.J. Park, Endothelial dysfunction: clinical implications in cardiovascular disease and therapeutic approaches, J. Kor. Med. Sci. 30 (2015) 1213–1225.
[36] P.O. Bonetti, L.O. Lerman, A. Lerman, Endothelial dysfunction: a marker of atherosclerotic risk, Arterioscler. Thromb. Vasc. Biol. 23 (2003) 168–175.
[37] S. Xu, S. Ogura, J. Chen, et al., LOX-1 in atherosclerosis: biological functions and pharmacological modifiers, Cell. Mol. Life Sci. 70 (2013) 2859–2872.
[38] R. Yoshimoto, Y. Fujita, A. Kakino, et al., The discovery of LOX-1, its ligands and clinical significance, Cardiovasc. Drugs Ther. 25 (2011) 379–391.
[39] A.J. Murphy, K.J. Woollard, High-density lipoprotein: a potent inhibitor of inflammation, Clin. Exp. Pharmacol. Physiol. 37 (2010) 710–718.
[40] B.A. Kingwell, M.J. Chapman, A. Kontush, et al., HDL-targeted therapies: progress, failures and future, Nat. Rev. Drug Discov. 13 (2014) 445–464.
[41] J.L. Martin-Ventura, R. Rodrigues-Diez, D. Martinez-Lopez, et al., Oxidative stress in human atherothrombosis: sources, markers and therapeutic targets, Int. J. Mol. Sci. 18 (2017) pii: E2315.
[42] E. Malle, G. Marsche, J. Arnhold, et al., Modification of low-density lipoprotein by myeloperoxidase-derived oxidants and reagent hypochlorous acid, Biochim. Biophys. Acta 1761 (2006) 392–415.
[43] A.M. Fogelman, I. Shechter, J. Seager, et al., Malondialdehyde alteration of low density lipoproteins leads to cholesteryl ester accumulation in human monocyte-macrophages, Proc. Natl. Acad. Sci. U. S. A. 77 (1980) 2214–2218.
[44] H.N. Yassine, A.M. Jackson, P.D. Reaven, et al., The application of multiple reaction monitoring to assess Apo A-I methionine oxidations in diabetes and cardiovascular disease, Transl. Proteom. 4–5 (2014) 18–24.
[45] S. Horkko, D.A. Bird, E. Miller, et al., Monoclonal autoantibodies specific for oxidized phospholipids or oxidized phospholipid-protein adducts inhibit macrophage uptake of oxidized low-density lipoproteins, J. Clin. Invest. 103 (1999) 117–128.
[46] X. Que, M.Y. Hung, C. Yeang, et al., Oxidized phospholipids are proinflammatory and proatherogenic in hypercholesterolaemic mice, Nature 558 (2018) 301–306.
[47] S.P. Forbes, L.J. Druhan, J.E. Guzman, et al., Mechanism of 4-HNE mediated inhibition of hDDAH-1: implications in no regulation, Biochemistry 47 (2008) 1819–1826.
[48] T. Okada, K. Morino, F. Nakagawa, et al., N-3 polyunsaturated fatty acids decrease the protein expression of soluble epoxide hydrolase via oxidative stress-induced P38 kinase in rat endothelial cells, Nutrients 9 (2017).
[49] Y.X. Wang, A. Ulu, L.N. Zhang, et al., Soluble epoxide hydrolase in atherosclerosis, Curr. Atheroscler. Rep. 12 (2010) 174–183.
[50] A. Ishikado, K. Morino, Y. Nishio, et al., 4-Hydroxy hexenal derived from docosahexaenoic acid protects endothelial cells via Nrf2 activation, PLoS One 8 (2013) e69415.
[51] G. Leonarduzzi, P. Gamba, S. Gargiulo, et al., Inflammation-related gene expression by lipid oxidation-derived products in the progression of atherosclerosis, Free Radic. Biol. Med. 52 (2012) 19–34.
[52] N. Shanmugam, J.L. Figarola, Y. Li, et al., Proinflammatory effects of advanced

lipoxidation end products in monocytes, Diabetes 57 (2008) 879–888.
[53] L.J. van Tits, R. Stienstra, P.L. van Lent, et al., Oxidized LDL enhances pro-inflammatory responses of alternatively activated M2 macrophages: a crucial role for Kruppel-like factor 2, Atherosclerosis 214 (2011) 345–349.
[54] C.E. Kim, S.J. Lee, K.W. Seo, et al., Acrolein increases 5-lipoxygenase expression in murine macrophages through activation of ERK pathway, Toxicol. Appl. Pharmacol. 245 (2010) 76–82.
[55] T.E. OToole, Y.T. Zheng, J. Hellmann, et al., Acrolein activates matrix metalloproteinases by increasing reactive oxygen species in macrophages, Toxicol. Appl. Pharmacol. 236 (2009) 194–201.
[56] A. Moghe, S. Ghare, B. Lamoreau, et al., Molecular mechanisms of acrolein toxicity: relevance to human disease, Toxicol. Sci. 143 (2015) 242–255.
[57] A.C. Schrimpe-Rutledge, K.Y. Fong, D.W. Wright, Impact of 4-hydroxynonenal on matrix metalloproteinase-9 regulation in lipopolysaccharide-stimulated RAW 264.7 cells, Cell Biochem. Funct. 33 (2015) 59–66.
[58] S.J. Lee, K.W. Seo, M.R. Yun, et al., 4-Hydroxynonenal enhances MMP-2 production in vascular smooth muscle cells via mitochondrial ROS-mediated activation of the Akt/NF-kappaB signaling pathways, Free Radic. Biol. Med. 45 (2008) 1487–1492.
[59] S. Akiba, S. Kumazawa, H. Yamaguchi, et al., Acceleration of matrix metalloproteinase-1 production and activation of platelet-derived growth factor receptor beta in human coronary smooth muscle cells by oxidized LDL and 4-hydroxynonenal, Biochim. Biophys. Acta 1763 (2006) 797–804.
[60] R. Vatsyayan, H. Kothari, U.R. Pendurthi, et al., 4-Hydroxy-2-nonenal enhances tissue factor activity in human monocytic cells via p38 mitogen-activated protein kinase activation-dependent phosphatidylserine exposure, Arterioscler. Thromb. Vasc. Biol. 33 (2013) 1601–1611.
[61] T.J. Lee, J.T. Lee, S.K. Moon, et al., Age-related differential growth rate and response to 4-hydroxynonenal in mouse aortic smooth muscle cells, Int. J. Mol. Med. 17 (2006) 29–35.
[62] T. Munzel, G.G. Camici, C. Maack, et al., Impact of oxidative stress on the heart and vasculature: part 2 of a 3-part series, J. Am. Coll. Cardiol. 70 (2017) 212–229.
[63] T.J. Guzik, J. Sadowski, B. Kapelak, et al., Systemic regulation of vascular NAD(P)H oxidase activity and nox isoform expression in human arteries and veins, Arterioscler. Thromb. Vasc. Biol. 24 (2004) 1614–1620.
[64] R. Stocker, J.F. Keaney Jr., New insights on oxidative stress in the artery wall, J. Thromb. Haemostasis 3 (2005) 1825–1834.
[65] K. Zarkovic, P. Larroque-Cardoso, M. Pucelle, et al., Elastin aging and lipid oxidation products in human aorta, Redox Biol. 4 (2015) 109–117.
[66] V.M. Subbotin, Neovascularization of coronary tunica intima (DIT) is the cause of coronary atherosclerosis. Lipoproteins invade coronary intima via neovascularization from adventitial vasa vasorum, but not from the arterial lumen: a hypothesis, Theor. Biol. Med. Model. 9 (2012) 11.
[67] P. Larroque-Cardoso, E. Mucher, M.H. Grazide, et al., 4-Hydroxynonenal impairs transforming growth factor-beta1-induced elastin synthesis via epidermal growth factor receptor activation in human and murine fibroblasts, Free Radic. Biol. Med. 71 (2014) 427–436.
[68] S.J. Lee, C.E. Kim, M.R. Yun, et al., 4-Hydroxynonenal enhances MMP-9 production in murine macrophages via 5-lipoxygenase-mediated activation of ERK and p38 MAPK, Toxicol. Appl. Pharmacol. 242 (2010) 191–198.
[69] S.C. Kolwicz Jr., S. Purohit, R. Tian, Cardiac metabolism and its interactions with contraction, growth, and survival of cardiomyocytes, Circ. Res. 113 (2013) 603–616.
[70] G.D. Lopaschuk, J.R. Ussher, C.D. Folmes, et al., Myocardial fatty acid metabolism in health and disease, Physiol. Rev. 90 (2010) 207–258.
[71] N. Fillmore, J. Mori, G.D. Lopaschuk, Mitochondrial fatty acid oxidation alterations in heart failure, ischaemic heart disease and diabetic cardiomyopathy, Br. J. Pharmacol. 171 (2014) 2080–2090.
[72] H.C. Chiu, A. Kovacs, R.M. Blanton, et al., Transgenic expression of fatty acid transport protein 1 in the heart causes lipotoxic cardiomyopathy, Circ. Res. 96 (2005) 225–233.
[73] B.N. Finck, J.J. Lehman, T.C. Leone, et al., The cardiac phenotype induced by PPARalpha overexpression mimics that caused by diabetes mellitus, J. Clin. Invest. 109 (2002) 121–130.
[74] K. Watanabe, H. Fujii, T. Takahashi, et al., Constitutive regulation of cardiac fatty acid metabolism through peroxisome proliferator-activated receptor alpha associated with age-dependent cardiac toxicity, J. Biol. Chem. 275 (2000) 22293–22299.
[75] E.M. Burkart, N. Sambandam, X. Han, et al., Nuclear receptors PPARbeta/delta and PPARalpha direct distinct metabolic regulatory programs in the mouse heart, J. Clin. Invest. 117 (2007) 3930–3939.
[76] T. Shiraki, N. Kamiya, S. Shiki, et al., Alpha,beta-unsaturated ketone is a core moiety of natural ligands for covalent binding to peroxisome proliferator-activated receptor gamma, J. Biol. Chem. 280 (2005) 14145–14153.
[77] T. Itoh, L. Fairall, K. Amin, et al., Structural basis for the activation of PPARgamma by oxidized fatty acids, Nat. Struct. Mol. Biol. 15 (2008) 924–931.
[78] V. Benedusi, F. Martorana, L. Brambilla, et al., The peroxisome proliferator-activated receptor gamma (PPARgamma) controls natural protective mechanisms against lipid peroxidation in amyotrophic lateral sclerosis, J. Biol. Chem. 287 (2012) 35899–35911.
[79] B.N. Finck, D.P. Kelly, Peroxisome proliferator-activated receptor gamma coactivator-1 (PGC-1) regulatory cascade in cardiac physiology and disease, Circulation 115 (2007) 2540–2548.
[80] B.Y. Nguyen, A. Ruiz-Velasco, T. Bui, et al., Mitochondrial function in the heart: the insight into mechanisms and therapeutic potentials, Br. J. Pharmacol. (2018) PMID: 29968316.
[81] E.J. Anderson, L.A. Katunga, M.S. Willis, Mitochondria as a source and target of lipid peroxidation products in healthy and diseased heart, Clin. Exp. Pharmacol. Physiol. 39 (2012) 179–193.
[82] A.J. Chicco, G.C. Sparagna, Role of cardiolipin alterations in mitochondrial dysfunction and disease, Am. J. Physiol. Cell Physiol. 292 (2007) C33–C44.
[83] J. Luo, B.G. Hill, Y. Gu, et al., Mechanisms of acrolein-induced myocardial dysfunction: implications for environmental and endogenous aldehyde exposure, Am. J. Physiol. Heart Circ. Physiol. 293 (2007) H3673–H3684.
[84] Z. Wu, E.Y. He, G.I. Scott, et al., alpha,beta-Unsaturated aldehyde pollutant acrolein suppresses cardiomyocyte contractile function: role of TRPV1 and oxidative stress, Environ. Toxicol. 30 (2015) 638–647.
[85] H.H. Refsgaard, L. Tsai, E.R. Stadtman, Modifications of proteins by polyunsaturated fatty acid peroxidation products, Proc. Natl. Acad. Sci. U. S. A. 97 (2000) 611–616.
[86] M. Glei, A. Schaeferhenrich, U. Claussen, et al., Comet fluorescence in situ hybridization analysis for oxidative stress-induced DNA damage in colon cancer relevant genes, Toxicol. Sci. 96 (2007) 279–284.
[87] A.G. Baker, D. Wiesler, M.V. Novotny, Tandem mass spectrometry of model peptides modified with trans-2-hexenal, a product of lipid peroxidation, J. Am. Soc. Mass Spectrom. 10 (1999) 613–624.
[88] P. Ping, C.P. Baines, Y. Gu, et al., Cardiac toxic effects of trans-2-hexenal are mediated by induction of cardiomyocyte apoptotic pathways, Cardiovasc. Toxicol. 3 (2003) 341–351.
[89] K. Uchida, 4-Hydroxy-2-nonenal: a product and mediator of oxidative stress, Prog. Lipid Res. 42 (2003) 318–343.
[90] S.J. Chapple, X. Cheng, G.E. Mann, Effects of 4-hydroxynonenal on vascular endothelial and smooth muscle cell redox signaling and function in health and disease, Redox Biol. 1 (2013) 319–331.
[91] Y. Zhang, M. Sano, K. Shinmura, et al., 4-hydroxy-2-nonenal protects against cardiac ischemia-reperfusion injury via the Nrf2-dependent pathway, J. Mol. Cell. Cardiol. 49 (2010) 576–586.
[92] E. Lopez-Bernardo, A. Anedda, P. Sanchez-Perez, et al., 4-Hydroxynonenal induces Nrf2-mediated UCP3 upregulation in mouse cardiomyocytes, Free Radic. Biol. Med. 88 (2015) 427–438.
[93] E. Nagy, A.L. Jermendy, B. Merkely, et al., Clinical importance of epicardial adipose tissue, Arch. Med. Sci. 13 (2017) 864–874.
[94] R. Li, W.Q. Wang, H. Zhang, et al., Adiponectin improves endothelial function in hyperlipidemic rats by reducing oxidative/nitrative stress and differential regulation of eNOS/iNOS activity, Am. J. Physiol. Endocrinol. Metab. 293 (2007) E1703–E1708.
[95] H.S. Sacks, J.N. Fain, Human epicardial adipose tissue: a review, Am. Heart J. 153 (2007) 907–917.
[96] A. Salgado-Somoza, E. Teijeira-Fernandez, A.L. Fernandez, et al., Proteomic analysis of epicardial and subcutaneous adipose tissue reveals differences in proteins involved in oxidative stress, Am. J. Physiol. Heart Circ. Physiol. 299 (2010) H202–H209.
[97] B. Demir, E. Demir, G. Aciksari, et al., The association between the epicardial adipose tissue thickness and oxidative stress parameters in isolated metabolic syndrome patients: a multimarker approach, Int. J. Endocrinol. 2014 (2014) 954045.
[98] H.E. Bays, Adiposopathy is "sick fat" a cardiovascular disease? J. Am. Coll. Cardiol. 57 (2011) 2461–2473.
[99] W. Shen, Z. Wang, M. Punyanita, et al., Adipose tissue quantification by imaging methods: a proposed classification, Obes. Res. 11 (2003) 5–16.
[100] S.B. Heymsfield, T.A. Wadden, Mechanisms, pathophysiology, and management of obesity, N. Engl. J. Med. 376 (2017) 1492.
[101] L.F. Van Gaal, I.L. Mertens, C.E. De Block, Mechanisms linking obesity with cardiovascular disease, Nature 444 (2006) 875–880.
[102] S.A. Ritchie, J.M. Connell, The link between abdominal obesity, metabolic syndrome and cardiovascular disease, Nutr. Metabol. Cardiovasc. Dis. 17 (2007) 319–326.
[103] S. Furukawa, T. Fujita, M. Shimabukuro, et al., Increased oxidative stress in obesity and its impact on metabolic syndrome, J. Clin. Invest. 114 (2004) 1752–1761.
[104] A.F. Soares, M. Guichardant, D. Cozzone, et al., Effects of oxidative stress on adiponectin secretion and lactate production in 3T3-L1 adipocytes, Free Radic. Biol. Med. 38 (2005) 882–889.
[105] G. Murdolo, M. Piroddi, F. Luchetti, et al., Oxidative stress and lipid peroxidation by-products at the crossroad between adipose organ dysregulation and obesity-linked insulin resistance, Biochimie 95 (2013) 585–594.
[106] S.P. Singh, M. Niemczyk, D. Saini, et al., Role of the electrophilic lipid peroxidation product 4-hydroxynonenal in the development and maintenance of obesity in mice, Biochemistry 47 (2008) 3900–3911.
[107] P.A. Grimsrud, M.J. Picklo, Sr, T.J. Griffin, et al., Carbonylation of adipose proteins in obesity and insulin resistance: identification of adipocyte fatty acid-binding protein as a cellular target of 4-hydroxynonenal, Mol. Cell. Proteomics 6 (2007) 624–637.
[108] F. Bost, M. Aouadi, L. Caron, et al., The role of MAPKs in adipocyte differentiation and obesity, Biochimie 87 (2005) 51–56.
[109] M.A. Elrayess, S. Almuraikhy, W. Kafienah, et al., 4-hydroxynonenal causes impairment of human subcutaneous adipogenesis and induction of adipocyte insulin resistance, Free Radic. Biol. Med. 104 (2017) 129–137.
[110] K.S. Echtay, T.C. Esteves, J.L. Pakay, et al., A signalling role for 4-hydroxy-2-nonenal in regulation of mitochondrial uncoupling, EMBO J. 22 (2003) 4103–4110.
[111] M. Csala, T. Kardon, B. Legeza, et al., On the role of 4-hydroxynonenal in health

and disease, Biochim. Biophys. Acta 1852 (2015) 826–838.
[112] A. Negre-Salvayre, C. Coatrieux, C. Ingueneau, et al., Advanced lipid peroxidation end products in oxidative damage to proteins. Potential role in diseases and therapeutic prospects for the inhibitors, Br. J. Pharmacol. 153 (2008) 6–20.
[113] Y.C. Awasthi, R. Sharma, A. Sharma, et al., Self-regulatory role of 4-hydroxynonenal in signaling for stress-induced programmed cell death, Free Radic. Biol. Med. 45 (2008) 111–118.
[114] C.M. Spickett, A.R. Pitt, Oxidative lipidomics coming of age: advances in analysis of oxidized phospholipids in physiology and pathology, Antioxidants Redox Signal. 22 (2015) 1646–1666.
[115] V. Serbulea, D. DeWeese, N. Leitinger, The effect of oxidized phospholipids on phenotypic polarization and function of macrophages, Free Radic. Biol. Med. 111 (2017) 156–168.
[116] L. Gros, A.A. Ishchenko, M. Saparbaev, Enzymology of repair of etheno-adducts, Mutat. Res. 531 (2003) 219–229.
[117] S.H. Lee, I.A. Blair, Oxidative DNA damage and cardiovascular disease, Trends Cardiovasc. Med. 11 (2001) 148–155.
[118] J. Nair, S. De Flora, A. Izzotti, et al., Lipid peroxidation-derived etheno-DNA adducts in human atherosclerotic lesions, Mutat. Res. 621 (2007) 95–105.
[119] R.J. Schaur, W. Siems, N. Bresgen, et al., 4-Hydroxy-nonenal-A bioactive lipid peroxidation product, Biomolecules 5 (2015) 2247–2337.
[120] M. Navab, S.T. Reddy, B.J. Van Lenten, et al., HDL and cardiovascular disease: atherogenic and atheroprotective mechanisms, Nat. Rev. Cardiol. 8 (2011) 222–232.
[121] A. Rossi, P. Kapahi, G. Natoli, et al., Anti-inflammatory cyclopentenone prostaglandins are direct inhibitors of IkappaB kinase, Nature 403 (2000) 103–108.
[122] D.S. Straus, G. Pascual, M. Li, et al., 15-deoxy-delta 12,14-prostaglandin J2 inhibits multiple steps in the NF-kappa B signaling pathway, Proc. Natl. Acad. Sci. U. S. A. 97 (2000) 4844–4849.
[123] E. Cernuda-Morollon, E. Pineda-Molina, F.J. Canada, et al., 15-Deoxy-Delta 12,14-prostaglandin J2 inhibition of NF-kappaB-DNA binding through covalent modification of the p50 subunit, J. Biol. Chem. 276 (2001) 35530–35536.
[124] T. Shiraki, N. Kamiya, H. Jingami, [Activation mechanism of PPARgamma by its endogenous ligands], Tanpakushitsu Kakusan Koso 50 (2005) 1660–1665.
[125] F. Lopez-Jimenez, M. Cortes-Bergoderi, Update: systemic diseases and the cardiovascular system (i): obesity and the heart, Rev. Esp. Cardiol. 64 (2011) 140–149.
[126] S. Pennathur, J.W. Heinecke, Mechanisms for oxidative stress in diabetic cardiovascular disease, Antioxidants Redox Signal. 9 (2007) 955–969.
[127] M.P. Mattson, Roles of the lipid peroxidation product 4-hydroxynonenal in obesity, the metabolic syndrome, and associated vascular and neurodegenerative disorders, Exp. Gerontol. 44 (2009) 625–633.
[128] H.K. Vincent, S.K. Powers, A.J. Dirks, et al., Mechanism for obesity-induced increase in myocardial lipid peroxidation, Int. J. Obes. Relat. Metab. Disord. 25 (2001) 378–388.
[129] X. Zhang, Z. Wang, J. Li, et al., Increased 4-hydroxynonenal formation contributes to obesity-related lipolytic activation in adipocytes, PLoS One 8 (2013) e70663.
[130] A.L. Kennedy, T.J. Lyons, Glycation, oxidation, and lipoxidation in the development of diabetic complications, Metabolism 46 (1997) 14–21.
[131] M. Brownlee, H. Vlassara, A. Cerami, Nonenzymatic glycosylation products on collagen covalently trap low-density lipoprotein, Diabetes 34 (1985) 938–941.
[132] A. Mezzetti, F. Cipollone, F. Cuccurullo, Oxidative stress and cardiovascular complications in diabetes: isoprostanes as new markers on an old paradigm, Cardiovasc. Res. 47 (2000) 475–488.
[133] R. Bucala, Z. Makita, G. Vega, et al., Modification of low density lipoprotein by advanced glycation end products contributes to the dyslipidemia of diabetes and renal insufficiency, Proc. Natl. Acad. Sci. U. S. A. 91 (1994) 9441–9445.
[134] C.B. Afonso, B.C. Sousa, A.R. Pitt, et al., A mass spectrometry approach for the identification and localization of small aldehyde modifications of proteins, Arch. Biochem. Biophys. 646 (2018) 38–45.
[135] D. Tsikas, Assessment of lipid peroxidation by measuring malondialdehyde (MDA) and relatives in biological samples: analytical and biological challenges, Anal. Biochem. 524 (2017) 13–30.
[136] C.M. Spickett, The lipid peroxidation product 4-hydroxy-2-nonenal: advances in chemistry and analysis, Redox Biol. 1 (2013) 145–152.
[137] N. Vidal, J.P. Cavaille, F. Graziani, et al., High throughput assay for evaluation of reactive carbonyl scavenging capacity, Redox Biol. 2 (2014) 590–598.
[138] L.J. Yan, M.J. Forster, Chemical probes for analysis of carbonylated proteins: a review, J. Chromatogr. B Analyt Technol. Biomed. Life Sci. 879 (2011) 1308–1315.
[139] S. Zelzer, H. Mangge, R. Oberreither, et al., Oxidative stress: determination of 4-hydroxy-2-nonenal by gas chromatography/mass spectrometry in human and rat plasma, Free Radic. Res. 49 (2015) 1233–1238.
[140] S. Rauli, M.D. Puppo, F. Magni, et al., Validation of malondialdehyde and 4-hydroxy-2-trans-nonenal measurement in plasma by NICI-GC-MS, J. Biochem. 123 (1998) 918–923.
[141] D. Spies-Martin, O. Sommerburg, C.D. Langhans, et al., Measurement of 4-hydroxynonenal in small volume blood plasma samples: modification of a gas chromatographic-mass spectrometric method for clinical settings, J. Chromatogr. B Analyt Technol. Biomed. Life Sci. 774 (2002) 231–239.
[142] M. Golizeh, T. Geib, L. Sleno, Identification of 4-hydroxynonenal protein targets in rat, mouse and human liver microsomes by two-dimensional liquid chromatography/tandem mass spectrometry, Rapid Commun. Mass Spectrom. 30 (2016) 1488–1494.
[143] A.M. Gioacchini, N. Calonghi, C. Boga, et al., Determination of 4-hydroxy-2-nonenal at cellular levels by means of electrospray mass spectrometry, Rapid Commun. Mass Spectrom. 13 (1999) 1573–1579.
[144] M. Colzani, G. Aldini, M. Carini, Mass spectrometric approaches for the identification and quantification of reactive carbonyl species protein adducts, J. Proteom. 92 (2013) 28–50.
[145] M. Carini, G. Aldini, R.M. Facino, Mass spectrometry for detection of 4-hydroxy-trans-2-nonenal (HNE) adducts with peptides and proteins, Mass Spectrom. Rev. 23 (2004) 281–305.
[146] K. Zarkovic, A. Jakovcevic, N. Zarkovic, Contribution of the HNE-immunohistochemistry to modern pathological concepts of major human diseases, Free Radic. Biol. Med. 111 (2017) 110–126.
[147] S. Borovic, F. Rabuzin, G. Waeg, et al., Enzyme-linked immunosorbent assay for 4-hydroxynonenal-histidine conjugates, Free Radic. Res. 40 (2006) 809–820.
[148] W. Palinski, S. Yla-Herttuala, M.E. Rosenfeld, et al., Antisera and monoclonal antibodies specific for epitopes generated during oxidative modification of low density lipoprotein, Arteriosclerosis 10 (1990) 325–335.
[149] Q. Chen, H. Esterbauer, G. Jurgens, Studies on epitopes on low-density lipoprotein modified by 4-hydroxynonenal. Biochemical characterization and determination, Biochem. J. 288 (Pt 1) (1992) 249–254.
[150] K. Uchida, K. Itakura, S. Kawakishi, et al., Characterization of epitopes recognized by 4-hydroxy-2-nonenal specific antibodies, Arch. Biochem. Biophys. 324 (1995) 241–248.
[151] K. Itakura, T. Oya-Ito, T. Osawa, et al., Detection of lipofuscin-like fluorophore in oxidized human low-density lipoprotein. 4-hydroxy-2-nonenal as a potential source of fluorescent chromophore, FEBS Lett. 473 (2000) 249–253.
[152] C. Wakita, K. Honda, T. Shibata, et al., A method for detection of 4-hydroxy-2-nonenal adducts in proteins, Free Radic. Biol. Med. 51 (2011) 1–4.
[153] S. Liu, W. Hou, H. Qin, et al., Oxidized LDL stimulates lipid peroxidation-derived DNA and protein adducts in human vascular endothelial and smooth muscle cells, J. Huazhong Univ. Sci. Technol. Med. Sci. 35 (2015) 200–205.
[154] A. Arcaro, M. Daga, G.P. Cetrangolo, et al., Generation of adducts of 4-Hydroxy-2-nonenal with heat shock 60 kDa protein 1 in human promyelocytic HL-60 and monocytic THP-1 cell lines, Oxid. Med. Cell Longev. 2015 (2015) 296146.
[155] K. Uchida, L.I. Szweda, H.Z. Chae, et al., Immunochemical detection of 4-hydroxynonenal protein adducts in oxidized hepatocytes, Proc. Natl. Acad. Sci. U. S. A. 90 (1993) 8742–8746.
[156] D. Weber, L. Milkovic, S.J. Bennett, et al., Measurement of HNE-protein adducts in human plasma and serum by ELISA-Comparison of two primary antibodies, Redox Biol. 1 (2013) 226–233.
[157] J.A. Doorn, D.R. Petersen, Covalent modification of amino acid nucleophiles by the lipid peroxidation products 4-hydroxy-2-nonenal and 4-oxo-2-nonenal, Chem. Res. Toxicol. 15 (2002) 1445–1450.
[158] A. Vila, K.A. Tallman, A.T. Jacobs, et al., Identification of protein targets of 4-hydroxynonenal using click chemistry for ex vivo biotinylation of azido and alkynyl derivatives, Chem. Res. Toxicol. 21 (2008) 432–444.
[159] N. Rauniyar, L. Prokai, Isotope-coded dimethyl tagging for differential quantification of posttranslational protein carbonylation by 4-hydroxy-2-nonenal, an end-product of lipid peroxidation, J. Mass Spectrom. 46 (2011) 976–985.
[160] J.D. Chavez, J. Wu, W. Bisson, et al., Site-specific proteomic analysis of lipoxidation adducts in cardiac mitochondria reveals chemical diversity of 2-alkenal adduction, J. Proteom. 74 (2011) 2417–2429.
[161] J. Wu, X. Luo, L.J. Yan, Two dimensional blue native/SDS-PAGE to identify mitochondrial complex I subunits modified by 4-hydroxynonenal (HNE), Front. Physiol. 6 (2015) 98.
[162] A. Pecorelli, C. Cervellati, A. Cortelazzo, et al., Proteomic analysis of 4-hydroxynonenal and nitrotyrosine modified proteins in RTT fibroblasts, Int. J. Biochem. Cell Biol. 81 (2016) 236–245.
[163] R.C. Gupta, V. Singh-Gupta, K. Zhang, et al., Abstract 12949: elamipretide (BendaviaTM) restores 4-hydroxy-2-nonenal protein adducts and aldehyde dehydrogenase-2 activity and mRNA expression in left ventricular myocardium of dogs with advanced heart failure, Circulation 134 (2018) A12949.
[164] K.M. Gomes, J.C. Campos, L.R. Bechara, et al., Aldehyde dehydrogenase 2 activation in heart failure restores mitochondrial function and improves ventricular function and remodelling, Cardiovasc. Res. 103 (2014) 498–508.
[165] K. Nakamura, K. Kusano, Y. Nakamura, et al., Carvedilol decreases elevated oxidative stress in human failing myocardium, Circulation 105 (2002) 2867–2871.
[166] S. Mak, D.C. Lehotay, M. Yazdanpanah, et al., Unsaturated aldehydes including 4-OH-nonenal are elevated in patients with congestive heart failure, J. Card. Fail. 6 (2000) 108–114.
[167] M. Giera, H. Lingeman, W.M. Niessen, Recent advancements in the LC- and GC-based analysis of malondialdehyde (MDA): a brief overview, Chromatographia 75 (2012) 433–440.
[168] K. Yagi, A simple fluorometric assay for lipoperoxide in blood plasma, Biochem. Med. 15 (1976) 212–216.
[169] J.A. Knight, R.K. Pieper, L. McClellan, Specificity of the thiobarbituric acid reaction: its use in studies of lipid peroxidation, Clin. Chem. 34 (1988) 2433–2438.
[170] J.C. Cooley, C.E. Lunte, Detection of malondialdehyde in vivo using microdialysis sampling with CE-fluorescence, Electrophoresis 32 (2011) 2994–2999.
[171] R. Agarwal, S.D. Chase, Rapid, fluorimetric-liquid chromatographic determination of malondialdehyde in biological samples, J. Chromatogr. B Analyt Technol. Biomed. Life Sci. 775 (2002) 121–126.
[172] D. Del Rio, N. Pellegrini, B. Colombi, et al., Rapid fluorimetric method to detect total plasma malondialdehyde with mild derivatization conditions, Clin. Chem. 49 (2003) 690–692.
[173] J.Y. Sheu, H.P. Ku, W.C. Tseng, et al., Determination of thiobarbituric acid adduct of malondialdehyde using on-line microdialysis coupled with high-performance liquid chromatography, Anal. Sci. 19 (2003) 621–624.
[174] G.W. Cheng, H.L. Wu, Y.L. Huang, Automated on-line microdialysis sampling

coupled with high-performance liquid chromatography for simultaneous determination of malondialdehyde and ofloxacin in whole blood, Talanta 79 (2009) 1071–1075.
[175] D. Tsikas, S. Rothmann, J.Y. Schneider, et al., Development, validation and biomedical applications of stable-isotope dilution GC-MS and GC-MS/MS techniques for circulating malondialdehyde (MDA) after pentafluorobenzyl bromide derivatization: MDA as a biomarker of oxidative stress and its relation to 15(S)-8-iso-prostaglandin F2alpha and nitric oxide (NO), J. Chromatogr. B Analyt Technol. Biomed. Life Sci. 1019 (2016) 95–111.
[176] J. Pilz, I. Meineke, C.H. Gleiter, Measurement of free and bound malondialdehyde in plasma by high-performance liquid chromatography as the 2,4-dinitrophenylhydrazine derivative, J. Chromatogr. B Biomed. Sci. Appl. 742 (2000) 315–325.
[177] O. Korchazhkina, C. Exley, S. Andrew Spencer, Measurement by reversed-phase high-performance liquid chromatography of malondialdehyde in normal human urine following derivatisation with 2,4-dinitrophenylhydrazine, J. Chromatogr. B Analyt Technol. Biomed. Life Sci. 794 (2003) 353–362.
[178] S. Zelzer, R. Oberreither, C. Bernecker, et al., Measurement of total and free malondialdehyde by gas-chromatography mass spectrometry–comparison with high-performance liquid chromatography methology, Free Radic. Res. 47 (2013) 651–656.
[179] R. Malaei, A.M. Ramezani, G. Absalan, Analysis of malondialdehyde in human plasma samples through derivatization with 2,4-dinitrophenylhydrazine by ultrasound-assisted dispersive liquid-liquid microextraction-GC-FID approach, J. Chromatogr. B Analyt Technol. Biomed. Life Sci. 1089 (2018) 60–69.
[180] J. Mao, H. Zhang, J. Luo, et al., New method for HPLC separation and fluorescence detection of malonaldehyde in normal human plasma, J. Chromatogr. B Analyt Technol. Biomed. Life Sci. 832 (2006) 103–108.
[181] H.L. Lord, J. Rosenfeld, V. Volovich, et al., Determination of malondialdehyde in human plasma by fully automated solid phase analytical derivatization, J. Chromatogr. B Analyt Technol. Biomed. Life Sci. 877 (2009) 1292–1298.
[182] D. Gerard-Monnier, I. Erdelmeier, K. Regnard, et al., Reactions of 1-methyl-2-phenylindole with malondialdehyde and 4-hydroxyalkenals. Analytical applications to a colorimetric assay of lipid peroxidation, Chem. Res. Toxicol. 11 (1998) 1176–1183.
[183] Y.H. Siddique, G. Ara, M. Afzal, Estimation of lipid peroxidation induced by hydrogen peroxide in cultured human lymphocytes, Dose Response 10 (2012) 1–10.
[184] J.P. Steghens, A.L. van Kappel, I. Denis, et al., Diaminonaphtalene, a new highly specific reagent for HPLC-UV measurement of total and free malondialdehyde in human plasma or serum, Free Radic. Biol. Med. 31 (2001) 242–249.
[185] M. Giera, D.P. Kloos, A. Raaphorst, et al., Mild and selective labeling of malondialdehyde with 2-aminoacridone: assessment of urinary malondialdehyde levels, Analyst 136 (2011) 2763–2769.
[186] P. Manini, R. Andreoli, S. Sforza, et al., Evaluation of Alternate Isotope-Coded Derivatization Assay (AIDA) in the LC-MS/MS analysis of aldehydes in exhaled breath condensate, J. Chromatogr. B Analyt Technol. Biomed. Life Sci. 878 (2010) 2616–2622.
[187] M. Eggink, S. Charret, M. Wijtmans, et al., Development of an on-line weak-cation exchange liquid chromatography-tandem mass spectrometric method for screening aldehyde products in biological matrices, J. Chromatogr. B Analyt Technol. Biomed. Life Sci. 877 (2009) 3937–3945.
[188] L. Yu, P. Liu, Y.L. Wang, et al., Profiling of aldehyde-containing compounds by stable isotope labelling-assisted mass spectrometry analysis, Analyst 140 (2015) 5276–5286.
[189] L. Sangalli, L.M. Chiesa, E. Passero, et al., Improved procedure for the determination of malonaldehyde by gas-chromatography with electron-capture detection as 2,4,6-trichlorophenylhydrazine derivative, J. Chromatogr. B Analyt Technol. Biomed. Life Sci. 796 (2003) 201–207.
[190] H.S. Shin, Determination of malondialdehyde in human blood by headspace-solid phase micro-extraction gas chromatography-mass spectrometry after derivatization with 2,2,2-trifluoroethylhydrazine, J. Chromatogr. B Analyt Technol. Biomed. Life Sci. 877 (2009) 3707–3711.
[191] U. Dreissigacker, M.T. Suchy, N. Maassen, et al., Human plasma concentrations of malondialdehyde (MDA) and the F2-isoprostane 15(S)-8-iso-PGF(2alpha) may be markedly compromised by hemolysis: evidence by GC-MS/MS and potential analytical and biological ramifications, Clin. Biochem. 43 (2010) 159–167.
[192] F. Karatas, M. Karatepe, A. Baysar, Determination of free malondialdehyde in human serum by high-performance liquid chromatography, Anal. Biochem. 311 (2002) 76–79.
[193] A. Zinellu, S. Sotgia, L. Deiana, et al., Field-amplified online sample stacking capillary electrophoresis UV detection for plasma malondialdehyde measurement, Electrophoresis 32 (2011) 1893–1897.
[194] K. Syslova, P. Kacer, M. Kuzma, et al., Rapid and easy method for monitoring oxidative stress markers in body fluids of patients with asbestos or silica-induced lung diseases, J. Chromatogr. B Analyt Technol. Biomed. Life Sci. 877 (2009) 2477–2486.
[195] C.A. Sobsey, J. Han, K. Lin, et al., Development and evaluation of a liquid chromatography-mass spectrometry method for rapid, accurate quantitation of malondialdehyde in human plasma, J. Chromatogr. B Analyt Technol. Biomed. Life Sci. 1029–1030 (2016) 205–212.
[196] D. Tsikas, S. Rothmann, J.Y. Schneider, et al., Simultaneous GC-MS/MS measurement of malondialdehyde and 4-hydroxy-2-nonenal in human plasma: effects of long-term L-arginine administration, Anal. Biochem. 524 (2017) 31–44.
[197] D.V. Folden, A. Gupta, A.C. Sharma, et al., Malondialdehyde inhibits cardiac contractile function in ventricular myocytes via a p38 mitogen-activated protein kinase-dependent mechanism, Br. J. Pharmacol. 139 (2003) 1310–1316.
[198] C.R. Diaz-Velez, S. Garcia-Castineiras, E. Mendoza-Ramos, et al., Increased malondialdehyde in peripheral blood of patients with congestive heart failure, Am. Heart J. 131 (1996) 146–152.
[199] J.J. Belch, A.B. Bridges, N. Scott, et al., Oxygen free radicals and congestive heart failure, Br. Heart J. 65 (1991) 245–248.
[200] A. Serdar, D. Yesilbursa, Z. Serdar, et al., Relation of functional capacity with the oxidative stress and antioxidants in chronic heart failure, Congest. Heart Fail. 7 (2001) 309–311.
[201] S. Radovanovic, A. Savic-Radojevic, M. Pljesa-Ercegovac, et al., Markers of oxidative damage and antioxidant enzyme activities as predictors of morbidity and mortality in patients with chronic heart failure, J. Card. Fail. 18 (2012) 493–501.
[202] R.A. Alarcon, Fluorometric determination of acrolein and related compounds with m-aminophenol, Anal. Chem. 40 (1968) 1704–1708.
[203] F. Bohnenstengel, M. Eichelbaum, E. Golbs, et al., High-performance liquid chromatographic determination of acrolein as a marker for cyclophosphamide bioactivation in human liver microsomes, J. Chromatogr. B Biomed. Sci. Appl. 692 (1997) 163–168.
[204] M. Togashi, Y. Urano, H. Kojima, et al., Sensitive detection of acrolein in serum using time-resolved luminescence, Org. Lett. 12 (2010) 1704–1707.
[205] M. Togashi, T. Terai, H. Kojima, et al., Practical fluorescence detection of acrolein in human plasma via a two-step tethering approach, Chem Commun (Camb). 50 (2014) 14946–14948.
[206] M.H. El-Maghrabey, N. Kishikawa, K. Ohyama, et al., Analytical method for lipoperoxidation relevant reactive aldehydes in human sera by high-performance liquid chromatography-fluorescence detection, Anal. Biochem. 464 (2014) 36–42.
[207] A. Paci, A. Rieutord, D. Guillaume, et al., Quantitative high-performance liquid chromatographic determination of acrolein in plasma after derivatization with Luminarin 3, J. Chromatogr. B Biomed. Sci. Appl. 739 (2000) 239–246.
[208] T. Imazato, M. Kanematsu, N. Kishikawa, et al., Determination of acrolein in serum by high-performance liquid chromatography with fluorescence detection after pre-column fluorogenic derivatization using 1,2-diamino-4,5-dimethoxybenzene, Biomed. Chromatogr. 29 (2015) 1304–1308.
[209] K. Uchida, M. Kanematsu, Y. Morimitsu, et al., Acrolein is a product of lipid peroxidation reaction. Formation of free acrolein and its conjugate with lysine residues in oxidized low density lipoproteins, J. Biol. Chem. 273 (1998) 16058–16066.
[210] J. Pan, B. Awoyemi, Z. Xuan, et al., Detection of acrolein-derived cyclic DNA adducts in human cells by monoclonal antibodies, Chem. Res. Toxicol. 25 (2012) 2788–2795.
[211] H. Li, J. Wang, B. Kaphalia, et al., Quantitation of acrolein-protein adducts: potential biomarker of acrolein exposure, J. Toxicol. Environ. Health 67 (2004) 513–524.
[212] M.A. Bradley, W.R. Markesbery, M.A. Lovell, Increased levels of 4-hydroxynonenal and acrolein in the brain in preclinical Alzheimer disease, Free Radic. Biol. Med. 48 (2010) 1570–1576.
[213] R. Andreoli, P. Manini, M. Corradi, et al., Determination of patterns of biologically relevant aldehydes in exhaled breath condensate of healthy subjects by liquid chromatography/atmospheric chemical ionization tandem mass spectrometry, Rapid Commun. Mass Spectrom. 17 (2003) 637–645.
[214] S. Uchiyama, Y. Inaba, N. Kunugita, Determination of acrolein and other carbonyls in cigarette smoke using coupled silica cartridges impregnated with hydroquinone and 2,4-dinitrophenylhydrazine, J. Chromatogr. A 1217 (2010) 4383–4388.
[215] I.G. Casella, M. Contursi, Determination of aliphatic aldehydes by liquid chromatography with pulsed amperometric detection, J. Chromatogr. A 1063 (2005) 129–135.
[216] J. Wu, J.F. Stevens, C.S. Maier, Mass spectrometry-based quantification of myocardial protein adducts with acrolein in an in vivo model of oxidative stress, Mol. Nutr. Food Res. 55 (2011) 1401–1410.
[217] T.P. Devasagayam, K.K. Boloor, T. Ramasarma, Methods for estimating lipid peroxidation: an analysis of merits and demerits, Indian J. Biochem. Biophys. 40 (2003) 300–308.
[218] J. Klawitter, M. Haschke, T. Shokati, et al., Quantification of 15-F2t-isoprostane in human plasma and urine: results from enzyme-linked immunoassay and liquid chromatography/tandem mass spectrometry cannot be compared, Rapid Commun. Mass Spectrom. 25 (2011) 463–468.
[219] D.R. Briskey, G.R. Wilson, R.G. Fassett, et al., Optimized method for quantification of total F(2)-isoprostanes using gas chromatography-tandem mass spectrometry, J. Pharmaceut. Biomed. Anal. 90 (2014) 161–166.
[220] G.L. Milne, Q. Dai, L.J. Roberts 2nd, The isoprostanes–25 years later, Biochim. Biophys. Acta 1851 (2015) 433–445.
[221] A.E. Barden, E. Mas, K.D. Croft, et al., Minimizing artifactual elevation of lipid peroxidation products (F2-isoprostanes) in plasma during collection and storage, Anal. Biochem. 449 (2014) 129–131.
[222] B. Halliwell, C.Y. Lee, Using isoprostanes as biomarkers of oxidative stress: some rarely considered issues, Antioxidants Redox Signal. 13 (2010) 145–156.
[223] A. Pekala-Wojciechowska, M. Poznanski, K. Szyszow, et al., Concentration of 8-isoprostanes in the exhaled breath condensate as a marker of oxidative stress in patients with type 1 diabetes, Adv. Respir. Med. 86 (2018) 3–6.
[224] S. Carrillo-Ibarra, J.I. Cerrillos-Gutierrez, A. Escalante-Nunez, et al., The oxidative and inflammatory state in patients with acute renal graft dysfunction treated with tacrolimus, Oxid. Med. Cell Longev. 2016 (2016) 5405847.
[225] X. Chu, Y. Ageishi, K. Nishimura, et al., Development of enzyme-linked immunosorbent assay for 8-iso-prostaglandin F2alpha, a biomarker of oxidative stress in vivo, and its application to the quantification in aged rats, J. Pharmaceut. Biomed. Anal. 50 (2009) 911–916.
[226] I.F. Wiswedel, (2)-isoprostanes: sensitive biomarkers of oxidative stress in vitro

and in vivo: a gas chromatography-mass spectrometric approach, Methods Mol. Biol. 580 (2009) 3–16.
[227] G.L. Milne, B. Gao, E.S. Terry, et al., Measurement of F2- isoprostanes and isofurans using gas chromatography-mass spectrometry, Free Radic. Biol. Med. 59 (2013) 36–44.
[228] V. Cavalca, F. Minardi, S. Scurati, et al., Simultaneous quantification of 8-iso-prostaglandin-F(2alpha) and 11-dehydro thromboxane B(2) in human urine by liquid chromatography-tandem mass spectrometry, Anal. Biochem. 397 (2010) 168–174.
[229] D. Tsikas, M.T. Suchy, Assessment of urinary F(2)-isoprostanes in experimental and clinical studies: mass spectrometry versus ELISA, Hypertension 60 (2012) e14.
[230] M.L. Langhorst, M.J. Hastings, W.H. Yokoyama, et al., Determination of F2-iso-prostanes in urine by online solid phase extraction coupled to liquid chromato-graphy with tandem mass spectrometry, J. Agric. Food Chem. 58 (2010) 6614–6620.
[231] S.A. Brose, A.G. Baker, M.Y. Golovko, A fast one-step extraction and UPLC-MS/MS analysis for E2/D 2 series prostaglandins and isoprostanes, Lipids 48 (2013) 411–419.
[232] D. Tsikas, M.T. Suchy, Protocols for the measurement of the F2-isoprostane, 15(S)-8-iso-prostaglandin F2alpha, in biological samples by GC-MS or GC-MS/MS cou-pled with immunoaffinity column chromatography, J. Chromatogr. B Analyt Technol. Biomed. Life Sci. 1019 (2016) 191–201.
[233] W. Liu, J.D. Morrow, H. Yin, Quantification of F2-isoprostanes as a reliable index of oxidative stress in vivo using gas chromatography-mass spectrometry (GC-MS) method, Free Radic. Biol. Med. 47 (2009) 1101–1107.
[234] V.B. Ritov, D.E. Kelley, V.E. Kagan, Derivatization of F2-isoprostanes with 1-pyr-enyldiazomethane and their subsequent determination by fluorescence high-per-formance liquid chromatography, Anal. Biochem. 311 (2002) 10–18.
[235] X. Liu, P.D. Whitefield, Y. Ma, Quantification of F(2)-isoprostane isomers in cul-tured human lung epithelial cells after silica oxide and metal oxide nanoparticle treatment by liquid chromatography/tandem mass spectrometry, Talanta 81 (2010) 1599–1606.
[236] A.W. Taylor, M.G. Traber, Quantitation of plasma total 15-series F(2)-isoprostanes by sequential solid phase and liquid-liquid extraction, Anal. Biochem. 396 (2010) 319–321.
[237] Y.Y. Lee, J.M. Galano, C. Oger, et al., Assessment of isoprostanes in human plasma: technical considerations and the use of mass spectrometry, Lipids 51 (2016) 1217–1229.
[238] A.W. Taylor, R.S. Bruno, M.G. Traber, Women and smokers have elevated urinary F(2)-isoprostane metabolites: a novel extraction and LC-MS methodology, Lipids 43 (2008) 925–936.
[239] T. Petrosino, M. Serafini, Matrix effect in F(2)-isoprostanes quantification by HPLC-MS/MS: a validated method for analysis of iPF(2)alpha-III and iPF(2)alpha-VI in human urine, J. Chromatogr. B Analyt Technol. Biomed. Life Sci. 965 (2014) 100–106.
[240] G. Rodríguez Patiño, M.A. Castillo Rodríguez, J.E. Ramírez Bribiesca, et al., Development of a method for the determination of 8-iso-PGF2alpha in sheep and goat plasma using solid phase micro-extraction and UPLC-MS/MS, Rapid Commun. Mass Spectrom. 32 (19) (2018) 1675–1682.
[241] P. Purwaha, Y. Gu, U. Kelavkar, et al., LC/ESR/MS study of pH-dependent radical generation from 15-LOX-catalyzed DPA peroxidation, Free Radic. Biol. Med. 51 (2011) 1461–1470.
[242] Y. Okimotoa, A. Watanabea, E. Nikia, et al., A novel fluorescent probe diphenyl-1-pyrenylphosphine to follow lipid peroxidation in cell membranes, FEBS Lett. 474 (2000) 137–140.
[243] I. Matot, Y. Manevich, A.B. Al-Mehdi, et al., Fluorescence imaging of lipid per-oxidation in isolated rat lungs during nonhypoxic lung ischemia, Free Radic. Biol. Med. 34 (2003) 785–790.
[244] G. Stubiger, O. Belgacem, P. Rehulka, et al., Analysis of oxidized phospholipids by MALDI mass spectrometry using 6-aza-2-thiothymine together with matrix ad-ditives and disposable target surfaces, Anal. Chem. 82 (2010) 5502–5510.
[245] L.J. Sparvero, A.A. Amoscato, C.E. Dixon, et al., Mapping of phospholipids by MALDI imaging (MALDI-MSI): realities and expectations, Chem. Phys. Lipids 165 (2012) 545–562.
[246] G. Stubiger, E. Aldover-Macasaet, W. Bicker, et al., Targeted profiling of athero-genic phospholipids in human plasma and lipoproteins of hyperlipidemic patients using MALDI-QIT-TOF-MS/MS, Atherosclerosis 224 (2012) 177–186.
[247] D. Gao, E.A. Podrez, Characterization of covalent modifications of HDL apopro-teins by endogenous oxidized phospholipids, Free Radic. Biol. Med. 115 (2018) 57–67.
[248] V. Bochkov, B. Gesslbauer, C. Mauerhofer, et al., Pleiotropic effects of oxidized phospholipids, Free Radic. Biol. Med. 111 (2017) 6–24.
[249] Z. Ni, G. Angelidou, R. Hoffmann, et al., LPPtiger software for lipidome-specific prediction and identification of oxidized phospholipids from LC-MS datasets, Sci. Rep. 7 (2017) 15138.
[250] H. Hinterwirth, G. Stubiger, W. Lindner, et al., Gold nanoparticle-conjugated anti-oxidized low-density lipoprotein antibodies for targeted lipidomics of oxidative stress biomarkers, Anal. Chem. 85 (2013) 8376–8384.
[251] K.A. Zemski Berry, W.W. Turner, M.S. VanNieuwenhze, et al., Characterization of oxidized phosphatidylethanolamine derived from RAW 264.7 cells using 4-(di-methylamino)benzoic acid derivatives, Eur. J. Mass Spectrom. 16 (2010) 463–470.
[252] G. Aldini, G. Vistoli, M. Stefek, et al., Molecular strategies to prevent, inhibit, and degrade advanced glycoxidation and advanced lipoxidation end products, Free Radic. Res. 47 (Suppl 1) (2013) 93–137.
[253] L. Horakova, S. Stolc, Antioxidant and pharmacodynamic effects of pyridoindole stobadine, Gen. Pharmacol. 30 (1998) 627–638.
[254] Z. Kyselova, A. Gajdosik, A. Gajdosikova, et al., Effect of the pyridoindole anti-oxidant stobadine on development of experimental diabetic cataract and on lens protein oxidation in rats: comparison with vitamin E and BHT, Mol. Vis. 11 (2005) 56–65.
[255] L. Horakova, A. Giessauf, G. Raber, et al., Effect of stobadine on Cu(++)-medi-ated oxidation of low-density lipoprotein, Biochem. Pharmacol. 51 (1996) 1277–1282.
[256] B. Pekiner, N.N. Ulusu, N. Das-Evcimen, et al., In vivo treatment with stobadine prevents lipid peroxidation, protein glycation and calcium overload but does not ameliorate Ca2+ -ATPase activity in heart and liver of streptozotocin-diabetic rats: comparison with vitamin E, Biochim. Biophys. Acta 1588 (2002) 71–78.
[257] S. Steenken, A.R. Sundquist, S.V. Jovanovic, et al., Antioxidant activity of the pyridoindole stobadine. Pulse radiolytic characterization of one-electron-oxidized stobadine and quenching of singlet molecular oxygen, Chem. Res. Toxicol. 5 (1992) 355–360.
[258] R. Nagai, D.B. Murray, T.O. Metz, et al., Chelation: a fundamental mechanism of action of AGE inhibitors, AGE breakers, and other inhibitors of diabetes compli-cations, Diabetes 61 (2012) 549–559.
[259] D.L. Price, P.M. Rhett, S.R. Thorpe, et al., Chelating activity of advanced glycation end-product inhibitors, J. Biol. Chem. 276 (2001) 48967–48972.
[260] I.A. Blair, Endogenous glutathione adducts, Curr. Drug Metabol. 7 (2006) 853–872.
[261] G. Aldini, A. Altomare, G. Baron, et al., N-Acetylcysteine as an antioxidant and disulphide breaking agent: the reasons why, Free Radic. Res. 52 (2018) 751–762.
[262] A.L. Furfaro, S. Menini, S. Patriarca, et al., HNE-dependent molecular damage in diabetic nephropathy and its possible prevention by N-acetyl-cysteine and oxer-utin, Biofactors 24 (2005) 291–298.
[263] J. Sochman, N-acetylcysteine in acute cardiology: 10 years later: what do we know and what would we like to know?!, J. Am. Coll. Cardiol. 39 (2002) 1422–1428.
[264] P.V. Dludla, S.C. Dias, N. Obonye, et al., A systematic review on the protective effect of N-acetyl cysteine against diabetes-associated cardiovascular complica-tions, Am. J. Cardiovasc. Drugs 18 (2018) 283–298.
[265] D.R.A. Reyes, M.J. Gomes, C.M. Rosa, et al., N-acetylcysteine influence on oxi-dative stress and cardiac remodeling in rats during transition from compensated left ventricular hypertrophy to heart failure, Cell. Physiol. Biochem. 44 (2017) 2310–2321.
[266] B. Giam, P.Y. Chu, S. Kuruppu, et al., N-acetylcysteine attenuates the development of cardiac fibrosis and remodeling in a mouse model of heart failure, Phys. Rep. 4 (2016).
[267] M. Sanson, N. Auge, C. Vindis, et al., Oxidized low-density lipoproteins trigger endoplasmic reticulum stress in vascular cells: prevention by oxygen-regulated protein 150 expression, Circ. Res. 104 (2009) 328–336.
[268] Y. Cui, C.A. Narasimhulu, L. Liu, et al., N-acetylcysteine inhibits in vivo oxidation of native low-density lipoprotein, Sci. Rep. 5 (2015) 16339.
[269] Y. Lu, W. Qin, T. Shen, et al., The antioxidant N-acetylcysteine promotes athero-sclerotic plaque stabilization through suppression of RAGE, MMPs and NF-kappaB in ApoE-deficient mice, J. Atherosclerosis Thromb. 18 (2011) 998–1008.
[270] B. Bouguerne, N. Belkheiri, F. Bedos-Belval, et al., Antiatherogenic effect of bis-vanillyl-hydralazone, a new hydralazine derivative with antioxidant, carbonyl scavenger, and antiapoptotic properties, Antioxidants Redox Signal. 14 (2011) 2093–2106.
[271] S. Galvani, C. Coatrieux, M. Elbaz, et al., Carbonyl scavenger and antiatherogenic effects of hydrazine derivatives, Free Radic. Biol. Med. 45 (2008) 1457–1467.
[272] C. Vindis, I. Escargueil-Blanc, M. Elbaz, et al., Desensitization of platelet-derived growth factor receptor-beta by oxidized lipids in vascular cells and atherosclerotic lesions: prevention by aldehyde scavengers, Circ. Res. 98 (2006) 785–792.
[273] S. Picard, S. Parthasarathy, J. Fruebis, et al., Aminoguanidine inhibits oxidative modification of low density lipoprotein protein and the subsequent increase in uptake by macrophage scavenger receptors, Proc. Natl. Acad. Sci. U. S. A. 89 (1992) 6876–6880.
[274] Z. Kang, H. Li, G. Li, et al., Reaction of pyridoxamine with malondialdehyde: mechanism of inhibition of formation of advanced lipoxidation end-products, Amino Acids 30 (2006) 55–61.
[275] J.M. Onorato, A.J. Jenkins, S.R. Thorpe, et al., Pyridoxamine, an inhibitor of ad-vanced glycation reactions, also inhibits advanced lipoxidation reactions. Mechanism of action of pyridoxamine, J. Biol. Chem. 275 (2000) 21177–21184.
[276] T.O. Metz, N.L. Alderson, M.E. Chachich, et al., Pyridoxamine traps intermediates in lipid peroxidation reactions in vivo: evidence on the role of lipids in chemical modification of protein and development of diabetic complications, J. Biol. Chem. 278 (2003) 42012–42019.
[277] S.H. Lee, A. Matsunaga, T. Oe, Inhibition effect of pyridoxamine on lipid hydro-peroxide-derived modifications to human serum albumin, PLoS One 13 (2018) e0196050.
[278] G.M. Cahuana, J.R. Tejedo, J. Jimenez, et al., Involvement of advanced lipoox-idation end products (ALEs) and protein oxidation in the apoptotic actions of nitric oxide in insulin secreting RINm5F cells, Biochem. Pharmacol. 66 (2003) 1963–1971.
[279] T.P. Degenhardt, N.L. Alderson, D.D. Arrington, et al., Pyridoxamine inhibits early renal disease and dyslipidemia in the streptozotocin-diabetic rat, Kidney Int. 61 (2002) 939–950.
[280] P.A. Voziyan, B.G. Hudson, Pyridoxamine as a multifunctional pharmaceutical: targeting pathogenic glycation and oxidative damage, Cell. Mol. Life Sci. 62 (2005) 1671–1681.
[281] A.A. Boldyrev, G. Aldini, W. Derave, Physiology and pathophysiology of carnosine, Physiol. Rev. 93 (2013) 1803–1845.
[282] A.R. Hipkiss, Carnosine and its possible roles in nutrition and health, Adv. Food

Nutr. Res. 57 (2009) 87–154.
[283] S. Zhou, E.A. Decker, Ability of carnosine and other skeletal muscle components to quench unsaturated aldehydic lipid oxidation products, J. Agric. Food Chem. 47 (1999) 51–55.
[284] M. Carini, G. Aldini, G. Beretta, et al., Acrolein-sequestering ability of endogenous dipeptides: characterization of carnosine and homocarnosine/acrolein adducts by electrospray ionization tandem mass spectrometry, J. Mass Spectrom. 38 (2003) 996–1006.
[285] G. Vistoli, M. Colzani, A. Mazzolari, et al., Quenching activity of carnosine derivatives towards reactive carbonyl species: focus on alpha-(methylglyoxal) and beta-(malondialdehyde) dicarbonyls, Biochem. Biophys. Res. Commun. 492 (2017) 487–492.
[286] M. Orioli, G. Aldini, M.C. Benfatto, et al., HNE Michael adducts to histidine and histidine-containing peptides as biomarkers of lipid-derived carbonyl stress in urines: LC-MS/MS profiling in Zucker obese rats, Anal. Chem. 79 (2007) 9174–9184.
[287] E.J. Anderson, G. Vistoli, L.A. Katunga, et al., A carnosine analog mitigates metabolic disorders of obesity by reducing carbonyl stress, J. Clin. Invest. 128 (2018) 5280–5293.
[288] S. Menini, C. Iacobini, C. Ricci, et al., D-Carnosine octylester attenuates atherosclerosis and renal disease in ApoE null mice fed a Western diet through reduction of carbonyl stress and inflammation, Br. J. Pharmacol. 166 (2012) 1344–1356.
[289] T. Grune, K.J. Davies, The proteasomal system and HNE-modified proteins, Mol. Aspect. Med. 24 (2003) 195–204.
[290] A. Gonen, L.F. Hansen, W.W. Turner, et al., Atheroprotective immunization with malondialdehyde-modified LDL is hapten specific and dependent on advanced MDA adducts: implications for development of an atheroprotective vaccine, J. Lipid Res. 55 (2014) 2137–2155.
[291] E. Ho, K. Karimi Galougahi, C.C. Liu, et al., Biological markers of oxidative stress: applications to cardiovascular research and practice, Redox Biol. 1 (2013) 483–491.
[292] K.K. Griendling, R.M. Touyz, J.L. Zweier, et al., Measurement of reactive oxygen species, reactive nitrogen species, and redox-dependent signaling in the cardiovascular system: a scientific statement from the American heart association, Circ. Res. 119 (2016) e39–75.
[293] I. Marrocco, F. Altieri, I. Peluso, Measurement and clinical significance of biomarkers of oxidative stress in humans, Oxid. Med. Cell Longev. 2017 (2017) 6501046.
[294] M.F. Walter, R.F. Jacob, R.E. Bjork, et al., Circulating lipid hydroperoxides predict cardiovascular events in patients with stable coronary artery disease: the PREVENT study, J. Am. Coll. Cardiol. 51 (2008) 1196–1202.
[295] C. Asselin, A. Ducharme, T. Ntimbane, et al., Circulating levels of linoleic acid and HDL-cholesterol are major determinants of 4-hydroxynonenal protein adducts in patients with heart failure, Redox Biol. 2 (2014) 148–155.
[296] R. Belardinelli, M. Solenghi, L. Volpe, et al., Trimetazidine improves endothelial dysfunction in chronic heart failure: an antioxidant effect, Eur. Heart J. 28 (2007) 1102–1108.
[297] I. Basarici, R.E. Altekin, I. Demir, et al., Urinary 8-isoprostane levels can indicate the presence, severity and extent of angiographic coronary artery disease, Acta Cardiol. 63 (2008) 415–422.
[298] B. Wang, J. Pan, L. Wang, et al., Associations of plasma 8-isoprostane levels with the presence and extent of coronary stenosis in patients with coronary artery disease, Atherosclerosis 184 (2006) 425–430.
[299] M.H. Shishehbor, R. Zhang, H. Medina, et al., Systemic elevations of free radical oxidation products of arachidonic acid are associated with angiographic evidence of coronary artery disease, Free Radic. Biol. Med. 41 (2006) 1678–1683.
[300] J.Y. Kim, Y.J. Hyun, Y. Jang, et al., Lipoprotein-associated phospholipase A2 activity is associated with coronary artery disease and markers of oxidative stress: a case-control study, Am. J. Clin. Nutr. 88 (2008) 630–637.
[301] F. Veglia, V. Cavalca, E. Tremoli, OXY-SCORE: a global index to improve evaluation of oxidative stress by combining pro- and antioxidant markers, Methods Mol. Biol. 594 (2010) 197–213.
[302] C. Vassalle, An easy and reliable automated method to estimate oxidative stress in the clinical setting, Methods Mol. Biol. 477 (2008) 31–39.
[303] F. Veglia, G. Cighetti, M. De Franceschi, et al., Age- and gender-related oxidative status determined in healthy subjects by means of OXY-SCORE, a potential new comprehensive index, Biomarkers 11 (2006) 562–573.
[304] K. Satoh, S. Yamada, Y. Koike, et al., A 1-hour enzyme-linked immunosorbent assay for quantitation of acrolein- and hydroxynonenal-modified proteins by epitope-bound casein matrix method, Anal. Biochem. 270 (1999) 323–328.
[305] X. Tang, L.M. Sayre, G.P. Tochtrop, A mass spectrometric analysis of 4-hydroxy-2-(E)-nonenal modification of cytochrome c, J. Mass Spectrom. 46 (2011) 290–297.
[306] A. Renner, M.R. Sagstetter, H. Harms, et al., Formation of 4-hydroxy-2-nonenal protein adducts in the ischemic rat heart after transplantation, J. Heart Lung Transplant. 24 (2005) 730–736.
[307] H. Ma, R. Guo, L. Yu, et al., Aldehyde dehydrogenase 2 (ALDH2) rescues myocardial ischaemia/reperfusion injury: role of autophagy paradox and toxic aldehyde, Eur. Heart J. 32 (2011) 1025–1038.
[308] Q. Gao, A. Sarkar, Y. Chen, et al., Overexpression of heart-type fatty acid binding protein enhances fatty acid-induced podocyte injury, Exp. Ther. Med. 15 (2018) 2054–2061.
[309] T.D. Calamaras, C. Lee, F. Lan, et al., Post-translational modification of serine/threonine kinase LKB1 via Adduction of the Reactive Lipid Species 4-Hydroxy-trans-2-nonenal (HNE) at lysine residue 97 directly inhibits kinase activity, J. Biol. Chem. 287 (2012) 42400–42406.
[310] S.W. Choi, Y.K. Jeon, S.H. Moon, et al., Suppression of hERG K(+) current and cardiac action potential prolongation by 4-hydroxynonenal via dual mechanisms, Redox Biol. 19 (2018) 190–199.
[311] M.F. Walter, R.F. Jacob, B. Jeffers, et al., Serum levels of thiobarbituric acid reactive substances predict cardiovascular events in patients with stable coronary artery disease: a longitudinal analysis of the PREVENT study, J. Am. Coll. Cardiol. 44 (2004) 1996–2002.
[312] M. White, A. Ducharme, R. Ibrahim, et al., Increased systemic inflammation and oxidative stress in patients with worsening congestive heart failure: improvement after short-term inotropic support, Clin. Sci. (Lond.) 110 (2006) 483–489.
[313] B. Shao, S. Pennathur, I. Pagani, et al., Modifying apolipoprotein A-I by malondialdehyde, but not by an array of other reactive carbonyls, blocks cholesterol efflux by the ABCA1 pathway, J. Biol. Chem. 285 (2010) 18473–18484.
[314] C.S. Yarian, I. Rebrin, R.S. Sohal, Aconitase and ATP synthase are targets of malondialdehyde modification and undergo an age-related decrease in activity in mouse heart mitochondria, Biochem. Biophys. Res. Commun. 330 (2005) 151–156.
[315] T. Obama, R. Kato, Y. Masuda, et al., Analysis of modified apolipoprotein B-100 structures formed in oxidized low-density lipoprotein using LC-MS/MS, Proteomics 7 (2007) 2132–2141.
[316] C. Gniwotta, J.D. Morrow, L.J. Roberts 2ndet al., Prostaglandin F2-like compounds, F2-isoprostanes, are present in increased amounts in human atherosclerotic lesions, Arterioscler. Thromb. Vasc. Biol. 17 (1997) 3236–3241.
[317] E. Schwedhelm, A. Bartling, H. Lenzen, et al., Urinary 8-iso-prostaglandin F2alpha as a risk marker in patients with coronary heart disease: a matched case-control study, Circulation 109 (2004) 843–848.
[318] A. Nishibe, Y. Kijima, M. Fukunaga, et al., Increased isoprostane content in coronary plaques obtained from vulnerable patients, Prostaglandins Leukot. Essent. Fatty Acids 78 (2008) 257–263.
[319] S.S. Davies, L.J. Roberts 2nd, F2-isoprostanes as an indicator and risk factor for coronary heart disease, Free Radic. Biol. Med. 50 (2011) 559–566.
[320] R.M. LeLeiko, C.S. Vaccari, S. Sola, et al., Usefulness of elevations in serum choline and free F2)-isoprostane to predict 30-day cardiovascular outcomes in patients with acute coronary syndrome, Am. J. Cardiol. 104 (2009) 638–643.
[321] R. De Cristofaro, B. Rocca, E. Vitacolonna, et al., Lipid and protein oxidation contribute to a prothrombotic state in patients with type 2 diabetes mellitus, J. Thromb. Haemostasis 1 (2003) 250–256.
[322] J. Bauer, A. Ripperger, S. Frantz, et al., Pathophysiology of isoprostanes in the cardiovascular system: implications of isoprostane-mediated thromboxane A2 receptor activation, Br. J. Pharmacol. 171 (2014) 3115–3131.

Journal of Proteomics 173 (2018) 62–76

Contents lists available at ScienceDirect

Journal of Proteomics

journal homepage: www.elsevier.com/locate/jprot

Proteomics in cardiovascular diseases: Unveiling sex and gender differences in the era of precision medicine

Roberta Baetta[a], Marta Pontremoli[a], Alma Martinez Fernandez[a], Corinne M. Spickett[b], Cristina Banfi[a,*]

[a] Centro Cardiologico Monzino, IRCCS, Milano, Italy
[b] School of Life & Health Sciences, Aston University, Birmingham, UK

ARTICLE INFO

Keywords:
Sex differences
Gender
Cardiovascular disease
Risk factors
Oxidative stress
Proteomics

ABSTRACT

Cardiovascular diseases (CVDs) represent the most important cause of mortality in women and in men. Contrary to the long-standing notion that the effects of the major risk factors on CVD outcomes are the same in both sexes, recent evidence recognizes new, potentially independent, sex/gender-related risk factors for CVDs, and sex/gender-differences in the clinical presentation of CVDs have been demonstrated. Furthermore, some therapeutic options may not be equally effective and safe in men and women. In this context, proteomics offers an extremely useful and versatile analytical platform for biomedical researches that expand from the screening of early diagnostic and prognostic biomarkers to the investigation of the molecular mechanisms underlying CDVs. In this review, we summarized the current applications of proteomics in the cardiovascular field, with emphasis on sex and gender-related differences in CVDs.

Significance: Increasing evidence supports the profound effect of sex and gender on cardiovascular physio-pathology and the response to drugs. A clear understanding of the mechanisms underlying sexual dimorphisms in CVDs would not only improve our knowledge of the etiology of these diseases, but could also inform health policy makers and guideline committees in tailoring specific interventions for the prevention, treatment and management of CVDs in both men and women.

1. Introduction

Cardiovascular diseases (CVDs) are the world's leading cause of morbidity and mortality, accounting for > 17 million deaths annually [1], and cause immense health and economic burdens [2,3]. In line with the recommendations of the World Health Organization (WHO), the principal health organizations in the field of heart diseases and stroke (such as the American Heart Association and the European Society of Cardiology) formulated recommendations to drive organizational priorities and guide actions to prevent CVDs in clinical practice [4,5]. In accordance with the strategic view of these recommendations, to achieve the goal of significantly reducing deaths attributable to CVDs continued emphasis is needed on the treatment and control of health behaviors and risk factors at both the population and the individual level [2,5]. In the era of precision medicine, the key challenge is to bridge the gaps in our knowledge about sex- and gender-related differences in the pathophysiology of the cardiovascular system, since increasing evidence supports the notion that an individual's sex is one of the most important modulators of disease risk and response to treatment [6–8] (Box 1).

Indeed, a large amount of correlative data unveils the existence of sexual diversities in human physiology and differential susceptibility to a wide variety of pathologies including CVDs [9,10]. Beyond environmental and social differences between men and women (e.g., occupational hazards, lifestyle, social stresses, access to healthcare) that can contribute to gender differences in CVDs, sex hormones have long been found to account for some sex-related differences in CVDs, and some molecular mechanisms mediating these effects have recently been elucidated [8,10,11]. Moreover, sex chromosomes are beginning to be recognized as important determinants of sexual dimorphism in the development of CVDs, independent of sex hormones [8,10–12]. In this Review, we consider the evidence for sex and gender differences in CVDs and summarize the proteomic research that has been conducted in this field.

2. Sex-specific and gender-specific cardiovascular research

CVDs have long been considered as male diseases, an assumption

* Corresponding author at: Centro Cardiologico Monzino, IRCCS, Via Parea 4, 20138 Milano, Italy.
E-mail address: cristina.banfi@ccfm.it (C. Banfi).

https://doi.org/10.1016/j.jprot.2017.11.012
Received 25 July 2017; Received in revised form 6 November 2017; Accepted 17 November 2017
Available online 24 November 2017
1874-3919/

Box 1
Sex vs. gender.

Sex and gender are different constructs. According to the WHO, sex "*refers to the set of biological characteristics that define humans as female or male*"; it is primarily associated with physical and physiological features including chromosomes, gene expression, hormone levels, and reproductive/sexual anatomy. Gender encompasses biology but is also influenced by experience and environment: it "*refers to the socially constructed roles, behaviors, activities, and attributes that a given society considers appropriate for men and women*"; it influences the distribution of power and resources, including access to healthcare. Sex and gender influence each other through complex interactions. Both sex and gender are critical variables in preclinical and clinical research.
http://www.who.int/reproductivehealth/topics/sexual_health/sh_definitions/en/
http://www.who.int/gender-equity-rights/understanding/gender-definition/en/

that stems largely from observations that CVDs in women develop later in life than in men, and the misperception that CVDs among women are not as severe as they are in men [13]. In line with this view, until recently cardiovascular research was predominantly conducted in men and it was assumed that clinical approaches based on research findings involving men were equally relevant for women [13]. However, a growing body of evidence has progressively revealed the importance of CVDs in women and has fostered the awareness of sex- and gender-related differences in the occurrence, management and outcomes of CVDs [13]. Marked progress has been made in the involvement of women in large-scale population studies and clinical trials. Nevertheless, several gaps in our understanding of sex- and gender-related diversities in cardiovascular health still persist. Moreover, the use of female animals, cells, or tissues, and sex-based reporting in preclinical investigations have not been equally implemented [14], in spite of the publication of a planned policy from the U.S. National Institutes of Health (NIH) to balance sex in cell and animal studies [15]. In this regard, it is important to highlight the value of preclinical studies for understanding the molecular bases of sex differences, since such studies: 1) enable scientists to take full advantage of the power of molecular genetics and 'omics technologies; 2) allow the control of variables such as diet, environment, exercise; and 3) offer the opportunity to quantify the extent of sex or gender contribution to the biological outcome, since in experimental animals gender has limited impact [9].

3. Sex and gender differences in CVD risk factors

Most of the traditional risk factors for CVDs, including elevated blood pressure, dyslipidemia, excess body weight and obesity, diabetes, and cigarette smoking, are similar between men and women, but for some of them the impact differs between the sexes; furthermore, recent evidence has emerged that recognizes new, potentially independent female-specific risk factors (Fig. 1) [8,16].

3.1. Major risk factors affecting both men and women

3.1.1. Elevated systolic blood pressure

Elevated systolic blood pressure (SBP) is one of the leading risk factors for global mortality and for CVDs. In 2015, the prevalence of raised blood pressure was around 20% in females aged 18 and over and around 24% in males [17]. Studies have reported conflicting results on whether the association between increments in SBP and CVDs differs between sexes [16]. A pooled analysis carried out in 2013, including data from prospective cohort studies on > 1.2 million individuals and over 50,000 cardiovascular events, found that every 10 mmHg increment in SBP was associated with a 15% increased risk of coronary heart disease (CHD) and a 25% increased risk of stroke in both men and women, indicating a similar impact of hypertension on cardiovascular outcomes in both sexes [18]. In contrast, results of a recent meta-regression analysis of US population-based studies indicate that women experienced a 10% greater risk in CVDs per 10 mmHg increment in SBP than men, after adjusting for age and baseline SBP [19].

3.1.2. Dyslipidemia

Raised total cholesterol (TC) is estimated to account for over 2.6 million deaths (4.5% of total) worldwide every year [20]. The prevalence of elevated TC is similar in men and women [20] and studies addressing the possible sex/gender-specific effects of TC on CVD risk have reported inconsistent results [21]. The first systematic meta-analysis evaluating the impact of TC on CVD risk in women compared with men included data from over one million individuals and > 20,000 CHD and 16,000 stroke events [21]. This analysis found that for every 1-mmol/L increment in TC, the risk of CHD increased by 20% in women and by 24% in men, indicating essentially a similar TC-related risk of CHD in both sexes [21].

In population studies, high-density lipoprotein cholesterol (HDL-C) is inversely related to the risk of myocardial infarction and death [22].

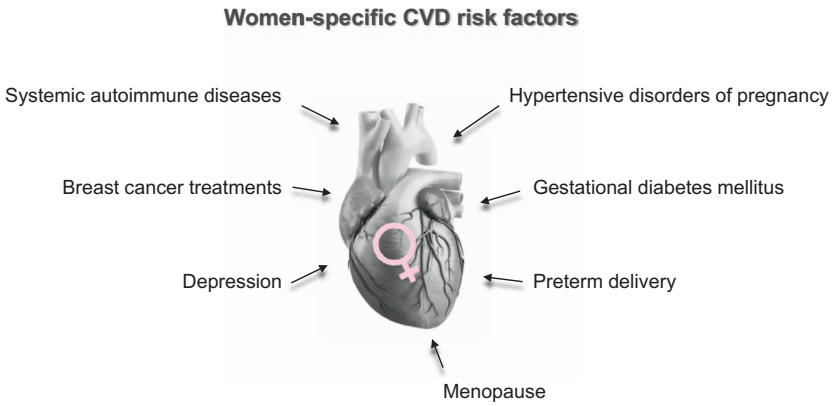

Fig. 1. Women-specific CVD risk factors. Women-specific conditions to consider in risk evaluation, diagnosis and treatment of CVDs include hypertensive disorders of pregnancy, gestational diabetes mellitus, preterm delivery, menopause, systemic autoimmune disease, breast cancer treatments, and depression.

Low HDL was initially suggested to be more predictive of coronary risk in women compared to men [23]; however, analyses of > 300,000 people from 68 long-term prospective studies contributing to the Emerging Risk Factors Collaboration (ERFC) analysis on the associations of major lipids and apolipoproteins with the risk of vascular disease indicated that, after adjustment for other cardiovascular risk factors, the association between HDL cholesterol levels and fatal CHD did not vary significantly by sex: each 1-SD increase in HDL-C lowered the risk of CHD mortality by 26% in women and by 21% in men [24].

3.1.3. Diabetes mellitus

Diabetes mellitus (DM) is an important predictor of a person's risk of vascular disease [25]. It is one of the largest global health emergencies of the 21st century, with an estimated global prevalence of over 400 million and a projected increase to 642 million by 2040, which poses an enormous burden on healthcare [26]. Although there is little gender difference in the global number of people with diabetes [26], compelling evidence indicates that women, compared to men, have a significant and clinically important higher excess risk of both CHD and stroke consequent to diabetes (44% and 27%, respectively) [27–29]. Furthermore, diabetic women have a higher risk of developing heart failure (HF) or peripheral arterial disease (PAD) compared with diabetic men [30]. Several hypotheses have been proposed to explain how diabetes confers a female disadvantage in terms of vascular risk, but the exact mechanisms remain unclear [16,31]. An attractive – but still unproven – hypothesis is that women live in a suboptimal glycemic ('prediabetic') state for a longer period of time than men, during which their metabolic profile continues to deteriorate relative to men, so that considerable vascular damage has already occurred by the time they are clinically diagnosed with diabetes [31].

3.1.4. Body fat, excess body weight and obesity

Excess body weight is another major risk factor for CVDs and currently one of the greatest public health issues worldwide [1]. According to the WHO global estimates, excess body weight has reached epidemic proportions globally: in 2016, > 1.9 billion adults were overweight (39% of men and 40% of women); of these, over 650 million were obese [32]. The association between body mass index (BMI) and CHD has been shown to be the same between men and women in the large-scale analyses of the Prospective Studies Collaboration [33] and the ERFC [34], and in a meta-analysis including data from 95 cohorts with > 1.2 million participants [35]. These results indicate that increased BMI has the same deleterious effects on the risk of CHD in women and men. However, there are numerous differences between males and females regarding body fat, excess body weight and obesity that could be due to either direct activation by sex steroids or by sex steroid-independent mechanisms. Although men generally have greater body weight than women, the proportion of body weight as fat is greater in women and there is a clear hormone-related sexual dimorphism in the patterns of body fat storage and fat metabolism [36]. In their fertile age, females store the lipids in excess in subcutaneous deposits (such as the gluteal femoral region) that are believed to be associated with lower cardiometabolic risk than the abdominal (visceral) fat accumulation that predominates in men [36]. When ovarian activity ceases with the onset of menopause, this female advantage is lost and women become more vulnerable to the risks of an obesogenic environment [9]. In addition, the concept has recently emerged that the complex and different effects of obesity on CVDs could in different cases be detrimental, or innocuous, or even protective [37]. Indeed, the possible existence of a metabolically healthy obese phenotype (more appropriately defined as a lower risk form of obesity), the important role of regional body fat distribution and ectopic fat accumulation, and the presence of an "obesity paradox" in patients with CVDs, are all observations which emphasize the remarkable heterogeneity of obesity [37]. Thus, given the complex metabolic roles of the adipose tissue [38] and the importance of obesity as a driver of several major CVD risk factors [31], more research is needed on gender-specific pathophysiology of obesity development.

3.1.5. Cigarette smoking

Smoking (including second-hand smoking) is an established cause of a myriad of diseases and according to the WHO it is currently responsible of > 7 million deaths across the world each year [39]. With regard to CVDs, it is well known that smoking negatively affects endothelial function, oxidative processes, platelet function, fibrinolysis, inflammation, and vasomotor function, thus promoting the development of both atherosclerosis and the superimposed thrombotic complications [5]. According to these proatherogenic roles of cigarette smoking, the 10-year risk of fatal events is approximately doubled in smokers compared to non-smokers [5]. While the beneficial effects of smoking cessation on coronary risk are similar in women and men, the mortality from CVDs is higher in female than male smokers, even after adjustment for other risk factors [40]. Furthermore, a meta-analysis of data from 75 prospective cohort studies and nearly 2.4 million subjects showed that female smokers had a 25% higher risk of developing CHD than men with the same exposure to tobacco smoke [41]. With regard to stroke, a second meta-analysis, involving data from 81 cohorts worldwide and nearly 4 million individuals did not find an overall greater excess risk of smoking in women compared with men, but it found a 10% higher risk in female smokers in Western populations, where smoking is a long-standing habit also among women [42]. The molecular basis underlying such differential female susceptibility to tobacco smoke is not currently understood. Interestingly, a recent report on genome-wide profiling in white blood cells found that the expression or methylation of several genes with a key role in the pathogenesis of CVDs (especially genes involved in thrombin signaling) is altered by smoking significantly more in females than in males [43]. These results underline the potential of blood-based omics profiling in sex/gender-specific risk assessment.

3.2. Women-specific risk factors

The unique aspects of cardiovascular health in women have been comprehensively reviewed by Garcia and colleagues [30], who provided an in-depth analysis on sex and gender differences related to clinical practice in the prevention, diagnosis, and treatment of CVDs. Sex steroid hormones, especially estrogen (the major sex steroid in females), have a plethora of physiological effects on the cardiovascular system, as well as indirect effects mediated through changes in metabolism and coagulation [8,11,44]. In view of that, it is thought that changes in circulating levels of endogenous sex hormones, such as those that occur in women during pregnancy and menopause, can affect current and future CVD risk [8]. In addition, exogenous hormones in the form of hormonal contraceptives and menopausal hormone therapy modulate the hormonal environment, and subsequently women-specific CVD risk [8]. The latter topics are not addressed in this review but have been covered previously [8,45–47].

3.2.1. Hypertensive disorders of pregnancy and gestational diabetes mellitus

The vascular, metabolic and immunological adaptations that occur to a woman's body during pregnancy pose a substantial challenge to the cardiovascular system, and pregnancy-associated disorders are often the result of the mother's inability to adapt to this vascular and metabolic stress [8,16]. Accordingly, complications such as hypertensive disorders (including the conditions of gestational hypertension and preeclampsia) or gestational DM represent important women-specific factors to consider in risk assessment, since they can place a woman at long-term risk of developing CVDs, or reveal a preexistent cardiovascular dysfunction [8,16]. Preeclampsia (defined as pregnancy-related hypertension accompanied by proteinuria) occurs in 1–2% of all pregnancies [5]. A meta-analysis by Bellamy et al. [48] found that in comparison to women with normal pregnancies, women who suffered

from preeclampsia had a greater relative risk for developing hypertension, CHD, and stroke later in life. Gestational hypertension affects 10–15% of all pregnancies [5]. The associated risk of later CVDs is lower than for preeclampsia, but is still elevated [49]. Gestational DM has a prevalence of 3–5% of all pregnancy and is similarly associated with an increased risk of future CVDs. Most of this risk appears to be mediated by a sharply elevated likelihood of future type 2 DM in women with gestational DM compared to women with normoglycemic pregnancies, with up to 50% developing type 2 DM within 5 years [50]. Interestingly, women with a history of hypertensive disease in pregnancy have a higher risk for developing type 2 DM [49] and women with gestational DM have a higher risk for gestational hypertension and preeclampsia [51], suggesting a close link between the vascular and the metabolic complications of pregnancy, which are both associated with increased risk of CVDs later in life.

3.2.2. Menopause

In their fertile age, women are relatively protected against CVDs, compared with age-matched men. However, this sex gap narrows after menopause [30]. The decrease in ovarian activity during and after menopause goes hand in hand with an increased risk of CVDs in women, partially because the deleterious biological changes consequent to the loss of endogenous estrogens favor hypertension, diabetes, hyperlipidemia, central obesity and the metabolic syndrome [8,16,52]. Two meta-analyses that assessed the relationship between age at menopause and CVD risk found that menopause before age 50 was associated with a 25% higher risk of CVDs [53], while natural menopause < 40 years, better defined as primary ovarian insufficiency, was related to an increased hazard ratio (HR) of CHD of 1.69 and an HR of 1.61 for total CVDs [54]. However, menopausal hormone therapy increases the risks of serious disease, such as breast or endometrial cancers, and its cardiovascular effects are controversial; thus, the current consensus is that it should never be prescribed for the aim of preventing CVDs [8,30,47].

3.2.3. Other emerging, non-traditional CVD risk factors in women

Other conditions that are emerging as non-traditional CVD risk factors in women include preterm delivery, systemic autoimmune diseases (such as rheumatoid arthritis and systemic lupus erythematosus), breast cancer treatments, and depression [16,30] (Fig. 1).

Spontaneous preterm delivery appears to be an independent risk factor for the development of ischemic heart disease (IHD), stroke, and overall CVDs according to a meta-analysis including 10 cohort studies from five north western European countries and follow-ups that ranged from 12 to 35 years [55]. Using data from ≈70,000 participants in the Nurses' Health Study II, Tanz et al. [56] recently demonstrated that preterm delivery (< 37 weeks gestation) was associated with an increased risk of future CVDs (HR of 1.42); remarkably, only a modest proportion of the increased risk was accounted for by the postpartum development of conventional CVD risk factors, which suggests that the association between spontaneous preterm delivery and CVD risk is mediated by alternative mechanisms [56]. At present, these mechanisms are not well understood, but it has been suggested that the increased inflammatory status observed in women with preterm delivery may play a role [55,56].

Many population studies attest the association between excess cardiovascular burden and systemic autoimmune diseases [57]. Little is known about the relationships between systemic autoimmune diseases and sex, but it has been proposed that the microvasculature may play an important role in the predisposition of women with autoimmune diseases to develop accelerated CVDs [58]. Since systemic autoimmune diseases are generally more prevalent among female subjects, they represent more common CVD risk factors in women compared to men [30,58].

Breast cancer treatments also represent important causes of excess CVD risk in women, due to incidental exposure of the heart to the deleterious effects of ionizing radiations and to the cardiotoxicity of the breast cancers chemotherapeutic agents [30,59]. Since there has been an enormous improvement in the survival rates of breast cancer, the focus on cardiac health in breast cancer patients is becoming a priority.

Increasing evidence indicates that depression is a prevalent risk factor for the development of CHD and a predictor of unfavorable outcomes after a CHD event [60]. Overall, hundreds of studies investigated the relationship between depression and the onset and progression of CHD [60]. These investigations suggest that, although depression is associated with other cardiac risk factors (such as sedentary life), it is an independent risk factor for CHD morbidity and mortality [60]. Since depressive disorders are more common in female subjects, especially young women, they can affect women's CVD risk disproportionately [61,62]. Many possible pathogenetic mechanisms have been proposed to explain the relationship between CVDs and depression. Recently, we (C.B.) found an association between the brain-derived neurotrophic factor (BDNF) Val66Met polymorphism and the enhancement of thrombosis in an experimental model of carotid injury or the increased occurrence of acute coronary syndromes in a human coronary artery disease (CAD) cohort [63]. These findings provide a potential mechanistic link between depression and CAD; however, major challenges remain to be addressed for assessing the potential cause–effect relationships of this association in humans. Given the enormous public health impact of depression and heart disease, efforts are needed to gain further insights into gender and individual differences in the susceptibility for depression and CVDs, which could contribute to the improvement of both prevention and treatment.

4. Sex and gender differences in CVD manifestations and underlying pathophysiological mechanisms

CVDs occur and progress differently in the two sexes [10,11]. An overview of sex and gender differences in the manifestations of CVDs and the underlying pathophysiological mechanisms is provided below.

4.1. Ischemic heart disease

In the context of IHD, evidence of an uniquely female pattern of disease is emerging, including not only atherosclerotic CAD, but also an expanded spectrum of coronary disease, comprising coronary microvascular dysfunction (CMD), spontaneous coronary dissection (SCAD), and Takotsubo cardiomyopathy [30]. Furthermore, women with IHD typically have a poorer prognosis then men [30].

With regard to CAD, women have often a non-obstructive pattern that differs from the traditional male model of obstructive CAD [30]. Moreover, several histological observations attest the existence of differences in the morphology of atherosclerotic plaques underlying CAD in men and women [7]. According to registry data of patients dying from coronary thrombosis, plaque rupture is more frequent in men than women, whereas plaque erosion is more frequent in women than men [64,65]. In women, this pattern seems to be affected by the hormonal status, since pathological observations indicate that the incidence of plaque rupture is higher than that of erosion in postmenopausal compared to premenopausal women (87% vs. 17%, P = 0.001) [65].

CMD, defined as limited coronary flow reserve and coronary endothelial dysfunction, is another frequent cause of IHD in women, associated with increased rate of cardiac death, stroke, or HF. It is characterised by a decrease in the size of epicardial vessels and microvasculature, diffuse atherosclerotic disease, increased arterial stiffness and fibrosis, altered remodeling, and the presence of endothelial or smooth muscle dysfunction [30]. Interestingly, impaired coronary flow reserve in the absence of obstructive CAD has recently been associated with excess cardiovascular risk in women [66].

SCAD is an uncommon cause of acute myocardial ischemia that occurs when a tear forms between the layers of a coronary artery, and most frequently (> 90%) affects women below 60 years of age [30,65].

The classic presentation is of a young healthy woman, without traditional atherosclerotic CVD risk factors, and sudden onset of acute coronary syndrome [30].

Takotsubo cardiomyopathy, affecting postmenopausal women in nearly 90% of the reported cases, is another sex-specific cause of transient acute ischemic heart disease. The etiopathology of Takotsubo cardiomyopathy is not clear; proposed mechanisms include multivessel coronary artery spasm, impaired cardiac microvascular function, endogenous catecholamine-induced myocardial stunning and myocarditis [30,65].

4.2. Heart failure

HF, which occurs when the heart muscle is weakened and cannot pump enough blood to meet the body's needs for blood and oxygen, has a high prevalence in old age, affecting > 10% of those above 70 years in Western societies and typically more women than men [11]. In particular, women are ≈ twice as likely as men to develop HF with preserved ejection fraction, a condition for which no treatment has yet proved effective [11,30].

4.3. Other vascular diseases

Other manifestations of CVD showing sex/gender-related differences include ischemic stroke, peripheral arterial disease (PAD), and abdominal aortic aneurysm (AAA).

Women have an increased lifetime incidence of stroke compared with men, largely because of a sharp increase in stroke risk in older postmenopausal women, and an increased lifetime prevalence of stroke risk factors, including hypertension, abdominal obesity and metabolic syndrome [30]. Furthermore, elderly women have more severe strokes and greater disability compared with age-matched men [67]. With regard to the underlying pathohistological characteristics, evidence suggests that carotid plaque morphology differs between men and women: women with a carotid stenosis have more stable plaques than men, independent of clinical presentation and cardiovascular risk profile [68], while plaques from men are associated with more cellularity, more inflammatory infiltrates, and more neovascularization [69].

PAD is now recognized to be associated with comparable morbidity and mortality to CAD and stroke, and is associated with significantly reduced quality of life [30]. Similar to CAD, PAD is more prevalent in men than women at younger ages, but the incidence rises in women after menopause; in addition, women generally display more severe PAD compared to men and experience greater complications [67].

AAA is a localized ballooning of the abdominal aorta. It is 4 to 6 times more prevalent in men than women, and develops in women ≈ 10 years later than in men, although it has worse outcomes in women [30]. The underlying reasons for males being predisposed are still not completely clear because of the disease's complex pathogenesis [67].

5. Gender proteomics in CVD

A clear understanding of the mechanisms underlying sexual dimorphisms in pathophysiology is crucial for precision medicine, in which the knowledge of the molecular bases of diseases is considered essential for the definition of appropriate preventive and therapeutic approaches [9]. In this context, proteomics, and 'omics approaches in general, can provide powerful tools to analyse physiological and disease-induced biological states at the molecular level, taking into account both the organism's intrinsic properties, such as genetic factors, and the effects of lifestyle, diet, and environment. The development of sophisticated analytic platforms to handle increasingly complex data now enables the analysis of complex biological samples with a high throughput rate, offering an extremely useful and versatile analytical tool for biomedical researches that expand from the screening of early diagnostic and prognostic biomarkers to the investigation of the molecular mechanisms underlying CDVs. Proteomic studies focused on sex and gender-related differences in CVDs are still very rare, but they are expected to increase in the coming years and will provide novel insights into the pathophysiology and clinical manifestations of these diseases.

In the following paragraphs, we illustrate the most relevant examples of proteomics studies to date that have focused on sex/gender-related differences performed to date in the context of CVDs.

5.1. Proteomics of biological fluids

5.1.1. Plasma and serum

Although proteomics of biological fluids has the potential to identify novel proteins that can improve the accuracy of cardiovascular risk prediction, many challenges still exist. Nowadays the plasma, with > 10,000 proteins identified (http://www.plasmaproteomedatabase.org), represents the most challenging proteome due to the exceptionally wide concentration range of the proteins, from micromolar to femtomolar level [70], and the presence of highly abundant proteins (e.g. albumin; immunoglobulins) that constitute > 99% of the total protein amount. As a consequence, discovering and validating novel protein biomarkers for CVDs in plasma is very challenging [71], especially when the aim is the detection of gender-specific biomarkers.

Interest in gender differences in plasma dates back to the 1960s, when some papers described such aspects mainly in animal studies, such as in monkey and fish [72,73]. More recently, studies performed on serum of cardiovascular patients have highlighted gender-related differences. Serum adipocyte fatty acid-binding protein (A-FABP) levels, for example, have a greater impact on atherosclerosis in women, being independently associated with carotid intima-media thickness, probably due to the higher fat percentage in women, to a difference in regional fat distribution, or to sex hormones regulation [74]. Furthermore, in the non-diabetic population, smoking associates differently with subclinical inflammation in the two sexes, with a decreased adiponectin level in women and with an increased hs-CRP level in men [75].

The first systematic proteomic study specifically addressing differences in serum protein composition between healthy male and female subjects, was conducted by Miike et al. in 2010 [76]. By removing highly abundant proteins and combining iTRAQ labeling, HPLC, nano-LC and MS, the authors succeeded in identifying and analysing 4000 proteins from the human serum. They found differences in the serum proteome of males and females: proteins more abundant in females participated in cascades commonly involved in female diseases, such as breast cancer and arthritis, whereas proteins more abundant in males were involved in hormonal response and were usually activated in conditions such as hypertrichosis and virilism [76].

To circumvent the limitations of immunodepletion-based strategies, which may lead to biases because of cross-reactions of the antibodies used or by proteins bound to carrier proteins such as albumin [77,78], a subproteome enrichment by size-exclusion chromatography followed by iTRAQ 2D-LC-nESI-FTMS analysis of whole serum of obese adults was performed by Al-Daghri et al. [79]. Among the 2472 identified proteins, 248 proteins exhibited significant modulation between women and men. A key observation was the gender-specific differences in proteins associated with β-estradiol signaling and immune system, which were less abundant in males than in females, whereas the opposite occurred for proteins involved in lipid and testosterone metabolism, vitamin D signaling, and coagulation [79].

The utility of proteomics to identify disease markers is becoming increasingly evident in multifactorial diseases, such as CVDs, for which the value of using more than one marker has been highlighted in several studies [80,81]. Zethelius et al. [80] suggested that a combination of biomarkers reflecting the myocardial cell damage (i.e. troponin I), left ventricular dysfunction (i.e. N-terminal pro-brain natriuretic peptide), renal failure (i.e. cystatin C), and inflammation (i.e. C-reactive protein)

could improve the risk stratification with respect to a model essentially based on established risk factors. A more extensive study, including 47 selected markers of inflammation, lipoprotein metabolism, adipocyte metabolism, calcification and thrombosis measured by a multiplex immunoassay, was performed in 2561 men and women of African-American and non-Hispanic White ethnicity [81]. The authors reported an association between female sex and levels of inflammatory and calcification markers, insulin-resistance promoting adipokines, natriuretic peptides, and coagulation factor levels and activity, independently of potential confounding variables [81].

5.1.2. Urine

Another interesting biological fluid in proteomics is urine; similarly to plasma, it provides information not only from the urinary track, but also from other organs, potentially providing biomarkers for other systemic diseases. Moreover, urinary proteomics may be advantageous in terms of non-invasiveness of urine sampling, low dynamic range of analytes which facilitates the detection and analysis of biomarkers, lack of requirement for special sample preparation, and relative stability of the stored sample [82]. Of course, the interest in urinary proteome developed first in the field of urologic and kidney diseases, in particular in IgA nephropathy [83] and prostate cancer [84], but there is now an increasing interest in investigating urine as an orthogonal sample for studying systemic diseases [85]. Indeed, ongoing clinical trials involving urinary proteomics for protein biomarker discovery or validation (registered at clinicaltrials.gov) included studies in urologic and kidney diseases, as well as studies analysing urine along with orthogonal bodily fluids or tissue samples in diseases spanning neurology, cancer, and cardiology, among others [85].

The central question about individual variability or gender-related variations in the normal urine proteome was first addressed by Thongboonkerd et al. [86], who observed using two-dimensional electrophoresis (2-DE) that total protein was higher in male urine compared to female urine, but there were fewer protein spots. Recently, a study based on a 2D-LC-MS/MS and iTRAQ approach provided evidence of significant differences between the male and female urinary proteomes [87]. In particular, the females had higher abundance of some lipid and carbohydrate metabolism-related proteins. The analysis also revealed a larger inter-individual variation in the female urinary proteome than in males, maybe due to the higher variation in the levels of proteins associated with inflammatory response and cell movement and migration [87].

The analysis of the urinary proteome in females and males is extremely timely considering the diagnostic utility of the urinary proteomics in the cardiovascular field. In 2012, Kuznetsova et al. [88] found a panel of urinary proteins that were specific for essential hypertension with left ventricular dysfunction from a discovery set in asymptomatic hypertensive patients; this set also distinguished, in a validation test, hypertensive patients with HF from healthy controls. The same authors also found that, in the general population, the urinary proteome correlated with diastolic LV dysfunction [89], and that the urinary peptide-based classifier, but not systolic pressure, predicted the incidence of fatal and nonfatal cardiovascular and cardiac events over a follow-up period of 5 years in 791 randomly recruited Flemish subjects [90].

5.2. Tissue proteome

5.2.1. The aging myocardium

The first proteomic study with a particular emphasis on myocardial gender differences was performed in a primate model of aging heart and published by Yan et al. in 2004 [91]. By employing 2-DE coupled to mass spectrometry (2-DE/MS), the authors found that only in the left ventricular samples of male monkeys there was a decreased abundance of enzymes participating in glycolysis (e.g. pyruvate kinase, α-enolase), glucose oxidation (pyruvate dehydrogenase E1 β), the tricarboxylic acid cycle (oxoglutarate dehydrogenase), and the electron transport system (complexes III–V) accompanied by a reduced capacity of mitochondria for oxygen consumption. As these differences were also present in the human failing heart [92,93], they could be involved in the pathogenesis of the disease, whereas the absence of these changes in females might explain their delayed cardiovascular risk.

5.2.2. Sex differences in pressure overloaded heart

Left ventricular hypertrophy (LVH), characterised by the growth in left ventricular mass caused by increased cardiomyocyte size, can be a physiological adaptation to strenuous physical exercise or a pathological condition, which is either genetic or secondary to left ventricular overload. While physiological LVH is usually benign and regressive, pathological LVH is a compensatory phenomenon, which eventually may become maladaptive and evolve towards progressive left ventricular dysfunction and HF. A large number of studies have recognized the influence of sex and/or gender on pathological cardiac remodeling and have shown differences in clinical outcomes and therapeutic responses, with males more prone than females to develop greater cardiac remodeling responses in hypertensive condition and aortic stenosis (reviewed in [94]). In the latter case, the cardiac performance is more preserved in female compared with male patients with a similar degree of aortic stenosis [95,96]. Whether sex/gender-related differences result from intrinsic differences in molecular adaptation to pressure overload, or are related to age, degree of stenosis, left ventricle geometry or other factors extrinsic to the myocardium is not currently known. By employing the transverse aortic constriction model to simulate pressure overload in male and female wild-type (WT) and estrogen receptor β (ERβ) knockout mice, Kararigas et al. [97] found that in WT mice, hypertrophy was significantly more pronounced in males than females, an effect that was abolished in ERβ knockout mice, thus supporting the hypothesis of a cardioprotective effect of estrogen in pressure overload [98]. To provide mechanistic insights into the influence of sex and ERβ on the heart response to pressure overload, they used 2-DE/MS and found decreased levels of several metabolic and mitochondrial proteins, a finding compatible with the negative outcome in males. For example, males with pressure overload had a reduced level of aldehyde dehydrogenase, which has been shown to play a major role in cardioprotection and maintenance of contractile function in alcohol-induced left ventricular hypertrophy and ischemia/reperfusion injury [99,100]. Furthermore, in male ERβ knockout mice with pressure overload there was a substantial decrease in the levels of several myosin heavy chain isoforms compared with the sham control group, suggesting an increased susceptibility of male ERβ knockout mice to impairments in the functional and structural adaptation to pressure overload. On the other hand, in female mice proteins that might confer cardioprotection, such as cytoskeletal and structural proteins, appeared to be elevated in response to pressure overload [98]. Vinculin, for example, is an important protein of the cytoskeleton, an actin-binding protein whose mutations can cause dilated cardiomyopathy in humans [101]. Thus, this proteomic analysis suggests that the response of the heart to pressure overload is highly modulated by sex and that ERβ is crucial for the tight regulation of mechanisms active in the development of left ventricular hypertrophy.

5.2.3. Cardioplegia

Cardioprotection afforded by cardioplegia, a reproducible and safe method to induce and maintain electromechanical cardiac quiescence during surgeries, has been found to be significantly lower in the aged female compared with the aged male rabbit heart [102]. These findings are in accordance with human studies indicating that women have a significantly higher risk and worse outcomes after cardiac surgery with respect to men [103,104]. Furthermore, in patients undergoing coronary artery bypass grafting (CABG), women have a significantly higher operative mortality and less favorable long-term survival than men [104]. Multivariate analysis also shows that women have higher

mortality rates than men in low-risk and medium-risk groups. Only among very high-risk patients is gender not found to be an independent predictor of adverse outcomes [104]. Among possible mechanisms involved in these gender differences, mitochondrial function seems to be modulated by gender, as well as by age, suggesting a role in the gender-related responses to global ischemia and to the cardioprotection afforded by cardioplegia [105].

A proteomic report by Black et al. [106] showed that specific pathways associated with the mitochondrion modulated cardioprotection using cardioplegia in the mature rabbit male and female hearts. Specifically, glycolysis/gluconeogenesis and the pentose phosphate pathway were affected in the aged male hearts, whereas glyoxylate/dicarboxylate metabolism was significantly altered only in female hearts. The authors suggested that an alteration of these pathways might contribute to decreased myocardial functional recovery and myonecrosis following ischemia [106]. It is expected that improved understanding will pave the way to future cardioprotective approaches.

5.2.4. Atherosclerotic plaque

Notwithstanding the high heterogeneity of atherosclerotic lesions, which makes plaque analysis a challenging task, proteomic profiling of human plaque samples has been shown to be a feasible approach for the analysis of proteins within the atherosclerotic lesion [107,108]. A variety of proteomics techniques have been used, from 2-DE with peptide mass fingerprinting, to more complex mass spectrometry techniques, utilising LC-MS/MS, or a combination of these techniques [107,108]. Up to now, the only study that investigated the potential sexual dimorphism in plaque proteome was performed by Liang and colleagues, which used 2-DE combined with MALDI-TOF MS, as well as nLC-MS/MS for secondary confirmation, to analyse the proteomic profile of different regions of human carotid plaques [109]. Twenty six patients undergoing carotid endarterectomy were enrolled in the study, which had an equal gender ratio and very similar mean ages for men (72.6 ± 1.8 years) and women (71.4 ± 1.7 years). Different regions of human carotid plaques were studied, specifically fatty streak, plaque shoulder, plaque centre, and fibrous cap; these were compared to an internal control [109]. In this study, 2-DE/MS analysis identified 52 unique proteins, 41 of which were confirmed by nLC-MS/MS analysis, including proteins such as procollagen C-endopeptidase enhancer 1, biglycan, hepatoma-derived growth factor, calmodulin, SH3 domain-binding glutamic acid-rich like, and Protein S100-A11, which had not previously been mapped in human carotid plaques. By 2-DE/MS, the abundance of 18 proteins was found to be significantly altered in plaque regions compared to the internal control region. Of these proteins, 5 showed gender-specific alterations with 2-DE/MS, including ferritin light chain and transthyretin, which were also validated using nLC-MS/MS [109]. In men, a significantly higher content of ferritin light chain was detected in fibrous cap, in line with previous proteomic investigations showing an increased abundance of ferritin light chain in atherosclerotic plaque [110,111]. In contrast, the abundance of ferritin light chain was found to be significantly decreased in female carotid plaque relative to the respective internal control site [109]. These findings deserve further investigation, since ferritin light chain is responsible for the storage of iron in cells and the accumulation of tissue iron has been implicated in the progression of atherosclerosis [112]. On the other hand, the content of transthyretin was found to be significantly higher in female carotid plaque [109]. Transthyretin is an evolutionarily conserved carrier protein associated with cardiac amyloidosis and a serine peptidase that is suspected to play multiple pathophysiologic roles, including the cleavage of substrates such as apolipoprotein A-I, that might affect the development of atherosclerosis [113,114]. Its function within the atherosclerotic lesion and the significance of the gender difference in its abundance in human carotid atheroma, reported for the first time by Liang and colleagues [109], is unknown.

5.2.5. Adipose tissue

The first proteomic analysis addressing gender differences in visceral adipose tissue from type 2 DM patients was published in 2016 by Gomez-Serrano et al. [115]. Protein abundance changes reported in this study revealed distinctive male and female phenotypes in terms of the antioxidant response: levels of SOD1, SOD3 and several GST proteins were higher in men, and the peroxide-scavenging enzymes GPX1 and GPX3 were higher in women. Interestingly, the levels of fatty acid synthase were found to be increased in women, supporting the notion that visceral adipose tissue in women correlates with dysfunctional hypertrophic adipocytes characterised by a significant increase in cell size, in contrast to men who showed more numerous and smaller adipocytes (adipocyte hyperplasia). According to the authors, these novel findings suggest a worsening of the obese phenotype in women once type 2 DM emerges, due to an increased pro-inflammatory state and decreased visceral adipose tissue adipocyte hyperplasia compared to men, resulting overall in a more dysfunctional adipose tissue [115].

5.3. Circulating cells: platelets

That gender might influence platelet biology was anticipated over 30 years ago [116,117]. A state-of-the-art paper by Patti et al. [118] highlights that, although less represented in clinical studies, the female gender may obtain different benefits from antiplatelet therapy with respect to men. Also, the thrombotic and bleeding risks, as well as outcomes after a cardiovascular event, appear to differ between genders. Among the multiple factors involved in these effects, hormonal mechanisms and differences in platelet biology might contribute to different gender characteristics. From a biochemical point of view, it is well known that many differences occur in platelets between females and males: the platelet count differs significantly, with higher values in women than in men [119]; in women, platelets have a higher number of surface receptors and bind a greater amount of fibrinogen (reviewed in [118]); their reactivity is also different, both with and without antiplatelet therapy [120]. The increased platelet responsiveness in females, at least in animal models, appears to be an intrinsic feature of the platelet itself, independent of the platelet size and the expression of surface adhesion molecules [121].

In recent years, it has become increasingly evident that proteomics can provide novel insights into basic research questions regarding the protein composition and the post-translational modifications (PTMs) occurring in platelets, which might be useful to understand the impact of the diseases and, eventually, of therapeutic interventions [122]. Indeed, platelet signaling is much more complicated and nonlinear than originally anticipated, involving a considerable level of cross talk among signaling pathways. However, as yet no proteomic study has addressed the issue of sex/gender-specificity of platelet proteomics in the cardiovascular system, with the exception of a single paper on human platelets derived from volunteers [123]. In this study, using protein microarrays, Eidelman et al. showed that gender differences appeared in the low abundance signaling proteome, whereas 2-DE revealed only high abundance proteins that did not differ between genders. Considering that there are still gaps in knowledge on gender-specific platelet biology and antiplatelet therapy, and that the percentage of women included in clinical trials evaluating the impact of antiplatelet drugs on cardiovascular outcomes (≈ 30%) has not changed in the last 20 years, it is evident that more women need to be included in order to produce strong evidence-based recommendations on the topic.

5.4. Gender dependence of nutritional effects on proteomics

In the nascent arena of nutriproteomics, proteomics aims to characterise the molecular and cellular changes occurring at the protein level following exposure to food nutrients. Indeed, proteomics in nutritional sciences can help indeed to understand the impact of nutrients

on living systems, to identify potential biomarkers that can aid in lifestyle changes or dietary habits, and, finally, to assess food safety and functionality [124].

As discussed by Anand et al., short-term controlled-feeding studies with CVD risk factors as outcomes, long-term prospective cohort studies with CAD, stroke, and type 2 DM as outcomes, and a limited number of randomized controlled trials with CVD endpoints collectively show that multiple aspects of diet substantially influence CVD risk [125]. This review, as many others [126,127] underlines that the traditional Mediterranean-type diet, characterised by a high intake of olive oil, fruit, nuts, vegetables, and cereals; a moderate intake of fish and poultry; a low intake of dairy products, red meat, processed meats, and sweets; and wine in moderation, provides a well-tested healthy dietary pattern to reduce CVD risk by about a third. A series of papers by Bedard [128–131] showed that men have greater cardiometabolic changes than premenopausal women in response to the Mediterranean diet. Up to now, some proteomics studies have been performed to investigate the effects of nutrients typical of the Mediterranean diet, i.e. olive oil and omega-3 fatty acids, on different specimens (lipoproteins, urine, peripheral blood mononuclear cells, platelets) in the context of CVDs [132–138], but no one has specifically addressed sex or gender differences.

Beyond the impact of food on the proteome, there is convincing evidence, at least from animal models, that caloric restriction benefits health by slowing the aging process and delaying the onset of age-associated chronic diseases, including CVD. Several studies have now demonstrated that cardiovascular aging can be affected by changes in food intake [139,140], mainly due to reductions in inflammation and oxidative stress: in the vasculature, caloric restriction appears to protect against endothelial dysfunction and arterial stiffness and attenuates atherogenesis by improving several cardiometabolic risk factors; in the heart, it reduces cardiomyocyte apoptosis, protects against fibrosis, and preserves or improves left ventricular diastolic function [141]. While there is strong evidence supporting the inclusion of modest caloric restriction in lifestyle programs targeting cardiovascular health, the impact of caloric restriction on human health is not fully understood and deserves further investigation [142].

The aging process is further complicated by the sex differences in lifespan, which is a world-wide phenomenon with women outliving men by more than a decade in some countries, and not unique to humans because most sexually reproducing species show sex differences in patterns of aging. A comprehensive explanation does not currently exist, even if interference of sex-steroids and altered activity of nutrient-sensing pathways may contribute [143]. Up to now, only one paper has addressed the combined effects of gender and caloric restriction at the proteomic level. Valle et al. found that females differ remarkably from males in the mechanisms that regulate substrate utilisation and energy metabolism, in the antioxidant systems, and in the stress response [144]. Caloric restriction also affects overlapping sets of proteins and many of the gender differences are attenuated by caloric restriction suggesting that cellular pathways are similarly regulated in females and caloric restricted rats and could be related with a greater longevity [144].

6. Gender differences in oxidative stress and oxidative PTMs in CVDs

6.1. Oxidative stress in CVDs

Partially reduced oxygen species (PROS; e.g. superoxide radical anion, hydrogen peroxide, hydroxyl radical) and oxynitro species (e.g. nitric oxide, peroxynitrite) at physiological levels play an important role as regulatory mediators in fundamental cell functions and contribute to the maintenance of cell homeostasis [145]. In contrast, a redox imbalance in favor of pro-oxidant processes leads to oxidative stress and oxidative damage, which have been implicated in the pathogenesis of a wide variety of diseases including cancer, neurodegenerative diseases, and vascular diseases [145]. In particular, oxidative stress is one of the most potent inducers of endothelial dysfunction and is involved in the initiation, progression and clinical manifestation of atherosclerosis [146–148]. Moreover, several conditions that represent risk factors for CVD, such as hypertension, diabetes mellitus, metabolic syndrome, obesity and cigarette smoking, are strongly linked to oxidative stress [149].

Evidence is emerging for gender differences in the occurrence and susceptibility of redox imbalance and oxidative stress, including in the cardiovascular system. For example, gender differences have been found in circulating leptin, which has proinflammatory properties, and leptin levels were found to correlate with increased total glutathione [150]. Markers of oxidative stress have mostly been reported to be lower in females than males during the first decades of life, but oxidative stress appears to be elevated in post-menopausal women when compared to pre-menopausal women, and is thought to play a major role in menopause symptoms such as hot flushes and osteoporosis, which argues for the involvement of female sex-hormones in maintaining low oxidative status [151]. In elderly people the redox balance seems to be inverted; for example, higher serum hydroperoxide levels have been observed in female CAD patients compared to males with CAD [151,152]. As a result, it has been suggested that estimation of oxidative stress could be a useful biomarker for cardiovascular risk especially in elderly women [153]. However, “oxidative stress” is a composite of many different parameters and therefore comes in a variety of forms; there is no single universal measure. This emphasizes the importance of using a panel of redox biomarkers appropriate to the disease condition [154]. In atherosclerosis and other vascular dysfunctions, the presence of lipid oxidation products such as lipid hydroperoxides, small reactive aldehydes (malondialdehyde, hydroxynonenal) or oxidized LDL have commonly been analysed by a variety of methods [149,155].

Oxidative stress can lead to oxidative modifications of proteins, with a variety of (mostly deleterious) effects on the functions of those proteins, and it is increasingly appreciated that a full understanding of the proteome and how it is altered by physiological conditions (such as gender) or disease requires analysis of all different protein forms, as discussed below.

6.2. PTMs and protein speciation in CVDs

The existence of PTMs and their effect on protein function has been recognized for many years: for example, phosphorylation is an archetypal PTM that regulates activity of many enzymes and interactions of proteins, but the number and types of PTMs existing is now known to be very extensive [156]. However, many proteomics studies simply seek to identify proteins in samples, and the issue of variability in protein structure is thus often ignored. This approach has significant limitations for understanding cellular processes, as explained by Jungblut et al. (2008), who coined the termed “protein speciation” to reflect the enormous variety in protein chemical structures over and above the amino acid sequence [157]. “Protein species” are defined as different protein forms resulting from covalent modifications of the protein with functional relevance [158]; they are thought to occur for most mammalian genes, and it has been estimated that, while the number of genes encoding human proteins is approximately 20,000, the number of human protein species is in the range of 1 billion. Species variation arises at every step from gene expression to protein degradation, and influences subcellular localization, degradation, subunit assembly, tertiary structure or enzyme activity.

Nowadays it is clear that information at the protein species level cannot be ignored to obtain biological relevant information on a protein. Indeed, the success rate of FDA approved diagnostic markers to date is very low compared to the number of published disease markers, and it has been suggested by Steffen et al. [159] that the biochemistry

of the proteins and especially the occurrence of a multitude of protein species originating from a single gene is a major reason for this. This is particularly important in the setting of heart disease, which comprises a diverse range of acute (such as ischemia/reperfusion), chronic (such as heart failure, dilated cardiomyopathy) and genetic (such as hypertrophic cardiomyopathy) disease states, all of which have been associated with protein PTMs [160]. These notions on relationships of function to the exact chemical formula of the protein species have recently been discussed in a Special Issue of the Journal of Proteomics (2016), with recommendations on how to improve studies of a proteome, particularly in the disease state, in the future [161]. In CVD research, the protein species concept has been introduced by Schwab et al., who performed a 2-DE/ESI-LC-MS approach to assess the effect of a dietary supplement with the phytoestrogen genistein on the protein patterns involved in the maintenance of normal heart physiology at the protein species level [162,163]. By this approach, the authors observed a substantial impact of sex, age, and genistein on the abundance of a multitude of protein species, especially mitochondrial enzymes involved in the fatty acid metabolism or playing a role in the tricarboxylic acid cycle or the respiratory chain [163].

Because it is not possible in this review to consider all of the possible PTMs, the next sections focus on oxidative modifications, as there is growing interest in proteomics and analysis of oxidative PTMs (oxPTMs) to proteins in CVDs. While many oxidative modifications to proteins can occur, including oxidations of cysteines, methionines, prolines, as well as hydroxylations, chlorinations and nitrations of tyrosines or tryptophans, only a subsection of these are thought to have regulatory effects [156]. Many other modifications may have no functional effect, or simply cause loss of activity. Another interesting category of oxPTMs are those caused by adduct formation by small reactive aldehydes, which includes the formation of AGEs (advanced glycation end products) and ALEs (advanced lipoxidation end products); some functional effects have been described for these modifications, such as altered binding to the receptor for AGEs or altered subcellular localization.

Analysis of all of these oxPTMs by mass spectrometry is extremely challenging [164], and this is especially true of glycation and lipoxidation [164–166]. Unlike enzymatically-induced modifications, such as phosphorylation, ubiquitinylation or farnesylation, which occur on specific residues, oxPTMs tend to occur randomly on a number of susceptible residues and proteins, making it extremely difficult to define all protein species. Thus improved enrichment processes and mass spectrometry-based methods for detection of oxPTMs including AGEs and ALEs are urgently required. Development of untargeted and semi-targeted bottom-up MS methods together with improved data mining algorithms are currently being developed with the H2020 innovative training network MASSTRPLAN (Project ID: 675132; http://cordis.europa.eu/project/rcn/198275_en.html), and will ultimately help to identify a larger fraction of protein species and their role in CVDs. However, at the current time most work on oxPTMs in CVDs have been carried out by more conventional proteomics approaches, as described in the following section.

6.3. Emerging role of oxPTMs in CVDs

In the context of CVDs, the interest towards PTMs and especially oxPTMs of proteins has grown considerably. The analysis of PTMs should provide useful information for the identification of mechanisms potentially involved in the genesis and/or progression of CVD. Ranging from immediate and reversible modifications, such as phosphorylation and some oxidative modifications, which enable rapid response to changes in the cellular environment, to long-term and irreversible modifications, such as AGE formation, analysis of the PTM status of proteins can provide clues to the molecular basis of the underlying pathology. Furthermore, emerging evidence supports a major role of PTMs in regulating multiple pathways of the intracellular quality control mechanisms evoked by the cell to minimize the level and toxicity of misfolded proteins and defective organelles in the cell. Indeed, poor quality control is associated with many forms of heart diseases [167,168]. Liddy et al. [160] nicely described the most relevant PTMs that seem to be of emerging significance in cardiac disease, but within the Human Proteome Project further work is going on to identify and characterise as many PTMs as possible, including oxPTMs [169].

At the organelle level, the discovery and knowledge of PTMs occurring in the mitochondrial proteome have recently exploded with the advent of mass spectrometry and the most characterised PTMs and oxPTMs have been nicely reviewed by Stram et al. [170]. Many mitochondrial PTMs have a relevant role in signal transduction pathways, energy generation, apoptosis, autophagy, metabolism, and tissue response to ischemic injury, but the functional significance of the various mitochondrial PTMs in regard to their impact on the pathophysiology of disease remains an intense area of investigation [170]. Mitochondrial dysfunction almost certainly has a role in CVDs, such as stroke, HF, and cardiac ischemia/reperfusion injury [171,172]. Based on these assumptions, it is likely that prevention or reversal of mitochondrial damages might represent a potential target for the treatment of CVDs. At the time of writing, the only study that investigated PTMs in the mitochondrial proteome linked to gender differences was performed in rat hearts by Lagranha et al. [173], likely due to the lack of standardized methods to analyse mitochondrial proteome [174]. The authors found an increased phosphorylation of aldehyde dehydrogenase 2 and of the E2 subunit of alpha-ketoglutarate dehydrogenase in females, an event that may be responsible of the lower production of oxidants and of the cardioprotection of the female heart in the ischemia-reperfusion model.

7. Conclusions

The differences between females and males begin even before implantation of the zygote in the uterus and continue throughout prenatal development phases, in childhood and adulthood. These differences include diverse susceptibility to some diseases, such as certain types of cancer and autoimmunity, in which females have an overall higher susceptibility [175]. The existence of sexual diversities in the onset, manifestation, and outcome has now been recognized also in CVDs [6–8]. The endogenous causes of the sex differences observed in many diseases are largely unknown, and the situation in CVD research is not much different. Beyond environmental and social differences between men and women (e.g., occupational hazards, lifestyle, social stresses, access to healthcare) that can contribute to gender differences in CVDs, sex hormones and sex chromosomes have been found to account for some sex differences in CVDs [8,10–12]. However, several gaps in our understanding of sex- and gender-related diversities in cardiovascular health still exist. The search for sex/gender-related mechanisms is further complicated by the still-increasing sex bias in preclinical research [14], despite the fact that in 2014 the NIH announced that sex should be considered as a biological variable in applications for preclinical research funding [15].

By generating large sets of molecular data, ‘omics technologies, including genomics/transcriptomics, proteomics, metabolomics, lipidomics and others, can provide deep biological insight into human health and disease. Applications of these technologies to investigations aimed at elucidating the causes underlying sex- and gender-related diversities in pathophysiology is a challenging task. While great technological progress has been made and some excellent bioinformatic methods are currently available for computational analysis, further improvements in the acquisition, storage, handling and integration of large volumes of data are needed [176]. In particular, a crucial aspect of ‘omics studies on complex phenotypes such as CVDs is the collection of high-quality biological samples providing the basis for the creation of large data sets that can accurately incorporate the many sources of variability (including key variables as race/ethnicity, age, and sex/

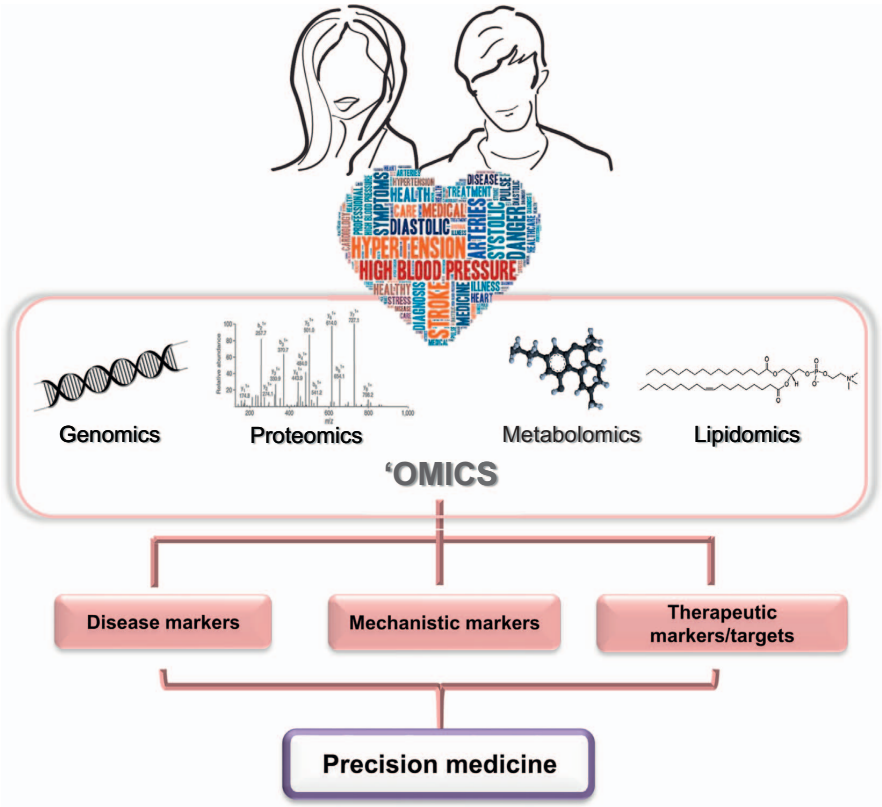

Fig. 2. 'Omics applications in cardiovascular research: unveiling sex/gender-differences in CVDs. The figure highlights the role of proteomics in biomedical researches that expand from the screening of early diagnostic and prognostic biomarkers to the investigation of the molecular pathways underlying CDVs. The deciphering of proteomes via protein speciation, and its integration with genomics/transcriptomics, metabolomics, and lipidomics, may reveal novel mechanisms responsible for sex/gender-differences in CVDs, thus providing new opportunities oriented towards precision medicine.

gender) into rigorous statistical models [176]. Notwithstanding these challenges, it is hoped that, by exploiting multi-omics approaches to integrate information about gene expression and protein species composition of an organism with metabolic fingerprints and lipid profiles (Fig. 2), we will gain a more comprehensive understanding on how sex and gender impact cardiovascular health. This is an exciting field where 'omics approaches could make a significant contribution to precision medicine [177].

Finally, the current knowledge of the relationship between the function and the exact structural formula of protein species to health and disease suggests that the focus on disease-associated protein species in the future will bring to more specific disease markers. Last, the exact chemical composition including not one but every posttranslational modification and complete sequence coverage at the protein species level should be achievable with further progress in sample preparation techniques, especially concerning separation techniques at the protein level, mass spectrometry and algorithms for mass spectrometric data processing.

Executive summary

Clinically important sex- and gender-related differences exist in risk factors, occurrence, management and outcomes of cardiovascular diseases (CVDs).

Traditional CVD risk factors affecting both men and women

- Hypertension
  - Slightly higher prevalence in men than in women
  - Uncertain whether the association between increments in systolic blood pressure and CVDs differs between men and women
- Dyslipidemia
  - Similar prevalence of elevated total cholesterol (TC) in men and in women
  - Similar TC-related risk of CHD in men and in women
- Diabetes mellitus (DM)
  - Similar prevalence in men and in women
  - Higher excess risk of coronary heart disease (CHD), stroke, heart failure (HF), and peripheral arterial disease (PAD) in diabetic women compared with diabetic men
- Excess body weight
  - Similar prevalence in men and in women
  - Similar association between body mass index (BMI) and CHD in men and in women
  - Hormone-related sex dimorphism in patterns of body fat storage and fat metabolism potentially affecting the relationship between excess body weight and CVD risk
- Cigarette smoking
  - Mortality from CVDs higher in women than in men who smoke
  - Higher risk of developing CHD in women than men with the same exposure to tobacco smoke
  - Similar beneficial effects of smoking cessation on CVD risk in women and in men

Women-specific CVD Risk Factors

- Pregnancy complications
  - Hypertensive disorders of pregnancy and gestational DM are important women-specific factors to consider in CVD risk assessment
- Age at menopause
  - Women who undergo menopause before age 50 or primary ovarian insufficiency have an increased risk of CVDs
  - Controversy remains regarding the cardiovascular effects of menopausal hormone therapy; the current consensus is that it should never be prescribed for the aim of preventing CVDs
- Emerging, non-traditional CVD risk factors in women
  - Preterm delivery, systemic autoimmune diseases, breast cancer treatments, and depression are new emerging factors that can affect CVD risk in women

Sex/gender-differences in CVD manifestations and underlying pathophysiology

- Coronary artery disease (CAD)
  - Prevalence higher in men than women at younger ages, but the incidence rises in women after menopause
  - Prevalence of obstructive CAD phenotype in men vs. non-obstructive CAD in women
  - Plaque rupture more frequent in men than in women; plaque erosion more frequent in premenopausal women than in men
  - Poorer prognosis in women compared to men
- CVDs more prevalent in women
  - Expanded spectrum of coronary disease in women, comprising coronary microvascular dysfunction (CMD), spontaneous coronary dissection (SCAD), and Takotsubo cardiomyopathy
  - HF (particularly with preserved ejection fraction) affects typically more women than men
- Ischemic stroke
- Increased lifetime incidence in women compared with men
- More severe strokes and greater disability in elderly women compared with age-matched men
- PAD
  - Prevalence higher in men than women at younger ages, but the incidence rises in women after menopause
  - More severe PAD in women compared to men
- Abdominal aortic aneurysm (AAA)
  - Prevalence higher in men than women
  - Worse outcomes in women

Role of oxidative stress in CVDs

- Several conditions that represent risk factors for CVDs are strongly linked to oxidative stress
- Oxidative stress is involved in the initiation, progression and clinical manifestation of atherosclerosis
- Evidence is emerging for gender differences in the susceptibility to oxidative stress
- Oxidative stress can lead to oxidative modifications of proteins (oxPTMs), with a variety of (mostly deleterious) effects on their functions
- oxPTMs, together with other post-translational modifications, are actually an intense area of investigations by proteomics

Gender proteomics in CVDs

- Applications of ‘omics technologies to investigations aimed at elucidating the causes underlying sex- and gender-related diversities in pathophysiology is a challenging task
- A full understanding of the proteome and how it is altered by physiological conditions (such as gender) or disease requires analysis of all different protein forms
- Proteomic studies in this field are still very rare, but they are expected to increase over the next years
- Several gaps in our knowledge of sex/gender-related diversities in CVDs still exist. The successful integration of ‘omics technologies (including genomics/transcriptomics, proteomics, metabolomics, lipidomics, and others) could make a significant contribution to precision medicine developed on top of sex/gender-based assessments.

Transparency document

The Transparency document associated with this article can be found, in online version.

Funding

This work was supported by the European Union's Horizon 2020 research and innovation programme under the Marie Sklodowska-Curie grant agreement number 675132.

Financial and competing interest disclosure

The authors report no conflict of interest.

References

[1] W.H.O. (WHO), Cardiovascular diseases (CVDs). Fact sheet, http://www.who.int/mediacentre/factsheets/fs317/en/, (2017).
[2] D. Mozaffarian, E.J. Benjamin, A.S. Go, D.K. Arnett, M.J. Blaha, M. Cushman, S.R. Das, S. de Ferranti, J.P. Despres, H.J. Fullerton, V.J. Howard, M.D. Huffman, C.R. Isasi, M.C. Jimenez, S.E. Judd, B.M. Kissela, J.H. Lichtman, L.D. Lisabeth, S. Liu, R.H. Mackey, D.J. Magid, D.K. McGuire, E.R. Mohler III, C.S. Moy, P. Muntner, M.E. Mussolino, K. Nasir, R.W. Neumar, G. Nichol, L. Palaniappan, D.K. Pandey, M.J. Reeves, C.J. Rodriguez, W. Rosamond, P.D. Sorlie, J. Stein, A. Towfighi, T.N. Turan, S.S. Virani, D. Woo, R.W. Yeh, M.B. Turner, Heart disease and stroke statistics-2016 update: a report from the American Heart Association, Circulation 133 (4) (2016) e38–360.
[3] M. Nichols, N. Townsend, P. Scarborough, M. Rayner, European Cardiovascular Disease Statistics, (2012).
[4] D.M. Lloyd-Jones, Y. Hong, D. Labarthe, D. Mozaffarian, L.J. Appel, L. Van Horn, K. Greenlund, S. Daniels, G. Nichol, G.F. Tomaselli, D.K. Arnett, G.C. Fonarow, P.M. Ho, M.S. Lauer, F.A. Masoudi, R.M. Robertson, V. Roger, L.H. Schwamm, P. Sorlie, C.W. Yancy, W.D. Rosamond, Defining and setting national goals for cardiovascular health promotion and disease reduction: the American Heart Association's strategic impact goal through 2020 and beyond, Circulation 121 (4) (2010) 586–613.
[5] M.F. Piepoli, A.W. Hoes, S. Agewall, C. Albus, C. Brotons, A.L. Catapano, M.T. Cooney, U. Corra, B. Cosyns, C. Deaton, I. Graham, M.S. Hall, F.D. Hobbs, M.L. Lochen, H. Lollgen, P. Marques-Vidal, J. Perk, E. Prescott, J. Redon, D.J. Richter, N. Sattar, Y. Smulders, M. Tiberi, H.B. van der Worp, I. van Dis, W.M. Verschuren, 2016 European Guidelines on cardiovascular disease prevention in clinical practice: the Sixth Joint Task Force of the European Society of Cardiology and Other Societies on Cardiovascular Disease Prevention in Clinical Practice (constituted by representatives of 10 societies and by invited experts) developed with the special contribution of the European Association for Cardiovascular Prevention & Rehabilitation (EACPR), Eur. Heart J. 37 (29) (2016) 2315–2381.
[6] L. Mosca, S.M. Grundy, D. Judelson, K. King, M. Limacher, S. Oparil, R. Pasternak, T.A. Pearson, R.F. Redberg, S.C. Smith Jr., M. Winston, S. Zinberg, AHA/ACC scientific statement: consensus panel statement. Guide to preventive cardiology for women. American Heart Association/American College of Cardiology, J. Am. Coll. Cardiol. 33 (6) (1999) 1751–1755.
[7] H.M. den Ruijter, S. Haitjema, F.W. Asselbergs, G. Pasterkamp, Sex matters to the heart: a special issue dedicated to the impact of sex related differences of cardiovascular diseases, Atherosclerosis 241 (1) (2015) 205–207.
[8] R.E. Harvey, K.E. Coffman, V.M. Miller, Women-specific factors to consider in risk, diagnosis and treatment of cardiovascular disease, Women's Health (Lond. Engl.) 11 (2) (2015) 239–257.
[9] S. Della Torre, A. Maggi, Sex differences: a resultant of an evolutionary pressure? Cell Metab. 25 (3) (2017) 499–505.
[10] A.P. Arnold, L.A. Cassis, M. Eghbali, K. Reue, K. Sandberg, Sex hormones and sex chromosomes cause sex differences in the development of cardiovascular diseases, Arterioscler. Thromb. Vasc. Biol. 37 (5) (2017) 746–756.

[11] V. Regitz-Zagrosek, G. Kararigas, Mechanistic pathways of sex differences in cardiovascular disease, Physiol. Rev. 97 (1) (2017) 1–37.
[12] S.J. Winham, M. de Andrade, V.M. Miller, Genetics of cardiovascular disease: importance of sex and ethnicity, Atherosclerosis 241 (1) (2015) 219–228.
[13] S.A.E. Peters, M. Woodward, V. Jha, S. Kennedy, R. Norton, Women's health: a new global agenda, BMJ Glob. Health 1 (3) (2016) e000080.
[14] F.D. Ramirez, P. Motazedian, R.G. Jung, P. Di Santo, Z. MacDonald, T. Simard, A.A. Clancy, J.J. Russo, V. Welch, G.A. Wells, B. Hibbert, Sex bias is increasingly prevalent in preclinical cardiovascular research: implications for translational medicine and health equity for women: a systematic assessment of leading cardiovascular journals over a 10-year period, Circulation 135 (6) (2017) 625–626.
[15] J.A. Clayton, Studying both sexes: a guiding principle for biomedicine, FASEB J. 30 (2) (2016) 519–524.
[16] Y. Appelman, B.B. van Rijn, M.E. Ten Haaf, E. Boersma, S.A. Peters, Sex differences in cardiovascular risk factors and disease prevention, Atherosclerosis 241 (1) (2015) 211–218.
[17] W.H.O. (WHO), Raised blood pressure. Situation and trends, http://www.who.int/gho/ncd/risk_factors/blood_pressure_text/en/.
[18] S.A. Peters, R.R. Huxley, M. Woodward, Comparison of the sex-specific associations between systolic blood pressure and the risk of cardiovascular disease: a systematic review and meta-analysis of 124 cohort studies, including 1.2 million individuals, Stroke 44 (9) (2013) 2394–2401.
[19] Y.C. Wei, N.I. George, C.W. Chang, K.A. Hicks, Assessing sex differences in the risk of cardiovascular disease and mortality per increment in systolic blood pressure: a systematic review and meta-analysis of follow-up studies in the United States, PLoS One 12 (1) (2017) e0170218.
[20] W.H.O. (WHO), Raised cholesterol: situation and trends, http://www.who.int/gho/ncd/risk_factors/cholesterol_text/en/, (2015).
[21] S.A. Peters, Y. Singhateh, D. Mackay, R.R. Huxley, M. Woodward, Total cholesterol as a risk factor for coronary heart disease and stroke in women compared with men: a systematic review and meta-analysis, Atherosclerosis 248 (2016) 123–131.
[22] T.F. Luscher, U. Landmesser, A. von Eckardstein, A.M. Fogelman, High-density lipoprotein: vascular protective effects, dysfunction, and potential as therapeutic target, Circ. Res. 114 (1) (2014) 171–182.
[23] J.W. Rich-Edwards, J.E. Manson, C.H. Hennekens, J.E. Buring, The primary prevention of coronary heart disease in women, N. Engl. J. Med. 332 (26) (1995) 1758–1766.
[24] E. Di Angelantonio, N. Sarwar, P. Perry, S. Kaptoge, K.K. Ray, A. Thompson, A.M. Wood, S. Lewington, N. Sattar, C.J. Packard, R. Collins, S.G. Thompson, J. Danesh, Major lipids, apolipoproteins, and risk of vascular disease, JAMA 302 (18) (2009) 1993–2000.
[25] N. Sarwar, P. Gao, S.R. Seshasai, R. Gobin, S. Kaptoge, E. Di Angelantonio, E. Ingelsson, D.A. Lawlor, E. Selvin, M. Stampfer, C.D. Stehouwer, S. Lewington, L. Pennells, A. Thompson, N. Sattar, I.R. White, K.K. Ray, J. Danesh, Diabetes mellitus, fasting blood glucose concentration, and risk of vascular disease: a collaborative meta-analysis of 102 prospective studies, Lancet 375 (9733) (2010) 2215–2222.
[26] I.D.F. (IDF), IDF Diabetes Atlas, 7th edn, International Diabetes Federation, Brussel, Belgium, 2015http://www.diabetesatlas.org.
[27] R. Huxley, F. Barzi, M. Woodward, Excess risk of fatal coronary heart disease associated with diabetes in men and women: meta-analysis of 37 prospective cohort studies, BMJ 332 (7533) (2006) 73–78.
[28] S.A. Peters, R.R. Huxley, M. Woodward, Diabetes as a risk factor for stroke in women compared with men: a systematic review and meta-analysis of 64 cohorts, including 775,385 individuals and 12,539 strokes, Lancet 383 (9933) (2014) 1973–1980.
[29] S.A. Peters, R.R. Huxley, M. Woodward, Diabetes as risk factor for incident coronary heart disease in women compared with men: a systematic review and meta-analysis of 64 cohorts including 858,507 individuals and 28,203 coronary events, Diabetologia 57 (8) (2014) 1542–1551.
[30] M. Garcia, S.L. Mulvagh, C.N. Merz, J.E. Buring, J.E. Manson, Cardiovascular disease in women: clinical perspectives, Circ. Res. 118 (8) (2016) 1273–1293.
[31] M. Woodward, S.A. Peters, R.R. Huxley, Diabetes and the female disadvantage, Women's Health (Lond. Engl.) 11 (6) (2015) 833–839.
[32] W.H.O. (WHO), Obesity and Overweight. Fact Sheet, (2017) http://www.who.int/mediacentre/factsheets/fs311/en/.
[33] G. Whitlock, S. Lewington, P. Sherliker, R. Clarke, J. Emberson, J. Halsey, N. Qizilbash, R. Collins, R. Peto, Body-mass index and cause-specific mortality in 900 000 adults: collaborative analyses of 57 prospective studies, Lancet 373 (9669) (2009) 1083–1096.
[34] D. Wormser, S. Kaptoge, E. Di Angelantonio, A.M. Wood, L. Pennells, A. Thompson, N. Sarwar, J.R. Kizer, D.A. Lawlor, B.G. Nordestgaard, P. Ridker, V. Salomaa, J. Stevens, M. Woodward, N. Sattar, R. Collins, S.G. Thompson, G. Whitlock, J. Danesh, Separate and combined associations of body-mass index and abdominal adiposity with cardiovascular disease: collaborative analysis of 58 prospective studies, Lancet 377 (9771) (2011) 1085–1095.
[35] M.L. Mongraw-Chaffin, S.A. Peters, R.R. Huxley, M. Woodward, The sex-specific association between BMI and coronary heart disease: a systematic review and meta-analysis of 95 cohorts with 1.2 million participants, Lancet Diabetes Endocrinol. 3 (6) (2015) 437–449.
[36] B.F. Palmer, D.J. Clegg, The sexual dimorphism of obesity, Mol. Cell. Endocrinol. 402 (2015) 113–119.
[37] S.H. Kim, J.P. Despres, K.K. Koh, Obesity and cardiovascular disease: friend or foe? Eur. Heart J. 37 (48) (2016) 3560–3568.
[38] E.E. Kershaw, J.S. Flier, Adipose tissue as an endocrine organ, J. Clin. Endocrinol. Metab. 89 (6) (2004) 2548–2556.
[39] W.H.O. (WHO), Tobacco. Fact Sheet, (2017) http://www.who.int/mediacentre/factsheets/fs339/en/.
[40] I. Graham, D. Atar, K. Borch-Johnsen, G. Boysen, G. Burell, R. Cifkova, J. Dallongeville, G. De Backer, S. Ebrahim, B. Gjelsvik, C. Herrmann-Lingen, A. Hoes, S. Humphries, M. Knapton, J. Perk, S.G. Priori, K. Pyorala, Z. Reiner, L. Ruilope, S. Sans-Menendez, W.S. Op Reimer, P. Weissberg, D. Wood, J. Yarnell, J.L. Zamorano, E. Walma, T. Fitzgerald, M.T. Cooney, A. Dudina, A. Vahanian, J. Camm, R. De Caterina, V. Dean, K. Dickstein, C. Funck-Brentano, G. Filippatos, I. Hellemans, S.D. Kristensen, K. McGregor, U. Sechtem, S. Silber, M. Tendera, P. Widimsky, A. Altiner, E. Bonora, P.N. Durrington, R. Fagard, S. Giampaoli, H. Hemingway, J. Hakansson, S.E. Kjeldsen, M.L. Larsen, G. Mancia, A.J. Manolis, K. Orth-Gomer, T. Pedersen, M. Rayner, L. Ryden, M. Sammut, N. Schneiderman, A.F. Stalenhoef, L. Tokgozoglu, O. Wiklund, A. Zampelas, European guidelines on cardiovascular disease prevention in clinical practice: full text. Fourth Joint Task Force of the European Society of Cardiology and other societies on cardiovascular disease prevention in clinical practice (constituted by representatives of nine societies and by invited experts), Eur. J. Cardiovasc. Prev. Rehabil. 14 (Suppl. 2) (2007) S1–113.
[41] R.R. Huxley, M. Woodward, Cigarette smoking as a risk factor for coronary heart disease in women compared with men: a systematic review and meta-analysis of prospective cohort studies, Lancet 378 (9799) (2011) 1297–1305.
[42] S.A. Peters, R.R. Huxley, M. Woodward, Smoking as a risk factor for stroke in women compared with men: a systematic review and meta-analysis of 81 cohorts, including 3,980,359 individuals and 42,401 strokes, Stroke 44 (10) (2013) 2821–2828.
[43] A. Chatziioannou, P. Georgiadis, D.G. Hebels, I. Liampa, I. Valavanis, I.A. Bergdahl, A. Johansson, D. Palli, M. Chadeau-Hyam, A.P. Siskos, H. Keun, M. Botsivali, T.M. de Kok, A.E. Perez, J.C. Kleinjans, P. Vineis, S.A. Kyrtopoulos, Blood-based omic profiling supports female susceptibility to tobacco smoke-induced cardiovascular diseases, Sci. Rep. 7 (2017) 42870.
[44] M.E. Mendelsohn, Protective effects of estrogen on the cardiovascular system, Am. J. Cardiol. 89 (12A) (2002) 12E–17E (discussion 17E-18E).
[45] O. Lidegaard, E. Lokkegaard, A.L. Svendsen, C. Agger, Hormonal contraception and risk of venous thromboembolism: national follow-up study, BMJ 339 (2009) b2890.
[46] O. Lidegaard, E. Lokkegaard, A. Jensen, C.W. Skovlund, N. Keiding, Thrombotic stroke and myocardial infarction with hormonal contraception, N. Engl. J. Med. 366 (24) (2012) 2257–2266.
[47] E. Banks, An evidence-based future for menopausal hormone therapy, Women's Health (Lond. Engl.) 11 (6) (2015) 785–788.
[48] L. Bellamy, J.P. Casas, A.D. Hingorani, D.J. Williams, Pre-eclampsia and risk of cardiovascular disease and cancer in later life: systematic review and meta-analysis, BMJ 335 (7627) (2007) 974.
[49] J.A. Lykke, J. Langhoff-Roos, B.M. Sibai, E.F. Funai, E.W. Triche, M.J. Paidas, Hypertensive pregnancy disorders and subsequent cardiovascular morbidity and type 2 diabetes mellitus in the mother, Hypertension 53 (6) (2009) 944–951.
[50] L. Bellamy, J.P. Casas, A.D. Hingorani, D. Williams, Type 2 diabetes mellitus after gestational diabetes: a systematic review and meta-analysis, Lancet 373 (9677) (2009) 1773–1779.
[51] J. Harreiter, G. Dovjak, A. Kautzky-Willer, Gestational diabetes mellitus and cardiovascular risk after pregnancy, Women's Health (Lond. Engl.) 10 (1) (2014) 91–108.
[52] A.H. Maas, Y.T. van der Schouw, V. Regitz-Zagrosek, E. Swahn, Y.E. Appelman, G. Pasterkamp, H. Ten Cate, P.M. Nilsson, M.V. Huisman, H.C. Stam, K. Eizema, M. Stramba-Badiale, Red alert for women's heart: the urgent need for more research and knowledge on cardiovascular disease in women: proceedings of the workshop held in Brussels on gender differences in cardiovascular disease, 29 September 2010, Eur. Heart J. 32 (11) (2011) 1362–1368.
[53] F. Atsma, M.L. Bartelink, D.E. Grobbee, Y.T. van der Schouw, Postmenopausal status and early menopause as independent risk factors for cardiovascular disease: a meta-analysis, Menopause 13 (2) (2006) 265–279.
[54] J.E. Roeters van Lennep, K.Y. Heida, M.L. Bots, A. Hoek, Cardiovascular disease risk in women with premature ovarian insufficiency: a systematic review and meta-analysis, Eur. J. Prev. Cardiol. 23 (2) (2016) 178–186.
[55] K.Y. Heida, B.K. Velthuis, M.A. Oudijk, J.B. Reitsma, M.L. Bots, A. Franx, F.M. van Dunne, Cardiovascular disease risk in women with a history of spontaneous preterm delivery: a systematic review and meta-analysis, Eur. J. Prev. Cardiol. 23 (3) (2016) 253–263.
[56] L.J. Tanz, J.J. Stuart, P.L. Williams, E.B. Rimm, S.A. Missmer, K.M. Rexrode, K.J. Mukamal, J.W. Rich-Edwards, Preterm delivery and maternal cardiovascular disease in young and middle-aged adult women, Circulation 135 (6) (2017) 578–589.
[57] M.J. Peters, D.P. Symmons, D. McCarey, B.A. Dijkmans, P. Nicola, T.K. Kvien, I.B. McInnes, H. Haentzschel, M.A. Gonzalez-Gay, S. Provan, A. Semb, P. Sidiropoulos, G. Kitas, Y.M. Smulders, M. Soubrier, Z. Szekanecz, N. Sattar, M.T. Nurmohamed, EULAR evidence-based recommendations for cardiovascular risk management in patients with rheumatoid arthritis and other forms of inflammatory arthritis, Ann. Rheum. Dis. 69 (2) (2010) 325–331.
[58] L. Gianturco, B.D. Bodini, F. Atzeni, C. Colombo, D. Stella, P. Sarzi-Puttini, L. Drago, S. Galaverna, M. Turiel, Cardiovascular and autoimmune diseases in females: the role of microvasculature and dysfunctional endothelium, Atherosclerosis 241 (1) (2015) 259–263.
[59] J.L. Zamorano, P. Lancellotti, D. Rodriguez Munoz, V. Aboyans, R. Asteggiano, M. Galderisi, G. Habib, D.J. Lenihan, G.Y. Lip, A.R. Lyon, T. Lopez Fernandez, D. Mohty, M.F. Piepoli, J. Tamargo, A. Torbicki, T.M. Suter, 2016 ESC Position

Paper on cancer treatments and cardiovascular toxicity developed under the auspices of the ESC Committee for Practice Guidelines: the task force for cancer treatments and cardiovascular toxicity of the European Society of Cardiology (ESC), Eur. Heart J. 37 (36) (2016) 2768–2801.
[60] R.M. Carney, K.E. Freedland, Depression and coronary heart disease, Nat. Rev. Cardiol. 14 (3) (2017) 145–155.
[61] E.M. Bucholz, K.M. Strait, R.P. Dreyer, S.T. Lindau, G. D'Onofrio, M. Geda, E.S. Spatz, J.F. Beltrame, J.H. Lichtman, N.P. Lorenze, H. Bueno, H.M. Krumholz, Sex differences in young patients with acute myocardial infarction: a VIRGO study analysis, Eur. Heart J. Acute Cardiovasc. Care 6 (7) (2017) 610–622.
[62] A. O'Neil, A.J. Fisher, K.J. Kibbey, F.N. Jacka, M.A. Kotowicz, L.J. Williams, A.L. Stuart, M. Berk, P.A. Lewandowski, C.B. Taylor, J.A. Pasco, Depression is a risk factor for incident coronary heart disease in women: an 18-year longitudinal study, J. Affect. Disord. 196 (2016) 117–124.
[63] P. Amadio, G.I. Colombo, E. Tarantino, S. Gianellini, A. Ieraci, M. Brioschi, C. Banfi, J.P. Werba, A. Parolari, F.S. Lee, E. Tremoli, S.S. Barbieri, BDNFVal66met polymorphism: a potential bridge between depression and thrombosis, Eur. Heart J. 38 (18) (2017) 1426–1435.
[64] E. Arbustini, B. Dal Bello, P. Morbini, A.P. Burke, M. Bocciarelli, G. Specchia, R. Virmani, Plaque erosion is a major substrate for coronary thrombosis in acute myocardial infarction, Heart 82 (3) (1999) 269–272.
[65] K. Yahagi, H.R. Davis, E. Arbustini, R. Virmani, Sex differences in coronary artery disease: pathological observations, Atherosclerosis 239 (1) (2015) 260–267.
[66] V.R. Taqueti, L.J. Shaw, N.R. Cook, V.L. Murthy, N.R. Shah, C.R. Foster, J. Hainer, R. Blankstein, S. Dorbala, M.F. Di Carli, Excess cardiovascular risk in women relative to men referred for coronary angiography is associated with severely impaired coronary flow reserve, not obstructive disease, Circulation 135 (6) (2017) 566–577.
[67] A.C. Boese, S.C. Kim, K.J. Yin, J.P. Lee, M.H. Hamblin, Sex differences in vascular physiology and pathophysiology: estrogen and androgen signaling in health and disease, Am. J. Physiol. Heart Circ. Physiol. 313 (3) (2017) H524–H545 (ajpheart 00217 2016).
[68] W.E. Hellings, G. Pasterkamp, B.A. Verhoeven, D.P. De Kleijn, J.P. De Vries, K.A. Seldenrijk, T. van den Broek, F.L. Moll, Gender-associated differences in plaque phenotype of patients undergoing carotid endarterectomy, J. Vasc. Surg. 45 (2) (2007) 289–296 (discussion 296-7).
[69] C. Wendorff, H. Wendorff, J. Pelisek, P. Tsantilas, A. Zimmermann, A. Zernecke, A. Kuehnl, H.H. Eckstein, Carotid plaque morphology is significantly associated with sex, age, and history of neurological symptoms, Stroke 46 (11) (2015) 3213–3219.
[70] G.L. Hortin, D. Sviridov, N.L. Anderson, High-abundance polypeptides of the human plasma proteome comprising the top 4 logs of polypeptide abundance, Clin. Chem. 54 (10) (2008) 1608–1616.
[71] H.C. Beck, M. Overgaard, L.M. Rasmussen, Plasma proteomics to identify biomarkers – application to cardiovascular diseases, Transl. Proteomics 7 (2015) 40–48.
[72] J.L. Miguel, M.T. Agapito, J.M. Recio, Sex differences of hematological and biochemical parameters in healthy rainbow trout (*Salmo gairdneri*, R), Rev. Esp. Fisiol. 44 (2) (1988) 215–219.
[73] M. Ihrig, L.G. Tassinary, B. Bernacky, M.E. Keeling, Hematologic and serum biochemical reference intervals for the chimpanzee (*Pan troglodytes*) categorized by age and sex, Comp. Med. 51 (1) (2001) 30–37.
[74] D.C. Yeung, A. Xu, C.W. Cheung, N.M. Wat, M.H. Yau, C.H. Fong, M.T. Chau, K.S. Lam, Serum adipocyte fatty acid-binding protein levels were independently associated with carotid atherosclerosis, Arterioscler. Thromb. Vasc. Biol. 27 (8) (2007) 1796–1802.
[75] T.M. Ahonen, H.J. Kautiainen, S.M. Keinanen-Kiukaanniemi, E.A. Kumpusalo, M.J. Vanhala, Gender difference among smoking, adiponectin, and high-sensitivity C-reactive protein, Am. J. Prev. Med. 35 (6) (2008) 598–601.
[76] K. Miike, M. Aoki, R. Yamashita, Y. Takegawa, H. Saya, T. Miike, K. Yamamura, Proteome profiling reveals gender differences in the composition of human serum, Proteomics 10 (14) (2010) 2678–2691.
[77] C. Tu, P.A. Rudnick, M.Y. Martinez, K.L. Cheek, S.E. Stein, R.J. Slebos, D.C. Liebler, Depletion of abundant plasma proteins and limitations of plasma proteomics, J. Proteome Res. 9 (10) (2010) 4982–4991.
[78] E. Bellei, S. Bergamini, E. Monari, L.I. Fantoni, A. Cuoghi, T. Ozben, A. Tomasi, High-abundance proteins depletion for serum proteomic analysis: concomitant removal of non-targeted proteins, Amino Acids 40 (1) (2011) 145–156.
[79] N.M. Al-Daghri, O.S. Al-Attas, H.E. Johnston, A. Singhania, M.S. Alokail, K.M. Alkharfy, S.H. Abd-Alrahman, S.L. Sabico, T.I. Roumeliotis, A. Manousopoulou-Garbis, P.A. Townsend, C.H. Woelk, G.P. Chrousos, S.D. Garbis, Whole serum 3D LC-nESI-FTMS quantitative proteomics reveals sexual dimorphism in the milieu interieur of overweight and obese adults, J. Proteome Res. 13 (11) (2014) 5094–5105.
[80] B. Zethelius, L. Berglund, J. Sundstrom, E. Ingelsson, S. Basu, A. Larsson, P. Venge, J. Arnlov, Use of multiple biomarkers to improve the prediction of death from cardiovascular causes, N. Engl. J. Med. 358 (20) (2008) 2107–2116.
[81] C.X. Kim, K.R. Bailey, G.G. Klee, A.A. Ellington, G. Liu, T.H. Mosley Jr., H. Rehman, I.J. Kullo, Sex and ethnic differences in 47 candidate proteomic markers of cardiovascular disease: the Mayo Clinic proteomic markers of arteriosclerosis study, PLoS One 5 (2) (2010) e9065.
[82] S. Siebert, D. Porter, C. Paterson, R. Hampson, D. Gaya, A. Latosinska, H. Mischak, J. Schanstra, W. Mullen, I. McInnes, Urinary proteomics can define distinct diagnostic inflammatory arthritis subgroups, Sci. Rep. 7 (2017) 40473.
[83] M. Haubitz, S. Wittke, E.M. Weissinger, M. Walden, H.D. Rupprecht, J. Floege, H. Haller, H. Mischak, Urine protein patterns can serve as diagnostic tools in patients with IgA nephropathy, Kidney Int. 67 (6) (2005) 2313–2320.
[84] D. Theodorescu, E. Schiffer, H.W. Bauer, F. Douwes, F. Eichhorn, R. Polley, T. Schmidt, W. Schofer, P. Zurbig, D.M. Good, J.J. Coon, H. Mischak, Discovery and validation of urinary biomarkers for prostate cancer, Proteomics Clin. Appl. 2 (4) (2008) 556–570.
[85] S. Thomas, L. Hao, W.A. Ricke, L. Li, Biomarker discovery in mass spectrometry-based urinary proteomics, Proteomics Clin. Appl. 10 (4) (2016) 358–370.
[86] V. Thongboonkerd, S. Chutipongtanate, R. Kanlaya, Systematic evaluation of sample preparation methods for gel-based human urinary proteomics: quantity, quality, and variability, J. Proteome Res. 5 (1) (2006) 183–191.
[87] Z. Guo, Y. Zhang, L. Zou, D. Wang, C. Shao, Y. Wang, W. Sun, L. Zhang, A proteomic analysis of individual and gender variations in normal human urine and cerebrospinal fluid using iTRAQ quantification, PLoS One 10 (7) (2015) e0133270.
[88] T. Kuznetsova, H. Mischak, W. Mullen, J.A. Staessen, Urinary proteome analysis in hypertensive patients with left ventricular diastolic dysfunction, Eur. Heart J. 33 (18) (2012) 2342–2350.
[89] Z. Zhang, J.A. Staessen, L. Thijs, Y. Gu, Y. Liu, L. Jacobs, T. Koeck, P. Zurbig, H. Mischak, T. Kuznetsova, Left ventricular diastolic function in relation to the urinary proteome: a proof-of-concept study in a general population, Int. J. Cardiol. 176 (1) (2014) 158–165.
[90] Z.Y. Zhang, L. Thijs, T. Petit, Y.M. Gu, L. Jacobs, W.Y. Yang, Y.P. Liu, T. Koeck, P. Zurbig, Y. Jin, P. Verhamme, J.U. Voigt, T. Kuznetsova, H. Mischak, J.A. Staessen, Urinary proteome and systolic blood pressure as predictors of 5-year cardiovascular and cardiac outcomes in a general population, Hypertension 66 (1) (2015) 52–60.
[91] L. Yan, H. Ge, H. Li, S.C. Lieber, F. Natividad, R.R. Resuello, S.J. Kim, S. Akeju, A. Sun, K. Loo, A.P. Peppas, F. Rossi, E.D. Lewandowski, A.P. Thomas, S.F. Vatner, D.E. Vatner, Gender-specific proteomic alterations in glycolytic and mitochondrial pathways in aging monkey hearts, J. Mol. Cell. Cardiol. 37 (5) (2004) 921–929.
[92] D. Jarreta, J. Orus, A. Barrientos, O. Miro, E. Roig, M. Heras, C.T. Moraes, F. Cardellach, J. Casademont, Mitochondrial function in heart muscle from patients with idiopathic dilated cardiomyopathy, Cardiovasc. Res. 45 (4) (2000) 860–865.
[93] W.C. Stanley, M.P. Chandler, Energy metabolism in the normal and failing heart: potential for therapeutic interventions, Heart Fail. Rev. 7 (2) (2002) 115–130.
[94] M. Patrizio, G. Marano, Gender differences in cardiac hypertrophic remodeling, Ann. Ist. Super. Sanita 52 (2) (2016) 223–229.
[95] J.D. Carroll, E.P. Carroll, T. Feldman, D.M. Ward, R.M. Lang, D. McGaughey, R.B. Karp, Sex-associated differences in left ventricular function in aortic stenosis of the elderly, Circulation 86 (4) (1992) 1099–1107.
[96] P. Buttrick, J. Scheuer, Sex-associated differences in left ventricular function in aortic stenosis of the elderly, Circulation 86 (4) (1992) 1336–1338.
[97] G. Kararigas, D. Fliegner, S. Forler, O. Klein, C. Schubert, J.A. Gustafsson, J. Klose, V. Regitz-Zagrosek, Comparative proteomic analysis reveals sex and estrogen receptor beta effects in the pressure overloaded heart, J. Proteome Res. 13 (12) (2014) 5829–5836.
[98] F.A. Babiker, D. Lips, R. Meyer, E. Delvaux, P. Zandberg, B. Janssen, G. van Eys, C. Grohe, P.A. Doevendans, Estrogen receptor beta protects the murine heart against left ventricular hypertrophy, Arterioscler. Thromb. Vasc. Biol. 26 (7) (2006) 1524–1530.
[99] T.A. Doser, S. Turdi, D.P. Thomas, P.N. Epstein, S.Y. Li, J. Ren, Transgenic overexpression of aldehyde dehydrogenase-2 rescues chronic alcohol intake-induced myocardial hypertrophy and contractile dysfunction, Circulation 119 (14) (2009) 1941–1949.
[100] Y. Yu, X.J. Jia, Q.F. Zong, G.J. Zhang, H.W. Ye, J. Hu, Q. Gao, S.D. Guan, Remote ischemic postconditioning protects the heart by upregulating ALDH2 expression levels through the PI3K/Akt signaling pathway, Mol. Med. Rep. 10 (1) (2014) 536–542.
[101] V.C. Vasile, S.R. Ommen, W.D. Edwards, M.J. Ackerman, A missense mutation in a ubiquitously expressed protein, vinculin, confers susceptibility to hypertrophic cardiomyopathy, Biochem. Biophys. Res. Commun. 345 (3) (2006) 998–1003.
[102] J.D. McCully, Y. Toyoda, H. Wakiyama, A.J. Rousou, R.A. Parker, S. Levitsky, Age- and gender-related differences in ischemia/reperfusion injury and cardioprotection: effects of diazoxide, Ann. Thorac. Surg. 82 (1) (2006) 117–123.
[103] J. Butterworth, R. James, R. Prielipp, J. Cerese, J. Livingston, D. Burnett, Female gender associates with increased duration of intubation and length of stay after coronary artery surgery. CABG clinical benchmarking database participants, Anesthesiology 92 (2) (2000) 414–424.
[104] D. Abramov, M.G. Tamariz, J.Y. Sever, G.T. Christakis, G. Bhatnagar, A.L. Heenan, B.S. Goldman, S.E. Fremes, The influence of gender on the outcome of coronary artery bypass surgery, Ann. Thorac. Surg. 70 (3) (2000) 800–805 (discussion 806).
[105] J.D. McCully, A.J. Rousou, R.A. Parker, S. Levitsky, Age- and gender-related differences in mitochondrial oxygen consumption and calcium with cardioplegia and diazoxide, Ann. Thorac. Surg. 83 (3) (2007) 1102–1109.
[106] K.M. Black, R.J. Barnett, M.K. Bhasin, C. Daly, S.T. Dillon, T.A. Libermann, S. Levitsky, J.D. McCully, Microarray and proteomic analysis of the cardioprotective effects of cold blood cardioplegia in the mature and aged male and female, Physiol. Genomics 44 (21) (2012) 1027–1041.
[107] I. Eberini, R. Wait, L. Calabresi, C. Sensi, I. Miller, E. Gianazza, A proteomic portrait of atherosclerosis, J. Proteome 82 (2013) 92–112.
[108] O.B. Bleijerveld, Y.N. Zhang, S. Beldar, I.E. Hoefer, S.K. Sze, G. Pasterkamp, D.P. de Kleijn, Proteomics of plaques and novel sources of potential biomarkers for atherosclerosis, Proteomics Clin. Appl. 7 (7–8) (2013) 490–503.
[109] W. Liang, L.J. Ward, H. Karlsson, S.A. Ljunggren, W. Li, M. Lindahl, X.M. Yuan, Distinctive proteomic profiles among different regions of human carotid plaques in

men and women, Sci. Rep. 6 (2016) 26231.
[110] S.A. You, S.R. Archacki, G. Angheloiu, C.S. Moravec, S. Rao, M. Kinter, E.J. Topol, Q. Wang, Proteomic approach to coronary atherosclerosis shows ferritin light chain as a significant marker: evidence consistent with iron hypothesis in atherosclerosis, Physiol. Genomics 13 (1) (2003) 25–30.
[111] A.J. Lepedda, A. Cigliano, G.M. Cherchi, R. Spirito, M. Maggioni, F. Carta, F. Turrini, C. Edelstein, A.M. Scanu, M. Formato, A proteomic approach to differentiate histologically classified stable and unstable plaques from human carotid arteries, Atherosclerosis 203 (1) (2009) 112–118.
[112] L. Guo, E. Harari, R. Virmani, A.V. Finn, Linking hemorrhage, angiogenesis, macrophages, and iron metabolism in atherosclerotic vascular diseases, Arterioscler. Thromb. Vasc. Biol. 37 (4) (2017) e33–e39.
[113] J.N. Buxbaum, N. Reixach, Transthyretin: the servant of many masters, Cell. Mol. Life Sci. 66 (19) (2009) 3095–3101.
[114] M.A. Liz, S.C. Leite, L. Juliano, M.J. Saraiva, A.M. Damas, D. Bur, M.M. Sousa, Transthyretin is a metallopeptidase with an inducible active site, Biochem. J. 443 (3) (2012) 769–778.
[115] M. Gomez-Serrano, E. Camafeita, E. Garcia-Santos, J.A. Lopez, M.A. Rubio, A. Sanchez-Pernaute, A. Torres, J. Vazquez, B. Peral, Proteome-wide alterations on adipose tissue from obese patients as age-, diabetes- and gender-specific hallmarks, Sci. Rep. 6 (2016) 25756.
[116] M. Johnson, E. Ramey, P.W. Ramwell, Sex and age differences in human platelet aggregation, Nature 253 (5490) (1975) 355–357.
[117] B. Bain, T. Forster, A sex difference in the bleeding time, Thromb. Haemost. 43 (2) (1980) 131–132.
[118] G. Patti, R. De Caterina, R. Abbate, F. Andreotti, L.M. Biasucci, P. Calabro, G. Cioni, G. Davi, G. Di Sciascio, E. Golia, P. Golino, G. Malatesta, F. Mangiacapra, R. Marcucci, A. Nusca, V.M. Parato, V. Pengo, D. Prisco, F. Pulcinelli, G. Renda, E. Ricottini, B. Ruggieri, F. Santilli, F. Sofi, M. Zimarino, Platelet function and long-term antiplatelet therapy in women: is there a gender-specificity? A 'state-of-the-art' paper, Eur. Heart J. 35 (33) (2014) 2213-23b.
[119] J.B. Segal, A.R. Moliterno, Platelet counts differ by sex, ethnicity, and age in the United States, Ann. Epidemiol. 16 (2) (2006) 123–130.
[120] P. Bobbert, C. Stellbaum, D. Steffens, C. Schutte, T. Bobbert, H.P. Schultheiss, U. Rauch, Postmenopausal women have an increased maximal platelet reactivity compared to men despite dual antiplatelet therapy, Blood Coagul. Fibrinolysis 23 (8) (2012) 723–728.
[121] X.H. Leng, S.Y. Hong, S. Larrucea, W. Zhang, T.T. Li, J.A. Lopez, P.F. Bray, Platelets of female mice are intrinsically more sensitive to agonists than are platelets of males, Arterioscler. Thromb. Vasc. Biol. 24 (2) (2004) 376–381.
[122] J.M. Burkhart, S. Gambaryan, S.P. Watson, K. Jurk, U. Walter, A. Sickmann, J.W. Heemskerk, R.P. Zahedi, What can proteomics tell us about platelets? Circ. Res. 114 (7) (2014) 1204–1219.
[123] O. Eidelman, C. Jozwik, W. Huang, M. Srivastava, S.W. Rothwell, D.M. Jacobowitz, X. Ji, X. Zhang, W. Guggino, J. Wright, J. Kiefer, C. Olsen, N. Adimi, G.P. Mueller, H.B. Pollard, Gender dependence for a subset of the low-abundance signaling proteome in human platelets, Hum. Genomics Proteomics 2010 (2010) 164906.
[124] V. Ganesh, N.S. Hettiarachchy, Nutriproteomics: a promising tool to link diet and diseases in nutritional research, Biochim. Biophys. Acta 1824 (10) (2012) 1107–1117.
[125] S.S. Anand, C. Hawkes, R.J. de Souza, A. Mente, M. Dehghan, R. Nugent, M.A. Zulyniak, T. Weis, A.M. Bernstein, R.M. Krauss, D. Kromhout, D.J. Jenkins, V. Malik, M.A. Martinez-Gonzalez, D. Mozaffarian, S. Yusuf, W.C. Willett, B.M. Popkin, Food consumption and its impact on cardiovascular disease: importance of solutions focused on the globalized food system: a report from the workshop convened by the World Heart Federation, J. Am. Coll. Cardiol. 66 (14) (2015) 1590–1614.
[126] R. Estruch, E. Ros, J. Salas-Salvado, M.I. Covas, D. Corella, F. Aros, E. Gomez-Gracia, V. Ruiz-Gutierrez, M. Fiol, J. Lapetra, R.M. Lamuela-Raventos, L. Serra-Majem, X. Pinto, J. Basora, M.A. Munoz, J.V. Sorli, J.A. Martinez, M.A. Martinez-Gonzalez, Primary prevention of cardiovascular disease with a Mediterranean diet, N. Engl. J. Med. 368 (14) (2013) 1279–1290.
[127] D.D. Wang, E. Toledo, A. Hruby, B.A. Rosner, W.C. Willett, Q. Sun, C. Razquin, Y. Zheng, M. Ruiz-Canela, M. Guasch-Ferre, D. Corella, E. Gomez-Gracia, M. Fiol, R. Estruch, E. Ros, J. Lapetra, M. Fito, F. Aros, L. Serra-Majem, C.H. Lee, C.B. Clish, L. Liang, J. Salas-Salvado, M.A. Martinez-Gonzalez, F.B. Hu, Plasma ceramides, Mediterranean diet, and incident cardiovascular disease in the PREDIMED trial (Prevencion con Dieta Mediterranea), Circulation 135 (21) (2017) 2028–2040.
[128] A. Bedard, M. Riverin, S. Dodin, L. Corneau, S. Lemieux, Sex differences in the impact of the Mediterranean diet on cardiovascular risk profile, Br. J. Nutr. 108 (8) (2012) 1428–1434.
[129] A. Bedard, A. Tchernof, B. Lamarche, L. Corneau, S. Dodin, S. Lemieux, Effects of the traditional Mediterranean diet on adiponectin and leptin concentrations in men and premenopausal women: do sex differences exist? Eur. J. Clin. Nutr. 68 (5) (2014) 561–566.
[130] A. Bedard, L. Corneau, B. Lamarche, S. Dodin, S. Lemieux, Sex differences in the impact of the Mediterranean diet on LDL particle size distribution and oxidation, Nutrients 7 (5) (2015) 3705–3723.
[131] A. Bedard, B. Lamarche, L. Corneau, S. Dodin, S. Lemieux, Sex differences in the impact of the Mediterranean diet on systemic inflammation, Nutr. J. 14 (2015) 46.
[132] E. Burillo, R. Mateo-Gallego, A. Cenarro, S. Fiddyment, A.M. Bea, I. Jorge, J. Vazquez, F. Civeira, Beneficial effects of omega-3 fatty acids in the proteome of high-density lipoprotein proteome, Lipids Health Dis. 11 (2012) 116.
[133] A. Pedret, U. Catalan, S. Fernandez-Castillejo, M. Farras, R.M. Valls, L. Rubio, N. Canela, G. Aragones, M. Romeu, O. Castaner, R. de la Torre, M.I. Covas, M. Fito, M.J. Motilva, R. Sola, Impact of virgin olive oil and phenol-enriched virgin olive oils on the HDL proteome in hypercholesterolemic subjects: a double blind, randomized, controlled, cross-over clinical trial (VOHF study), PLoS One 10 (6) (2015) e0129160.
[134] W. Mullen, J. Gonzalez, J. Siwy, J. Franke, N. Sattar, A. Mullan, S. Roberts, C. Delles, H. Mischak, A. Albalat, A pilot study on the effect of short-term consumption of a polyphenol rich drink on biomarkers of coronary artery disease defined by urinary proteomics, J. Agric. Food Chem. 59 (24) (2011) 12850–12857.
[135] S. Silva, M.R. Bronze, M.E. Figueira, J. Siwy, H. Mischak, E. Combet, W. Mullen, Impact of a 6-wk olive oil supplementation in healthy adults on urinary proteomic biomarkers of coronary artery disease, chronic kidney disease, and diabetes (types 1 and 2): a randomized, parallel, controlled, double-blind study, Am. J. Clin. Nutr. 101 (1) (2015) 44–54.
[136] A. Camargo, O.A. Rangel-Zuniga, P. Pena-Orihuela, C. Marin, P. Perez-Martinez, J. Delgado-Lista, F.M. Gutierrez-Mariscal, M.M. Malagon, H.M. Roche, F.J. Tinahones, F. Perez-Jimenez, J. Lopez-Miranda, Postprandial changes in the proteome are modulated by dietary fat in patients with metabolic syndrome, J. Nutr. Biochem. 24 (1) (2013) 318–324.
[137] O.A. Rangel-Zuniga, A. Camargo, C. Marin, P. Pena-Orihuela, P. Perez-Martinez, J. Delgado-Lista, L. Gonzalez-Guardia, E.M. Yubero-Serrano, F.J. Tinahones, M.M. Malagon, F. Perez-Jimenez, H.M. Roche, J. Lopez-Miranda, Proteome from patients with metabolic syndrome is regulated by quantity and quality of dietary lipids, BMC Genomics 16 (2015) 509.
[138] B. de Roos, X. Zhang, G. Rodriguez Gutierrez, S. Wood, G.J. Rucklidge, M.D. Reid, G.J. Duncan, L.L. Cantlay, G.G. Duthie, N. O'Kennedy, Anti-platelet effects of olive oil extract: in vitro functional and proteomic studies, Eur. J. Nutr. 50 (7) (2011) 553–562.
[139] L. Fontana, S. Klein, Aging, adiposity, and calorie restriction, JAMA 297 (9) (2007) 986–994.
[140] L. Fontana, L. Partridge, V.D. Longo, Extending healthy life span—from yeast to humans, Science 328 (5976) (2010) 321–326.
[141] E.P. Weiss, L. Fontana, Caloric restriction: powerful protection for the aging heart and vasculature, Am. J. Physiol. Heart Circ. Physiol. 301 (4) (2011) H1205–19.
[142] C.W. Bales, W.E. Kraus, Caloric restriction: implications for human cardiometabolic health, J. Cardiopulm. Rehabil. Prev. 33 (4) (2013) 201–208.
[143] J.C. Regan, L. Partridge, Gender and longevity: why do men die earlier than women? Comparative and experimental evidence, Best Pract. Res. Clin. Endocrinol. Metab. 27 (4) (2013) 467–479.
[144] A. Valle, E. Silvestri, M. Moreno, A. Chambery, J. Oliver, P. Roca, F. Goglia, Combined effect of gender and caloric restriction on liver proteomic expression profile, J. Proteome Res. 7 (7) (2008) 2872–2881.
[145] W. Droge, Free radicals in the physiological control of cell function, Physiol. Rev. 82 (1) (2002) 47–95.
[146] C.K. Glass, J.L. Witztum, Atherosclerosis. The road ahead, Cell 104 (4) (2001) 503–516.
[147] D. Harrison, K.K. Griendling, U. Landmesser, B. Hornig, H. Drexler, Role of oxidative stress in atherosclerosis, Am. J. Cardiol. 91 (3A) (2003) 7A–11A.
[148] R. Schnabel, S. Blankenberg, Oxidative stress in cardiovascular disease: successful translation from bench to bedside? Circulation 116 (12) (2007) 1338–1340.
[149] F. Santilli, D. D'Ardes, G. Davi, Oxidative stress in chronic vascular disease: from prediction to prevention, Vasc. Pharmacol. 74 (2015) 23–37.
[150] A. Agrawal, E.V. Lourenco, S. Gupta, A. La Cava, Gender-based differences in leptinemia in healthy aging, non-obese individuals associate with increased marker of oxidative stress, Int. J. Clin. Exp. Med. 1 (4) (2008) 305–309.
[151] C. Vassalle, A. Mercuri, S. Maffei, Oxidative status and cardiovascular risk in women: keeping pink at heart, World J. Cardiol. 1 (1) (2009) 26–30.
[152] C. Vassalle, S. Maffei, C. Boni, G.C. Zucchelli, Gender-related differences in oxidative stress levels among elderly patients with coronary artery disease, Fertil. Steril. 89 (3) (2008) 608–613.
[153] M.C. Kander, Y. Cui, Z. Liu, Gender difference in oxidative stress: a new look at the mechanisms for cardiovascular diseases, J. Cell. Mol. Med. 21 (5) (2017) 1024–1032.
[154] J. Frijhoff, P.G. Winyard, N. Zarkovic, S.S. Davies, R. Stocker, D. Cheng, A.R. Knight, E.L. Taylor, J. Oettrich, T. Ruskovska, A.C. Gasparovic, A. Cuadrado, D. Weber, H.E. Poulsen, T. Grune, H.H. Schmidt, P. Ghezzi, Clinical relevance of biomarkers of oxidative stress, Antioxid. Redox Signal. 23 (14) (2015) 1144–1170.
[155] H.N. Siti, Y. Kamisah, J. Kamsiah, The role of oxidative stress, antioxidants and vascular inflammation in cardiovascular disease (a review), Vasc. Pharmacol. 71 (2015) 40–56.
[156] C.M. Spickett, A.R. Pitt, N. Morrice, W. Kolch, Proteomic analysis of phosphorylation, oxidation and nitrosylation in signal transduction, Biochim. Biophys. Acta 1764 (12) (2006) 1823–1841.
[157] P.R. Jungblut, H.G. Holzhutter, R. Apweiler, H. Schluter, The speciation of the proteome, Chem. Cent. J. 2 (2008) 16.
[158] P. Jungblut, B. Thiede, U. Zimny-Arndt, E.C. Muller, C. Scheler, B. Wittmann-Liebold, A. Otto, Resolution power of two-dimensional electrophoresis and identification of proteins from gels, Electrophoresis 17 (5) (1996) 839–847.
[159] P. Steffen, M. Kwiatkowski, W.D. Robertson, A. Zarrine-Afsar, D. Deterra, V. Richter, H. Schluter, Protein species as diagnostic markers, J. Proteome 134 (2016) 5–18.
[160] K.A. Liddy, M.Y. White, S.J. Cordwell, Functional decorations: post-translational modifications and heart disease delineated by targeted proteomics, Genome Med. 5 (2) (2013) 20.
[161] P.R. Jungblut, B. Thiede, H. Schluter, Towards deciphering proteomes via the proteoform, protein speciation, moonlighting and protein code concepts, J. Proteome 134 (2016) 1–4.

[162] K. Schwab, B. Neumann, C. Scheler, P.R. Jungblut, F. Theuring, Adaptation of proteomic techniques for the identification and characterization of protein species from murine heart, Amino Acids 41 (2) (2011) 401–414.
[163] K. Schwab, B. Neumann, N. Vignon-Zellweger, A. Fischer, R. Stein, P.R. Jungblut, C. Scheler, F. Theuring, Dietary phytoestrogen supplementation induces sex differences in the myocardial protein pattern of mice: a comparative proteomics study, Proteomics 11 (19) (2011) 3887–3904.
[164] I. Verrastro, S. Pasha, K.T. Jensen, A.R. Pitt, C.M. Spickett, Mass spectrometry-based methods for identifying oxidized proteins in disease: advances and challenges, Biomol. Ther. 5 (2) (2015) 378–411.
[165] R.M. Domingues, P. Domingues, T. Melo, D. Perez-Sala, A. Reis, C.M. Spickett, Lipoxidation adducts with peptides and proteins: deleterious modifications or signaling mechanisms? J. Proteome 92 (2013) 110–131.
[166] G. Aldini, M.R. Domingues, C.M. Spickett, P. Domingues, A. Altomare, F.J. Sanchez-Gomez, C.L. Oeste, D. Perez-Sala, Protein lipoxidation: detection strategies and challenges, Redox Biol. 5 (2015) 253–266.
[167] X. Wang, J.S. Pattison, H. Su, Posttranslational modification and quality control, Circ. Res. 112 (2) (2013) 367–381.
[168] J. Li, K.M. Horak, H. Su, A. Sanbe, J. Robbins, X. Wang, Enhancement of proteasomal function protects against cardiac proteinopathy and ischemia/reperfusion injury in mice, J. Clin. Invest. 121 (9) (2011) 3689–3700.
[169] G.S. Omenn, L. Lane, E.K. Lundberg, R.C. Beavis, C.M. Overall, E.W. Deutsch, Metrics for the Human Proteome Project 2016: progress on identifying and characterizing the human proteome, including post-translational modifications, J. Proteome Res. 15 (11) (2016) 3951–3960.
[170] A.R. Stram, R.M. Payne, Post-translational modifications in mitochondria: protein signaling in the powerhouse, Cell. Mol. Life Sci. 73 (21) (2016) 4063–4073.
[171] A.P. Halestrap, A pore way to die: the role of mitochondria in reperfusion injury and cardioprotection, Biochem. Soc. Trans. 38 (4) (2010) 841–860.
[172] M.G. Rosca, C.L. Hoppel, Mitochondria in heart failure, Cardiovasc. Res. 88 (1) (2010) 40–50.
[173] C.J. Lagranha, A. Deschamps, A. Aponte, C. Steenbergen, E. Murphy, Sex differences in the phosphorylation of mitochondrial proteins result in reduced production of reactive oxygen species and cardioprotection in females, Circ. Res. 106 (11) (2010) 1681–1691.
[174] T. Alberio, L. Pieroni, M. Ronci, C. Banfi, I. Bongarzone, P. Bottoni, M. Brioschi, M. Caterino, C. Chinello, A. Cormio, F. Cozzolino, V. Cunsolo, S. Fontana, B. Garavaglia, L. Giusti, V. Greco, A. Lucacchini, E. Maffioli, F. Magni, F. Monteleone, M. Monti, V. Monti, C. Musicco, G. Petrosillo, V. Porcelli, R. Saletti, R. Scatena, A. Soggiu, G. Tedeschi, M. Zilocchi, P. Roncada, A. Urbani, M. Fasano, Toward the standardization of mitochondrial proteomics: the Italian mitochondrial human proteome project initiative, J. Proteome Res. (2017), http://dx.doi.org/10.1021/acs.jproteome.7b00350.
[175] M.T. Dorak, E. Karpuzoglu, Gender differences in cancer susceptibility: an inadequately addressed issue, Front. Genet. 3 (2012) 268.
[176] E. Commision, Use of '-omics' technologies in the development of personalised medicine, http://ec.europa.eu/research/health/pdf/2013-10_personalised_medicine_en.pdf, (2013).
[177] A Report of the Mary Horrigan Connors Center for Women's Health & Gender Biology, Precision Medicine: How Sex and Gender Drive Innovation, Brigham and Women's Hospital, Boston MA, 2016.

Glossary

2-DE two-dimensional electrophoresis:
2D-LC-MS/MS two-dimensional liquid chromatography/tandem mass spectrometry:
2-DE/MS two-dimensional electrophoresis coupled to mass spectrometry:
8-plex iTRAQ:
AAA abdominal aortic aneurysm:
BMI body mass index:
CAD coronary artery disease:
CHD coronary heart disease:
CMD coronary microvascular dysfunction:
CVD cardiovascular disease:
DM diabetes mellitus:
ERFC Emerging Risk Factors Collaboration:
ERβ estrogen receptor β:
GPX glutathione peroxidase:
GST glutathione S-transferase:
HDL-C high-density lipoprotein cholesterol:
HF heart failure:
HR hazard ratio:
IHD ischemic heart disease:
iTRAQ isobaric tags for relative and absolute quantitation:
LVH left ventricular hypertrophy:
MALDI-TOF MS matrix-assisted laser-desorption ionization- time of flight mass spectrometry:
NIH National Institutes of Health:
nLC-MS/MS nano liquid chromatography/tandem mass spectrometry:
oxPTM oxidative post-translational modification:
PAD peripheral arterial disease:
PTM post-translational modification:
SBP systolic blood pressure:
SCAD spontaneous coronary dissection:
SOD superoxide dismutase:
TC total cholesterol:

Expert Review of Proteomics

ISSN: 1478-9450 (Print) 1744-8387 (Online) Journal homepage: http://www.tandfonline.com/loi/ieru20

Exploring the biochemistry of the prenylome and its role in disease through proteomics: progress and potential

Maura Brioschi, Alma Martinez Fernandez & Cristina Banfi

To cite this article: Maura Brioschi, Alma Martinez Fernandez & Cristina Banfi (2017): Exploring the biochemistry of the prenylome and its role in disease through proteomics: progress and potential, Expert Review of Proteomics, DOI: 10.1080/14789450.2017.1332998

To link to this article: http://dx.doi.org/10.1080/14789450.2017.1332998

Accepted author version posted online: 18 May 2017.
Published online: 26 May 2017.

EXPERT REVIEW OF PROTEOMICS, 2017
https://doi.org/10.1080/14789450.2017.1332998

Taylor & Francis
Taylor & Francis Group

REVIEW

Exploring the biochemistry of the prenylome and its role in disease through proteomics: progress and potential

Maura Brioschi, Alma Martinez Fernandez and Cristina Banfi

Centro Cardiologico Monzino, IRCCS, Milano, Italy

ABSTRACT

Introduction: Protein prenylation is a ubiquitous covalent post-translational modification characterized by the addition of farnesyl or geranylgeranyl isoprenoid groups to a cysteine residue located near the carboxyl terminal of a protein. It is essential for the proper localization and cellular activity of numerous proteins, including Ras family GTPases and G-proteins. In addition to its roles in cellular physiology, the prenylation process has important implications in human diseases and in the recent years, it has become attractive target of inhibitors with therapeutic potential.

Areas covered: This review attempts to summarize the basic aspects of prenylation integrating them with biological functions in diseases and giving an account of the current status of prenylation inhibitors as potential therapeutics. We also summarize the methodologies for the characterization of this modification.

Expert commentary: The growing body of evidence suggesting an important role of prenylation in diseases and the subsequent development of inhibitors of the enzymes responsible for this modification lead to the urgent need to identify the full spectrum of prenylated proteins that are altered in the disease or affected by drugs. Proteomic tools to analyze prenylated proteins are recently emerging, thanks to the advancement in the field of mass spectrometry coupled to enrichment strategies.

ARTICLE HISTORY
Received 25 January 2017
Accepted 17 May 2017

KEYWORDS
Bioorthogonal labeling; diseases; mass spectrometry; post-translational modifications; prenylation; prenylation inhibitors; proteomics

1. Introduction

Among posttranslational modifications (PTMs), protein lipidation is unique owing to its structural versatility and the ability to directly control the attachment of soluble proteins to cell membranes without the requirement of other mediators. Indeed, numerous membrane proteins require a temporary membrane association to fulfill their biological functions. This can be achieved via interaction with membrane lipids (i.e. phospholipids or sphingolipids), through conserved lipid-binding domains present in the protein, or by covalent attachment of lipid groups (reviewed in [1]).

Different lipid classes, namely fatty acids, isoprenoids, sterols, phospholipids, and glycosylphosphatidylinositol anchors, are known to be enzymatically attached, and, with the exception of palmitoylation, lipid modifications (N-myristoylation, cholesterylation, and prenylation) are all irreversible.

Originally discovered in fungi in 1978 [2], the first prenylated protein was identified in mammalian cells about 10 years later [3], and the number of identified prenylated proteins is still increasing, thanks to novel analytical strategies based on mass spectrometry (MS) (170 entries in UniProt database, UniProt release 2017_01).

A number of exhaustive reviews have described the pathways and enzymes involved in the prenylation process [4–18]. Briefly, prenylation is a multistep enzymatic process in which three prenyltransferases (PTases) catalyze this modification adding hydrophobic prenyl moieties to proteins: farnesyltransferase (FTase), geranygeranyltransferase I (GGTase I), and Rab geranylgeranyltransferase (RabGGTase or GGTase II) (Figure 1). As their names suggest, these enzymes carry out farnesylation, whereby a C15 moiety (three isoprene units) is transferred to a cysteine side chain, or geranylgeranylation, in which a C20 moiety (four isoprene units) is transferred. FTase and GGTase I are often referred to as CAAX PTases because they recognize a four-amino-acid C-terminal motif that is termed the CAAX box where C is cysteine, A is usually an aliphatic amino acid, and X can be a variety of amino acids. Proteins can then be further processed by RAS-converting CAAX endopeptidase 1 (RCE1), which removes the AAX residues, followed by isoprenylcysteine carboxyl methyltransferase (ICMT), which 'caps' the carboxyl group on the now carboxy-terminal isoprenoid-modified cysteine residue with a methyl group. RabGGTase differs both structurally and functionally from the CAAX PTases because it recognizes the overall structure of Rab proteins instead of a short C-terminal sequence. This recognition is mediated by an accessory Rab escort protein that can bind mammalian Rab proteins and present them to the catalytic subunit of RabGGTase.

The protein substrates of the three PTases are very diverse in nature. This group includes the γ-subunits of heterotrimeric G proteins, centromeric proteins, regulators of the cell cycle and apoptosis, nuclear structural proteins such as lamins, enzymes of glycogen metabolism, and proteins of the visual cascade, but the largest, and most extensively studied group, is composed by the small GTPase superfamilies including the well-known Ras, Rab, Rho, and Rac. Small GTPases are essential signaling proteins that regulate a variety of cell processes and functions, such as cell growth, differentiation, cytoskeletal organization, and vesicle trafficking. The prenylation status of

CONTACT Cristina Banfi cristina.banfi@ccfm.it Centro Cardiologico Monzino, IRCCS, Via Parea 4, 20138 Milano, Italy

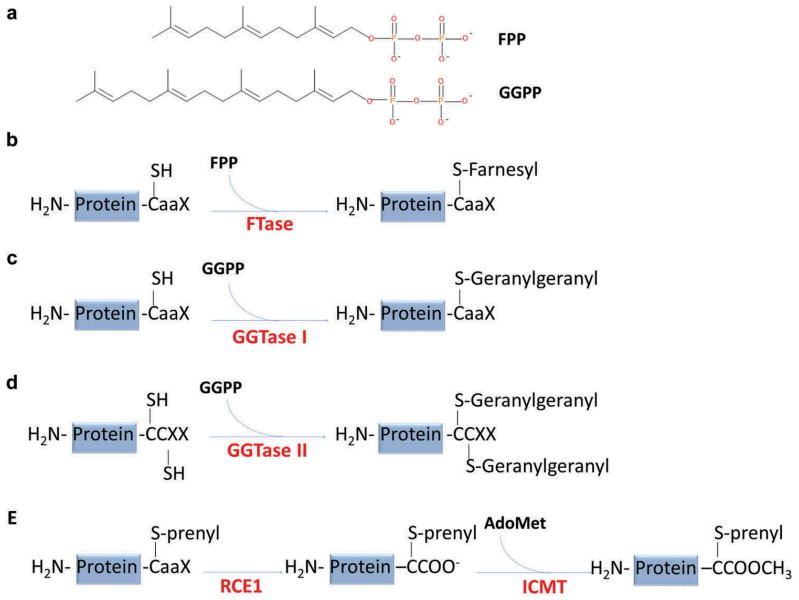

Figure 1. **Overview of prenylation reactions**. (A) Isoprenoids substrates for prenylation (FPP, farnesyl pyrophosphate, Structure 1; GGPP, geranylgeranyl pyrophosphate, Structure 2). (B-D) Mechanism of action of farnesyltransferase (FTase) (panel B), geranygeranyltransferase I (GGTase I) (panel C), and Rab geranylgeranyltransferase (RabGGTase or GGTase II) (panel D). (E) Processing of farnesylated or geranylgeranylated CAAX-proteins catalyzed by RAS-converting CAAX endopeptidase 1 (RCE1), which removes the -AAX residues, followed by isoprenylcysteine carboxyl methyltransferase (ICMT), which adds a methyl group from S-adenosylmethionine (AdoMet) to the carboxy-terminal isoprenoid-modified Cys residue.

small GTPases affects their intracellular trafficking, subcellular localization, and interactions with substrates. Therefore, prenylation modifies the functions of small GTPases as well as the functions of their downstream effectors [4–18].

In addition to their roles in cellular physiology, the prenylation and post-prenylation of CAAX proteins have important implications in human diseases as discussed later, and in the recent years, these proteins have become attractive targets in the search for inhibitors with therapeutic potential.

2. Prenylation in diseases

2.1. Prenylation in progeria

Studies on lamin proteins, a group of proteins that, being localized near the inner side of the nuclear membrane, form the nuclear lamina and affect many nucleus functions, were among the first to show farnesylation of mammalian proteins [5]. Indeed, posttranslational farnesylation had previously been demonstrated for fungal mating pheromones [19], and the first direct evidence of the relationship between the CAAX motif and farnesylation was obtained by nuclear magnetic resonance (NMR) of the *Saccharomyces* a-factor [20]. The preference for lamin farnesylation, over geranylgeranylation, derives entirely from the C-terminal methionine residue, being the human lamin CAAX boxes CSIM for prelamin A, CAIM for mammalian lamin B1, and CYVM for lamin B2. The functional role of the CAAX-box modification of prelamin A is unique among mammalian proteins because it is eliminated during prelamin A maturation.

Indeed, the sequential processing steps to generate the mature forms of lamin A, lamin B1, and lamin B (reviewed in [21] and [22]) include (a) addition of a 15-carbon farnesyl isoprenoid to the CAAX by FTase and (b) modification by a prenyl-CAAX-specific endoprotease that removes the tripeptide at the carboxyl terminus of prelamin A and lamin B. RCE1 is responsible for the cleavage of the peptide in B-type lamins, while RCE1 as well as ZMPSTE24, the Zn-metallopeptidase that is also required for the final proteolytic step of prelamin A, has been implicated in the cleavage of the -SIM tail from prelamin A. Third, the carboxyl terminal farnesylcysteine is then methylated by an ICMT. Finally, while B-type lamins are permanently farnesylated and carboxymethylated, prelamin A undergoes an additional cleavage of the carboxyl terminal 15 amino acids mediated by ZMPSTE24, leading to the release of the mature, unfarnesylated, and unmethylated lamin A.

Up to this date, more than 400 mutations have been identified in the protein-coding region of the *LMNA* gene (http://www.umd.be/LMNA). Some of these mutations are unique for lamin A, while others are located in the region encoding for both lamin A and C. These mutations cause the onset of several distinct forms of laminopathies, but one of the most striking and devastating is the fatal Hutchinson–Gilford progeria syndrome (HGPS), a sporadic autosomal dominant segmental genetic disease leading to premature aging affecting 1 subject every 4 million [23].

HGPS is caused by a series of single point mutation in the *LMNA* gene that, although silent, induce an alternative splicing leading to the translation of the disease-causing abnormal

lamin A protein, progerin [24]. The main HGPS-causing mutation in *LMNA* is a single-nucleotide substitution that alters the splicing of the prelamin A transcript, leading to the in-frame deletion of 50 amino acids [24].

This deletion leaves the CAAX motif of prelamin A intact and available for farnesylation and methylation, but it eliminates the ZMPSTE24 cleavage site, preventing the conversion of the mutant prelamin A (generally called progerin) into lamin A. Progerin accumulation also leads to misshapen cell nuclei in cultured fibroblasts and is responsible for all of the disease phenotypes of HGPS [24].

Yang et al. generated knock-in mice expressing farnesylated progerin (LmnaHG/+) and tested whether their progeria-like disease phenotypes might be ameliorated by an FTase inhibitor (FTI). They showed that FTI treatment lessened the severity of disease phenotypes in LmnaHG/+ mice [25]. The favorable results with FTI therapy in LmnaHG/+ mice have raised hopes for positive results from the FTI trial in humans. Nevertheless, recent studies in mice have suggested that the FTI treatment strategy may be destined to fall short of a complete cure. Yang et al. [26] generated knock-in mice expressing a 'non-farnesylated' version of progerin (LmnaHG/+) and showed that those animals developed severe progeria, but less severe than in mice bearing farnesylated progerin. The understanding that non-farnesylated progerin elicits disease suggested that an altered primary structure (i.e. the 50 amino acid deletion), and not merely the farnesyl lipid, contributes to the pathogenesis of HGPS.

The first FTI used in human clinical trial for HGPS was lonafarnib [27]. Cardiovascular and neurovascular benefits were demonstrated including decreased vascular stiffness, incidence of stroke, headache, and transient ischemic attack, after 2 years of treatment. There was also evidence for skeletal and audiologic benefits. However, lonafarnib was not able to improve all disease phenotypes and not all subjects benefit from this treatment [28]. The possibility that targeting ICMT could be an effective strategy for treating HGPS was addressed by Ibrahim et al. [29] who found that a hypomorphic allele of ICMT improved disease phenotype by increasing body weight, normalizing grip strength, and preventing bone fractures and death in ZMPSTE24-deficient mice. Furthermore, ICMT inhibition increased proliferation and delayed senescence in human HGPS fibroblasts [29].

2.2. Prenylation and Alzheimer's disease

Alzheimer's disease (AD) is a progressive neurodegenerative disorder affecting approximately 11% of the population aged 65 years and older and is clinically characterized by impaired episodic memory. The pathological signs of AD are intracellular neurofibrillary tangles and deposits of aggregated amyloid-βprotein (Aβ) in neuritic plaques and cerebral vessels, an event that compromises the plasticity and structural integrity of the synapses [30]. However, the relationship between the neuropathology of AD and the behavioral changes is not completely clear. Emerging evidence demonstrates that protein prenylation and alterations in the level and function of some small GTPases may contribute to the pathogenesis of AD (reviewed in [31] and [32]).

For example, atorvastatin-induced depletion of isoprenoids is associated with the reduction of protein prenylation and the stimulation of non-amyloidogenic processing of amyloid precursor protein (APP) through the α-secretase activity, which, cleaving within the sequence of Aβ, precludes the formation of intact Aβ in favor of the neurotrophic soluble fragment sAPPα [33].

In contrast, other *in vitro* studies reported that lovastatin or simvastatin augments intracellular levels of APP and Aβ, paralleled by a decrease of secreted Aβ, in a geranylgeranylpyrophosphate (GGPP)-dependent manner [34]. The mechanisms proposed include the increase/activation of β-secretase [34], inhibition of vesicle trafficking [35], and inhibition of γ-secretase activity [36]. Independently from the effects exerted by different statins, these data indicate that prenylation is involved in determining levels of intracellular Aβ.

Interestingly, the interplay between prenylation and APP/Aβ metabolism seems to be reciprocal. Indeed, the activities of the enzymes involved in the mevalonate pathway may be directly regulated by Aβ and other APP cleavage products, such as APP intracellular domain, influencing the levels of isoprenoids and other lipids [37].

In accordance, the levels of farnesylpyrophosphate (FPP) and GGPP, as well as that of FPP synthase and Ras, in the cytosol or in the membranes (prenylated forms) are higher in the brains of AD patients, suggesting that also protein prenylation could be increased in AD brains [38,39].

In addition to APP/Aβ metabolism, prenylation/GTPases have been demonstrated to be involved in different aspects of AD pathogenesis. For example, inhibition of Rho GTPases prenylation leads to attenuation of Aβ-induced neuroinflammation [40].

Despite these premises, results from epidemiological studies show that the risk of AD is decreased by statins even if prospective studies have produced mixed results. The discrepancies among these studies are most likely caused by differences in the choice and dose of statins, the selection of patient populations, the treatment durations, and the criteria of outcome measures (reviewed in [41,42]). However, another critical aspect is the fact that statins reduce FPP and GGPP levels simultaneously and consequently alter both farnesylation and geranylgeranylation pathways, which are both involved in the regulation of different cellular functions. Recent studies demonstrated that selective inhibition of protein farnesylation, but not geranylgeranylation, improves synaptic and cognitive function with a reduction of AD pathology, suggesting the potentiality of these inhibitors as therapeutic agents for AD. Interestingly, inhibiting the level of FPP, but not GGPP, enhances hippocampal synaptic plasticity in brain slices of mature C57BL/6 mice [43]. Consistently, Cheng et al. demonstrated that haplodeficiency in FTase, but not in GGTase-1, rescues cognitive function and attenuates Aβ-associated neuroinflammation and neuropathology in a mouse model of AD [44]. Thus, FTIs have also been proposed for the treatment of neurodegenerative diseases and one FTI (LNK-754), developed by Link Medicine Corp. [45–47], has been tested in Phase I clinical trials in subjects with mild AD and in healthy elderly volunteers to evaluate tolerability, safety, and pharmacokinetics (http://clinicaltrials.gov, NCT01013610 and NCT00903253). However, additional studies are needed to clarify the role of protein farnesylation on the onset and progression of AD.

2.3. Prenylation and hepatitis

Chronic hepatitis delta is a severe liver disease occurring in subjects that carry the hepatitis B surface antigen (HBsAg) and are also infected with the hepatitis delta virus (HDV), the smallest virus in human virology with a genome of about 1700 nucleotides coding for the hepatitis delta antigen (HDAg) of 195 amino acids [48].

Treatment still relies on interferon, first introduced empirically in the 1980s, but results are limited [49]. Therapy is problematic because the minimalist HDV does not encode for any enzymatic function and has no replicative machinery of its own to be targeted by antivirals.

The crucial role of prenylation, which is an essential step for virion assembly and packaging of viral particles [50], has led to the hypothesis that disruption of this PTM by drugs could prevent virion morphogenesis. The prenyl-lipid on the HDAg is farnesyl, and FTase inhibitors were used with success *in vitro* and in the mouse model to diminish HDV release [51].

Koh and colleagues [52] provided the first proof-of-concept that a prenylation inhibitor, lonafarnib, can decrease HDV mRNA in a dose-dependent manner and indicated a new unconventional strategy to attack a virus resistant to conventional therapies. One potential advantage of the use of FTase as antiviral target is that it is more difficult to develop resistance against a host target.

In clinical practice, several problems need to be considered before lonafarnib becomes a therapeutic option in human HDV disease, and future studies will need to address if monotherapy with a prenylation inhibitor can be sufficient to cure HDV or if combination therapies, for example, with pegylated interferon alfa will be required.

As far as hepatitis C is concerned, the analysis of prenylated proteins by using a combination of [H^3] mevalonate labeling, coimmunoprecipitation, and bioinformatics search led to the identification of a geranylgeranylated host protein called FBL2, which forming a specific complex with the HCV NS5A protein is crucial for HCV RNA replication [49].

2.4. Prenylation in infective diseases

During the last decade, the advanced detection methods of PTMs, including the modified peptide enrichment combined with high-accuracy MS, the sequencing of pathogen genomes for PTMs activity prediction, and the functional studies of the host–pathogen relationships, highlight that bacteria have also developed several PTMs, in order to use host cell pathways for their benefit, to bypass the host defenses, and finally to promote their replication (reviewed in [53]). *Legionella pneumophila*, the etiological agent of the severe pneumonia legionellosis, is a paradigm of highly adapted intravacuolar pathogens that have set up sophisticated biochemical strategies to hijack host cell processes. Similar to many bacteria, *Legionella* interacts with the host cell through secretion of effector proteins which serve as substrates for protein–protein interactions with proteins from the host cell or other bacteria but also as substrates for PTMs using the eukaryotic machinery. These effectors contain the CAAX motifs that after prenylation are targeted to host organelles, thus facilitating intracellular infection [53,54].

An important role in the control of cell growth and morphogenesis of microbial pathogen is also exerted by prenylated Ras-like GTPase family proteins. For instance, Ras1 protein prenylation, in *Candida albicans*, is required for a correct membrane localization to support hyphal growth, which is a virulence-associated phenotype for this organism [55]. Similar effects have been demonstrated in *Aspergillus fumigatus* in which an altered hyphal growth, defective cell walls, and reduced virulence have been also associated with mislocalization of RasA from the plasma membrane [56]. In addition, other components of the prenylation pathway, such as PTases, could affect fungal virulence. It has been demonstrated that the expression of a gene encoding for a subunit of both FTase and GGTase-I, RAM2, is crucial for the viability of *C. albicans* [57] and *Candida glabrata*, *in vitro* as well as in infected mice [58]. Furthermore, for the human fungal pathogen *Cryptococcus neoformans*, not only farnesylation and geranylgeranylation but also post-prenylation processing have been shown to influence the virulence of this fungus [59]. Finally, as reviewed by Eastman et al. [60], protein prenylation occurs in a wide variety of pathogenic protozoa, including *Trypanosoma brucei*, *Trypanosoma cruzi*, *Leishmania species*, *Plasmodium falciparum*, *Toxoplasma gondii*, *Giardia lamblia*, and *Entamoeba histolytica*. Growth of the protozoan parasites has been shown to be seriously damaged by the inhibition of protein farnesylation in comparison with mammalian cells, suggesting high potential of the enzyme protein FTase as an antiparasitic drug target. Indeed, FTIs have already been shown to be efficacious in the treatment of eukaryotic pathogens in animal models, including infection with both *T. brucei*, the causative agent of African sleeping sickness, and *P. falciparum*, one of the causative agents of malaria [61].

2.5. Prenylation and cancer

Members of the Ras family of GTPases, which almost all contain the CAAX motif, have attracted a great interest because of their well-established role in oncogenesis [62]. Besides Ras, several other CAAX proteins are involved in the initiation and progression of cancer: the Rho family of GTPases, which includes Rac and Cdc42, and many phosphatases and kinases (reviewed in [63]). As nicely discussed by Wang et al. [64], the discovery of the essential role of prenylation in modulating Ras function generated enormous enthusiasm for the development of prenylation inhibitors, in particular FTase inhibitors, with more than 400 patents registered in less than a decade [65]. The impressive results obtained in animal model of tumor promptly led to clinical trials, but the results were quite contradictory. Indeed, the outcome of Phase II and Phase III clinical trials was, in general, rather disappointing, considering that many FTIs failed to demonstrate antitumor activity in Ras-dependent cancers, presumably because one of the most frequent mutated form of Ras in human cancers (K-Ras) is able to avoid FTI blockade through cross-prenylation by the related enzyme GGTase I [66]. Thus, the recognition of alternative prenylation of RAS enhanced attention on targeting GGTase I, which processing additional proteins, such as Rho, has the potential to modulate also inflammation. So far,

geranylgeranyl trasferase inhibitors (GGTIs) have shown significant efficacy in several animal models of both cancer and inflammatory diseases. However, there is still much to be learned about the modifications and functions of the CAAX proteins. The effects of GGTase I appear to be very complex as suggested by the surprising results showing that the gene deletion of GGTase I in mice, instead of protecting from inflammatory symptoms, on the basis of the inflammatory effects of Rho GTPases, induced severe joint inflammation [67]. Overall, these findings highlight the cell context-specific interplay of the biological processes determined by the CAAX protein prenylation.

2.6. Prenylation and spermatogenesis defects

Protein prenylation in the seminiferous epithelium is crucial in early stage of spermatogenesis before sexual maturity [68]. This finding comes from the observation that male rats treated with the HMG-CoA inhibitor, rosuvastatin, present a delay in the age of puberty onset and epididymal development accompanied by testicular and epididymal alterations [69]. Moreover, Wang et al. suggest that male infertility due to mumps virus infection before puberty could be ascribed to reduced levels of prenylation caused by deficiency of geranylgeranyl diphosphate synthase, which induce excessive synthesis and secretion of chemokine and cytokine in Sertoli cells, leading to spermatogonia apoptosis and subsequent adult infertility, as demonstrated in a mouse model [70]. The same authors further demonstrated the importance of protein farnesylation as cell-intrinsic regulator, able to stimulate the mTORC1 signaling pathway influencing the expression of differentiation-related genes. Indeed, geranylgeranyl diphosphate synthase reduction is associated with FPP accumulation, changing the ratio between protein geranylgeranylation and farnesylation, which regulate spermatogonial stem cell differentiation in early stage of spermatogenesis, thus providing a potential basis for primary male sterility treatment, which is caused by spermatogonial stem cell exhaustion and germ cell depletion [68].

2.7. Other diseases

Many studies reviewed by Roosing et al. [71] suggest that the retina specifically requires proteins modified with lipid moieties, most probably due to the membranous structure of the photoreceptors. The retina, therefore, may be particularly susceptible to prenylation of proteins, which would give rise to retinal symptoms before (if at all) affecting other tissues. Several genes implicated in inherited retinal diseases encode proteins involved in the prenylation process as mediator or target. Mutations in these genes may result in diminished or abolished protein synthesis, but can also cause protein inactivation and accumulation of inactive prenylated proteins, with deleterious effects in photoreceptor cells and subsequent progressive degeneration of photoreceptors, the retinal pigment epithelium, and the choroid.

Very recently, it has been demonstrated that alteration of glucose homeostasis in complex diseases such as infection, obesity, and type 2 diabetes might be due to sustained inflammation which suppressing CYP7A1 leads to accumulation of intermediate metabolites of the mevalonate pathway. This phenomenon results in prenylation of RHOC, which is concomitantly induced by inflammatory cytokines, and in the elevation of plasma glucose [72].

3. Proteomics and prenylation

The growing body of evidence suggesting an important role of prenylation in diseases is leading to the development of several inhibitors of the enzymes responsible for this modification [73]. Thus, prenylome-wide approaches are urgently needed to identify the subsets of prenylated proteins that are affected by FTIs and/or GGTIs, which in turn should help to elucidate the link between physiological effects of PTase inhibitors (PTIs) and their targets.

However, tools to analyze prenylated proteins from a global point of view are only recently emerging. Indeed, the study of lipid modification, and in particular prenylation, is a really difficult task, due to not only their low abundance, typical of many PTMs, but also the extremely high hydrophobicity that complicates protein extraction and separation and their MS analysis [74]. After in-gel digestion of modified proteins, lipidated peptides are not efficiently eluted [75], and lipidated proteins or peptides display also reduced efficiency in terms of ionization and fragmentation by tandem MS (MS/MS), making their analysis more difficult by liquid chromatography (LC) coupled to MS [18,76]. It is therefore clear that there is strong need of tools to modify and enrich prenylated proteins to reach a comprehensive knowledge of the prenylome and to quantify it.

An enormous step forward into the analysis of posttranslationally modified proteins has been done in the recent years, thanks to the technological advancement in the field of MS, the most powerful tool to address this challenging issue.

However, since almost all PTMs present lower stoichiometry in comparison with unmodified proteins, MS sensitivity is still not enough, and specific enrichment techniques are essential to achieve detection and characterization of these low-abundant components in complex mixtures of proteins from cell or tissue lysates (Figure 2). Several enrichment strategies at protein or peptide level have been developed so far to deal with the different types of PTM before MS analysis for their identification and localization of the modification site. Affinity enrichment strategies using antibodies have been successfully applied to the study of tyrosine phosphorylation and nitration, arginine methylation, and lysine acetylation [77] through the immunopurification of modified proteins or peptides with high-quality antibody that are, unfortunately, not available for all the PTMs. Other affinity purification methods using, for example, lectin have been used for the enrichment of N-glycosylated proteins, while in the case of phosphorylation, the chemical characteristics of the phosphate group allow their enrichment with matrix-immobilized metal ions, such as IMAC or TiO2-based methods, with an high efficiency [78,79]. Other PTMs, such as O-glycosylation or glycosylphosphatidylinositol (GPI) modification, have been investigated using modification-specific enzymes that allow the release of the PTM, such as PNGase, for the release of N-linked oligosaccharides [80] or their tagging with biotin for subsequent enrichment [81–83]. Alternatively, a series of methods using

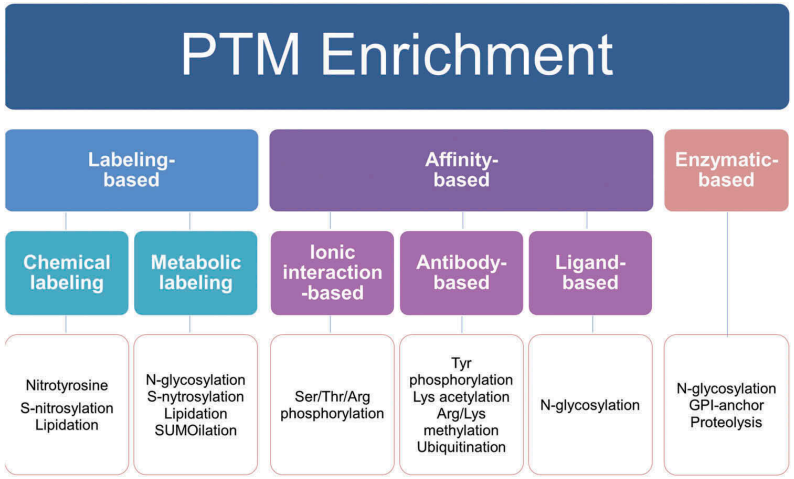

Figure 2. **Enrichment strategies for PTM analysis**. Proteomic analysis of post-translationally modified proteins often require enrichment strategies before gel-based or MS-based methods for the identification of the modified proteins and the modification site. These strategies can be based on labeling, affinity purification or enzymatic reactions.

in vivo metabolic labeling or *in vitro* chemical labeling has been developed to convert the PTMs (i.e. palmitoylation and myristoylation) in molecules that can be easily traced or tagged with biotin for enrichment [77].

As far as prenylation is concerned, several methods based on biochemistry and molecular biology are available in the literature to study this modification, but most of these studies are tailored to individual proteins and are based on enzyme overexpression and inhibition or labeling with radioactive isoprenoids.

Radioactive labeling was the first method employed to evaluate protein prenylation *in vitro*, and it is based on the treatment of cells with a labeled H^3-mevalonate, which is converted by the cells in H^3-FPP and H^3-GGPP and incorporated in prenylated proteins through the action of PTases. The labeled prenylated protein can be detected by autoradiography and the combination with immunoprecipitation of a protein of interest has proven to be the method of choice to determine the prenylation of individual proteins. Using H^3-mevalonate, it is impossible to discriminate between the two types of prenylation, and to do that, it is necessary to use alternatively H^3-labeled FPP or GGPP as isoprenoids donors [84]. To further confirm the presence of prenylation, additional experiment can be performed to visualize by Western blotting the change of apparent molecular weight of the protein of interest upon inhibition of prenylation or the subcellular localization of prenylated proteins in membrane fractions. These radioactive-based methods are in general used in combination with the generation of mutants in which the cysteine, target of prenylation, is substituted by a serine in order to confirm the modification site.

Despite the evident disadvantages, they have been successfully applied in many cases. For example, Wang et al. demonstrated that the geranylgeranylation of a specific host protein is necessary for RNA replication of hepatitis C virus (HCV) using cell labeling with H^3-mevalonate, molecular biology, bioinformatics, and immunoprecipitation experiments [85]. Based on previous observations suggesting that HCV geranylgeranylation was essential for HCV RNA replication [86,87], they overexpressed a tagged form of one of the HCV protein (NS5A), and, studying its radioactive interactors, they were able to hypothesize the prenylation of F-box/leucine-rich repeat protein 2 (FBL2). Indeed, overexpressing a tagged form of FBL2, wild type (Myc-FBL2WT) or mutated to eliminate the putative modification site (myc-FBl2-C420S), they evidenced that only the immunoprecipitated Myc-FBL2WT was positive for autoradiography because of prenylated but not the mutated form. Furthermore, they demonstrated that the Myc-FBL2WT was able to localize in membrane fraction, while the mutated one was mainly located in the cytosol, and the treatment with GGTI, but not FTI, lead to a relocalization in the cytosol for Myc-FBL2WT [85].

However, this approach has several drawbacks linked to the safety of working with radiochemicals, the costs, and the quantity of time required to obtain results with autoradiography (up to 3 months) [84]. For these reasons, it is not suitable for broad-based proteomic studies to identify novel prenylated proteins in complex mixtures [18,84].

Antibodies against specific prenylated proteins are commercially available for immunohistochemistry, ELISA, or Western blotting analysis [84]. On the other hand, antibodies against the prenyl groups that could be used for affinity purification of prenylated proteins in combination with MS-based methods are still sparse, and, to the best of our knowledge, no examples of antibody-based enrichment of prenylated proteins exist.

Hereinafter in this review, we describe the emerging broad-based strategies developed to identify and quantify protein prenylation *in vivo* and *in vitro*. Indeed, in order to analyze protein prenylation from a global point of view, several

techniques have been developed based on MS coupled, for example, with prenyl group derivatization, bioorthogonal labeling, or *in vitro* reactions with recombinant PTases.

3.1. Strategies to study prenylated proteins

3.1.1. MS-based methods for prenylome analysis

The growing knowledge of the complexity of PTMs occurred in the last decade is strictly connected with the improvements in the performances of LC and the advancements in MS with the introduction of novel high-resolution instruments, for a more precise measurement of precursor and products and different types of fragmentation (electron capture- and electron transfer-based fragmentation) essential for sequencing and identification of the modification site [88].

Though prenylation has been extensively studied in the past two decades, systematic MS-based analyses are still rare.

Prenyl group structures have been studied by MS coupled to gas chromatography [89] or high-performance liquid chromatography (HPLC) after hydrogenation, cleavage of the thioether bond by Raney nickel cleavage, and isolation of free lipids [90]. Fewer examples exist in which MS has been applied to obtain the exact location of the modification, beyond the characterization of the lipid moieties [75].

Analyzing synthetic peptides, by electrospray ionization (ESI) or matrix-assisted laser desorption ionization (MALDI) MS/MS, it has been demonstrated that the fragmentation of farnesylated peptides during collision-induced dissociation (CID) produces a neutral loss of 204 Da, which equate the farnesyl group, or a marker ion of 205 Da corresponding to the protonated form of the farnesyl group, together with some fragment ions (135, 149, and 163 m/z) that could help in the identification of putative farnesylated peptides [91]. In particular, monitoring of the neutral loss seems to be the preferential method for the analysis of prenylated peptides by MALDI, while with ESI the marker ions would be better [91].

Several HPLC methods have been proposed to separate peptides bearing lipid modification before MS analysis, but the high hydrophobicity renders this task still challenging, especially if the modified and unmodified peptides need to be separated in a single HPLC run [92]. To circumvent this limitation, Wotske et al. demonstrated that farnesylated peptides could be identified also in complex mixtures by MS, despite their low abundance, exploiting the separation efficiency of multidimensional protein identification technology (MudPIT) chromatography avoiding other enrichment steps. Indeed, peptides from *in vitro* farnesylated Rab proteins were detected and identified in a complex mixture of HeLa cell lysate coupling a first separation by strong cation exchange chromatography with a second separation by reverse-phase chromatography. They demonstrated that the low-abundant farnesylated peptides, identified by the presence of a farnesyl neutral loss during fragmentation, were eluted significantly later than their non-farnesylated counterpart near the end of the gradient (5–80% acetonitrile) after the majority of peptides. However, it should be noticed that the farnesyl group occasionally split off the peptide during ionization complicating the interpretation of the results [92].

More recently, Bhawal et al. developed a novel 'MS cleavable strategy' based on the derivatization of the prenyl groups with m-chloroperoxybenzoic acid (mCPBA) introducing a mono-oxidized thioether bond that, during CID in the gas phase of the MS, produces a neutral loss that allows the unambiguous distinction of farnesylated or geranylgeranylated peptides in a single experiment. In addition to the introduction of a mono-oxidized thioether bond on modified cysteines, that is very labile and can be easily broken [93] to release the neutral RSOH group (R is the mass of the epoxidized prenyl group), it produces also the epoxydation of a variable number of isoprenoid groups that could be very useful in the characterization of prenylated peptides and for the addition of an enrichment tag (Figure 3). The mCPBA reaction introduces a maximum of five epoxy group in the farnesylated peptides and six in the geranylgeranylated peptides, generating several targets for MS/MS analysis with no effects of hydrolysis after long HPLC gradients [76]. To further clarify the potential application of this method, Bhawal et al. tested a different fragmentation technique (electron-transfer dissociation [ETD]) in combination with CID to study epoxidized prenylated peptides, and they evidenced a more efficient fragmentation of the backbone with ETD, but with the loss of the signature fragment due to mono-oxidized thioether bond cleavage, which is prevalent with CID

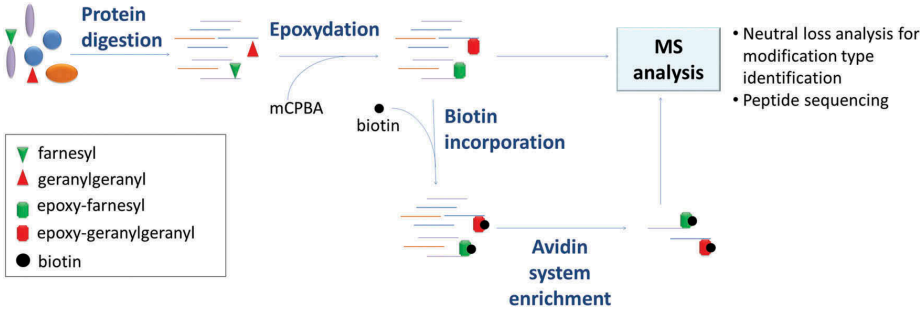

Figure 3. **Prenylated protein analysis by the 'mass spectrometry cleavable strategy'**. After protein digestion prenylated peptides can be epoxydized with m-chloroperoxybenzoic acid (mCPBA). This treatment allows the direct analysis of prenylated peptides by MS, with the identification of the type of modification (farnesyl or geranylgeranyl) on the basis of the presence of a specific neutral loss signature followed by peptide sequencing. Otherwise prenylated peptides can be derivatized with a biotin probe and enriched by means of an avidin system before MS analysis.

fragmentation, suggesting that a combination of CID and ETD could be useful for an efficient analysis of prenylated peptide by MS [94]. This MS-based method offers several additional advantages: after neutral loss, the newly generated precursors can be more easily fragmented and therefore sequenced; the epoxidation of unsaturated attached lipids reduce the extreme hydrophobicity of prenylated peptides with a consequent better performance of the reverse-phase chromatography separation; and the epoxy groups could be used for enrichment strategy based on the introduction of enrichment tags such as azide biotin [76].

The method has been validated with spiking experiment with prenylated peptides in a matrix of unmodified peptides; however, up to this date, no examples exist for its application in complex samples, and a dedicated search algorithm is going to be developed. Nevertheless, this is a promising approach that could be applied not only *in vitro*, but also *in vivo* in animal models and in clinical samples, avoiding any type of labeling and exploiting the ability of MS for relative and absolute quantitation.

3.1.2. Metabolic labeling for prenylome analysis

In order to avoid radioactive labeling, other analogs have been proposed for *in situ* metabolic labeling of prenylated proteins in the so-called 'bioorthogonal labeling' approach. This approach is based on the use of lipid analogs containing functional groups, such as alkyne or azide modifications, which are cell permeable and metabolically stable, but normally absent in biological samples and largely inert toward biological molecules. These molecules could be the target of a bioorthogonal reaction based on the 'click chemistry' with chemical tags for fluorescence detection or enrichment.

The term 'click' chemistry coined by Sharpless [95] describes chemical reactions such as the Huisgen copper(I)-catalyzed azide-alkyne 1,3-dipolar cycloaddition (CuAAC) reaction between azides and alkynes that offers high yields generating only inoffensive products. Fluorophore ligation allows prenylated protein imaging in cells or in gels, while biotin ligation could be used for enrichment of prenylated proteins for identification and quantitation of single target by Western blotting or proteome wide profiling and quantification of protein prenylation by MS (Figure 4).

In particular, isoprenol analogs (such as alkyne-farnesol, Alk-FOH) are preferred to pyrophosphate for their increased cell permeability. Furthermore, it has been demonstrated that exogenous isoprenols can be used by mammalian cells to generate isoprenoid diphosphate substrates by kinases, independently from the mevalonate pathways, and this process is upregulated with the inhibition of mevalonate pathway [96]. Indeed, this bioorthogonal approach is in general combined with statin treatment to reduce the pools of endogenous isoprenoids even if this affects the bioorthogonality of the reaction considering the multiple effects exerted by statin [96].

Metabolic labeling of living cell has been demonstrated to be powerful for the definition of the specificity of PTase, for the assessment of PTI efficiency, and for the discovery of novel prenylated proteins, notwithstanding obvious limitations exist for the application to clinical samples [74]

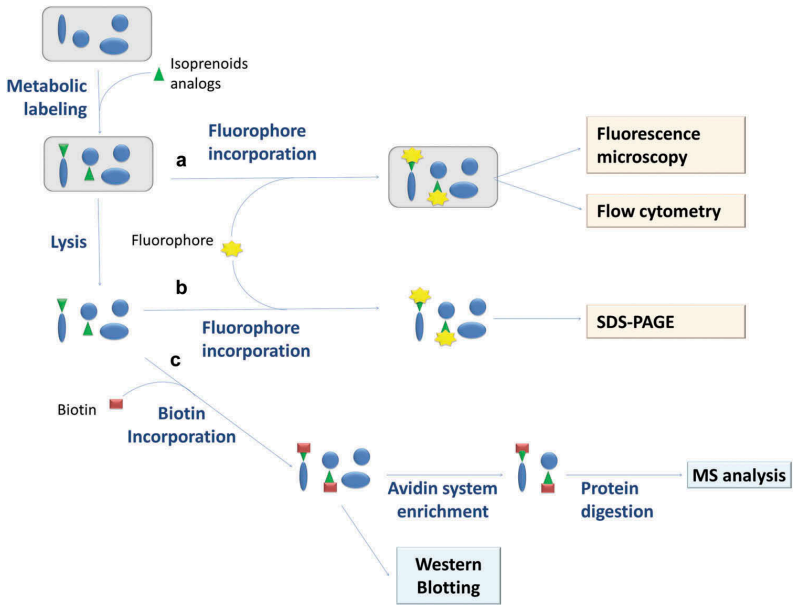

Figure 4. **Workflow for prenylated protein analysis by bioorthogonal labeling**. Cells are metabolically labeled using isoprenoids analogs containing alkyne or azide groups (i.e. alkyne farnesol, C15Alk) and subsequently derivatized in several ways for their identification or visualization. A) Labeled cells can be fixed and permeabilized before fluorochrome incorporation for analysis of prenylated proteins by fluorescence microscopy or flow cytometry. B) Labelled cells can be lysed and derivatized with fluorochrome to be visualized with an imaging system for fluorescence detection after protein separation by SDS-PAGE. C) Labeled cells can be derivatized with biotin probes and visualized by Western blotting or enriched with an avidin system before protein digestion for MS analysis.

Several azide or alkyne analogs have been used so far, such as anilinogeraniol in combination with detection with anti-anilinogeranyl antibody [97], azidogeranylgeranyl analog derivatized using tetramethyl-rhodamine for fluorescence detection [98], and C15Alk used in combination with differential gel electrophoresis (DIGE) [99]. In particular, Degraw et al. explored the use of several alkyne-containing analogs to study protein prenylation, in the presence of various inhibitors and in different cell lines, in comparison with azides [100]. In all these cases, proteins are separated by 2-DE and only prenylated proteins are detected, and differentially expressed proteins are identified by in-gel digestion and MS [97–99]. A recent paper by Palsuledesai et al. proposed also metabolic labeling with C15Alk followed by cycloaddition of a fluorophore for imaging of prenylated proteins using microscopy and quantification using flow cytometry for the evaluation of the global prenylome state [101].

On the other hand, bioorthogonal labeling using biotin tag demonstrated its efficacy for the first time in the study from Kho et al. in which FPP-azide-modified proteins were selectively ligated with a phosphine capture reagent via the Staudinger reaction, instead of the azide/alkyne click reaction, and subsequently enriched by affinity purification leading to the identification of 18 farnesylated proteins [102].

A pull-down approach, employing an alkyne farnesol analog as reporter and CuAAC, was also applied in the study from Charron et al. to identify more than 100 prenylated proteins in the prenylome of macrophages. Together with known small GTPases, unannotated proteins were also identified as putative target of prenylation such as the zinc-finger antiviral protein, for which farnesylation was demonstrated to be essential for its targeting in lysosomes and late endosomes and for its antiviral activity [103].

More recently, Suazo et al. used the C15AlkOPP probe to tag prenylated proteins for both in-gel fluorescence labeling and pull-down for proteomic analysis to study the prenylome of *P. falciparum*, which is mainly composed of Rab GTPases together with few proteins involved in membrane trafficking [104].

The main advantage of this approach is the compatibility with subsequent proteomic analysis by MS. Indeed, the selection of a short clickable lipid analog reduces the hydrophobicity of the modified proteins, ameliorating their extraction and separation; the biotin tagging allows the efficient enrichment of prenylated proteins; quantitative data can be obtained; the ionization efficiency is increased by the addition of a positive-charged linker region, and better fragmentation spectra can be obtained after tag removal [18].

However, some limitations exist. Metabolic labeling in animal models, by direct introduction into the bloodstream or injection into specific organ or xenograft tissue, is still in its infancy and requires studies to determine pharmacokinetic and pharmacodynamic behavior of the isoprenoid analogs [105].

Furthermore, results need to be validated with other techniques. Some unspecific protein identifications could be obtained due to the *in vivo* metabolism of these analogs into other lipid molecules [106], and the intracellular localization of modified proteins could be incorrect due to the presence in some analogs of an artificial ether linkage that renders the probes not completely biomimetic [74].

In comparison with the MS-based methods described previously, concomitant detection of farnesylated and geranylgeranylated proteins is currently complicated by the quality of analogs that are not suitable or nonselective for geranylgeranylation [105], and the exact location of the modification site could be obtained only through mutagenesis.

3.1.3. *In vitro* prenylation assays

In order to analyze protein prenylation in samples that are not accessible to metabolic labeling, some tools for *in vitro* prenylation (IVP) have been developed. These approaches are based on the treatment of cells or tissue lysates with exogenous recombinant PTases and synthetic substrates, bearing fluorophores or enrichment tags, to induce protein prenylation of those sites that are not *in vivo* prenylated (Figure 5) [74]. Fluorescent isoprenyl pyrophosphates, such as 7-nitrobenzo[1,2,5]oxadiazol-4-ylamino (NBD) conjugated to FPP or GGPP, have been used to evaluate prenylation catalyzed by FTase and GGTase-I on selected small GTPases evaluating the fluorescence after SDS-PAGE of treated cell lysates or in living cells, thanks to its cell permeability [107].

The implementation of this method for proteomic studies is really complex because the synthetic substrates need to have an affinity for PTase similar to that of native substrate despite the tag, and for this reason, engineered protein PTases need to be developed [106,108].

Nguyen et al. developed a functionalized substrate, biotin-geranylpyrophosphate (BGPP), optimized to function as a lipid donor in all the protein prenylation reactions, using a set of engineered mammalian PTases able to selectively conjugate BGPP to the prenylation substrates (Figure 5). This method allowed the characterization and quantitative analysis of the prenylome of COS7 cells treated with compactin, a mevalonate pathway inhibitor, thanks to the possibility to isolate the biotin-labeled unprenylated proteins for proteomic analysis by MudPIT. They also demonstrated that this approach could be used to test the selectivity of prenylation inhibitors, incubating the cells with the PTI and subsequently the lysates with BGPP and different PTases [108].

This method was also successfully applied to study the prenylation of Rab proteins in Choroideremia disease, a disease resulting from the genetic deletion of Rep1 in which unprenylated Rabs accumulate in the eye, demonstrating that the presence of unprenylated Rab38, which is not functional, could be responsible for the observed eye defects [109].

More recently, Ali et al. optimized this approach to deal with the possible effects on prenylation exerted by a bisphosphonate drug used for bone disorders treatment, zoledronic acid (ZOL). Employing recombinant geranylgeranyltransferase RabGGTase/REP1 and the biotinylated substrate BGPP, they were able to evidence the effects of ZOL on prenylation of J477 macrophages proteins and demonstrated that IVP assay is more sensitive (>10 times) than Western blotting for the detection of unprenylated Rap1. Furthermore, by combining IVP with quantitative MS based on stable isotope labeling with amino acids in cell culture (SILAC) and biotin–avidin enrichment, they identified 18 different unprenylated Rab proteins in J774 cells after ZOL

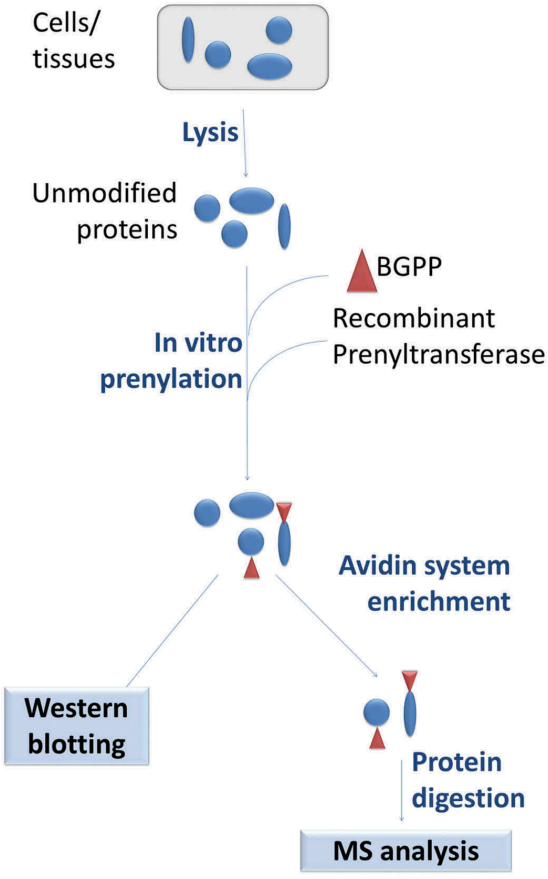

Figure 5. **Workflow for *in vitro* prenylation assays**. After cell or tissue lysis, the extracted proteins that are not modified can be prenylated by recombinant prenyltransferases in the presence of a chemical substrate, such as biotin-geranyl pyrophosphate (BGPP). Prenylated proteins are now biotinilated and can be visualized by Western blotting or analyzed by mass spectrometry after enrichment through the avidin system and protein digestion.

treatment, mainly Rab proteins associated with the endophagosome pathway (such as Rab1, Rab5, Rab6, Rab7, Rab11, Rab14, and Rab21), and also RhoA and Rac2. They also demonstrated the effectiveness of IVP assay in animal models and, in particular, in peritoneal macrophages isolated from mice treated with ZOL, confirming the prenylation of endophagosome-associated Rabs [110].

The methods described above represent powerful tools to study prenylation because they bypass the use of radioactivity, and biotin tagging allows the enrichment of prenylated proteins for a broad-based proteomic analysis and could be used in a variety of samples from cell-free systems [108,109] to clinical samples to quantitatively compare protein prenylation. However, limitations arise from the generation of synthetic substrates modified by the addition of fluorophore or biotin groups, which reduced their cell permeability and could modify the affinity for the PTases [106]. Furthermore, the rate of prenylation of proteins in lysates can be established only by identifying proteins that were not modified, and this is often forced through statin treatment to reduce endogenous isoprenoids reservoirs. Thus, information about *in vivo*-prenylated proteins could only be deduced, and possible cross talk between PTase could not be ruled out [74].

4. Conclusion

PTMs represent the most delicate and complex regulatory networks in eukaryotic cells. In particular, the role of prenylation in several disease state ranging from infective disease to cancer has been demonstrated, leading to the development of many PTIs that are under evaluation for their therapeutic application. However, only few studies have tackled these complex PTMs from a global point view, due to the lack of dedicated proteomic tools. The methods that are now available for the analysis of prenylated proteins *in vitro* and *in vivo* are mainly based on the application of MS analysis coupled with specific enrichment strategies to overcome the low abundance of modified proteins and the effects of prenylation on the efficiency of protein extraction and analysis.

5. Expert commentary

One of the challenges facing the field of prenylation is the variety and complexity of prenylated proteins. Even though numerous biologically important proteins have been identified to undergo prenylation [13], the number of the prenylome components is still unknown [111]. Based on the literature, several hundred proteins are subjected to prenylation [73,112], but only 170 human proteins result to be annotated in UniProt as prenylated (http://www.uniprot.org/; UniProt release 2017_01). Thus, the impact of prenylated proteins certainly extends beyond what has been demonstrated up to now.

The majority of the studies has focused on the prenylation of individual proteins and therefore has only touched the tip of the iceberg.

Several methods are recently being developed to characterize protein prenylation globally, including sequence-based computer programs specially designed to predict if proteins are prenylated [111]; but the most important progresses have been made over the past few years, thanks to the development of quantitative proteomic approaches based on MS, that could be applied to the study of protein prenylation not only *in vitro*, but also *in vivo*. The combination of MS with prenyl group derivatization or tagging of prenylated proteins with isoprenoid analogs, obtained by metabolic labeling [74] or by IVP reactions, has proven particularly powerful and will help to provide unique insights into prenylation targets and PTI selectivity.

However, the analysis of protein prenylation *in vivo* in mammalian tissue and in the clinical setting is still a challenging task. Indeed, metabolic labeling is complicated by the pharmacokinetic and pharmacodynamic issues of the lipid analogs used for labeling [105]. Furthermore, the so-called IVP assays can be applied to mammalian tissues to compare the levels of prenylation of proteins in different physiopathological conditions, but this is not a direct evaluation of the

amount of prenylated protein because only unmodified proteins can react and thus *in vivo* levels could only be inferred [108]. In this context, the strategy proposed by Bhawal et al. [76], which is based on prenyl group derivatization, is promising, but additional studies need to be performed to demonstrate the feasibility in complex samples.

In order to identify specific prenylated proteins, conditional knockout mice, in which FTase and GGTase activities can be ablated in a tissue-specific manner, have been generated and used as *in vivo* model system to investigate the targets of prenylation inhibition. In conjunction with the aforementioned approaches to characterize the prenylome, animal models with conditional knockout of FTases and GGTases in specific tissues [113] offer powerful tools for elucidating the mechanisms of a disease, identifying and validating therapeutic targets, and ultimately improving the outcomes of clinical trials.

It is important to note that, when dealing with prenylation, one should also take into consideration that prenylated protein could undergo further processing leading to removal of the C-terminal tripeptide and methylation of the new C-terminal cysteine. Indeed, it has been demonstrated that some proteins, like Gγ, could be present both in the unmethylated and in the methylated form [114]. This aspect was tackled by Kassai et al. using a top–down MS-based approach that allowed them to provide the evidence, from the MS/MS spectra, that mouse Tγ is farnesylated and carboxyl methylated at the C-terminal residue [115]. Thus, it is necessary to consider also the proteolytic cleavage and methylation of C-terminal cysteine as a possible variable modification for database search in global proteomic studies using MS. However, not all the approaches described in this review could address this issue. Indeed, by performing an IVP assay, only unprenylated proteins can be modified after cell/tissue lysis; thus, any information on post-prenylation processing is lost.

Overall, the novel strategies described in this review represent important progresses in the field of protein prenylation analysis, improving the sensitivity of the detection and allowing the identification of modified proteins in a high-throughput manner, thanks to affinity-enrichment steps. However, despite great advances have been obtained, tools and methodologies still need to be better characterized.

6. Five-year view

A deeper knowledge of prenylation process would improve the understanding of disease mechanisms with amelioration of therapy and diagnosis. We believe that the application of the novel strategies described in this review represents a step forward in the identification and characterization of the prenylation targets in broad-based studies, meeting the challenge of analyzing these large and hydrophobic PTMs.

However, another challenge still exists which is represented by the PTM cross talk. Various publications have demonstrated that multiple PTMs can coexist on the same protein influencing each other [77,116,117], and, in particular, a cross talk exists between lipid modification and other PTMs such as phosphorylation [118,119], glycosylation [120], or ubiquitination [18,121,122]. To this regard, recent advances in nonrestrictive sequence alignment algorithms provide a possible means for identifying all types of PTMs in a protein [77,123–126].

In order to determine how these multiple PTMs act together, proteomic studies in which multiple PTMs are contemporarily analyzed would be useful. However, up to this date, workflows for the comprehensive analysis of multiple PTM, including prenylation, are still lacking and need to be developed to analyze PTM cross talk on a global scale, further increasing the sensitivity and the range of abundance of the detected proteins.

Notwithstanding enormous progress has been obtained in the last few years, for many questions about prenylation an answer is still lacking, despite enormous investment in development of novel, potent, and selective inhibitors of PTases. Understanding the global effects of this PTM would increase the possibility to exploit therapeutic potential of PTI in several diseases.

Thanks to these approaches, a quantitative proteome-wide analysis of the regulation of protein prenylation and its modulation by therapeutic agents could be obtained, and their application in prenylome profiling of individuals in clinical settings could facilitate personalized medicine, decoding inter-individual differences in the response to drug treatments.

Key issues

- Prenylation is a multistep enzymatic process in which three known prenyltransferases (PTase) catalyze this modification adding hydrophobic prenyl moieties to proteins.
- The known protein substrates of PTases are very diverse in nature, but we are far from a comprehensive knowledge of all the existing prenylated proteins.
- In addition to the roles in cellular physiology, the prenylation and post-prenylation of CAAX proteins have important implications in several human diseases, such as cancer, Alzheimer's disease, progeria, hepatitis, infertility and infective disease.
- The role of prenylation in diseases is leading to the development of several inhibitors of the enzymes responsible for this modification.
- The available methods for the analysis of prenylome, *in vitro* and/or *in vivo*, are mainly based on MS coupled, for example, with prenyl groups derivatization, bioorthogonal labeling or *in vitro* reactions with recombinant prenyltransferases, for their enrichment
- Prenylome-wide approaches are only recently emerging to mine prenylated proteins and to identify the subsets of prenylated proteins that are affected by FTIs and/or GGTIs.

Funding

This work was supported by the European Union's Horizon 2020 research and innovation programme under the Marie Sklodowska-Curie grant agreement number 675132.

Declaration of interest

The authors have no relevant affiliations or financial involvement with any organization or entity with a financial interest in or financial conflict with the subject matter or materials discussed in the manuscript. This includes employment, consultancies, honoraria, stock ownership or options, expert testimony, grants or patents received or pending, or royalties.

References

Papers of special note have been highlighted as either of interest (•) or of considerable interest (••) to readers.

1. Gelb MH. Protein prenylation, et cetera: signal transduction in two dimensions. Science. 1997;275(5307):1750–1751.
2. Tsuchiya E, Fukui S. Binding of rhodotorucine A, a lipopeptidyl mating hormone, to a cells of *Rhodosporidium toruloides* for induction of sexual differentiation. Biochem Biophys Res Commun. 1978;85(1):473–479.
3. Wolda SL, Glomset JA. Evidence for modification of lamin B by a product of mevalonic acid. J Biol Chem. 1988;263(13):5997–6000.
4. Casey PJ. Biochemistry of protein prenylation. J Lipid Res. 1992;33 (12):1731–1740.
5. Zhang FL, Casey PJ. Protein prenylation: molecular mechanisms and functional consequences. Annu Rev Biochem. 1996;65:241–269.
   • **A pioneer paper describing the enzymology of prenyl protein processing.**
6. Higgins JB, Casey PJ. The role of prenylation in G-protein assembly and function. Cell Signal. 1996;8(6):433–437.
7. Resh MD. Regulation of cellular signalling by fatty acid acylation and prenylation of signal transduction proteins. Cell Signal. 1996;8 (6):403–412.
8. Parish CA, Rando RR. Isoprenylation/methylation of proteins enhances membrane association by a hydrophobic mechanism. Biochemistry. 1996;35(26):8473–8477.
9. Liang PH, Ko TP, Wang AH. Structure, mechanism and function of prenyltransferases. Eur J Biochem. 2002;269(14):3339–3354.
10. Roskoski R Jr. Protein prenylation: a pivotal posttranslational process. Biochem Biophys Res Commun. 2003;303(1):1–7.
11. Magee T, Seabra MC. Fatty acylation and prenylation of proteins: what's hot in fat. Curr Opin Cell Biol. 2005;17(2):190–196.
12. Wright LP, Philips MR. Thematic review series: lipid posttranslational modifications. CAAX modification and membrane targeting of Ras. J Lipid Res. 2006;47(5):883–891.
13. Lane KT, Beese LS. Thematic review series: lipid posttranslational modifications. Structural biology of protein farnesyltransferase and geranylgeranyltransferase type I. J Lipid Res. 2006;47(4):681–699.
14. Leung KF, Baron R, Seabra MC. Thematic review series: lipid posttranslational modifications. Geranylgeranylation of Rab GTPases. J Lipid Res. 2006;47(3):467–475.
15. Nguyen UT, Goody RS, Alexandrov K. Understanding and exploiting protein prenyltransferases. Chembiochem. 2010;11(9):1194–1201.
   •• **This review describes the mechanisms of protein prenylation and recent developments in the analysis and biotechnological exploitation of these modifications.**
16. Novelli G, D'Apice MR. Protein farnesylation and disease. J Inherit Metab Dis. 2012;35(5):917–926.
17. Zverina EA, Lamphear CL, Wright EN, et al. Recent advances in protein prenyltransferases: substrate identification, regulation, and disease interventions. Curr Opin Chem Biol. 2012;16(5–6):544–552.
18. Hentschel A, Zahedi RP, Ahrends R. Protein lipid modifications – more than just a greasy ballast. Proteomics. 2016;16(5):759–782.
   •• **A recent review that gives a comprehensive and detailed overview about enzymatic and nonenzymatic lipidation events, their role in cellular biology, their relevance in diseases, and the available bioanalytical strategies to analyze this challenging type of modification.**
19. Kamiya Y, Sakurai A, Takahashi N. Metabolites of mating pheromone, rhodotorucine A, by a cells of *Rhodosporidium toruloides*. Biochem Biophys Res Commun. 1980;94(3):855–860.
20. Anderegg RJ, Betz R, Carr SA, et al. Structure of *Saccharomyces cerevisiae* mating hormone a-factor. Identification of S-farnesyl cysteine as a structural component. J Biol Chem. 1988;263(34):18236–18240.
21. Young SG, Yang SH, Davies BS, et al. Targeting protein prenylation in progeria. Sci Transl Med. 2013;5(171):171ps3.
   • **In this review, the authors discuss the mutation that causes HGPS, the rationale for inhibiting protein farnesyl transferase, the potential limitations of this therapeutic approach, and new potential strategies for treating the disease.**
22. Rusinol AE, Sinensky MS. Farnesylated lamins, progeroid syndromes and farnesyl transferase inhibitors. J Cell Sci. 2006;119(Pt 16):3265–3272.
23. Broers JL, Ramaekers FC, Bonne G, et al. Nuclear lamins: laminopathies and their role in premature ageing. Physiol Rev. 2006;86 (3):967–1008.
24. Eriksson M, Brown WT, Gordon LB, et al. Recurrent de novo point mutations in lamin A cause Hutchinson-Gilford progeria syndrome. Nature. 2003;423(6937):293–298.
25. Yang SH, Bergo MO, Toth JI, et al. Blocking protein farnesyltransferase improves nuclear blebbing in mouse fibroblasts with a targeted Hutchinson-Gilford progeria syndrome mutation. Proc Natl Acad Sci U S A. 2005;102(29):10291–10296.
26. Yang SH, Andres DA, Spielmann HP, et al. Progerin elicits disease phenotypes of progeria in mice whether or not it is farnesylated. J Clin Invest. 2008;118(10):3291–3300.
27. Gordon LB, Kleinman ME, Massaro J, et al. Clinical trial of the protein farnesylation inhibitors lonafarnib, pravastatin, and zoledronic acid in children with Hutchinson-Gilford progeria syndrome. Circulation. 2016;134(2):114–125.
28. Gordon LB, Massaro J, D'Agostino RB Sr., et al. Impact of farnesylation inhibitors on survival in Hutchinson-Gilford progeria syndrome. Circulation. 2014;130(1):27–34.
29. Ibrahim MX, Sayin VI, Akula MK, et al. Targeting isoprenylcysteine methylation ameliorates disease in a mouse model of progeria. Science. 2013;340(6138):1330–1333.
30. Serrano-Pozo A, Frosch MP, Masliah E, et al. Neuropathological alterations in Alzheimer disease. Cold Spring Harb Perspect Med. 2011;1(1):a006189.
31. Li L, Zhang W, Cheng S, et al. Isoprenoids and related pharmacological interventions: potential application in Alzheimer's disease. Mol Neurobiol. 2012;46(1):64–77.
32. Hottman DA, Li L. Protein prenylation and synaptic plasticity: implications for Alzheimer's disease. Mol Neurobiol. 2014;50 (1):177–185.
33. Pedrini S, Carter TL, Prendergast G, et al. Modulation of statin-activated shedding of Alzheimer APP ectodomain by ROCK. Plos Med. 2005;2(1):e18.
34. Cole SL, Grudzien A, Manhart IO, et al. Statins cause intracellular accumulation of amyloid precursor protein, beta-secretase-cleaved fragments, and amyloid beta-peptide via an isoprenoid-dependent mechanism. J Biol Chem. 2005;280(19):18755–18770.
35. Ostrowski SM, Wilkinson BL, Golde TE, et al. Statins reduce amyloid-beta production through inhibition of protein isoprenylation. J Biol Chem. 2007;282(37):26832–26844.
36. Zhou Y, Suram A, Venugopal C, et al. Geranylgeranyl pyrophosphate stimulates gamma-secretase to increase the generation of Abeta and APP-CTFgamma. Faseb J. 2008;22(1):47–54.
37. Grimm MO, Grimm HS, Patzold AJ, et al. Regulation of cholesterol and sphingomyelin metabolism by amyloid-beta and presenilin. Nat Cell Biol. 2005;7(11):1118–1123.
38. Eckert GP, Hooff GP, Strandjord DM, et al. Regulation of the brain isoprenoids farnesyl- and geranylgeranylpyrophosphate is altered in male Alzheimer patients. Neurobiol Dis. 2009;35 (2):251–257.
39. Gartner U, Holzer M, Arendt T. Elevated expression of p21ras is an early event in Alzheimer's disease and precedes neurofibrillary degeneration. Neuroscience. 1999;91(1):1–5.
40. Cordle A, Landreth G. 3-Hydroxy-3-methylglutaryl-coenzyme A reductase inhibitors attenuate beta-amyloid-induced microglial inflammatory responses. J Neurosci. 2005;25(2):299–307.
41. Shepardson NE, Shankar GM, Selkoe DJ. Cholesterol level and statin use in Alzheimer disease: II review of human trials and recommendations. Arch Neurol. 2011;68(11):1385–1392.
42. Shepardson NE, Shankar GM, Selkoe DJ. Cholesterol level and statin use in Alzheimer disease: I. Review of epidemiological and preclinical studies. Arch Neurol. 2011;68(10):1239–1244.
43. Mans RA, Chowdhury N, Cao D, et al. Simvastatin enhances hippocampal long-term potentiation in C57BL/6 mice. Neuroscience. 2010;166(2):435–444.

44. Cheng S, Cao D, Hottman DA, et al. Farnesyltransferase haplodeficiency reduces neuropathology and rescues cognitive function in a mouse model of Alzheimer disease. J Biol Chem. 2013;288(50):35952–35960.
45. Kaplan A, Stockwell BR. Therapeutic approaches to preventing cell death in Huntington disease. Prog Neurobiol. 2012;99(3):262–280.
46. Sommer DB, Stacy MA. What's in the pipeline for the treatment of Parkinson's disease? Expert Rev Neurother. 2008;8(12):1829–1839.
47. Gagnon KT. HD therapeutics – CHDI Fifth Annual Conference. IDrugs. 2010;13(4):219–223.
48. Rizzetto M, Hepatitis D. Thirty years after. J Hepatol. 2009;50(5):1043–1050.
49. Ciancio A, Rizzetto M. Chronic hepatitis D at a standstill: where do we go from here? Nat Rev Gastroenterol Hepatol. 2014;11(1):68–71.
50. Glenn JS, Watson JA, Havel CM, et al. Identification of a prenylation site in delta virus large antigen. Science. 1992;256(5061):1331–1333.
51. Bordier BB, Ohkanda J, Liu P, et al. In vivo antiviral efficacy of prenylation inhibitors against hepatitis delta virus. J Clin Invest. 2003;112(3):407–414.
52. Koh C, Canini L, Dahari H, et al. Oral prenylation inhibition with lonafarnib in chronic hepatitis D infection: a proof-of-concept randomised, double-blind, placebo-controlled phase 2A trial. Lancet Infect Dis. 2015;15(10):1167–1174.
53. Amaya M, Baranova A, van Hoek ML. Protein prenylation: a new mode of host-pathogen interaction. Biochem Biophys Res Commun. 2011;416(1–2):1–6.
54. Ivanov SS, Charron G, Hang HC, et al. Lipidation by the host prenyltransferase machinery facilitates membrane localization of *Legionella pneumophila* effector proteins. J Biol Chem. 2010;285(45):34686–34698.
55. Piispanen AE, Bonnefoi O, Carden S, et al. Roles of Ras1 membrane localization during *Candida albicans* hyphal growth and farnesol response. Eukaryot Cell. 2011;10(11):1473–1484.
56. Fortwendel JR, Juvvadi PR, Rogg LE, et al. Plasma membrane localization is required for RasA-mediated polarized morphogenesis and virulence of *Aspergillus fumigatus*. Eukaryot Cell. 2012;11(8):966–977.
57. Song JL, White TC. RAM2: an essential gene in the prenylation pathway of *Candida albicans*. Microbiology. 2003;149(Pt 1):249–259.
58. Nakayama H, Ueno K, Uno J, et al. Growth defects resulting from inhibiting ERG20 and RAM2 in *Candida glabrata*. FEMS Microbiol Lett. 2011;317(1):27–33.
59. Esher SK, Ost KS, Kozubowski L, et al. Relative contributions of prenylation and postprenylation processing in *Cryptococcus neoformans* pathogenesis. Msphere. 2016;1(2):e00084–00015.
60. Eastman RT, Buckner FS, Yokoyama K, et al. Thematic review series: lipid posttranslational modifications. Fighting parasitic disease by blocking protein farnesylation. J Lipid Res. 2006;47(2):233–240.
61. Sharma K. A review on *Plasmodium falciparum*-protein farnesyltransferase inhibitors as antimalarial drug targets. Curr Drug Targets. 2016;17:1–11.
62. Samatar AA, Poulikakos PI. Targeting RAS-ERK signalling in cancer: promises and challenges. Nat Rev Drug Discov. 2014;13(12):928–942.
63. Winter-Vann AM, Casey PJ. Post-prenylation-processing enzymes as new targets in oncogenesis. Nat Rev Cancer. 2005;5(5):405–412.
64. Wang M, Casey PJ. Protein prenylation: unique fats make their mark on biology. Nat Rev Mol Cell Biol. 2016;17(2):110–122.
65. Cox AD, Fesik SW, Kimmelman AC, et al. Drugging the undruggable RAS: mission possible? Nat Rev Drug Discov. 2014;13(11):828–851.
66. Sousa SF, Fernandes PA, Ramos MJ. Farnesyltransferase inhibitors: a detailed chemical view on an elusive biological problem. Curr Med Chem. 2008;15(15):1478–1492.
67. Khan OM, Ibrahim MX, Jonsson IM, et al. Geranylgeranyltransferase type I (GGTase-I) deficiency hyperactivates macrophages and induces erosive arthritis in mice. J Clin Invest. 2011;121(2):628–639.
68. Diao F, Jiang C, Wang XX, et al. Alteration of protein prenylation promotes spermatogonial differentiation and exhausts spermatogonial stem cells in newborn mice. Sci Rep. 2016;6:28917.
69. Leite GA, Rosa Jde L, Sanabria M, et al. Delayed reproductive development in pubertal male rats exposed to the hypolipemiant agent rosuvastatin since prepuberty. Reprod Toxicol. 2014;44:93–103.
70. Wang XX, Ying P, Diao F, et al. Altered protein prenylation in Sertoli cells is associated with adult infertility resulting from childhood mumps infection. J Exp Med. 2013;210(8):1559–1574.
71. Roosing S, Collin RW, Den Hollander AI, et al. Prenylation defects in inherited retinal diseases. J Med Genet. 2014;51(3):143–151.
72. Okin D, Medzhitov R. The effect of sustained inflammation on hepatic mevalonate pathway results in hyperglycemia. Cell. 2016;165(2):343–356.
73. Berndt N, Hamilton AD, Sebti SM. Targeting protein prenylation for cancer therapy. Nat Rev Cancer. 2011;11(11):775–791.
74. Tate EW, Kalesh KA, Lanyon-Hogg T, et al. Global profiling of protein lipidation using chemical proteomic technologies. Curr Opin Chem Biol. 2015;24:48–57.
• **Review describing the application of bioorthogonal labeling to the study of protein lipidation.**
75. Suzuki T, Ito M, Ezure T, et al. Protein prenylation in an insect cell-free protein synthesis system and identification of products by mass spectrometry. Proteomics. 2007;7(12):1942–1950.
76. Bhawal RP, Sadananda SC, Bugarin A, et al. Mass spectrometry cleavable strategy for identification and differentiation of prenylated peptides. Anal Chem. 2015;87(4):2178–2186.
•• **A recent paper that describes the development of a novel mass-spectrometry-based method for detection of farnesylated and geranylgeranylated proteins.**
77. Zhao Y, Jensen ON. Modification-specific proteomics: strategies for characterization of post-translational modifications using enrichment techniques. Proteomics. 2009;9(20):4632–4641.
78. Thingholm TE, Larsen MR, Ingrell CR, et al. TiO(2)-based phosphoproteomic analysis of the plasma membrane and the effects of phosphatase inhibitor treatment. J Proteome Res. 2008;7(8):3304–3313.
79. Olsen JV, Blagoev B, Gnad F, et al. Global, in vivo, and site-specific phosphorylation dynamics in signaling networks. Cell. 2006;127(3):635–648.
80. Elortza F, Nuhse TS, Foster LJ, et al. Proteomic analysis of glycosylphosphatidylinositol-anchored membrane proteins. Mol Cell Proteomics. 2003;2(12):1261–1270.
81. Yoshihara HA, Mahrus S, Wells JA. Tags for labeling protein N-termini with subtiligase for proteomics. Bioorg Med Chem Lett. 2008;18(22):6000–6003.
82. Wiita AP, Seaman JE, Wells JA. Global analysis of cellular proteolysis by selective enzymatic labeling of protein N-termini. Methods Enzymol. 2014;544:327–358.
83. Khidekel N, Ficarro SB, Peters EC, et al. Exploring the O-GlcNAc proteome: direct identification of O-GlcNAc-modified proteins from the brain. Proc Natl Acad Sci U S A. 2004;101(36):13132–13137.
84. Berndt N, Sebti SM. Measurement of protein farnesylation and geranylgeranylation in vitro, in cultured cells and in biopsies, and the effects of prenyl transferase inhibitors. Nat Protoc. 2011;6(11):1775–1791.
85. Wang C, Gale M Jr., Keller BC, et al. Identification of FBL2 as a geranylgeranylated cellular protein required for hepatitis C virus RNA replication. Mol Cell. 2005;18(4):425–434.
86. Kapadia SB, Chisari FV. Hepatitis C virus RNA replication is regulated by host geranylgeranylation and fatty acids. Proc Natl Acad Sci USA. 2005;102(7):2561–2566.
87. Ye J, Wang C, Sumpter R Jr., et al. Disruption of hepatitis C virus RNA replication through inhibition of host protein geranylgeranylation. Proc Natl Acad Sci U S A. 2003;100(26):15865–15870.
88. Doll S, Burlingame AL. Mass spectrometry-based detection and assignment of protein posttranslational modifications. ACS Chem Biol. 2015;10(1):63–71.
89. Lai RK, Perez-Sala D, Canada FJ, et al. The gamma subunit of transducin is farnesylated. Proc Natl Acad Sci USA. 1990;87(19):7673–7677.
90. Sorek N, Akerman A, Yalovsky S. Analysis of protein prenylation and S-acylation using gas chromatography-coupled mass spectrometry. Methods Mol Biol. 2013;1043:121–134.

91. Hoffman MD, Kast J. Mass spectrometric characterization of lipid-modified peptides for the analysis of acylated proteins. J Mass Spectrom. 2006;41(2):229–241.
92. Wotske M, Wu Y, Wolters DA. Liquid chromatographic analysis and mass spectrometric identification of farnesylated peptides. Anal Chem. 2012;84(15):6848–6855.
93. Chowdhury SM, Munske GR, Ronald RC, et al. Evaluation of low energy CID and ECD fragmentation behavior of mono-oxidized thio-ether bonds in peptides. J Am Soc Mass Spectrom. 2007;18 (3):493–501.
94. Bhawal RP, Shahinuzzaman AD, Chowdhury SM. Gas-phase fragmentation behavior of oxidized prenyl peptides by CID and ETD tandem mass spectrometry. J Am Soc Mass Spectrom. 2017;28 (4):704–707.
95. Kolb HC, Finn MG, Sharpless KB. Click chemistry: diverse chemical function from a few good reactions. Angew Chem Int Ed Engl. 2001;40(11):2004–2021.
96. Onono F, Subramanian T, Sunkara M, et al. Efficient use of exogenous isoprenols for protein isoprenylation by MDA-MB-231 cells is regulated independently of the mevalonate pathway. J Biol Chem. 2013;288(38):27444–27455.
97. Onono FO, Morgan MA, Spielmann HP, et al. A tagging-via-substrate approach to detect the farnesylated proteome using two-dimensional electrophoresis coupled with Western blotting. Mol Cell Proteomics. 2010;9(4):742–751.
98. Chan LN, Hart C, Guo L, et al. A novel approach to tag and identify geranylgeranylated proteins. Electrophoresis. 2009;30(20):3598–3606.
99. Palsuledesai CC, Ochocki JD, Markowski TW, et al. A combination of metabolic labeling and 2D-DIGE analysis in response to a farnesyltransferase inhibitor facilitates the discovery of new prenylated proteins. Mol Biosyst. 2014;10(5):1094–1103.
100. DeGraw AJ, Palsuledesai C, Ochocki JD, et al. Evaluation of alkyne-modified isoprenoids as chemical reporters of protein prenylation. Chem Biol Drug Des. 2010;76(6):460–471.
101. Palsuledesai CC, Ochocki JD, Kuhns MM, et al. Metabolic labeling with an alkyne-modified isoprenoid analog facilitates imaging and quantification of the prenylome in cells. ACS Chem Biol. 2016;11 (10):2820–2828.
102. Kho Y, Kim SC, Jiang C, et al. A tagging-via-substrate technology for detection and proteomics of farnesylated proteins. Proc Natl Acad Sci U S A. 2004;101(34):12479–12484.
103. Charron G, Li MM, MacDonald MR, et al. Prenylome profiling reveals S-farnesylation is crucial for membrane targeting and antiviral activity of ZAP long-isoform. Proc Natl Acad Sci U S A. 2013;110 (27):11085–11090.
104. Suazo KF, Schaber C, Palsuledesai CC, et al. Global proteomic analysis of prenylated proteins in *Plasmodium falciparum* using an alkyne-modified isoprenoid analogue. Sci Rep. 2016;6:38615.
105. Storck EM, Serwa RA, Tate EW. Chemical proteomics: a powerful tool for exploring protein lipidation. Biochem Soc Trans. 2013;41 (1):56–61.
106. Couvertier SM, Zhou Y, Weerapana E. Chemical-proteomic strategies to investigate cysteine posttranslational modifications. Biochim Biophys Acta. 2014;1844(12):2315–2330.
107. Dursina B, Reents R, Delon C, et al. Identification and specificity profiling of protein prenyltransferase inhibitors using new fluorescent phosphoisoprenoids. J Am Chem Soc. 2006;128(9):2822–2835.
108. Nguyen UT, Guo Z, Delon C, et al. Analysis of the eukaryotic prenylome by isoprenoid affinity tagging. Nat Chem Biol. 2009;5 (4):227–235.
•• **This paper describes the application of *in vitro* prenylation assay for the identification of protein targets of prenylatransferases and PTI inhibitor selectivity.**
109. Kohnke M, Delon C, Hastie ML, et al. Rab GTPase prenylation hierarchy and its potential role in choroideremia disease. Plos One. 2013;8(12):e81758.
•• **This paper describes the application of *in vitro* prenylation assay for the identification of protein targets of prenylatransferases and PTI inhibitor selectivity.**
110. Ali N, Jurczyluk J, Shay G, et al. A highly sensitive prenylation assay reveals in vivo effects of bisphosphonate drug on the Rab prenylome of macrophages outside the skeleton. Small Gtpases. 2015;6 (4):202–211.
111. Maurer-Stroh S, Koranda M, Benetka W, et al. Towards complete sets of farnesylated and geranylgeranylated proteins. Plos Comput Biol. 2007;3(4):e66.
112. Perez-Sala D. Protein isoprenylation in biology and disease: general overview and perspectives from studies with genetically engineered animals. Front Biosci. 2007;12:4456–4472.
113. Liu M, Sjogren AK, Karlsson C, et al. Targeting the protein prenyltransferases efficiently reduces tumor development in mice with K-RAS-induced lung cancer. Proc Natl Acad Sci USA. 2010;107 (14):6471–6476.
114. Cook LA, Schey KL, Wilcox MD, et al. Proteomic analysis of bovine brain G protein gamma subunit processing heterogeneity. Mol Cell Proteomics. 2006;5(4):671–685.
115. Kassai H, Satomi Y, Fukada Y, et al. Top-down analysis of protein isoprenylation by electrospray ionization hybrid quadrupole time-of-flight tandem mass spectrometry; the mouse Tgamma protein. Rapid Commun Mass Spectrom. 2005;19(2):269–274.
116. Peng M, Scholten A, Heck AJ, et al. Identification of enriched PTM crosstalk motifs from large-scale experimental data sets. J Proteome Res. 2014;13(1):249–259.
117. Venne AS, Kollipara L, Zahedi RP. The next level of complexity: crosstalk of posttranslational modifications. Proteomics. 2014;14 (4–5):513–524.
118. Hayashi T, Rumbaugh G, Huganir RL. Differential regulation of AMPA receptor subunit trafficking by palmitoylation of two distinct sites. Neuron. 2005;47(5):709–723.
119. Hayashi T, Thomas GM, Huganir RL. Dual palmitoylation of NR2 subunits regulates NMDA receptor trafficking. Neuron. 2009;64 (2):213–226.
120. Komekado H, Yamamoto H, Chiba T, et al. Glycosylation and palmitoylation of Wnt-3a are coupled to produce an active form of Wnt-3a. Genes Cells. 2007;12(4):521–534.
121. Kong C, Lange JJ, Samovski D, et al. Ubiquitination and degradation of the hominoid-specific oncoprotein TBC1D3 is regulated by protein palmitoylation. Biochem Biophys Res Commun. 2013;434 (2):388–393.
122. Yount JS, Karssemeijer RA, Hang HC. S-palmitoylation and ubiquitination differentially regulate interferon-induced transmembrane protein 3 (IFITM3)-mediated resistance to influenza virus. J Biol Chem. 2012;287(23):19631–19641.
123. Hansen BT, Davey SW, Ham AJ, et al. P-Mod: an algorithm and software to map modifications to peptide sequences using tandem MS data. J Proteome Res. 2005;4(2):358–368.
124. Chen Y, Chen W, Cobb MH, et al. PTMap – a sequence alignment software for unrestricted, accurate, and full-spectrum identification of post-translational modification sites. Proc Natl Acad Sci USA. 2009;106(3):761–766.
125. Gupta N, Tanner S, Jaitly N, et al. Whole proteome analysis of post-translational modifications: applications of mass-spectrometry for proteogenomic annotation. Genome Res. 2007;17(9):1362–1377.
126. Savitski MM, Nielsen ML, Zubarev RA. ModifiComb, a new proteomic tool for mapping substoichiometric post-translational modifications, finding novel types of modifications, and fingerprinting complex protein mixtures. Mol Cell Proteomics. 2006;5(5):935–948.